FORAMINIFERAL PALEONTOLOGY AND SEQUENCE STRATIGRAPHY IN THE UPPER VISEAN – SERPUKHOVIAN DEPOSITS (ALADAĞ UNIT, EASTERN TAURIDES, TURKEY)

A THESIS SUBMITTED TO
THE GRADUATE SCHOOL OF NATURAL AND APPLIED SCIENCES
OF
MIDDLE EAST TECHNICAL UNIVERSITY

BY

SEDA DEMİREL

IN PARTIAL FULFILLMENT OF THE REQUIREMENTS
FOR
THE DEGREE OF MASTER OF SCIENCE
IN
GEOLOGICAL ENGINEERING

SEPTEMBER 2012

Approval of the thesis:

FORAMINIFERAL PALEONTOLOGY AND SEQUENCE STRATIGRAPHY IN THE UPPER VISEAN – SERPUKHOVIAN DEPOSITS (ALADAĞ UNIT, EASTERN TAURIDES, TURKEY)

submitted by **SEDA DEMİREL** in partial fulfillment of the requirements for the degree of **Master of Science in Geological Engineering Department, Middle East Technical University** by,

Prof. Dr. Canan ÖZGEN _____
Dean, Graduate School of **Natural and Applied Sciences**

Prof. Dr. Erdin BOZKURT _____
Head of Department, **Geological Engineering**

Prof. Dr. Demir ALTINER _____
Supervisor, **Geological Engineering Dept., METU**

Examining Committee Members:

Prof. Dr. M. Cemal GÖNCÜOĞLU _____
Geological Engineering Dept., METU

Prof. Dr. Demir ALTINER _____
Geological Engineering Dept., METU

Assoc. Prof. Dr. Bora ROJAY _____
Geological Engineering Dept., METU

Assoc. Prof. Dr. İ. Ömer YILMAZ _____
Geological Engineering Dept., METU

Dr. Zühtü Batı _____
Geological Engineering Dept., METU

Date: September 28, 2012

I hereby declare that all information in this document has been obtained and presented in accordance with academic rules and ethical conduct. I also declare that, as required by these rules and conduct, I have fully cited and referenced all material and results that are not original to this work.

Name, Last Name : Seda DEMİREL

Signature :

ABSTRACT

FORAMINIFERAL PALEONTOLOGY AND SEQUENCE STRATIGRAPHY IN THE UPPER VISEAN – SERPUKHOVIAN DEPOSITS (ALADAĞ UNIT, EASTERN TAURIDES, TURKEY)

Demirel, Seda

M.Sc., Department of Geological Engineering

Supervisor: Prof. Dr. Demir Altıner

September 2012, 360 pages

The aim of this study is to investigate the Upper Visean substages, delineate the Visean - Serpukhovian boundary with calcareous foraminifera and interpret the foraminiferal evolution and sequence stratigraphical framework by using sedimentary cyclicity across the boundary section. For this purpose a 59,61 m thick stratigraphic section consisting of mainly limestone and partly sandstone and shale is measured in the Aziziye Gediği and Oruçoğlu Formations in the Pınarbaşı Region of Eastern Taurides.

A detailed micropaleontological study has revealed presence of important foraminiferal groups namely, parathuramminids, earlandiids, endothyroids, archaediscids, biseriamminids, fusulinids, loeblichids, tournayellids and paleotextularids and 145 species and three biozones. The biozones are, in ascending order, *Eostaffella ikensis* – *Vissarionovella tujmasensis* Zone (Mikhailovsky; Late Visean), *Endothyranopsis* cf. *sphaerica* – *Biseriella parva* Zone (Venevsky; Late Visean) and

Eostaffella pseudostruvei – Archaediscids @ *tenuis* stage Zone (Taurssk; Early Serpukhovian).

A detailed microfacies analysis was carried out in order to understand the depositional history and sedimentary cyclicity and construct the sequence stratigraphic framework of the studied area. Three main depositional environments consisting of open marine, shoal or bank and tidal flat environments were interpreted based on the analysis of 12 major microfacies and 11 sub-microfacies types. Based on the vertical association of microfacies twenty-six cycles, two sequence boundaries and three sequences were recognized in the studied section and these two sequence boundaries, which correspond to the Mikhailovsky and Venevsky horizons, are the records of the global sea level changes during the Late Paleozoic Ice Age. Within this context Visean – Serpukhovian boundary falls in the transgressive system tract of the third sequence. The duration of cycles are calculated as 117 ky and interpreted as orbitally induced glacioeustatic cycles.

Keywords: Visean-Serpukhovian boundary, Foraminifera, Microfacies Analysis and Sequence Stratigraphy, Meter Scale Cycles, Eastern Taurides.

ÖZ

ÜST VİZEYEN - SERPUKOVİYEN ÇÖKELLERİNİN FORAMİNİFER PALEONTOLOJİSİ VE SEKANS STRATİGRAFİSİ (ALADAĞ BİRİMİ, DOĞU TOROSLAR, TÜRKİYE)

Demirel, Seda

Yüksek Lisans, Jeoloji Mühendisliği Bölümü

Tez Yöneticisi: Prof. Dr. Demir Altıner

Eylül 2012, 360 sayfa

Bu çalışmanın amacı Üst Vizeyen askatının bölümlerini ortaya koymak, Üst Vizeyen – Serpukoviyen sınırını foraminiferleri kullanarak belirlemek, kesit boyunca foraminiferlerin evrimini çalışmak ve sedimanter devirleri kullanarak sekans stratigrafik çatıyı oluşturmaktır. Bu amaçla, Doğu Torosların Pınarbaşı Bölgesi'nde bulunan Aziziye Gediği ve Oruçoğlu Formasyonlarının bir kısmını içine alan kireçtaşı hakim, kısmen kumtaşı ve şeyl içeren 59,61 m kalınlığında bir stratigrafik kesit ölçülmüştür.

Ayrıntılı bir mikropaleontolojik çalışma sonucunda önemli foraminifer gruplarından olan "parathuramminid, earlandiid, endothyroid, archaediscid, biseriamminid, fusulinid, loeblichid, tournayellid ve paleotextularidler" e ait 145 türün varlığı ortaya konmuş ve 3 biyozon tanımlanmıştır. Bu biyozonlar, aşağıdan yukarıya doğru *Eostaffella ikensis* – *Vissarionovella tujmasensis* Zonu (Mikhailovsky- Geç Vizeyen), *Endothyranopsis* cf. *sphaerica* – *Biseriella parva* Zonu (Venevsky-Geç Vizeyen) ve *Eostaffella pseudostruvei* – Archaediscid @ *tenuis* stage Zonu' dur (Taurssky Erken Serpukoviyen).

Çalışılan alanın çökelim tarihçesini ve sedimanter devirselliğini anlamak ve sekans stratigrafik çatıyı oluşturmak için detaylı bir mikrofasiyes çalışması yürütülmüştür. Açık deniz, karbonat sığlığı ve gelgit düzlüğü ortamlarından oluşan 3 ana çökelme alanı, 12 ana mikrofasiyes ve 11 alt mikrofasiyes tiplerinin ortaya konulması ile belirlenmiştir. Mikrofasiyeslerin dikey sıralanmalarına göre yirmi altı metre ölçekli devir, iki sekans sınırı ve üç sekans tespit edilmiş ve ortaya konulan sekans stratigrafik çatı içinde Mikhailovsky ve Venevsky ' deki iki sekans sınırının global ölçekte oluşan Geç Paleozoyik Buzul Devri deniz seviyesi değişimleri sırasında oluştuğu anlaşılmıştır. Bu durumda Vizeyen – Serpukoviyen sınırı üçüncü sekansın "transgressive system tract" ' i içinde yer almaktadır. Devirlerin depolanma süresinin 117 ky oluğu hesaplanmış ve bu devirlerin orbital değişimlerle tetiklenen buzul kontrollü östatik devirler olduğu yorumlanmıştır.

Anahta Kelimeler: Vizeyen-Serpukoviyen sınırı, Foraminifer, Mikrofasiyes Analizi ve Sekans Stratigrafisi, Metre Ölçekli devirsellik ve Doğu Toroslar.

To My Family...

ACKNOWLEDGEMENTS

I am deeply grateful to my supervisor Prof. Dr. Demir Altıner for his valuable guidance, encouragement and continued advice throughout the course of my M.Sc. studies. It is an honor for me to work with him.

I would like to express my appreciation to Prof. Dr. Sevinç ÖZKAN-ALTINER for her understanding approach, encouragements and valuable recommendations and during my studies.

I wish to thank my examining committee members, Prof. Dr. Cemal Göncüoğlu, Assoc. Prof. Dr. Bora Rojay, Assoc. Prof. Dr. İ. Ömer Yılmaz and Dr. Zühtü Batı for their valuable recommendations and criticism.

I am thankful to my friends especially Yavuz Kaya, Felat Dursun, Ezgi Ünal, Çiğdem Cankara, Burcu Erdemli and Ayten Koç for their encouragement, motivation and friendship. Special thanks to Mustafa Yücel Kaya and Ayşe Özdemir for our discussions on foraminiferal paleontology and geology and their friendship and endless encouragement throughout this study. I am also grateful to Yavuz Özdemir and Birce Bakdı for their helps throughout the field work.

I would like to thank to Mr. Orhan Karaman for the preparation of thin sections.

At last but definitely not the least, I would like to express my gratitude to my parents, Zübeyde Çalışır and İsmail Fevzi Çiçek, my sister Seçil Çiçek Koç and my husband Yücel Demirel for their patience, permanent encouragement and belief in me throughout this work.

TABLE OF CONTENTS

LIST OF TABLES

TABLES

LIST OF FIGURES

FIGURES

CHAPTER 1

INTRODUCTION

1.1 Purpose and Scope

This thesis aims to delineate the Upper Visean substage and the Visean - Serpukhovian boundary based on calcareous foraminifera in the allochthonous Aladağ Unit which is exposed in the Pınarbaşı region (Eastern Taurides) and to define the sedimentary cyclicity across the boundary. To be able to explain cyclicity, interpret the stacking patterns of strata and the evolution of carbonate platform in a sequence stratigraphic framework, it is essential to understand the evolution of depositional environments. For this purpose, a 59,61 m thick stratigraphic section has been measured in Aziziye Gediği and Oruçoğlu formations of the Aladağ Unit.

Since in the Visean-Serpukhovian transition second glacial episode of Late Paleozoic started in Gondwana (Isbell, 2003) and this transition coincided with significant climatic changes and marine biotic endemism, this boundary is significant in the geologic history (Davydov et al., 2004). One of the purposes of this study is to contribute to the international studies carried on the Visean-Serpukhovian transition by defining one of the boundary sections with foraminifera from Turkey and document the changes in depositional environments across the boundary. The boundary is defined between Russian Venevsky and Taurrsky Horizons and Brigantian and Pendelian or Namurian substages of the Western Europe. However, attempts are proceeding to place the boundary within the Brigantian substage with the first occurence of the conodont *L. ziegleri* (Richards et al., 2010). But this has not been voted

yet in the subcommision on Carboniferous of the International Commission of stratigraphy (Richards et al., 2010). Since this boundary has not been yet modified, the Visean-Serpukhovian boundary is placed between Venevsky and Taurrsky Horizons in this thesis by following traditional studies based on foraminifera (Cózar et al., 2008; Somerville, 2008; Hecker, 2009; Kulagina et al., 2009, Nigmadhaznov et al., 2010; Pazukhin et al., 2010; Pille et al., 2010). In order to delineate the boundary, a detailed taxonomic work on Upper Visean – Lower Serpukhovian foraminifera was carried out and a local biozonation was proposed. The measured section was divided into three biozones that correspond to Russian Horizons.

In order to define depositional environments and the evolution of depositional environments through Upper Visean – Lower Serpukhovian deposits in Pınarbaşı, a detailed microfacies analysis was carried out. Data handled from the microfacies analysis were also used to determine the sedimentary cyclicity since cycles are defined based on the vertical stacking patterns of microfacies. The higher order cyclic patterns can be the result of glacioeustasy driven by Milankovitch eccentricity. With the interpretation of vertical distribution of cycles, the studied section was placed in a sequence stratigraphic frame. In this thesis, bed scale cyclicity at the Visean – Serpukhovian beds was defined for the first time in Taurides.

1.2 Geographic Setting

The study area is located approximately 15 km northwest of the town Pınarbaşı and approximately 60 km to the east of the City of Kayseri (Figure 1.1). It is situated in the topographic map of Elbistan – K 36 – d2, of 1:25.000 scales. The coordinates of the measured section, according to UTM Zone 37, start at 256922 E – 4291666 N and ends at 257386 E- 4291768 N. The studied area can be accessed by using the Kayseri – Malatya highway. This road is crossed with the Melikgazi side road which could be followed.

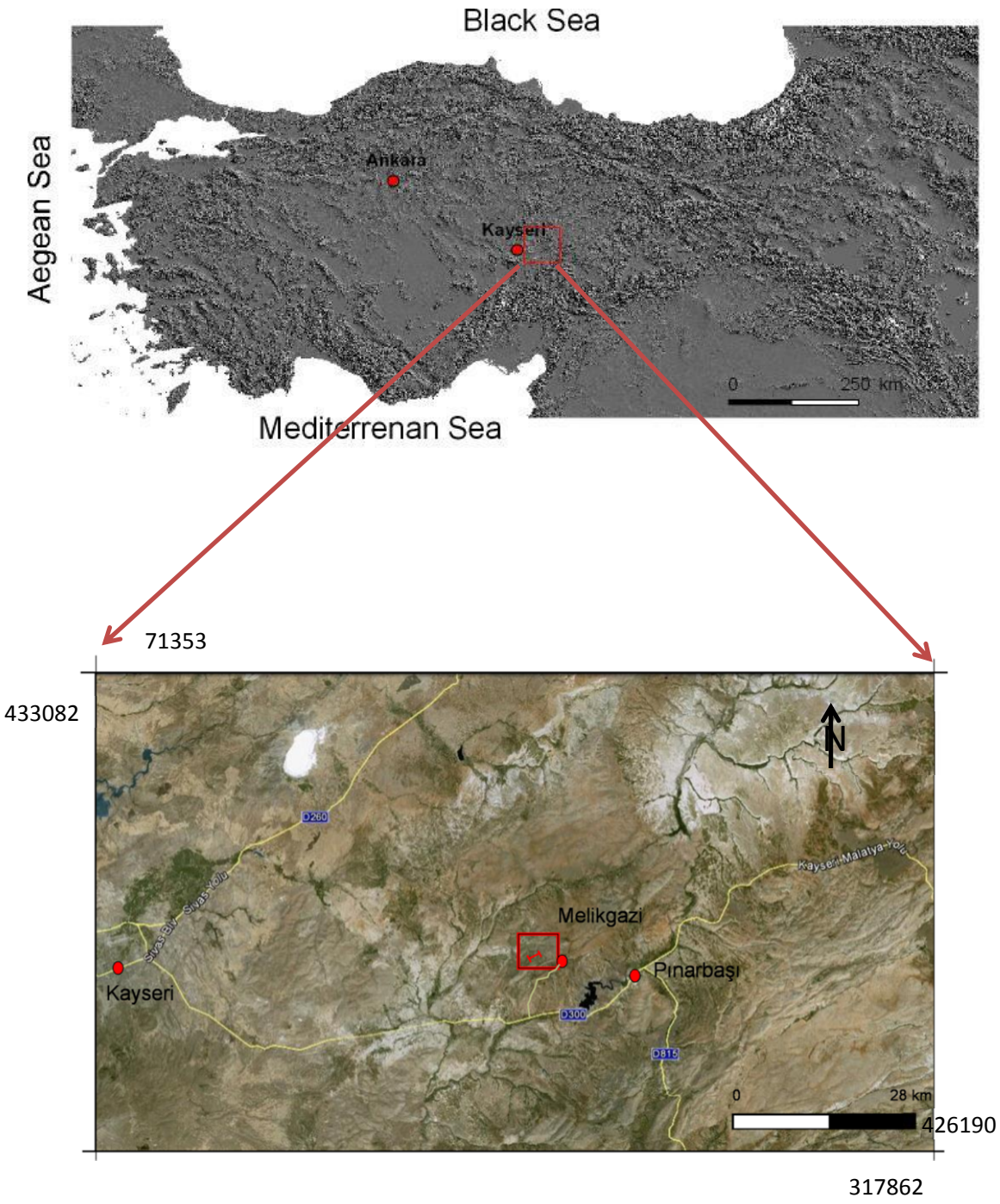

Figure 1. 1: Geographic setting of the study area and the location of the measured section (Red bar shows the approximate position of the measured section)

with a car up to the Melikgazi Village. To reach the measured section approximately 1.6 km air distance should be walked.

1.3 Methods of Study

In order to conduct this study field and laboratory works were needed. Field work included bed by bed measurement of the stratigraphic section and sampling of each bed. In this study, 59,61 m thick stratigraphic section was measured and 92 samples were collected from nearly each bed and were photographed (Figure 1.2). More than one sample were collected from some thicker beds. Samples were examined indetail in the field in order to locate the most fossiliferous zone.

Laboratory work includes microscope study. Thin sections were prepared from each sample collected from the field and they were studied under the microscope for micropaleontological and microfacies analysis. In the micropaleontological study foraminiferal content of the studied section was determined by morphological analysis of specimens. Dimensions of the specimens were measured. Individuals belonging to each species were photographed and classified according to the taxonomical hierarchy. After identification and discrimination of foraminifera, by using their distributions, foraminiferal zones for the studied section were constructed and the Visean-Serpukhovian boundary was delineated. Since the cyclic pattern of carbonates could not be interpreted in the field, vertical distribution of microfacies was used to determine the cyclicity. Microfacies were identified by the interpretation of types and abundance of allochems and the matrix in each thin section. Abundances of allochems and matrix were visually estimated and eye comparison charts were used. In addition, each thin section was photographed to display the microfacies properties. Cycle types which were determined by the vertical evolution of the microfacies were used in the interpretation of sequence stratigraphic framework since vertical stacking patterns of cycles defines types of system tracts and sequences are composed by systemtracts. Sequence boundaries were identified by drastic changes of the microfacies.

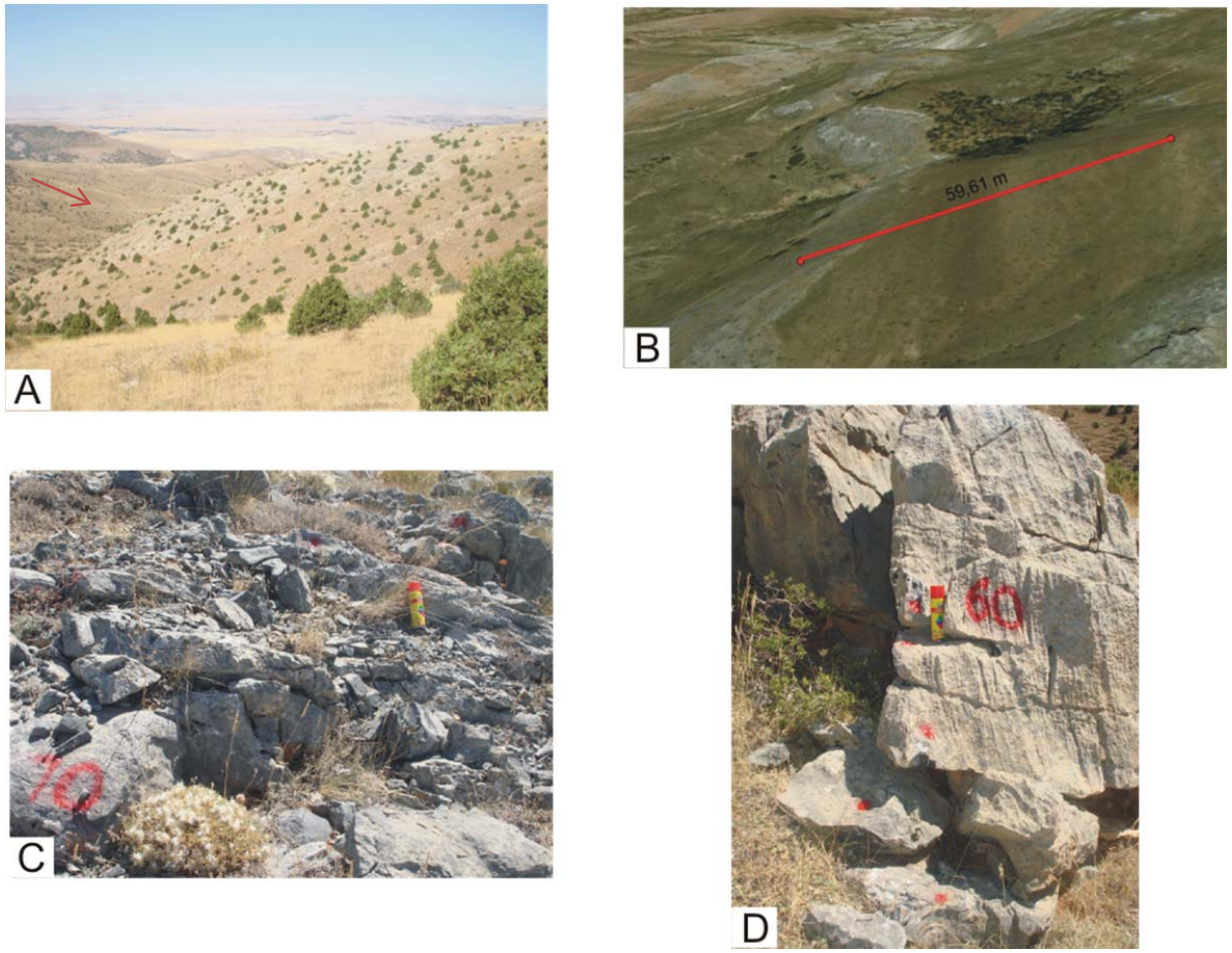

Figure 1. 2: Photographs from the field area. A. Location of the measured section (Red arrow shows the approximate location of the starting point, behind the hill); B. Location of the measured section (taken from Google Earth); C and D. Close up view of the sampled beds.

1.4 Previous Works

Taurides, which is an important part of Alpine Orogenic Belt, have drawn attention of many researchers since early twentieth century. Researches have been carried out for different purposes until today. Here, previous works that are related to the topic of the present study will be discussed. The pioneer of the studies in the Tauride Belt is Blumenthal. He systematically worked on the tectonics and stratigraphy of the Taurides between 1940's and 1950's (1944, 1947, 1951, 1956). Brunn et al. (1971, 1973) studied particularly the geology of the Western Taurides and named the Bozkır Unit of Özgül (1976) as Eastern Likia Nappes in the vicinity of Korkuteli. A group of French geologist also discussed the geology and tectonic movements in western Taurides (Monod, 1978; Dumont and Monod, 1976).

Şengör and Yılmaz (1981) discussed the evolution of Tethys from Permian to recent and they indicate the role of Anatolide-Tauride platform in this evolution. Göncüoğlu (1997) examined the Lower Paleozoic stratigraphic and paleogeographic constraints of the Tauride Belt.

Özgül who made great contributions to the understanding of the geology of the Tauride Belt, have started his studies in the Tauride Belt in 1967 and completed his studies in a number of papers published in 1971, 1976, 1983, 1984, 1985, 1997. Additionally, he studied with many other workers on Lower Paleozoic stratigraphy and fauna of various regions in Western, Central and Eastern Taurides (Özgül et al., 1972; Özgül and Gedik, 1973; Dean and Özgül, 1980; Dean and Özgül, 1994; Şenel et al., 1996 and Şenel et al., 1998). Lithostratigraphic properties and conodont fauna of Lower Paleozoic Çaltepe Limestone which is similar to Demirtaşlı formation in Tufanbeyli Region and Seydişehir Formation cropping out in the Seydişehir and Hadim regions was described by Özgül and Gedik (1973) and Cambrian of Çaltepe Limestone and its trilobite fauna studied by Dean and Özgül (1980). Şenel et al. (1998) studied the stratigraphy of the Beydağları-Karacahisar autocthon, Anamas-Akseki autocthon and

Antalya nappes. Carboniferous was observed in Beydağları-Karacahisar autocthon and Visean and Namurian is represented by bioclastic limestone and dolomite and clastic rocks respectively (Şenel et al., 1998).

In 1971, Özgül discussed the structural development of Hadim and Bozkır regions in the Central Taurides. In this study, "Unit" terminology was used in order to define an assemblage of different rock stratigraphic units which have been formed in the same depositional environment and subjected to the same tectonic processes. Özgül (1971) defined two autocthonous (Hadim and Geyikdağı Units) and two allochthonous (South Central Anatolia and Central Taurus Units) units. The Carboniferous of the Central Taurus Unit, which have been named as Hadim Nappe by Blumenthal (1944), is represented by quartzite, reefal limestone and shale. In 1976, Özgül defined six different tectonostratigraphic units in the Tauride Belt namely Bolkardağ Unit, Aladağ Unit, Geyikdağı Unit, Alanya Unit, Bozkır Unit and Antalya Unit. This study was a keystone to understand the tectonic structure of the Tauride Belt.

Şenel (1999) divided the Tauride Belt autochthonous-paraautochthonous and allochthonous rock units with a different approach. Autochthonous rock units were named from west to east as Beydağları autochthon, Anamas-Akseki autochthon and Southeast Anatolian autochthon. Allochthonous units are classified as Lycian Nappes, Antalya Nappes, Alanya Nappe, Beyşehir-Hoyran-Hadim-Bolkar Nappes, Yahyalı-Munzur Nappes and Bitlis-Pötürge-Malatya Nappes.

Evolution, tectonics and stratigraphy of the Aladağ Unit, which is exposed extensively in the study area, have been discussed by many workers since 1960's. Monod (1967, 1977) and Monod and Akay (1984) discussed the stratigraphy and structural geology of the Tauride carbonate platform including rock units in the Central Taurides which are named later as Aladağ Unit by Özgül (1976). Özgül (1976) defined the Aladağ Unit, as an allochthonous unit composed of Upper Devonian-Upper Cretaceous carbonate and clastic rocks. In the studies of Monod (1977) in the Beyşehir-Seydişehir region Aladağ

and Bozkır Units of Özgül (1976), were defined as "Beyşehir - Hoyran Nappes"and rock units of Aladağ Unit were named as "Bademli-Cevizli Unit". Roughly, the Carboniferous is defined by carbonates and intercalation of carbonates, quartz arenitic sandstone and dolomite in Monod (1977).

Additionally, Gutnic et al. (1979) studied in detail the stratigraphy and geology of various parts of Beyşehir - Hoyran Nappes. In 1979, they prepared tectonostratigraphic map of SW Turkey showing the positions Lycian Nappes, Beyşehir-Hoyran-Hadim Nappes, Antalya Complex and Alanya Complex. In this study, they indicated that Visean and Namurian rocks are made up of alternation of carbonates and quartz arenitic sandstone and dolomite.

Tekeli (1980) examined the structural evolution of Aladağ Mountains in the Taurus Belt and divided this process into phases as Late Triassic-Early Cretaceous, Senonian and Maastrichtian.

In Özgül (1984), he discussed the tectonic evolution and stratigraphy of the Central Taurides and Carboniferous of the Aladağ Unit is defined to be composed of shale, biostromal limestone and quartz arenitic sandstone. In 1997, Özgül worked on the stratigraphy of tectonostratigraphic units in the northern part of the Central Taurides. In this study, Aladağ Unit was divided into six different formations.

Demirtaşlı (1984) studied the stratigraphy and tectonics of the area between Silifke and Anamur in the Central Tauride where Aladağ Unit is exposed. Visean was distinguished in the Korucuk Formation cropping out in the Intermediate and Northern geotectonic zones and represented by bluish gray, medium to thick bedded wackestones with abundant foraminifera in the Intermediate zone and cream-colored medium to thick bedded limestone with dolomite intercalations in the Northern Zone.

Göncüoğlu et al. (2007) reviewed the previous literature on the Aladağ Unit in the Hadim region. In this study, the index fossils (foraminifera) of Visean in the Harlak

Formation of the Geyik Dağı Unit and the Halıcı Group of the Bolkar Dağı Unit are defined.

Mackintosh and Robertson (2012) discussed the sedimentary evolution of the Central Taurides from the Late Devonian to the Late Triassic. Aladağ Unit of Özgül (1976) was discussed under the name of Hadim Nappe in the study of Mackintosh and Robertson (2012). They measured two stratigraphic sections on the Hadim Nappe. In the first section, which is called as southern outcrop the Late Visean is composed of oolitic limestone, subordinate limestone, bioclastic limestone and nodular limestone. The succession from the Serpukhovian to Moscovian is represented by quartzose sandstone and carbonates. In the northern outcrop, Late Visean-Serpukhovian is represented by bioclastic grainstone-packstone to mictitic limestone intercalated with the oolitic limestone and quartzitic sandstone.

The Paleozoic of the Eastern Taurides studied by various workers. Özgül et al. (1972) discussed the Lower Paleozoic stratigraphy and fauna of Tufanbeyli in Eastern Taurides. Demirtaşlı et al. (1967, 1978, 1979) studied on the geology and Carboniferous of Pınarbaşı-Sarız vicinity and Pınarbaşı-Sarız-Tufanbeyli vicinity.

Aksay (1980) examined deposits of the Lower Carboniferous of Nohutluk Tepe (Eastern Taurides, Aladağ Unit) and analyzed microfacies. For the first time in this study, it is indicated that the Lower Carboniferous of Nohutluk Tepe sequence contains deep water facies.

Altıner (1981) defined several formations in Aygörmez Dağı Unit, which is the equivalent of the Aladağ Unit in the Eastern Taurides. Visean – Gzhelian aged Aziziye Gediği and Oruçoğlu formations defined by Altıner (1981) are within our studied section and composed of limestone and sandstone. Altıner (1981) worked on the geology, stratigraphy and biostratigraphy of the vicinity of Aygörmez Dağı near Kayseri, Pınarbaşı. He prepared the geologic map of the study are and interpreted three units namely para-autocthonous Aygörmez Dağı Unit, allochthonous Ophiolitic

Unit and Kocagedik Unit and the cover unit which is a sedimentary unit that was deposited after the arrival of the allochthonous units. The stratigraphy of the Carboniferous and the Permian was studied in detail and several stratigraphic sections were drown for the type sections of the formations named by Altıner (1981) in Aygörmez Dağı Unit.

Tekeli et al. (1984) discussed the structural features and stratigraphy of the Aladağ Mountains in Eastern Taurides. They stated that the Carboniferous crops out in Yahyalı Group of the Yahyalı Nappe, Siyah Aladağ Formation of the Siyah Aladağ Nappe and Nohutluk Formation of the Çataloturan Nappe. The presence of Visean and Serpukhovian in the Siyah Aladağ Formation and Nohutluk Formation was verified by the algea and foraminifera (Tekeli et al., 1984).

Metin et al. (1986), Demirkol (1989) and Çelik et al. (2007) investigated the stratigraphy, tectonics and geological evolution of the Eastern Taurides. In the study of Metin et al. (1986), the Carboniferous crops out in the Geyikdağı Unit and represented by clastic rocks at the lower, carbonate rocks at the upper part of the sequence. Demirkol (1989) and Çelik et al. (2007) observed the Carboniferous in the Karahamzakuşağı Formation and Köşkdere Formation of Siyah Aladağ Nappe, respectively.

Göncüoğlu et al. (2004) studied on the Paleozoic stratigraphy and conodont fauna of the Geyikdağı Unit in the Eastern Taurides and discussed the geological evolution along the Tauride Belt in order to contribute to the understanding of the Early Paleozoic paleogeography of the peri-Gondwana.

Various workers have carried out important studies on the foraminiferal paleontology and biostratigraphy of the Carboniferous in the Tauride Belt. Işık (1981) studied the Lower Carboniferus biostratigraphy in Nohutluk Tepe (Aladağ Region, Eastern Taurides). He identified twelve foraminiferal biozones from the Lower Tournaisian to the Upper Bashkirian. Altıner (1981) studied the micropaleontology and stratigraphy of Pınarbaşı (Eastern Taurides) in his Ph.D. thesis. He carried out detailed taxonomical

studies on the Late Paleozoic foraminifera. In this study Upper Visean (V3c) is defined by the first appearance of *Euxinita efremovi, Biseriella parva* and dissapperence of *Pojarkovella nibelis*. The boundary between Visean and Serpukhovian is marked by the first appearance of *Eostaffella pseudostruvei*.

In addition, Okuyucu (1999) defined a new species across the Carboniferous – Permian boundary in the Aladağ Unit of the Central Taurides. Moreover, Altıner and Özgül (2001) worked on the Carboniferous and Permian foraminiferal associations in Hadim (Central Taurides) and they identified several biozones. Upper Visean strata and Visean-Serpukhovian boundary were recognized by using these biozones. In the study of Altıner and Özgül (2001) both western Europe and Russian biozonations were used. Upper Visean Aleksinsky, Mikhailovsky and Venevsky horizons were defined by *Eostaffella proikensis*, *Eostaffella ikensis-Lysella Tujmasensis* and *Endostaffella parva-Biseriella parva* zones. The lowermost biozones of the Serpukhovian is identified as *Pseudoendothyra* ex gr. *illustria-Eostaffella pseudostruvei* zone by Altıner and Özgül (2001).

Atakul (2006), in her Ms. thesis, worked on the taxonomy of Serpukhovian and Bashkirian calcareous foraminifera to delineate the mid-Carboniferous boundary in Central Taurides. The result of this work was also published in 2011. Atakul et al. (2011) discuss the foraminiferal biostratigraphy across the mid Carboniferous boundary in Hadim region. They defined one biozone for the Upper Serpukhovian and three biozones for the Lower Bashkirian. Okuyucu and Vachard (2006) identified Late Visean foraminifera and algea in Çataloturan Nappe (Aladağ Mountains, Eastern Taurides). They proposed local biozonations for Asbian and Brigantian strata namely *Howchinia bradyana longa- Lituotubella magna- Koktjubina* (?) sp. zone for Asbian strata and *Bradyina rotula - Euxinita tauridina* and *Janischewskina typica - Biseriella aff. parva* zones for the Brigantian strata. Dinç (2009) focused on the taxonomy of the Lower Carboniferous (Upper Tournaisian) foraminifera in the Central Taurides.

Late Visean and Serpukhovian foraminifera are studied worldwide. Cózar (2004), Cózar et al. (2005), Somerville and Cózar (2005) and Vachard et al. (2006) focused on the Asbian-Brigantian boundary. Cózar (2004), Cózar et al. (2005) and Vachard et al. (2006) illustrated several species found in the Upper Visean strata of the southwestern Spain, northeastern Ireland and Central Morocco, respectively. Somerville and Cózar (2005) described and illustrated the assemblages that typify the Late Asbian and Early Brigantian strata of the southeast Ireland.

Late Visean foraminifera have been studied by Conil and Pirlet (1963), Vachard et al. (1991), Brenckle (2004) and Gallagher et al (2006). Conil and Lys (1964,1977), Conil and Pirlet (1970), Conil et al. (1979), Conil (1980) defined the foraminiferal associations of the Dinantien successions. Rich (1982) worked on the Middle Visean to Early Namurian foraminifera and he illustrated several specimens found in Georgia. In addition, he divided Middle Visean to Early Namurian strata of Georgia into foraminiferal bizones using Mamet's global scheme. Skompski et al. (1989) studied micropaleontology of the Upper Visean – Serpukhovian rocks of Pologne. Brenckle (1990) and Vdovenko et al. (1990) constructed foraminiferal biozonation of the Lower Carboniferous of North America and Russian Platform respectively and they defined Visean and Serpukhovian rocks with foraminifera. Cózar (2003) described the Lower Carboniferous foraminiferal fauna and biozonation from Spain. Cózar et al. (2008) interpreted Late Visean-Serpukhovian foraminifera and algae from the North Africa. Cózar et al. (2008) defined new foraminifers from the Visean - Serpukhovian boundary interval in Scotland. Somerville (2008) discusses the evolutionary trends and foraminiferal assamblages of the Upper Visean strata in the western Europe and he compares foraminiferal biozonations proposed by several workers across the Visean-Serpukhovian boundary. Marfenkova (1983, 2009) focused on Visean and Serpukhovian Archaediscids and Koktjubinids respectively. In Marfenkova (2009) he defines and illustrates some species of Koktjubinids and use them as "a base for stratigraphic and zonal divisions of stages". Hecker (2009) compared subzones of Dinantian in Belgium, Moscow and Donetz Basin and he proposed major index fossils to define the limits of these subzones. Kulagina et

al. (2009) revealed biozonation of the Upper Visean, Serpukhovian and Bashkirian rocks with foraminifera in Southern Urals. They proposed *Eostaffella ikensis-Endothyranopsis crassa, Eostaffella tenebrosa-Endothyranopsis sphaerica* and *Eolasiodiscus donbassicus - Janischewskina delicata* foraminiferal zones for the Mikhailovsky, Venevsky and Taurrsky horizons, respectively. In addition, they illustrated and identified foraminiferal species found in the biozones mentioned above. Nigmadhaznov et al. (2010) worked on the Visean-Serpukhovian boundary to be able to define the best section for the boundary in Uzbekhistan. They focused on an integrated ammonoid, conodont and foraminiferal biostratigraphy. They defined the Venevsky horizon with *Endothyranpsis crassa subzone* and the base of the Serpukhovian by *Neosrcaediscus regularis – Biseriella parva* zone. Aisenverg et al. (1979) described Serpukhovian faunas in Moscow Syneclise, Donetz Basin and Urals an Asia. They correlated the corresponding successions with those of in western Europe, North Africa, Japan and North America. Sebbar and Lys (1989) interpreted biostratigraphy of Serpukhovian rocks in Algeria and reported the early occurrences of some species. Pazukhin et al. (2010) proposed a complete condense section in the Southern Urals for the global stratotype of the lower boundary of the Serpukhovian stage. In this study they defined Visean and Serpukhovian strata with four faunal groups including foraminifera.

In the Tauride carbonate platform, sequence stratigraphical studies start with the works of Marine Micropaleontology Research Unit in METU. Several Ms. Thesis on the Permian (Pütürgeli, 2002), Permian-Triassic (Ünal, 2002; Esatoğlu, 2011), Jurassic - Cretaceous (Yılmaz, 1997) and Cretaceous (Akçar, 1998; Beyazıtoğlu, 1998; Ulusoy, 1999) sequence stratigraphy and meter scale cyclicity of the central Taurides was published.

Şen (2002) for the first time studied the Carboniferous sequence stratigraphy of the Taurides. He defined meter-scale subtidal cycles in the Middle Carboniferous carbonates of the central Taurides. Peynircioğlu (2005) measure two stratigraphic sections ascross the Tournaisian-Visean boundary in the central Taurides and he

detected thirteen shallowing upward subtidal cycles across one of the cycles. Atakul (2006) defined twenty-three shallowing upward cycles across the mid-Carboniferous boundary in the Hadim region (Central Taurides) and constructed the sequence stratigraphic framework based on the stacking patterns of the cycles. Dinç (2009) interpreted the cyclic pattern of the sedimentation in the Upper Tournaisian limestones in Hadim (Central Taurides). The result of these works was also published by several journals. These publications are Altıner et al. (1999), Yılmaz and Altıner (2001, 2006, 2007), Ünal et al. (2003), Atakul et al. (2011).

Present thesis, which defines twenty-six shallowing upward meter scale cycles, is the first study on the cyclicity and sequence stratigraphy in the Eastern Taurides. In addition, for the first time a sequence stratigraphic approach was applied on the Visean-Serpukhovian boundary beds in the Tauride carbonate platform.

1.4 Regional Geological Setting

Tauride Belt is west to east oriented Paleozoic-Mesozoic platform essentially composed of carbonates (Özgül, 1976; Şengör, 1981; Altıner, 1981). Taurides are a sub-unit of Tauride Anatolide composite terrain characterized by an Infra-Cambrian basement and its non-metamorphic cover composed of mainly platformal sediments (Göncüoğlu, 1997). Taurides geographically composed of three segments namely western, central and Eastern Taurides (Özgül, 1984). The study area is located in the Eastern Taurides.

Tauride Belt is composed of several rock units reflecting different depositional environmental conditions and they are named as ''Units'' by Özgül (1976). The contact between them is tectonic and there are six tectonostratigraphic units in the Taurides. These are Geyik Dağı, Aladağ, Bolkar Dağı, Bozkır, Antalya and Alanya Units. Geyik Dağı Unit is an autochthonous-parautochthonous unit but the other five are allochthonous (Özgül, 1984).

Different from Özgül (1976), Tekeli et al. (1984) divided Eastern Taurides into several napped structures formed by platform type carbonates. These are Upper Paleozoic-Mesozoic Yahyalı Nappe, Upper Paleozoic – Lower-Middle Triassic Siyah Aladağ Nappe, Upper Triassic Minaretepeler Nappe, Upper Paleozoic-Mesozoic Çataloturan Nappe, Mesozoic Beyaz Aladağ Nappe and Middle-Upper Triassic or Jurassic Aladağ ophiolite Nappe.

Tectonic Units cropping out in the Eastern Taurides are Geyik Dağı, Bolkar Dağı, Bozkır and Aladağ units are exposed in the Eastern Taurides (Özgül 1976) (Figure 1.3).

Geyik Dağı Unit is generally composed of platform type sediments and comprises Lower Paleozoic (Cambrian and Ordovician) rocks overlain by transgressive Upper Mesozoic-Lower Tertiary rocks in Central Taurides (Özgül, 1984). However, Geyik Dağı Unit has a continuous succession from the Lower Paleozoic to the Upper Cenozoic in Eastern Taurides. (Özgül, 1976, Metin et al., 1986). Geyik Dağı Unit is named as the Taurus Autochton by Metin et al. (1986) and according to these authors it is oriented

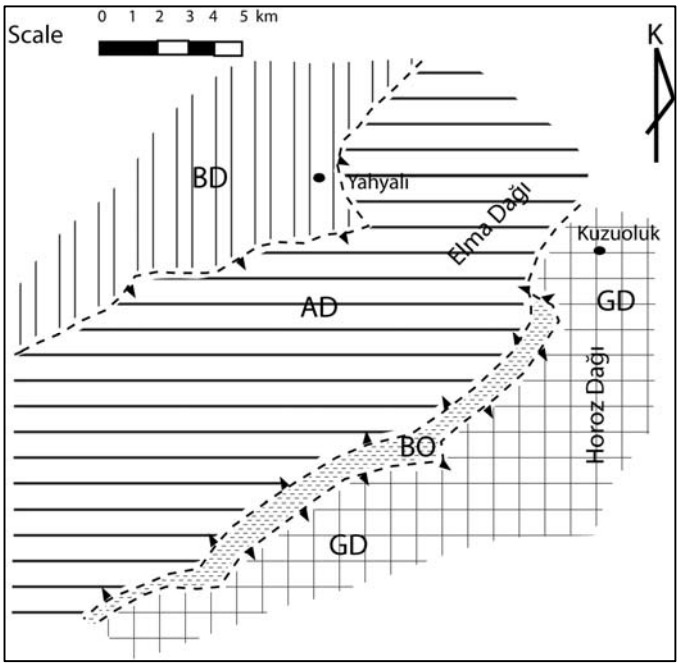

Figure 1. 3: Schematic map of Units in Eastern Taurides (redrawn from Özgül, 1976) (BD: Bolkar Dağı Unit, AD: Aladağ Unit, BO: Bozkır Unit, GD: Geyik Dağı Unit)

NE-SW from Kozan towards Sarız in the region. The Paleozoic of the Geyik Dağı Unit is generally represented by clastic and carbonate rocks. Cambrian sandstones, limestones and siltstones of the Geyik Dağı Unit is overlain conformably by clayey siltstone and shale intercalations of the Ordovician sequence. Silurian conglomerate sandstone and siltstone intercalation overlies conformably the Ordovician rocks. The Silurian succession continues with shale, limestone and sandstone-shale siltstone intercalation towards the top. Devonian is widely exposed in the region and conformably overlies the Silurian. Devonian is represented by sandstone, dolomitic limestone and limestone. Carboniferous overlies conformably Devonian rocks and represented by sandstone, marly limestone and limestone. Lower Carboniferous of the Geyik Dağı Unit is overlain unconformably by quartzite and fossiliferous limestone of the Permian. Triassic is composed of sandstone, siltstone, marl and limestone and it is conformable with the fossiliferous limestones of the Permian. However, the Late Triassic is absent in the region and Jurassic-Cretaceous are observed on the Triassic with an unconformity. Jurassic-Cretaceous is represented by micritic limestone and Upper Cretaceous is represented by rudistic limestone in the region. Paleogene sandstone-marl alternation unconformably overlies the Upper Cretaceous and it is unconformably overlain by the Neogene conglomerate, limestone, sandstone-marl alternation (Metin et al., 1986).

Bolkar Dağı Unit is located to the northern part of the Tauride Belt and composed of Middle-Upper Devonian – Lower Tertiary rock units (Özgül, 1976). This Unit is composed of shelf carbonates and clastics, and shows regional metamorphism (Özgül, 1984). The Bolkar Dağı Unit starts with Devonian schist and marble which are overlain conformably by the Carboniferous schist, quartzite and limestone intercalation. Permian is represented by quartzite intercalated with recrystallized limestone. The overlying Triassic is composed of shale, quartzite, limestone and dolostone, or schist intercalated with marble in the metamorphosed regions. Liassic is composed of conglomerates and is unconformably overlain by the Jurassic-Cretaceous limestone. The Upper Cretaceous is composed of Cenomanian-Turonian rudistic limestone and

Maastrichtian pelagic limestone. The uppermost part of the Bolkar Dağı Unit comprises Maastrichtian and/or Paleocene olistostroms. (Özgül, 1976).

Bozkır Unit comprises a variety of sequences and blocks with different ages (Özgül, 1976). These different sequences are Triassic-Cretaceous pelagic and neritic limestone, radiolorite, spilitic pillow basalts, tuffs and tectonic slices of diabase, ultramafic blocks and serpentinites (Özgül, 1984). Bozkır Unit includes four tectonic slices namely, Boyalı Tepe, Huğlu, Gencek and Kayabaşı Units.

Aladağ Unit, which widely exposed in the study area, consists of Upper Devonian-Upper Cretaceous carbonate and clastic rocks. This unit comprises Gölboğazı, Yarıcak, Çekiç Dağı, Gevne, Çambaşı and Zekeriya formations in Central Taurides (Özgül, 1997). Yarıcak Formation is correlated with Ekşimenlik, Aziziye Gediği and Oruçoğlu Formations of Altıner (1981) whereas the Çekiç Dağı formation is the equivalent of Taslı Güney Sırtı and Sarpkaya Tepe Formations in Pınarbaşı (Eastern Taurides) (Fig. 2.2). Gevne Formation was previously named as the Kokarkuyu Formation (Altıner, 1981) and the Küçüksu Formation (Tekeli et al., 1984) in the Eastern Taurides (Özgül, 1997).

Altıner (1981) defined three structural units in the Pınarbaşı region. They are para-autochthon unit is represented by the Aygörmez Dağı Unit (Upper Devonian-Upper Cretaceous) whereas the allocthonous units are represented by the Ophiolitic Unit and the Kocagedik Unit (Ladinian?-Norian) and cover units were deposited after the settlement of the allocthonous units in the region (Figure 1.4). Upper Devonian – Upper Cretaceous para-autochthon Aygörmez Dağı Unit comprises a Devonien Limestone Unit (Upper Devonian), Ekşimenlik Formation (Fammenian-Tournasian), Aziziye Gediği Formation (Visean), Oruçoğlu Formation (Upper Visean-Gzhalian), Taşlıgüney Sırtı Formation (Asselian-Artinskian), Sarpkaya Tepe Formation (Wordian-Changhsingian), Kokarkuyu Formation (Triassic), Karacat Dere Formation (Lower-Middle Lias), Pusuçukuru Formation (Upper Lias-Berriasian), Fakiekinciliği Formation

(Upper Berriasian-Cenomonian) and the Aygörmez Dağı Formation (Turonian-Maastrichtian) (Fig. 2.2).

The Aygörmez Dağı Unit is basicaly composed of limestone, sandstone, dolomitic limestone and limestone-sandstone alternations. Among the formations of the Aygörmez Dağı Unit, Aziziye Gediği and Oruçoğlu Formations are giving their extensive outcrops in the study area. The Aziziye Gediği Formation is composed of brecciated limestone in the lower part and continues with dark colored, well stratified crinoidal limestone. Oruçoğlu Formation consists of a limestone and quartz sandstone alternation in the lower and upper parts and a limestone unit in the middle part. Ophiolitic Unit (Paleozoic? and Triassic?) in the allochthonous Unit is formed by structurally low serpentinites, dunites, pyroxinites and gabbros, and structurally high radiolorite and limestone. Second Unit in the allochthonous Unit is the Kocagedik Unit and composed of limestone. Cover rocks comprise two main intervals. Lower cover is represented by Maastrichtian Kızılçukur Formation and unconformably overlying Eocene conglomerate, marl, sandstone and limestone. Upper cover is made up of Upper Miocene conglomerate and Plio-Quaternary tufs. Metamorphic Unit is composed of marble and quartzite. This unit is covered by the Lutetian conglomerates. (Altıner, 1981).

Within the regional geologic frame, the study area is located in the Aygörmez Dağı Unit (Altıner, 1981) which is the easternmost extension of the Aladağ Unit of Özgül (1976) in the Eastern Taurides. The measured section cross Aziziye Gediği and Oruçoğlu Formations.

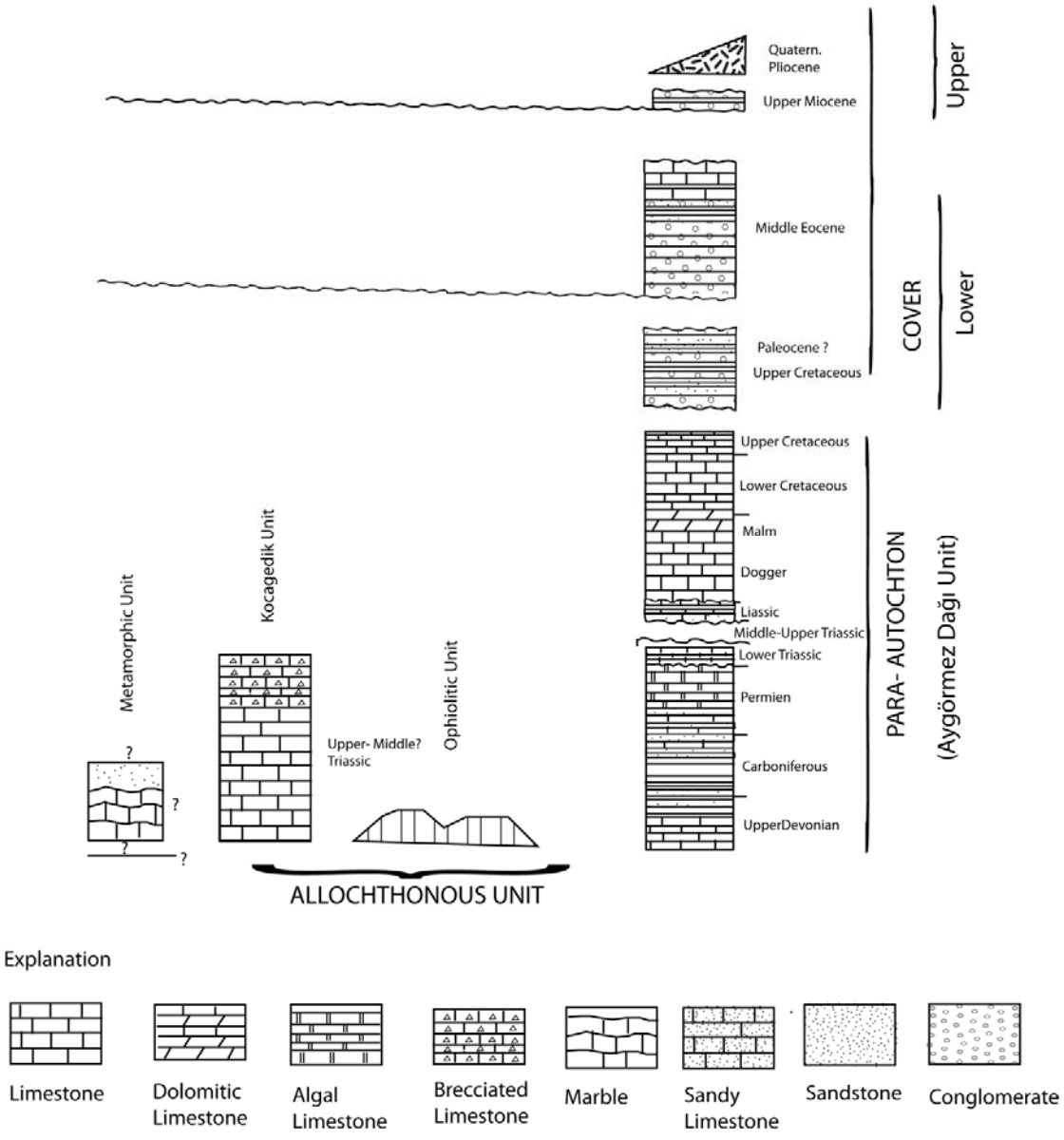

Figure 1. 4: Tectonic and stratigraphic units in the study area defined by Altıner (1981) (Redrawn from Altıner, 1981).

CHAPTER 2

LITHOSTRATIGRAPY AND BIOSTRATIGRAPHY

2.1 Lithostratigraphy

Studied section is composed of Upper Visean - Lower Serpukhovian deposits of Aladağ Unit which comprises Upper Devonian-Upper Cretaceous carbonate and clastic rocks (Özgül, 1977). Upper Devonian – Upper Cretaceous rocks in the Pınarbaşı region (Eastern Taurides) named as the Aygörmez Dağı Unit (Altıner, 1981). NE-SW oriented Aygörmez Dağı Unit is situated northern and southwestern part of the geologic map (Figure 2.1). The Triassic Kocagedik Unit is composed of limestone and exposed at the southern part of the Aygörmez Dağı Unit. The contact between the Aygörmez Dağı Unit and the Kocagedik Formation is tectonic (Figure 2.1). The Ophiolitic Unit, which exposes at the southeastern part of the study area, is composed of the Cretaceous Volcano-Sedimentary Unit and the Jurassic-Cretaceous Ultrabasic Unit (Figure 2.1). The contacts between the Kocagedik Formation and Volcano-Sedimentary Unit and Ultrabasic Unit and Volcano-Sedimentary Unit are tectonic. At the northwestern part of the study area the Lutetian conglomerates exposed and are tectonically bounded by the Upper Devonian Limestone Formation of the Aygörmez Dağı Unit (Figure 2.1).

Aygörmez Dağı Unit starts at its base with the Devonian Limestone Unit which is composed of an alternation of sandstone and limestone and shales at at bottom (Figure 2.2). Devonian Limestone Unit is overlain by the Upper Devonian – Lower Carboniferous Ekşimenlik Formation (Figure 2.2). This formation is made up of shale

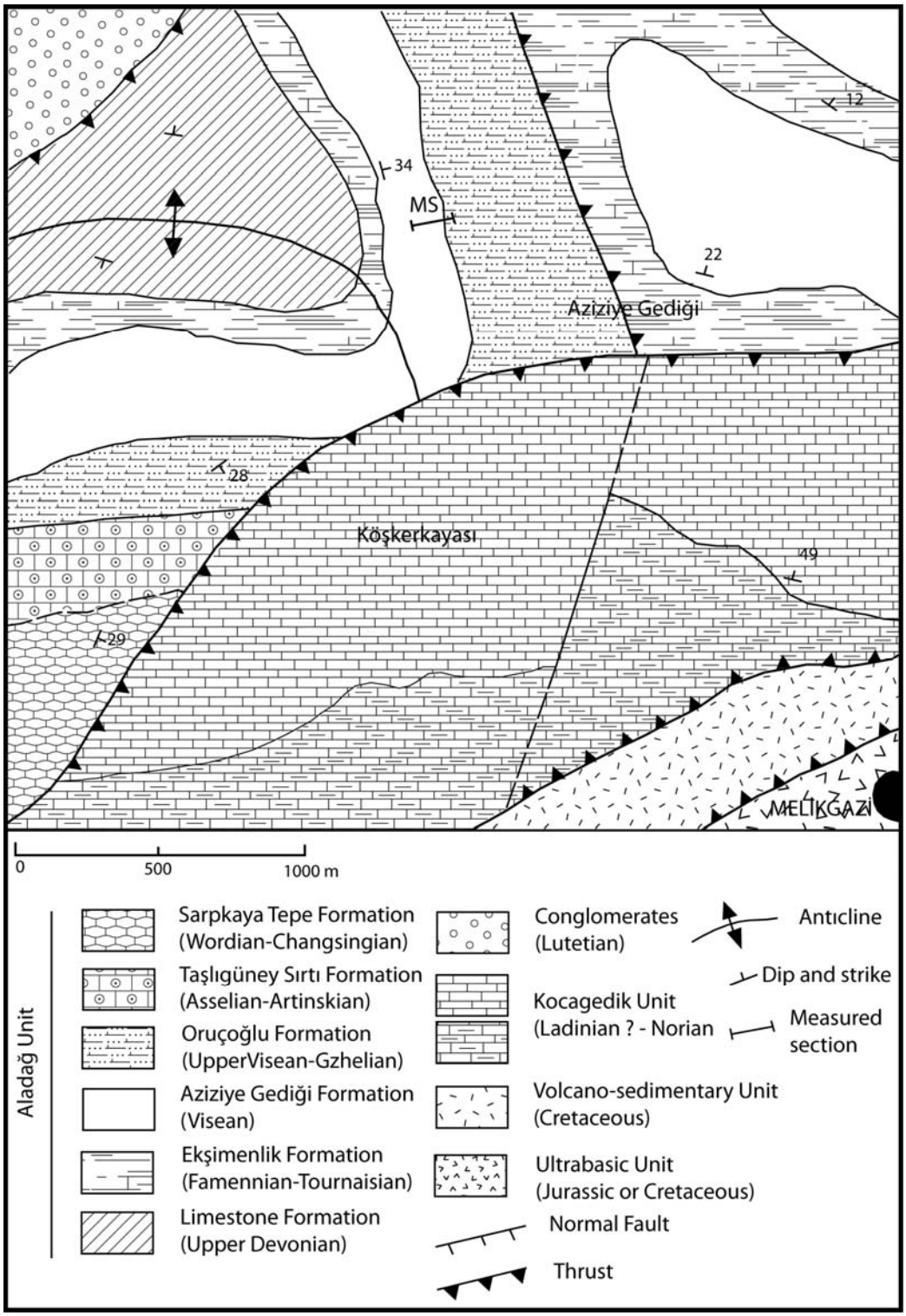

Figure 2. 1: Geological map of the study area (Redrawn and modified from Özkan-Altıner et al., 2007)

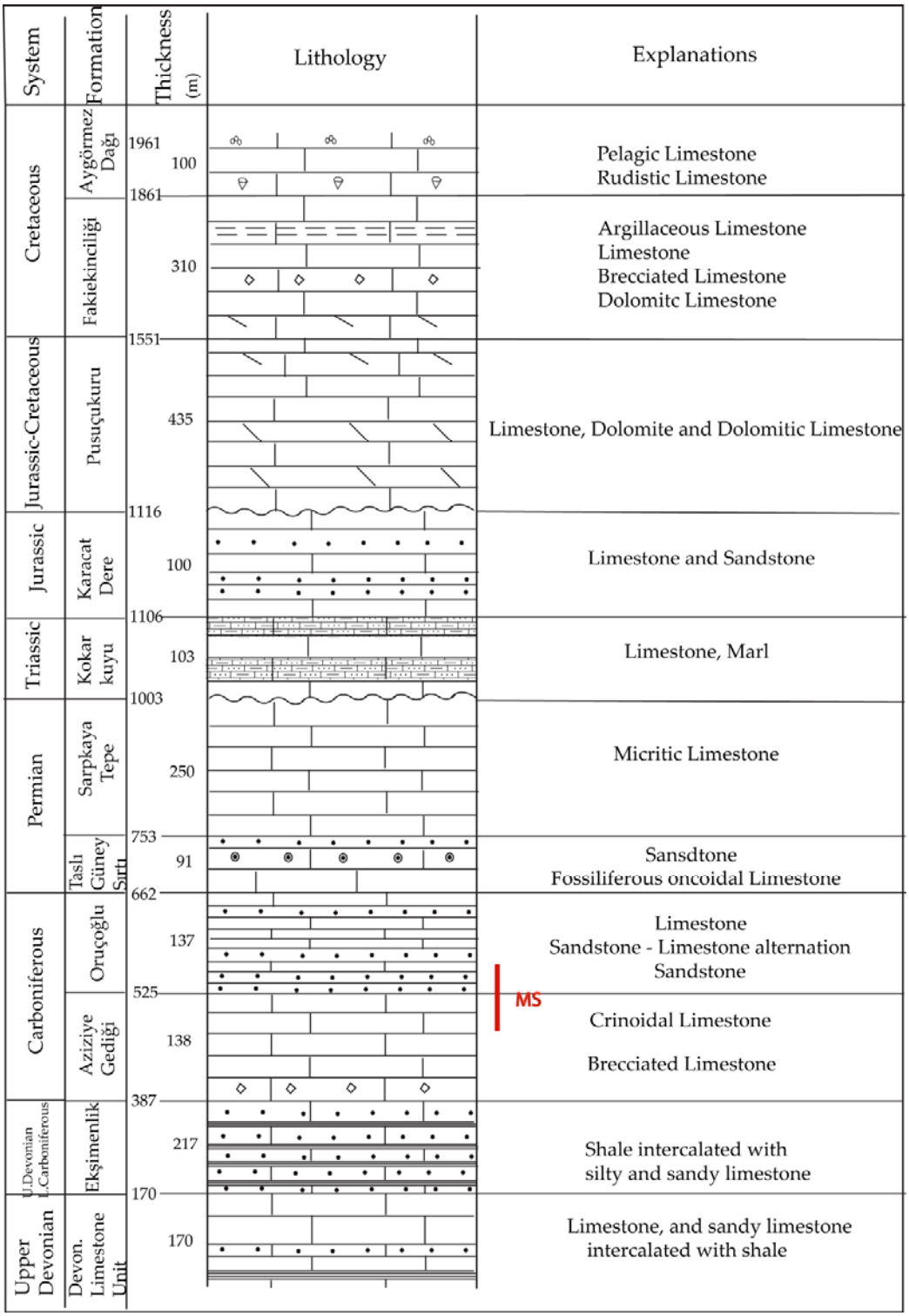

Figure 2. 2: Generalized columnar section of the Aygörmez Dağı (Aladağ Unit in Eastern Taurides) Unit in the Pınarbaşı region (MS indicates the stratigraphic position of the measured section) (Redrawn and modified from Altıner, 1981).

intercalated with siltstone, sandstone and limestone. The Lower Carboniferous Aziziye Gediği Formation conformably overlies the Ekşimenlik Formation and is composed of

brecciated limestone at its base and continues upward with dark colored, well stratified crinoidal limestone (Figure 2.2). From older to younger, the lithologic units of Oruçoğlu Formation which is observed above the Aziziye Gediği Formation are sandstone-limestone alternation, fossiliferous limestone, quartz sandstone and intercalation of limestone and sandstone (Figure 2.2). The overlying Taşlıgüney Sırtı Formation of Permian age is made up of oncoidal and fossiliferous limestones and sandstone at the upper levels. The Permian Sarpkaya Tepe Formation which is composed of greyish to blackish algal and foraminiferal micritic limestone conformably overlies the Taşlıgüney Sırtı Formation (Figure 2.1). Following an unconformity surface, the Triassic Kokarkuyu Formation overlies the Permian Sarpkaya Tepe Formation and is composed of greyish limestone and marl (Figure 2.1). Kokarkuyu Formation is unconformably overlain by the Jurassic Karacat Dere Formation consisting of dark colored limestone intercalated with sandstone (Figure 2.2). Jurassic-Cretaceous Pusuçukuru Formation overlies the Karacat Dere Formation with a possible unconformity surface and this formation is made up of limestone, dolomite and dolomitic limestone (Figure 2.2). Cretaceous Fakiekinciliği Formation starts with dolomitic limestone on top of the Pusuçukuru Formation and continues with dark colored limestone, brecciated limestone and argillaceous limestone (Figure 2.2). The last formation of the Aygörmez Dağı Unit is Upper Cretaceous Aygörmez Dağı Formation. The lithologic units of the formation from older to younger are black colored limestone, rudistic limestone and pelagic limestone (Figure 2.2).

Within the stratigraphic frame of the Pınarbaşı region, the studied stratigraphic section was measured in the uppermost part of the Aziziye Gediği Formation and in the lower part of the Oruçoğlu Formation. The section spans from the Upper Visean to the Lower Serpukhovian strata in the Carboniferous.

2.1.1 Aziziye Gediği Formation

The type section of the Aziziye Gediği Formation is nearly 1.5 km north of the Aziziye Gediği and where the unit is composed of 138 m thick dark fossiliferous limestone and brecciated or intraclastic limestone of Visean age. It overlies conformably the Ekşimenlik Formation of Late Devonian to Tournaisian age and is overlain by Oruçoğlu Formation of latest Visean to Gzhelian age (Altıner, 1981).

Aziziye Gediği Formation is made up of two informal members, namely brecciated limestone (member 1) at the bottom and the crinoidal limestone (member 2) at the top (Figure 2.2). Member 1 starts with well stratified dolomitic limestone and is followed by greyish to blackish colored poorly fossiliferous brecciated limestone. Member 2 is composed of fossiliferous, dark colored limestone alternating with intraclastic limestone in the upper part of the formation. At the contact between the Aziziye Gediği Formation and the Oruçoğlu Formation there is a marked facies change and the first appearance quartz sanstone markes the base of the Oruçoğlu Formation (Altıner, 1981).

2.1.2 Oruçoğlu Formation

Oruçoğlu Formation represents the Upper Carboniferous (Pennsylvanian) and Upper Lower Carboniferous (uppermost Visean and Serpukhovian) part of the Aygörmez Dağı Unit. Type section of Oruçoğlu Formation is 1.5 km northeast of the Oruçoğlu village and and it measures 137 m in thickness. It is composed of three informal members (Figure 2.2). Member 1 starts with reddish to whitish sandstone and is followed upwards by crinoidal, oolitic and intraclastic limestone intercalated with sandstone beds. Towards the top of this member limestone alternates with sandy limestone and sandstone. Corals are abundant in the limestone and sandy limestone levels and fusulinids are abundant in sandy oolitic limestone levels. Member 2 is composed of well-bedded, yellow colored limestone. This member is rich in fusulinids however corals are absent. Member 3 is made up of the alternation of yellow colored

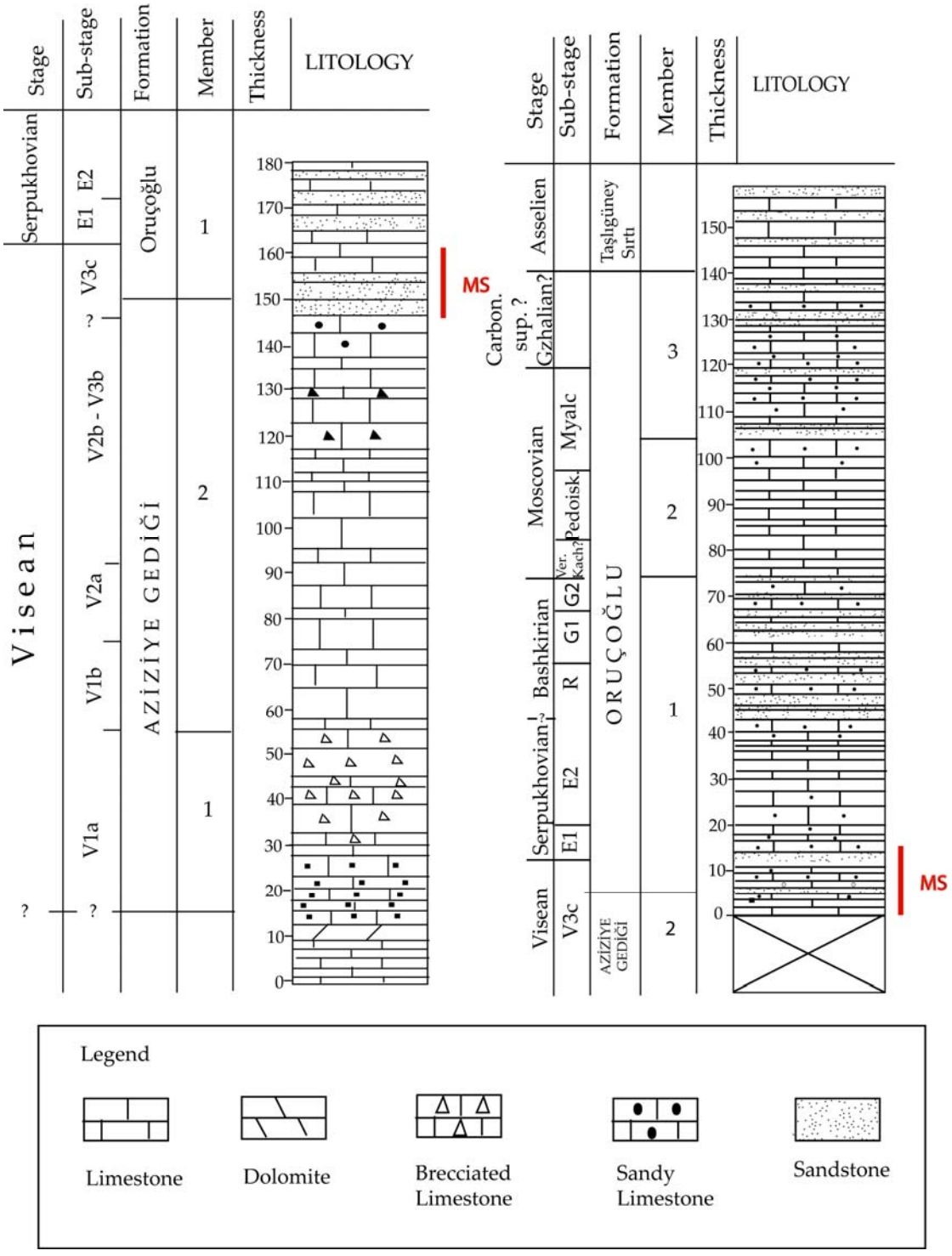

Figure 2. 3: Columnar sections of Aziziye Gediği (500 m N of Aziziye Gediği) and type section of Oruçoğlu Formations (1.5 km NE of the Oruçoğlu Vilage) (MS indicates the location of the measured section) (Redrawn from Altıner, 1981).

limestone of and reddish quartz arenitic sandstone and in the upper parts intercalated with sandy or intraclastic limestone (Altıner, 1981).

2.1.3 Measured Section

The measured section represents Upper Visean and Lower Serpukhovian deposits of Aziziye Gediği and Oruçoğlu Formations (Figure 2.3). Aziziye Gediği Formation in the studied section lies between the sample SC-1 and sample SC-72. The measured section (72 samples) begins with well bedded, greyish, bioclastic limestone rich particularly in foraminifera and crinoids (Figure 2.3). Approximately 11 m of the basal part of our measured section is composed of the alternation of dark grey bioclastic packstone and grainstone. In the first 5.9 m of the measured section (between samples SC-1 and SC-15), minor differences can be observed in the color of the beds. Dark color of the limestones changes from sample to sample. The color of packstones is darker than the color of grainstones. Above this grainstone packstone alternation lighter gray colored and macrofossil rich grainstone is seen in the samples SC-16, 17 and 18. Crystal size also increases in the samples SC-16, 17 and 18. This portion of the measured section is overlain by nearly 3 m thick grainstone packstone alternation which is represented by the samples from SC-19 to SC-27. In this grainstone packstone alternation the crystal sizes of grainstones are larger than those of packstones and they are also lighter colored. From the samples SC-28 to SC-29 nearly 1 m, light grey wackestone is observed. Above this wackestone, a 79 cm thick greyish to beige grainstone was deposited and represented by the sample SC-30. Between the samples SC-31 and SC-37, through 5.5 m, well bedded, grey colored grainstone is observed. After a 70 cm thick covered zone, 70 cm thick dark grey colored fossiliferous wackestone was deposited between the samples SC-38 and SC-39. Above wackestone, between the samples SC-40 and SC-41, through 1 m, dark grey mudstone was deposited. Between the samples SC-42 and SC-56 a 5.23 m thick, well bedded, dark grey colored grainstone is observed. Although grainstones are different from each other in microscopic scale, no differences

were identified in the field observations. Only the crystal sizes of the sample SC-49 is greater than those of other samples in this succession. Between the samples SC- 57 and SC-73, through 10 m, packstone-grainstone alternation is observed. The succession starts with a 1.3 m thick greyish colored packstone (between the samples SC-57 and SC-60) and continues with 3.4 m thick light grey colored grainstone (between the samples SC-61 and SC-66). The crystal sizes of the sample SC-66 is considerably high. After 30 cm thick covered area, 80 cm thick dark grey colored packstone, which is represented by the sample SC-67 was deposited and it is overlain by light grey colored, 3.66 m thick grainstone (between the samples SC-68 and SC-72). Sample SC- 72 belongs to the top of the Aziziye Gediği Formation. Oruçoğlu Formation, which covers sample SC-73 to sample SC-92 in the measured section, conformably overlies the Aziziye Gediği Formation. Oruçoğlu Formation starts with a poorly bedded, grey colored, 2 m thick limestone (between sample SC-73 and SC-74) and continues with 3 m thick, dark colored, fossiliferous wackestone (SC-75). Above the wackestone siliciclastic input rapidly increases in the system. Between the samples SC-75 and SC-77, through 9 m, yellow colored quartz arenitic sandstone was deposited. Between the samples SC- 78 and SC-79, through 2.5 m, poorly bedded dark grey colored grainstone was deposited and it is followed by 2 m thick light grey colored fenestral mudstone (SC-80). Above limestone, brownish to yellowish colored, 1 m thick shale is observed (SC-81). At the uppermost part of the section packstone-grainstone alternation was observed. Light grey colored, 9,27 m thick limestone (packstone grainstone alternation) was deposited between the samples SC-82 and SC-92). This limestone is rich in macrofossil fragments and its crystal size is obviously high. The thickness of the Aziziye Gediği Formation is 30,79 and the Oruçoğlu Formation is 28,77 m in the studied section.

Faunal content of the measured section will be discuss indetail in the Biostraigraphy part of this chapter. Detailed microfacies analysis and interpretation of depositional environments are given the the Microfacies Analysis Chapter (Chapter 3).

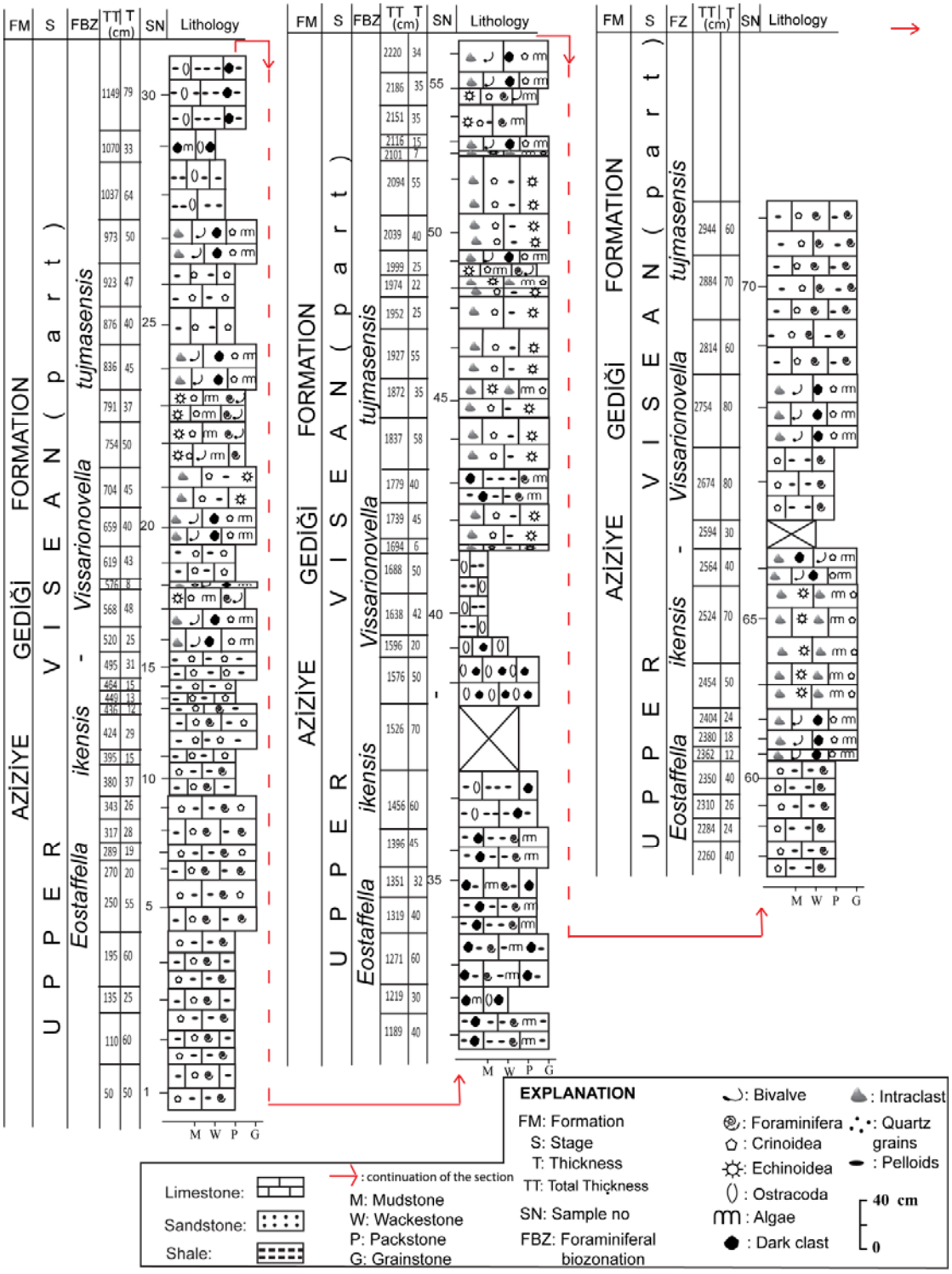

Figure 2. 4: Lithostratigraphy of measured section with biozones.

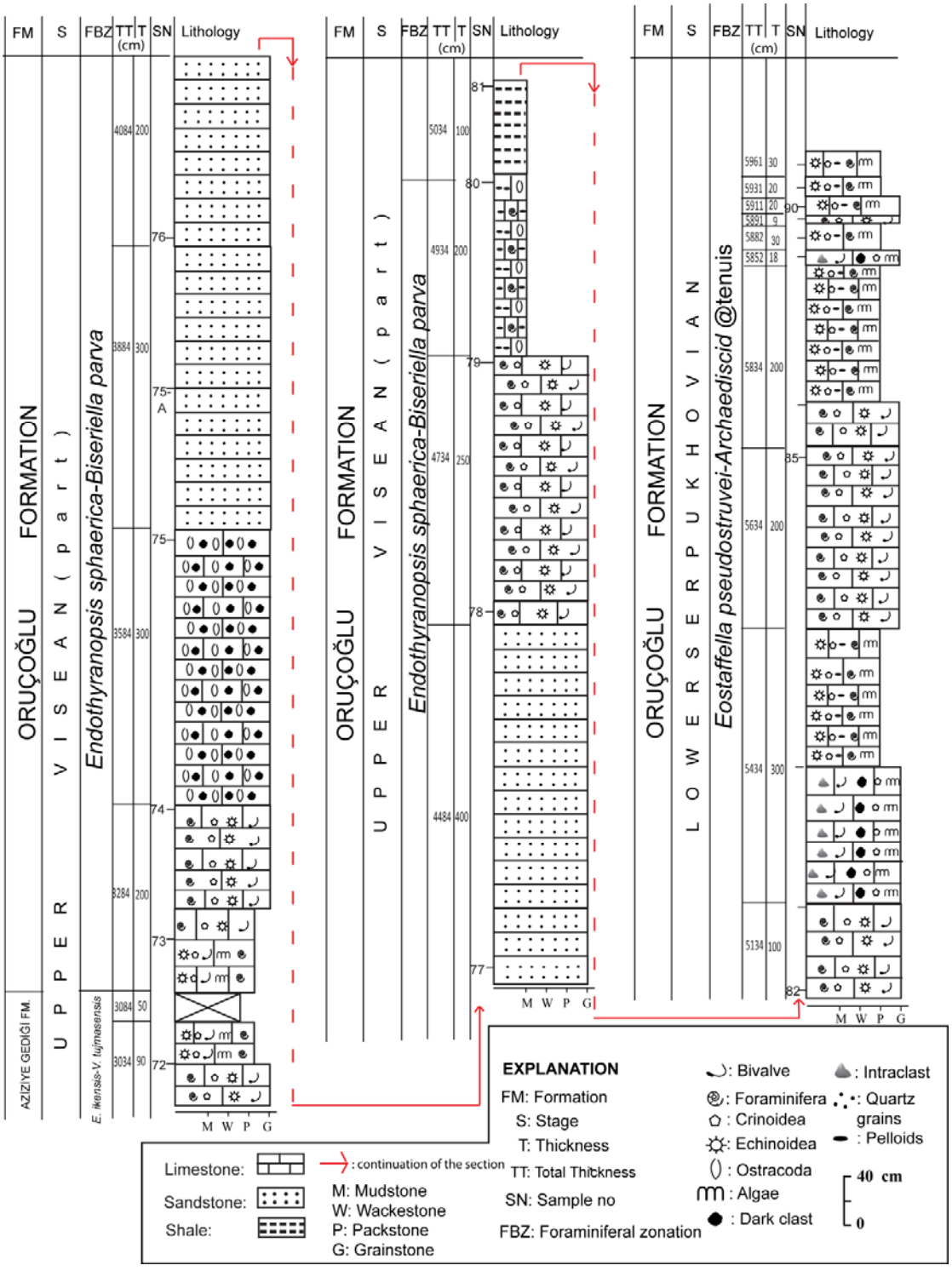

Figure 2. 4: (Continued)

2.2 Biostratigraphy

Studied section is composed of Upper Visean - Lower Serpukhovian bioclastic grainstones and packstones of Aziziye Gediği Formation and quartz arenitic sandstones, bioclastic packstones and grainstones of Oruçoğlu Formation.

Upper Visean and Serpukhovian stages correspond to different chronostratigraphic subdivisions in different regions such as South China, North America, Central and Western Europe and Russian Platform. Table 2.1 summarizes the regional correlation of Upper Visean and Serpukhovian stages. This summary table does not include substages of Britain because correlation of these stages with Russian Horizons is inconsistent in the literature (Table 2.3).

Many workers have proposed their own foraminiferal zonation for Upper Visean and Serpukhovian stages and all of these subzonations are widely used in the literature. Foraminiferal zonations proposed by various authors are shown in table 2.2.

Table 2. 1: Regional correlation of Upper Visean – Lower Serpukhovian stages (*: from A Geological Time Scale, 2004, **: from The Concise Geologic Time Scale, 2008)

<table>
<tr><th>Global Stratigraphic scales (2004* and 2008**)</th><th>South China Stages (2004* and 2008**)</th><th>North America (Stages) (2004* and 2008**)</th><th>(Western Europe)Belgian Stages, 2004*</th><th>Russian Platform, 2004*</th><th>(Western Europe)Belgian Stages, 2008**</th><th>Russian Platform, 2008**</th></tr>
<tr><td rowspan="2">Lower Serpukhovian</td><td rowspan="2">Dewunian-Shangsian</td><td rowspan="3">Chesterian</td><td rowspan="2">Pendleian</td><td rowspan="2">Taurissian</td><td>Pendelian(Part)</td><td>Tarusian</td></tr>
<tr><td rowspan="4">Warnantian</td><td rowspan="2">Venevian</td></tr>
<tr><td rowspan="3">Upper Visean</td><td rowspan="3">Jiusian</td><td rowspan="3">Warnantian</td><td>Venevian</td></tr>
<tr><td>Mikhailovian</td><td>Mikhailovian</td></tr>
<tr><td rowspan="2">Meramecian</td><td>Aleksian</td><td>Aleksian</td></tr>
<tr><td>Livian</td><td>Tullian</td><td>Livian</td><td>Livian</td></tr>
</table>

Table 2. 2: Upper Visean-Lower Serpukhovian chronostratigraphy and different foraminiferal zonations of Britain, Belgium and France and Western Tethys (modified from Cózar, 2004 and Somerville, 2008).

<table>
<tr><th rowspan="2">Global Stratigraphic scales</th><th colspan="2">Chronostratigraphy of</th><th rowspan="2">Poty et al., 2006</th><th rowspan="2">Conil et al., 1991 (Britain)</th><th rowspan="2">Conil et al, 1977; Vachard, 1977 (Belgium and France)</th><th rowspan="2">Mamet, 1974 (Western Tethys)</th></tr>
<tr><th>Britain and Ireland</th><th>Franco-Belgian Bassins</th></tr>
<tr><td>Serpukhovian</td><td>Pendelian</td><td>Pendelian</td><td rowspan="2">MFZ 15</td><td>Cf7 (part)</td><td>Nm1a-Nm1b</td><td>17-18</td></tr>
<tr><td rowspan="4">Upper Visean</td><td>Brigantian</td><td rowspan="3">Warnantian</td><td>Cf6 δ</td><td rowspan="2">V3c</td><td>16s</td></tr>
<tr><td rowspan="2">Asbian</td><td>MFZ 14</td><td>Cf6γ</td><td>V3bγ</td><td rowspan="2">16i</td></tr>
<tr><td>MFZ 13</td><td>Cf6α-β</td><td>V3bα-β</td><td rowspan="2">15</td></tr>
<tr><td>Holkerian</td><td>Livian</td><td>MFZ 12</td><td>Cf5</td><td>V2b-V3a</td><td>14-13</td></tr>
</table>

In the table 2.2, Russian horizons were not purposely used because; correlation of Russian zonations with other zonations differs in various studies. The correlation of Russian horizons and Western Europe Horizons in the literature is given in Table 2.3. Although Menning et al. (2006) suggest that Brigantian substage corresponds to Russian Venevian and a part of Mikhailovian Horizons and Asbian substage corresponds to a part of Mikhailovian and Aleksian Horizons, in Geological Time Scale (2004) Russian horizons of Venevian and Mikhailovian correspond to Brigantian and Asbian respectively. Moreover, according to this chart, Holkerian is correlated with the Aleksian and Tullian Horizons of central Russia. However, in the book "the Concise Geological Time Scale" (2008) the age of the boundary between Visean-Serpukhovian changes and a part of Russian Venevian Horizon and a part of Western Europe Brigantian sub-stage corresponds to the upper part of Visean. In the study of Altıner and Özgül (2001) carried out in Turkey, Russian Venevsky Horizon is correlated with the V3c (Brigantian) of Conil, (1977) and Mikhailovsky and Aleksinsky Horizons are correlated with V3b (Asbian) of Conil (1977). In another study in Turkey, Okuyucu and Vachard (2006) have accepted that Venevsky, Mikhailovsky and part of Aleksinsky horizons correspond to the Brigantian substage whereas, lower part of Aleksinsky horizon is correlated with the Asbian substage. Pillet at al. (2010) also used the

Table 2. 3: Correlation of Russian Horizons and Western Europe Horizons in different studies.

Global Stratigraphic scales	A geological time scale , 2004		Devonian- Carboniferous-Pemian Chart 2003 (DCP); Menning et al., 2006		The Concise Geologic Time Scale, 2008		Altıner and Özgül, 2001 (Turkey)			Cozar, 2004 (Morocco)		Vachard and Aretz,2004			Okuyucu and Vachard, 2006 (Turkey)				Hecker, 2009	
	Russian Platform	Western Europe	Central Russia	Central and Western Europe	Russia	Western Europe	Russian Horizons	Franco - Belgian Bassin, proposed by Conil, 1977	Western Europe	Moskow Basin Horizons	Stages, substages in Britain	Moskow Bassin	England Ireland Reginal Stage	Belgium composite subdivisio n	Russian Horizons	British Substages	Former subdivisions of Belgium		Moskow Basin	Belgium (Conil et al., 1990)
Serpukhovian (Part)	Taurissian	Pendleian	Taurissian	Pendelian	Tarusian	Pendelian (Part)	Taurssky	E1	Pendelian	not shown	not shown	not shown	not shown	not shown	not shown	not shown	not shown		Tarusa	Cf.7
					Venevian	Brigantian														
Upper Visean	Venevian	Brigantian	Venevian	Brigantian			Venevsky	V3c	Brigantian	Venevsky Mikhailovsky Aleksinsky	Brigantian	Venevsky Mikhailovsky Aleksinsky	Brigantian	V3c sup.	Venevsky	Brigantian	V3c	V3c sup.	Venevsky Mikhailovsky Aleksinsky	Cf6 δ
	Mikhailovian	Asbian	Mikhailovian		Mikhailovian		Miklailovsky	V3b	Asbian						Mikhailovsky					
	Aleksian	Holkerian	Aleksian	Asbian	Aleksian	Asbian	Aleksinsky							V3c inf.	Aleksinsky	Asbian	V3bγ	V3c inf.		
	Tullian		Tullian	Holkerian	Tulian	Holkerian	Tulsky	V2b-V3a	Holkerian	Tula	Asbian	Tulsky (part)	Asbian	V3b a-β-γ					Tula	Cf6α-β-γ

biozonation and correlation of Okuyucu and Vachard (2006) in their study in NW Turkey. Other workers namely, Cózar (2004), Vachard and Aretz (2004) and Hecker (2009) correlate Venevsky, Mikhailovsky and Aleksinsky Russian Horizons with the Brigantian Substage. In addition to all these data, Vladimir et al. (2010) proposed a calibration of the Global Carboniferous Time Scale with U-Pb zircon age and the summary of their article is used in the Newsletters on Carboniferous Stratigraphy (2010). In the calibration chart, they consider that Rusian Venevian Horizon is the equivalent of Brigantian and Russian Mikhailovian and Aleksinian Horizons are the equivalents of Asbian.

In Russian Platform Upper Visean substage is divided into three horizons namely; Tulsky, Aleksinsky and Mikhailovsky. Vdovenko et al. (1990) have proposed *Endothyranopsis compressa- Archaediscus krestovnikovi, Eostaffella proikensis – Archaediscus gigas, Eostaffella ikensis* and *Eostaffella tenebrosa- Endothyranopsis sphaerica* foraminiferal zones respectively (Table 2.4). Lower Serpukhovian corresponds to the Tarussky substage in Russian Platform and Vdovenko et al. (1990) calibrated the Tarussky substage with the *Pseudoendothyra globosa- Neoarchaediscus parvus* foraminiferal zone. This interval also corresponds to the first occurance of *Eostaffella pseudostruvei*, *Biseriella parva* and last appearance of *Endothyranopsis crassa* in the Russian Platform.

Altıner (1981) studied the foraminiferal paleontology and stratigraphy of the Eastern Taurides (Pınarbaşı region) and proposed the positions of V2b-V3b, V3c (Upper Visean) and E1 (Lower Serpuhhovian) horizons. V2b-V3c zone is determined with the first appearance of *Koskinotextularia* and *Urbanella nibelis* (*Urbanella nibelis* is equal to *pojarkovella nibelis* in the present study). The upper boundary of this zone is determined with the dissappearance of the *Pojarkovella nibelis.* The lower limit of V3c zone is defined by the first appearance of the *Euxinita efremovi* and *Globivalvulina parva (Globivalvulina parva* is the equivalent of *Biseriella parva* in the present study). These two forms appear immediately after the dissappearence of *Pojarkovella nibelis.* The upper limit is characterized by the first appearance of *Eostaffella pseudostruvei*. This limit is the

Visean-Serpukhovian boundary and the upper limit of the Serpukhovian is defined by the first appearance of *Eostaffella pseudostruvei*.

In the study of Altıner and Özgül (2001) carried out in Central Taurides, southern Turkey; three foraminiferal zones corresponding Aleksinsky, Mikhailovsky and Venevsky horizons were proposed (Table 2.4). These foraminiferal zones are *Eostaffella proikensis* (Vt4b), *Eostaffella ikensis - Lysella tujmasensis* (Vt4c) (*Lysella tujmasensis* is equivalent of *Vissarionovella tujmasensis* in the present study) and *Endostaffella parva – Biseriella parva* (Vt5) foraminiferal zones respectively. In addition, in this study, Vt4b and Vt4c zones are calibrated with V3b of Conil t al. (1976, 1979). The Lower Serpukhovian substages Tarussky and Steshevsky corresponding to E1 zone of Western Europe (Vdovenko at al., 1990) is considered to be the equivalant of *Pseudoendothyra ex gr. illustria – Eostaffella pseudostruvei* Zone (ST1).

The study of Okuyucu and Vachard (2006) was also carried out in southern Turkey, Eastern Taurides. They constructed their biozanation by frequently used forms in England and Ireland. Their Late Visean biozones are (1) *Howchinia bradyana longa-Lituotubella magna- Koktjubina* (?) sp. (Lower part of Aleksinsky and Cfγ1), (2) *Bradyina rotula - Euxinita tauridina* (Middle part of Aleksinsky and Cf6γ2), (3) *Janischewskina typica - Biseriella aff. parva* (Mikhailovsky and Upper Cf6(δ). In this zonation, the upper part of Aleksinsky horizon corresponding to Lower part of Cf6δ could not be characterized due to the scarcity of characteristic fossils.

A part of Upper Visean in Urals is represented by Aleksinian, Mikhailovian and Venevian Horizons. The proposed foraminiferal zones by Kulagina et al. (2009) are *Eostaffella proikensis, Eostaffella ikensis – Endothyranopsis crassa and Eostaffella tenebrosa – Endothyranopsis sphaerica* zones respectively. The Taurisian and part of Steshevian horizons of Urals were correlated with *Eostaffellina paraprotvae – Janischewskina delicata* foraminiferal zone.

Table 2. 4: Foraminiferal zones in different studies

Stage	In this study, Turkey, 2012	Altıner and Özgül, Turkey, 2001	Okuyucu and Vachard, Turkey,2006	DCP (2003), Menning et al., 2006	Vdovenko et al., 1990	Kulagina et al, Sothern Urals, 2009
Serpukhovian	*Eostaffella pseudostruvei* - Archaediscid @ *tenuis* stage	*Pseudoendothyra ex gr. Illustria* - *Eostaffella pseudostruvei* (ST1)			*Pseudoendothyra globosa*- *Neoarchaediscus parvus*	*Eolasiodiscus donbassicus* - *Janischewskina delicata*
Upper Visean	*Endothyranopsis* cf. *sphaerica* - *Bisearіella parva*	*Endostaffella parva* - *Biseriella parva* (VT5)	*Janischewskina typica*	*Endothyranopsis sphaerica*- *Eostaffella ikensis tenebrosa*	*Eostaffella tenebrosa*- *Endothyranopsis sphaerica*	*Eostaffella tenebrosa* - *Endothyranopsis sphaerica*
	Eostaffella ikensis - *Vissarionovella tujmasensis*	*Eostaffella ikensis* - *Lysella tujmasensis* (VT4c)	*Biseriella aff.parva*	*Eostaffella ikensis*	*Eostaffella ikensis*	*Eostaffella ikensis* - *Endothyranopsis crassa*
		Eostaffella proikensis (VT4b)	no characteristic fossil / *Bradyina rotula*- *Euxinita tauridina*	*Endothyranopsis crassa-Parastaffella luminosa*	*Eostaffella proikensis*- *Archaediscus gigas*	*Eostaffella proikensis*

Devonian- Carboniferous - Permian (DCP) Chart is constructed by Menning et al. (2006) in 2003 for the stratigraphic base of Project 1054 of the Deutsche Forschungsgemeinschaft (DFG) namely "The evolution of the Late Palaeozoic in the light of sedimentary geochemistry". Tournaisian, Visean and Serpukhovian stages of eastern Europe (Central Russia and Donetz Basin) were evaluated by Alekseev, Chuvashov, Devuyst, Hance and Weyer. They proposed a biostratigraphic zonation for the part of Upper Visean deposits. This Zonation is formed by (1) *Endothyranopsis crassa-Parastaffella luminosa* (Aleksinian), (2) *Eostaffella ikensis* (Mikhailovian), (3) *Endothyranopsis sphaerica –Eostaffella ikensis tenebrosa* (Venevian).

In Northern England, Cózar and Somerville (2004) have proposed 8 biostratigraphical assemblages comprising the Late Asbian to Early Namurian interval. The boundary between biostratigraphical assemblages 6 and 7 are correlated with the Early – Late Brigantian boundary and Late Brigantian (biostratigraphical assemblage 7) is characterized with the first appearances of *Endothyranopsis sphaerica, Planospirodiscus and Biseriella.* Moreover, *Neoarchaediscus incertus* is only known from the Namurian in

Northern England (Somerville and Cózar, 2005) however, *Neoaechaediscus incertus* with *Neoarchaediscus parvus* defines the Brigantian in NW Ireland (Cózar et al., 2006).

In Northeastern Ireland, *Endothyranopsis sphaerica, Janischewkina typica* and *Climacammina* first occur in the Late Brigantian. Some of the common Late Brigantian forms that are also found in our study are *Pojarkovella efremovi, Pseudoendothyra sublimis, Endostaffella* spp. and *Biseriella parva*. However, *Biseriella parva* mainly represents the latest Brigantian with common occurrence of *Pseudoglomospira* (Cózar et al., 2005). Although in many studies carried out in Ireland (Somerville, 2008; Somerville and Cozar, 2005; Cózar et al., 2005) the first occurrence of *Asteroarchaediscus* defines the Brigantian, in our studied section it appears first in the Serpukhovian.

Howchinia and *Janischewskina* first occur in the Brigantian in SE Spain (Cózar, 2004) and they are significant Brigantian markers. However, they were not recognized in this study.

In North Africa, *Endothyranopsis sphaerica* first occurs just below the Early – Late Brigantian boundary (Cózar et al., 2008). Other forms that are also observed in our study are *Biseriella* aff. *parva* and specimens of *Asteroarchaediscus*. However, *Biseriella* aff. *parva* and *Asteroarchaediscus rugosus* are more common in Latest Brigantian.

Following biozones were recognized along the measured section in our study.

2.2.1 *Eostaffella ikensis – Vissarionovella tujmasensis* Zone

This zone covers the longest part of the studied section from samples SC-1 to SC-72. It is formed by bioclastic packstone, bioclastic packstone to grainstone and bioclastic grainstone, skeletal intraclast grainstone, intraclastic grainstone, pelloidal packstone to grainstone and pelloidal grainstone, pelloidal packstone to wackestone, wackestone and mudstone (Figure 2.4). This zone is characterized by overlapping ranges of *Eostaffella ikensis* and *Vissarionovella tujmasensis*. The Upper boundary is defined by the

Table 2. 5: Foraminiferal distribution chart

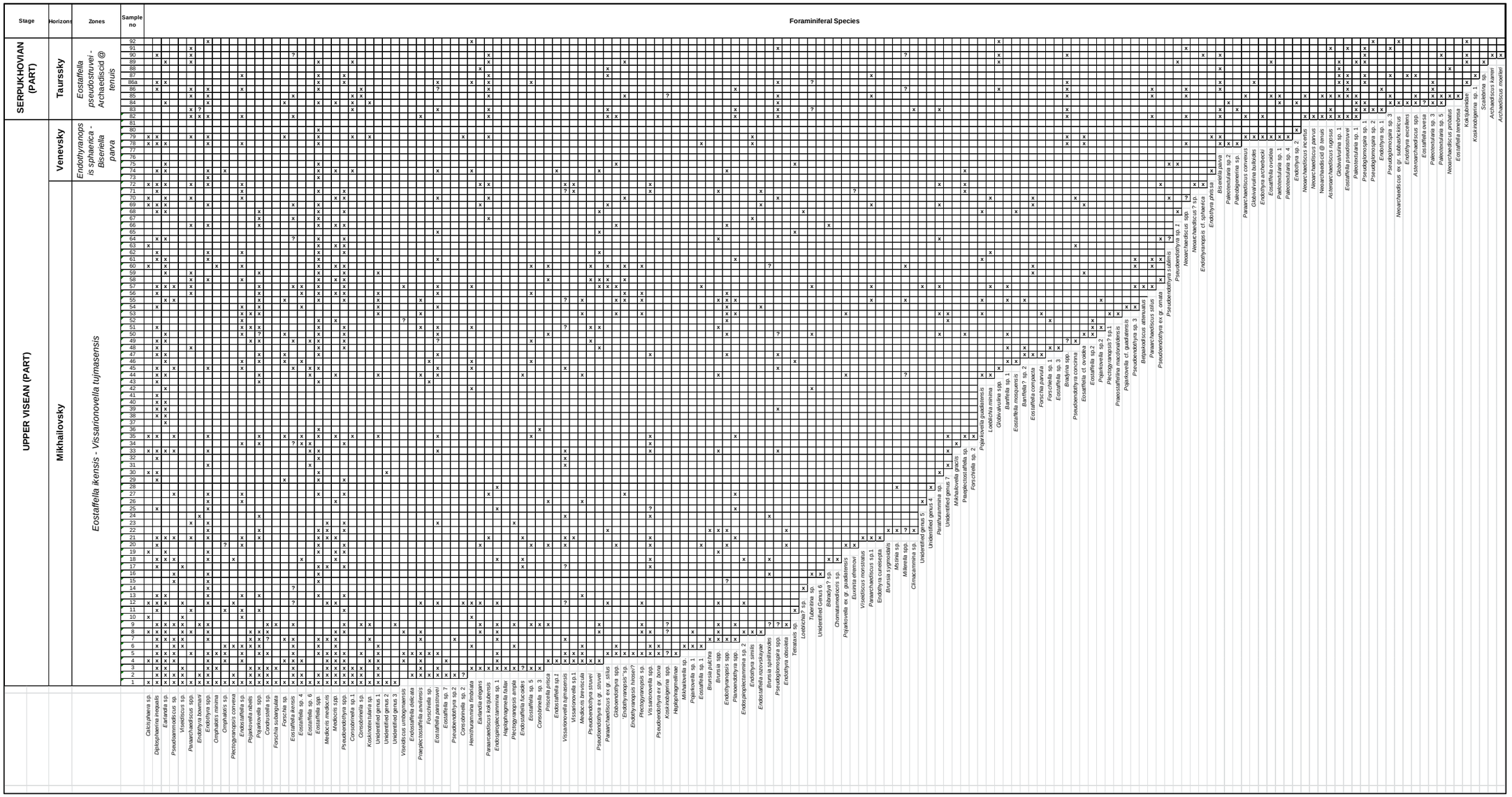

last occurrence of *Vissarionovella tujmasensis*. Since *Eostaffella ikensis* is observed from the first sample, the lower boundary cannot be defined. The thickness of this zone is 30,84 m.

There are many other forms present in this zone (Table 2.5) namely; *Diplosphaerina inequalis* (Pl. I, figs. 1-5, 10-11), *Calciciphaera* sp. (Pl. I, figs. 6-7), *Parathurammina* sp. (Pl. I, fig. 8-9), *Hemithurammina fimbriata* (Pl. I, figs. 14?, 15-16), *Earlandia elegans* (Pl. I, figs. 12-13), *Earlandia* sp., *Pseudoglomospira* spp. (Pl. III, figs. 16-21), *Paraarchaediscus stilus* (Pl. 6, Figs. 7-9), *Paraarchaediscus* ex gr. *stilus* (Pl. VI, figs. 10-15), *Paraarchaediscus koktjubensis* (Pl. IV, figs. 8-24; Pl. V, fig. 1?), *Paraarchaediscus* sp. 1 (Pl. VI, figs. 17-20), *Paraarchaediscus* spp. (Pl. V, figs. 2-14; Pl. VI, figs. 21-22), *Neoarchaediscus*? spp. (Pl. VII, figs. 16-18, 20?-23), *Globivalvulina* spp. (Pl. IX, fig. 1-6, 7?, 8-9), *Bradyina* spp. (Pl. X, fig. 1-10), *Endothyra bowmani* (Pl. XIII, figs. 17-19), *Endothyra similis* (Pl. XIII, figs. 1-3), *Endothyra* spp. (Pl. XIII, figs. 20-22, 25-26), *Globoendothyra* spp. (Pl. XI, figs. 1-10), *Omphalotis* sp. (Pl. XIII, figs. 8-9, 10?-11?, 12), **"***Endothyranopsis"* sp. (Pl. XIV, figs. 4-8), *Endothyranopsis* spp. (Pl. XIV, figs. 10-12, 14?), *Endostaffella* sp. 1 (Pl. XV, figs. 8-9), *Endostaffella* sp. (Pl. XV, figs. 10-21), *Planoendothyra* spp. (Pl. XVI, figs. 1-6), *Praeplectostaffella anvilensis* (Pl. XXVIII, figs. 2-9, 10?, 11-12), *Praeplectostaffella* sp. (Pl. XXVIII, figs. 13-14), *Forschia* sp. (Pl. XX, figs. 11-13), *Millerella* sp. (Pl. XVII, figs 17-19), *Eostaffella ikensis* (Pl. XXI, figs. 1-7), *Eostaffella parastruvei* (Pl. XII, figs. 1-11), *Eostaffella* cf. *ovoidea* (Pl. XXIII, figs. 4-6), *Eostaffella* sp. 1 (Pl. XXIII, figs. 11-14), *Eostaffella* sp. 5 (Pl. XXIV, figs. 6-11), *Eostaffella* spp. (Pl. XXIII, figs. 18?-19?, 20-26; Pl. XXV, figs. 6-11), *Mediocris* spp. (Pl. XXVII, figs. 1-13), *Pseudoendothyra sublimis* (Pl. XXX, figs. 6-7, 11), *Pseudoendothyra* sp. 1 (Pl. XXX, fig. 1), *Pseudoendothyra* spp. (Pl. XXIX, fig. 10; Pl. XXX, figs. 8-10), *Consobrinella* sp. 1 (Pl. XXXII, figs. 1-5), *Consobrinella* sp. 2 (Pl. XXXII, fig. 6, 9?), *Consobrinella* sp., *Koskinotextularia* sp. (Pl. XXXII, figs. 14-17), *Koskinobigerina*? sp. (XXXII, figs. 11-13), *Climacammina* sp. (XXXI, figs. 11-12), *Tetrataxis* sp. (Pl. XXXI, fig 13).

The following species are only found in this zone (Table 2.5). These forms are: *Brunsia pulchra* (Pl. II, figs. 3-5), *Brunsia spirillinoides* (Pl. II, figs. 1-2), *Brunsia sygmoidalis* (Pl. II,

fig. 10), *Brunsia* spp. (Pl. II, figs. 6-19), Pseudoammodiscus sp. (Pl. II, figs. 11-14), *Viseidiscus monstratus* (Pl. IV, fig. I), *Viseidiscus umbogmaensis* (Pl. IV, figs. 2-5), *Viseidiscus* spp. (Pl. IV, figs. 6-7), *Betpakodiscus attenuatus* (Pl. VI, fig. 6), *Bibradya*? sp. (Pl. X, figs. 11-12), *Endospiroplectammina* sp.1 (Pl. XXII, figs. 13-15), *Endospiroplectammina* sp. 2 (Pl. XII, fig. 16), *Endothyra cuneisepta* (Pl. XIII, fig. 15), *Endothyra obsoleta* (Pl. XIII, fig. 16), *Priscella prisca* (Pl. XIII, figs. 4-8), *Omphalotis minima* (Pl. XII, figs. 1-7), *Endothyranopsis hirosei*? (Pl. XIV, fig. 13), *Plectogyranopsis ampla* (Pl. XIV, figs. 18-19), *Plectogyranopsis convexa* (Pl. XIV, figs. 15-17), *Plectogyranopsis* sp. (Pl. XIV, figs. 21-22), *Plectogyranopsis*? sp. 1 (Pl. XIV, fig. 20), *Haplophragmella fallax* (Pl. XIV, fig. 1), *Mikhaiolovella gracilis* (Pl. XIV, fig. 2), *Mikhaiolovella* sp. (Pl. XIV, fig. 2), *Mstinia* (Pl XX, figs. 5-6), *Bibradya*? sp. (Pl. X, figs. 11-12), *Banffella* sp. 1 (Pl. XI, figs. 11-12), *Banffella*? sp. 2 (Pl. XI, figs 13-15), *Loeblichia minima* (Pl. XVI, fig. 9), *Loeblichia*? sp. (Pl. XVI, fig. 10), *Euxinita efremovi* (Pl. XVI, fig. 7, 8?), *Endostaffella delicata*? (Pl. XV, figs. 1-2), *Endostaffella fucoides* (Pl. XV, figs. 3,5, 4?), *Endostaffella rozovskayae* (Pl. XV, figs. 6-7), *Praeostaffellina macdonaldensis* (Pl. XXVIII, fig. 1), *Pojarkovella nibelis* (Pl. XVIII, figs. 1-9), *Pojarkovella guadiatensis* (Pl. XVII, fig. 1-4), *Pojarkovella* ex gr. *guadiatensis* (Pl. XVII, figs. 6-7), *Pojarkovella* cf. *guadiatensis* (Pl. XVII, fig. 5), *Pojarkovella* sp. 1 (Pl. XVIII, figs. 10-11), *Pojarkovella* sp. 2 (Pl. XVIII, figs. 12-13), *Pojarkovella* spp. (Pl. XII, figs. 8-17), *Vissarionovella tujmasensis* (Pl. XIX, figs. 1-7), *Vissarionovella* sp. 1 (Pl. XIX, figs. 9-12), *Vissarionovella* spp. (pl. XIX, figs. 8, 13-15), *Condrustella* sp. (Pl. XX, figs. 1-4), *Forschia parvula* (Pl. XX, fig. 7), *Forschia subangulata* (Pl. Pl. XX, figs. 8-10), *Forschiella* sp. 1 (Pl. XX, figs. 14-15), *Forschiella* sp. 2 (Pl. XX, fig. 16), *Forschiella* sp. (Pl. XX, fig. 17), *Eostaffella mosquensis* (Pl. XXII, fig. 12), *Eostaffela compacta* (Pl. XXII, fig. 13-14), *Eostaffella* sp. 2 (Pl. XXII, figs. 15-16), *Eostaffella* sp. 3 (Pl. XXIII, fig. 17),*Eostaffella* sp. 4 (Pl. XXIV, figs. 1-5), *Eostaffella* sp. 6 (Pl. XXIV, figs. 12-15; Pl. XXV, figs. 1-2), *Eostaffella*? sp. 7 (Pl. XXV, figs. 3-5), *Mediocris breviscula* (Pl. XXVI, figs. 11-15), *Mediocris mediocris* (Pl. XXVI, figs. 1-4, 5?, 6-10), *Chomatomediocris* sp. (Pl. XXVI, fig. 16), *Pseudoendothyra* ex gr. *bona* (Pl. XXIX, figs. 11-13), *Pseudoendothyra concinna* (Pl. XXX, fig. 2), *Pseudoendothyar* ex gr. *ornata* (Pl. XXX, figs. 3-5) *Pseudoendothyra struvei* (Pl. XXIX, figs. 1-2), *Pseudoendothyra* ex gr. *struvei* (Pl. XXIX, figs. 3-9), *Pseudoendothyra* sp. 2 (Pl.

XXX, fig. 12), *Pseudoendothyra* sp. 3 (Pl. XXX, figs. 13-14), *Consobrinella* sp. 3 (Pl. XXXII, figs. 7-8), Unidentified genus 1 (Pl. XXXIII, figs. 1-9), Unidentified genus 2 (Pl. XXXIII, figs. 10, 12), Unidentified genus 3 (Pl. XXXIII, fig. 11), Unidentified genus 4 (Pl. XXXIII, fig. 13), Unidentified genus 5 (Pl. XXXIII, fig. 14), Unidentified genus 6 (Pl. XXXIII, figs. 15-16), Unidentified genus 7 (Pl. XXXIII, fig. 17).

This zone is the equivalent of Mikhailovsky Horizon in the Russian Platform and it is considered to be the equivalent to Early Brigantian if recent studies in the literature are taken into account Cózar (2004), Vachard and Aretz (2004), Menning et al. (2006), Okuyucu and Vachard (2006), Ogg et al. (2008), Hecker (2009), Pillet et al (2010).

2.2.2 *Endothyranopsis* cf. *sphaerica – Biseriella parva* Zone

This zone is made up of quartz arenitic sandstone, shale, mudstone with fenestral fabric, intraclastic wackestone with ostracods, bioclastic packstone to grainstone, bioclastic grainstone and skeletal intraclast grainstone microfacies and covers the interval from SC- 73 to SC- 81. The thickness of this zone is 17,5 m. It is characterized by the first occurrences of *Endothyranopsis* cf. *sphaerica* and *Biseriella parva*. *Endothyranopsis* cf. *sphaerica* first appears just below the boundary and *Biseriella parva* first appears within this zone later than the first appearance of *Endothyranopsis* cf. *sphaerica*. The upper boundary is defined by the first occurrences of *Eostaffella pseudostruvei* and *Archaediscus @ tenuis* stage (Figure 2.4).

Several forms were recognized for the first time within this zone (Table 2.5) They are *Paraarchaediscus convexus* (Pl. VI. figs. 1-5), *Biseriella parva* (Pl. XIII, figs. 1-11, 12?), *Globivalvulina bulloides* (Pl. VIII, figs. 13-15?), *Endothyra archerbecki* (Pl. XIII, figs. 10-11), *Endothyra phrissa* (Pl. XIII, fig. 9), *Endothyra* sp. 2 (Pl. XIII, figs. 23-24), *Eostaffella ovoidea* (Pl. XXIII, figs. 1-3), *Paleotextularia* sp. 1 (Pl. XXXI, figs. 1-2), *Paleotextularia* sp. 2 (Pl.

XXXI, fig. 3), *Paleotextularia* sp. 4 (Pl. XXXI, fig. 5) and *Paleobigenerina* sp. (Pl. XXXI, figs. 9-10).

Other forms present in this zone are as follows (Table 2.5): *Diplosphaerina inequalis* (Pl. I, figs. 1-5, 10-11), *Calciciphaera* sp. (Pl. I, figs. 6-7), *Hemithurammina fimbriata* (Pl. I, figs. 14?, 15-16), *Earlandia* sp., *Paraarchaediscus* ex gr. *stilus* (Pl. VI, figs. 10-15), *Paraarchaediscus koktjubensis* (Pl. IV, figs. 8-24; Pl. V, fig. 1?), *Paraarchaediscus* spp. (Pl. V, figs. 2-14; Pl. VI, figs. 21-22), *Endothyra similis* (Pl. XIII, figs. 1-3), *Endothyra* spp. (Pl. XIII, figs. 20-22, 25-26), *Globoendothyra* spp. (Pl. XI, figs. 1-10), *Omphalotis* sp. (Pl. XIII, figs. 8-9, 10?-11?, 12), **"***Endothyranopsis"* sp. (Pl. XIV, figs. 4-8), *Endostaffella* sp. 1 (Pl. XV, figs. 8-9), *Endostaffella* sp. (Pl. XV, figs. 10-21), *Forschia* sp. (Pl. XX, figs. 11-13), *Eostaffella parastruvei* (Pl. XII, figs. 1-11), *Eostaffella* cf. *ovoidea* (Pl. XXIII, figs. 4-6), *Eostaffella* sp. 1 (Pl. XXIII, figs. 11-14), *Eostaffella* spp. (Pl. XXIII, figs. 18?-19?, 20-26; Pl. XXV, figs. 6-11), *Mediocris* spp. (Pl. XXVII, figs. 1-13), *Pseudoendothyra sublimis* (Pl. XXX, figs. 6-7), *Pseudoendothyra* sp. 1 (Pl. XXX, fig. 1), *Pseudoendothyra* spp. (Pl. XXIX, fig. 10; Pl. XXX, figs. 8-10), *Consobrinella* sp. 1 (Pl. XXXII, figs. 1-5), *Consobrinella* sp. 2 (Pl. XXXII, fig. 6,9?), *Koskinotextularia* (Pl. XXXII, figs. 14-17), *Climacammina* sp. (XXXI, figs. 11-12), *Tetrataxis* sp. (Pl. XXXI, fig 13).

This zone is correlated with the Russian Venevsky Horizon and it corresponds to the Late Brigantian.

2.2.3 *Eostaffella pseudostruvei* – Archaediscid @ *tenuis* stage Zone

This zone includes the upper part of the section covering the interval from SC-82 to SC-92 which has a thickness of 9,27 m. It is composed of bioclastic packstone and grainstone and skeletal intraclast grainstone, sandy bioclastic grainstone. This zone is characterized by the first occurrences of *Eostaffella pseudostruvei* and Archaediscid @ *tenuis* stage. Since the studied section ends with this zone, upper boundary was not

defined. The first appearance of *Neoarchaediscus parvus* can also be used to define the lower boundary of this zone (Figure 2.4).

The following species are first recognized within this zone (Table 2.5): *Pseudoglomospira* sp. 1 (Pl. III, figs. 1-8), *Pseudoglomospira* sp. 2 (Pl. III, figs. 9-10), *Pseudoglomospira* sp. 3 (Pl. III, figs. 11-15), *Archaediscus karreri* (Pl. V, fig. 15), *Archaediscus moelleri* (Pl. VI, fig. 16), *Neoarchaediscus* ex gr. *subbaschkiricus* (Pl. VII, figs. 14-15), *Neoarchaediscus incertus* (Pl. VII, figs. 7-8), *Neoarchaediscus probatus* (Pl. VII, figs. 12-13,*Neoarchaediscus* sp. (*@tenuis* stage), *Asteroarchaediscus rugosus* (Pl. VII, figs. 1-4, *Asteroarchaediscus* spp. (Pl. VII, figs. 5-6, *Globivalvulina* sp. 1 (Pl. VIII, figs. 16-20), Koktjubinidae (pl. IX, figs. 10-13), *Endothyra excellens* (Pl. XIII, fig. 14), *Endothyra* sp. 1 (Pl. XIII, figs. 12-13), *Eostaffella ovesa*? (Pl. XXIII, fig. 7), *Eostaffella pseudostruvei* (Pl. XXIII, figs. 8-10; Pl. XXVII, figs. 14-16), *Eostaffella tenebrosa* (Pl. XXI, fig. 8), *Paleotextularia* sp. 3 (Pl. XXXI, fig. 4), *Paleotextularia* sp. 5 (Pl. XXXI, figs. 6-8), *Koskinobigerina* sp. 1 (Pl. XXXII, fig. 10), *Scalebrina* sp. (Pl. III, fig. 22).

Following species that appear in the underlying zones are also present in this zone: *Diplosphaerina inequalis* (Pl. I, figs. 1-5, 10-11), *Parathurammina* sp. (Pl. I, fig. 8-9), *Hemithurammina fimbriata* (Pl. I, figs. 14?, 15-16), *Earlandia elegans* (Pl. I, figs. 12-13), *Pseudoglomospira* spp. (Pl. III, figs. 16-21), *Paraarchaediscus koktjubensis* (Pl. IV, figs. 8-24; Pl. V, fig. 1?), *Paraarchaediscus stilus* (Pl. 6, Figs. 7-9), *Paraarchaediscus* ex gr. *stilus* (Pl. VI, figs. 10-15), *Paraarchaediscus* sp. 1 (Pl. VI, figs. 17-20), *Paraarchaediscus* spp. (Pl. V, figs. 2-14; Pl. VI, figs. 21-22), *Globivalvulina* spp. (Pl. IX, fig. 1-6, 7?, 8-9), *Bradyina* spp. (Pl. X, fig. 1-10), *Endothyra bowmani* (Pl. XIII, figs. 17-19), *Endothyra* spp. (Pl. XIII, figs. 20-22, 25-26), *Globoendothyra* spp. (Pl. XI, figs. 1-10), **"***Endothyranopsis"* sp. (Pl. XIV, figs. 4-8), *Endostaffella* sp. (Pl. XV, figs. 10-21), *Planoendothyra* spp. (Pl. XVI, figs. 1-6), *Praeplectostaffella anvilensis* (Pl. XXVIII, figs. 2-9, 10?, 11-12), *Praeplectostaffella* sp. (Pl. XXVIII, figs. 13-14), *Forschia* sp. (Pl. XX, figs. 11-13), *Eostaffella ikensis* (Pl. XXI, figs. 1-7), *Eostaffella parastruvei* (Pl. XII, figs. 1-11), *Eostaffella* sp. 5 (Pl. XXIV, figs. 6-11), *Eostaffella* spp. (Pl. XXIII, figs. 18?-19?, 20-26; Pl. XXV, figs. 6-11), *Mediocris* spp. (Pl. XXVII, figs. 1-

13), *Millerella* sp. (Pl. XVII, figs 17-19), *Pseudoendothyra* spp. (Pl. XXIX, fig. 10; Pl. XXX, figs. 8-10), *Consobrinella* sp. 1 (Pl. XXXII, figs. 1-5), *Consobrinella* sp., *Koskinotextularia* (Pl. XXXII, figs. 14-17), *Koskinobigerina*? sp. (XXXII, figs. 11-13).

This zone is the equivalent of the lower part of Serpukhovian substage and it is correlated with the Taurrsky Horizon of the Russian Platform.

2.3 Visean – Serpukhovian Boundary and Foraminifers Across the Boundary

In the book "A Geologic Time Scale" (2004) the Visean – Serpukhovian boundary coincides with the boundary between Venevsky and Taurissky Horizons of the Russian Platform. It also coincident with Brigantian – Pendelian or Namurian boundary of the Western Europe. This boundary was chosen based on the first appearance of conodont *Lochria cruciformis*. Many studies in the literature use this correlation. However, the base of the Serpukhovian is revised in the book "the Concise Geologic Time Scale" (2008) and defined based on the first appearance of *L. ziegleri* in the *L. nodosa-L. ziegleri* linage of conodonts. This level is below the proposed level for the base of Serpukhovian in 2004 and it lies within the Russian Venevian and Western European Brigantian Horizons.

Although in 2008, the first appearance of *L. ziegleri* in the *L. nodosa-L. ziegleri* linage is proposed to define the boundary, definition of the boundary by various fossil groups, including conodonts, is still debatable. In studies of the working groups carried out later 2008, this lineage has been documented in many sections in Europe and Asia however; the validity of usage of this lineage to define the boundary was not certainly determined (Richards et al., 2010). Moreover in many other studies since 2008, Russian Venevsky Horizon and Western Europe Brigantian substage have been incorporated in Upper Visean not in Serpukhovian (Cózar et al., 2008; Somerville, 2008; Hecker, 2009; Kulagina et al., 2009, Nigmadhaznov et al., 2010; Pazukhin et al., 2010; Pille et al., 2010).

There are many suggestions to define the boundary with benthic foraminifera. In Moskow Basin, lower boundary of Serpukhovian is coincident with *Pseudoendothyra globosa – Neoarchadiscus parvus* zone (Davydov et al., 2005). Gibsman (2001 in Davydov et al., 2005) placed the boundary between the latest Visean *Eostaffella tenebrosa* zone and the earliest Serpukhovian *Neoarchaediscus parvus* zone. However, *Neoarchaediscus parvus* defines Brigantian in NW Ireland (Cózar et al., 2006) while it first occurs in the Sepukhovian of Georgia (Rich, 1982).

While in Great Britain Archaediscids *@ tenuis* stage are significant in Early Serpukhovian, in Ireland they were observed first in the Late Brigantian (Gallagher, et al., 2006) and the latest Brigantian (Cózar et al., 2006; Somerville, 2008). However, Cózar et al. (2008) observed Archaediscids @ tenuis stage at the base of the Serpukhovian in Midland Valley (Scotland) but they also observed Archaediscids transitional angulatus stage to tenuis stage in Upper Brigantian and Serpukhovian rocks in Scotland, Ireland and Northen England.

Cózar and Somerville (2004) define the Namurian limestones of Northern England with a significant change in morphology and size of the eostaffellids namely the presence of giant *Eostaffella* ex gr. *parastruvei* and first occurrence of *Eostaffella* ex gr. *pseudostruvei* and *Millerella* sp.

In Africa Lower Serpukhovian is defined by the first occurrences of *Eostaffella pseudostruvei*, *Archaediscus @ tenuis* stage, *Biseriella* ? sp. 1, small *Euxinita* spp. and *Endothyranopsis plana* (Cózar et al., 2008).

In China *Eostaffella pseudostruvei* and *Globivalvulina parva* appear in the uppermost Visean (Vachard et al;, 1991). However, they also indicated that these species are characteristic for the lowermost Serpukhovian.

In Turkey, the boundary between Visean and Serpukhovian is determined by the first occurrences of *Pseudoendothyra* ex gr. *illustria* and *Eostaffella pseudostruvei* (Altıner and

Özgül, 2001). However, *Eostaffella pseudostruvei* had been used as a boundary marker already in Altıner (1981).

In the present study the boundary between Visean and Serpukhovian stages is located in between the *Endothyranopsis* cf. *sphaerica – Biseriella parva* Zone and *Eostaffella pseudostruvei* – Archaediscids @ *tenuis* stage Zone where *Eostaffella pseudostruvei* and Archaediscids @ *tenuis* stage had their first appearences.

CHAPTER 3

MICROFACIES ANALYSIS

3.1 Microfacies Types and Depositional Environments

Despite the fact that early studies handled the microfacies concepts as simply petrographic and paleontological criteria studied in thin sections, today this perspective has changed. At the present time, microfacies is defined as "the total of all sedimentological and paleontological data which can be described and classified from thin sections, peels, polished slabs or rock samples" (Flügel, 2004).

Identification of microfacies mainly consists of determination of composition and texture of limestone. Simple petrographic analysis of limestone mostly aims the interpretation of depositional environments. For this reason, classifications associating grain properties and fabric to environmental properties such as energy level are the most useful ones (Tucker and Wright, 1990). Dunham (1962) and Folk (1959, 1962) are the most widely used textural classifications. Dunham classification is revised and expanded by Embry and Klovan (1971) (Flügel, 2004). Although both of them are based on depositional texture, Flügel (2004) stated that Dunham (1962) classification can well be applied in the field, in laboratory studies and in investigations of cores equally and it is most widely used classification, however, Folk classification is more restricted to laboratory studies. For these reasons, Dunham classification is used in this study.

Since one of the aims of this work is to interpret the environment of deposition of Visean-Serpukhovian limestones in Aladağ Unit, main depositional facies models have been reviewed. In 1975, Wilson proposed a conceptual model including 9 Standard Facies Zones from shore to basin in a rimmed carbonate platform (Figure 3.2). He has designated a new concept namely, Standard Microfacies Types (SMF) and defined 24 Standard Microfacies Types. Flügel revised the Wilson model and in 2004 (Figure 3.1), he also proposed generalized facies models for rimmed carbonate platform (Figure 3.3) and homoclinal carbonate ramp (Figure 3.4). He has benefited from grain types, grain frequency, matrix types, depositional fabrics, fossils and depositional texture types in order to determine Standard Microfacies Types associated with his models. He has described 26 microfacies types (SMF) in rimmed carbonate platform and 30 microfacies types (RMF) in homoclinal carbonate ramp.

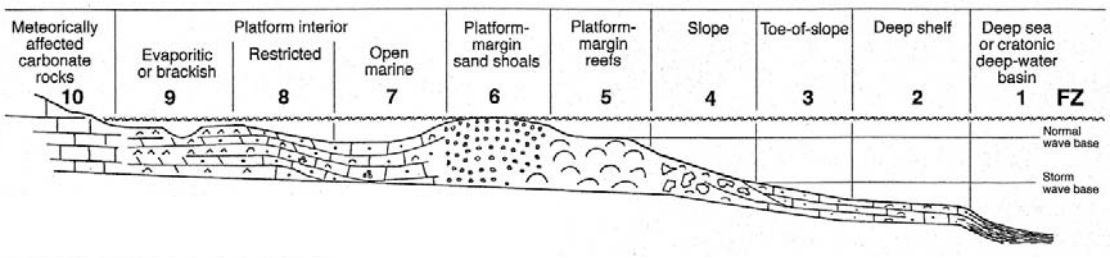

Figure 3. 1: Rimmed carbonate platform: The standard facies zones of the modified Wilson model (taken from Flügel, 2004)

In this study, for determination of microfacies as well as textural criteria, the composition and abundance of allochems are used. Allochems and matrix type and their relative abundance are crucial in the identification of facies types. Figure 3.5 and 3.6 shows thin section photographs of main allochem types and depositional textures used in microfacies analysis.

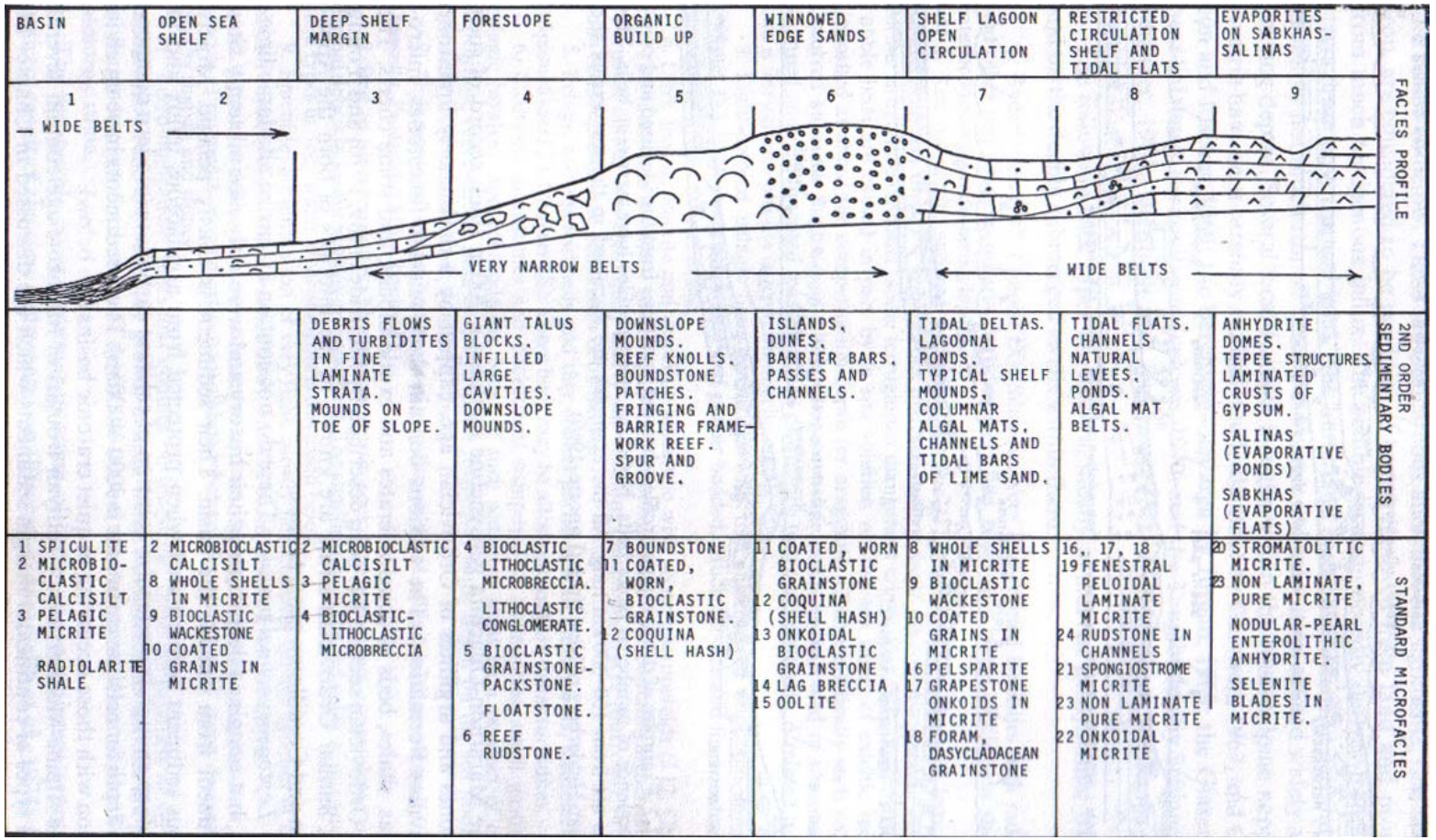

Figure 3. 2: Carbonate depositional model showing Standard Facies Belts and associated microfacies (Wilson, 1975).

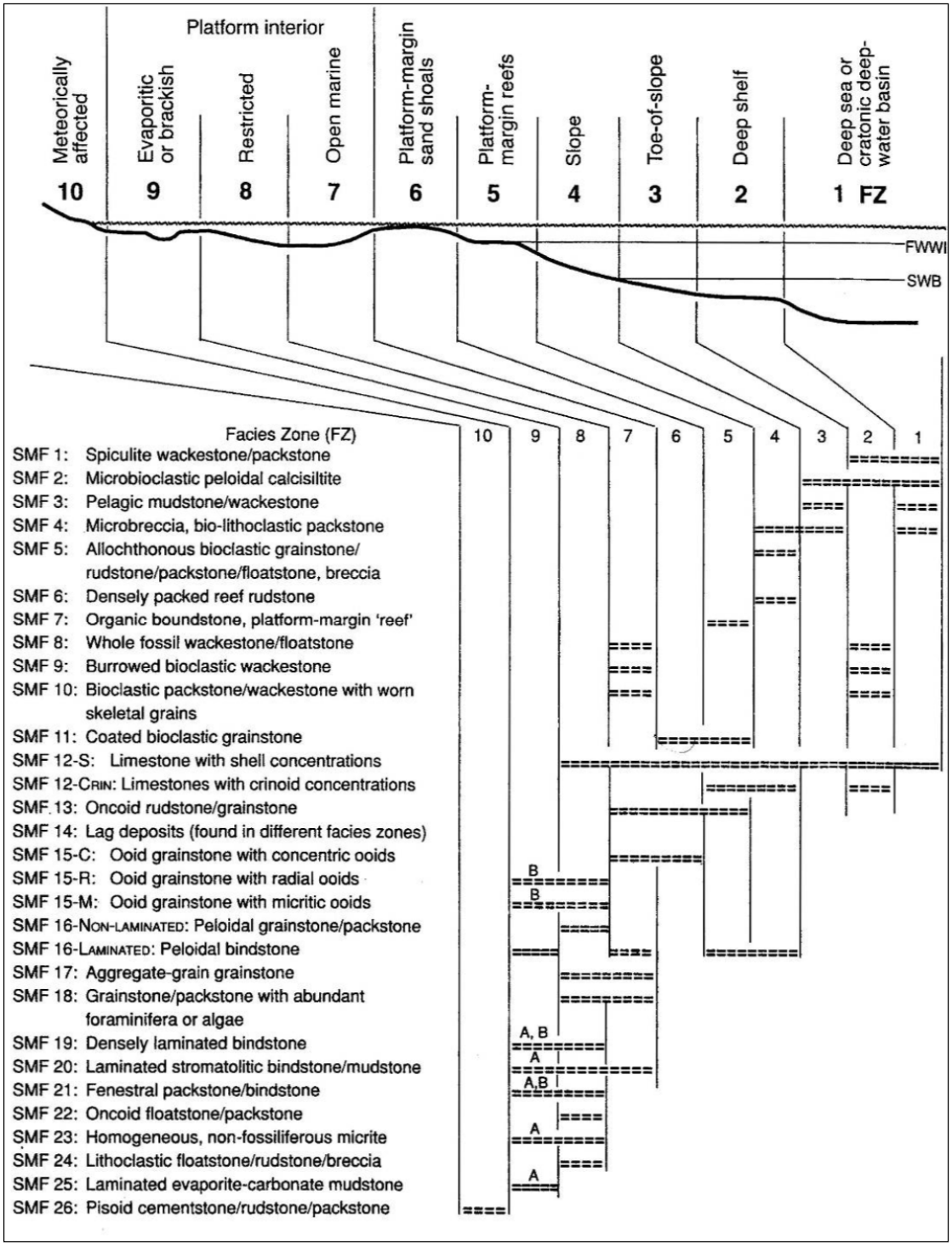

Figure 3. 3: Distribution of Standard Microfacies type (SMF) in the Facies Zones (FZ) of the rimmed carbonate platform model (Flügel, 2004) (A: evaporitic, B: brackish)

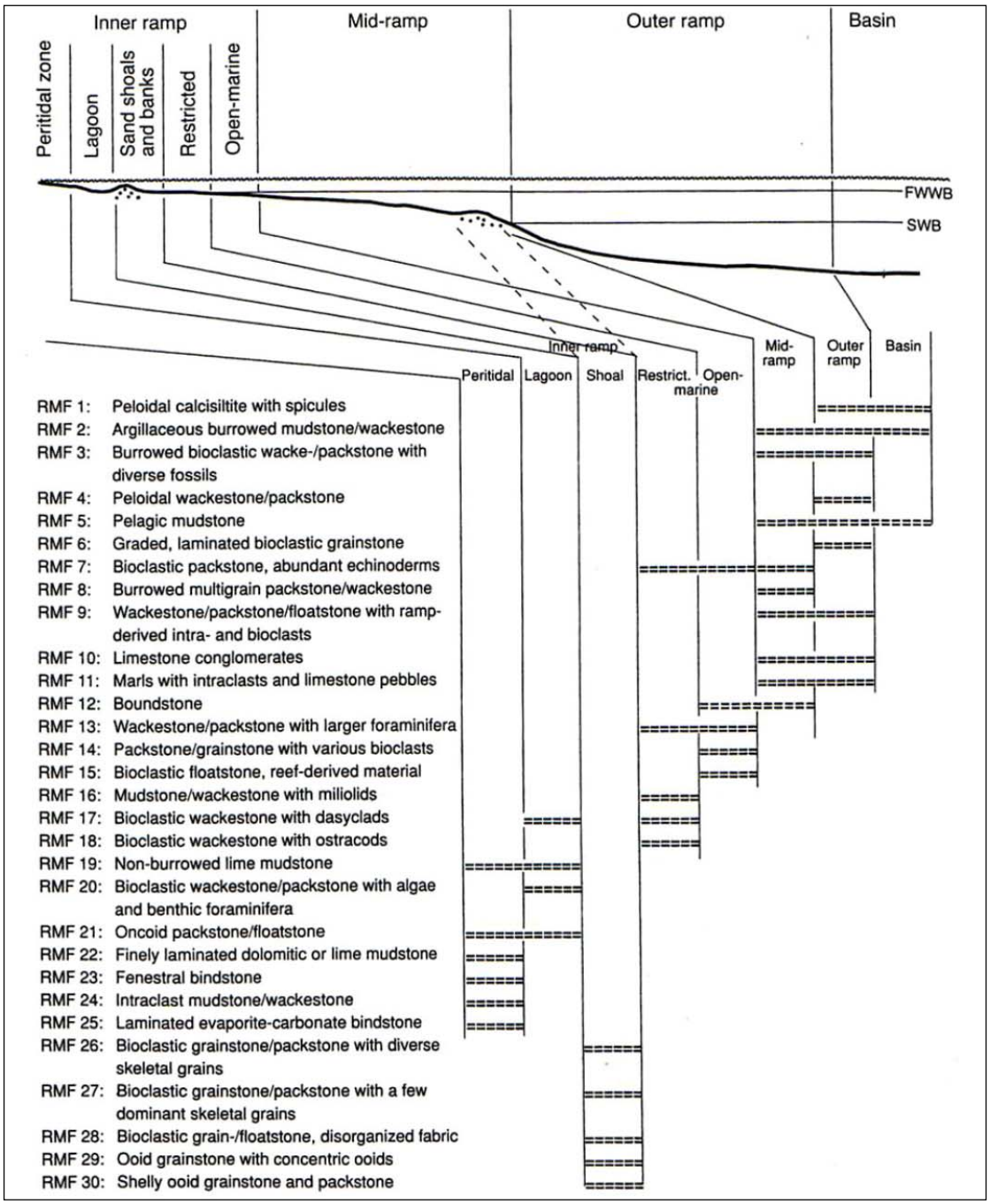

Figure 3.4: Generalized distribution of microfacies types in different parts of a homoclinal carbonate ramp (Flügel, 2004).

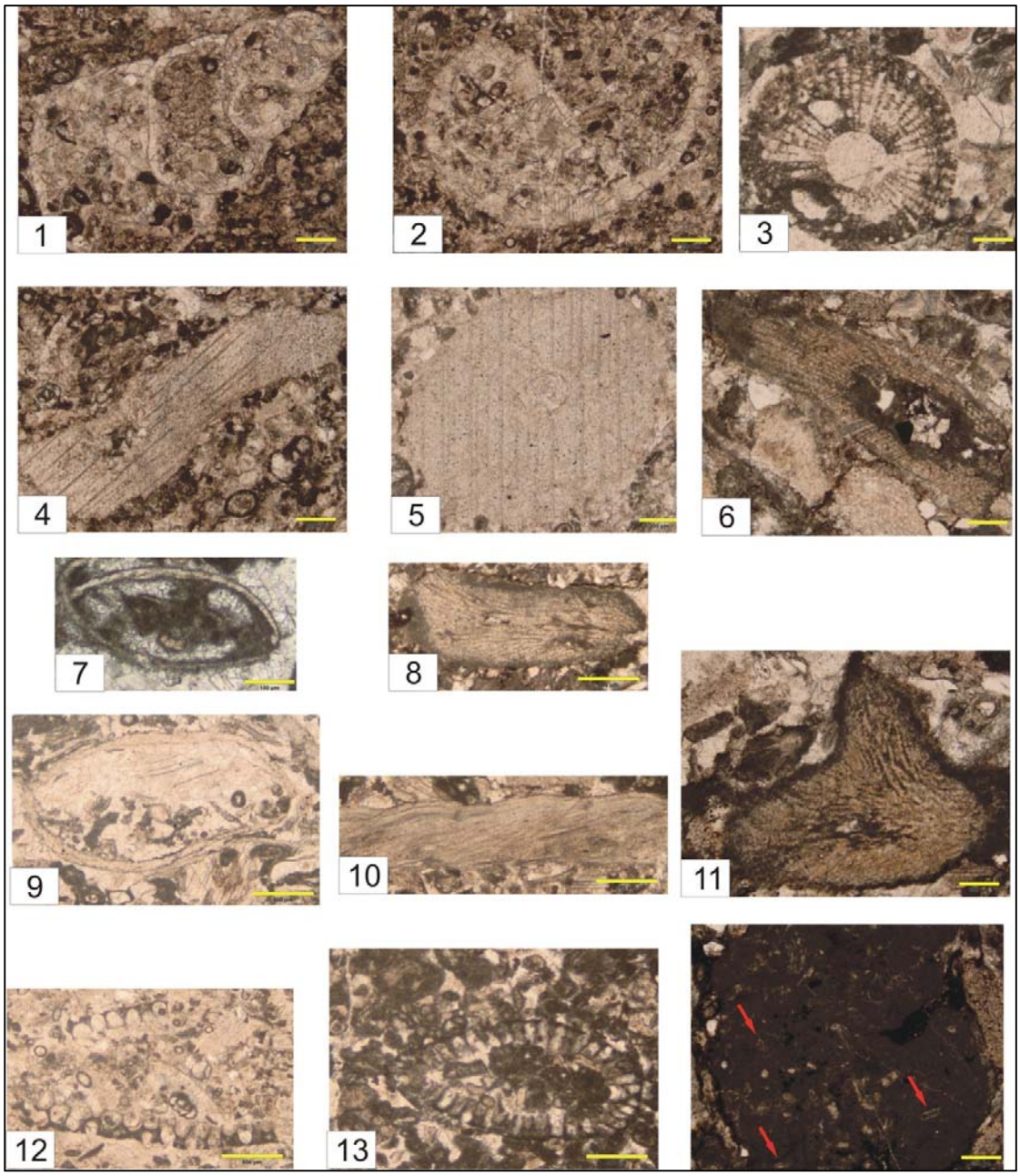

Figure 3.5: Skeletal grains used in microfacies analysis. **1-2:** Gastropoda shell (SC-2). **3, 6:** Echinoderm spine (SC-16, SC-89). **4-5:** Crinoid fragment (SC-2 and SC-6). **7:** Ostracoda (SC-37). **8, 11:** Ungdarella (SC-89). **9-10:** Bivalve fragment (SC-17, SC-16). **12-13:** *Koninckopora* (Sc-9, SC-22). **14:** *Kamaenella*? (SC-89) (Red arrows show *Kamaenella*?). Scale bar: 100 μ for 7; 200 μ for 1,2,3,4,5,11,14; 500 μ for 8, 9, 10, 12, 13.

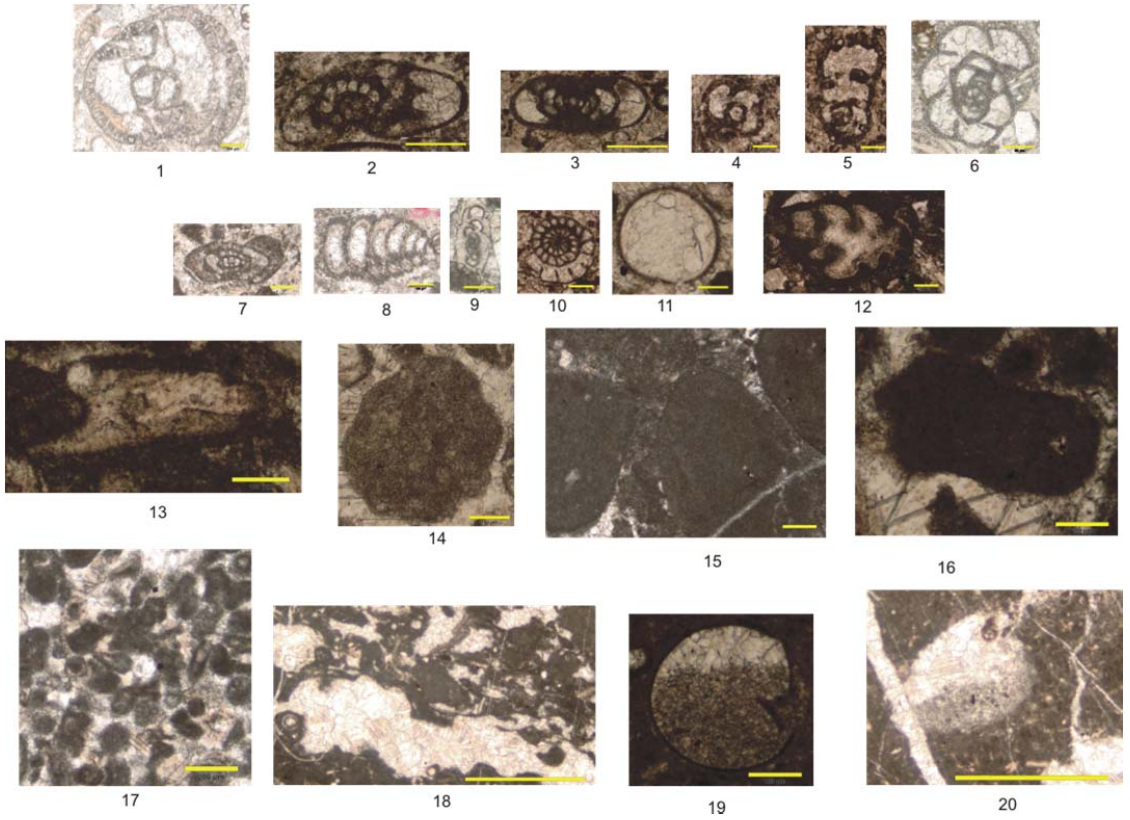

Figure 3.6: Allochems and depositional textures used in microfacies analysis. **1:** Foraminifera (Bradyina) (SC-82). **2-4:** Foraminifera (Pojarkovella, Mediocris, Condrustella) (SC-1). **5:** Foraminifera (Nevillea) (SC-2). **6:** Foraminifera (Endothyra) (SC-82). **7:** Foraminifera (*Eostaffella*) (SC-50). **8-9:** Foraminifera (*Paleotextularia, Paraarchaediscus*) (SC-82). 10: Foraminifera (*Eostaffella*) (SC-2). **11:** Calciciperidae (SC-1). **12:** Foraminifera (*Climacammina*) (SC-22) **13:** Cortoid (SC-22). **14:** Micritized skeletal grain (SC-18). **15:** Dark clasts (SC-29). **16:** Intraclast (SC-22). **17:** Pelloids (SC-5). **18:** Fenestral fabric (SC-30). **19:** Vadose silt (SC-40). **20.** Geopetal filling (SC-40). Scale bar: 100 μ for 6, 11, 13, 14, 16, 19; 200 μ for 1, 2, 3, 4, 5, 7, 8, 10, 12, 15, 17; 1 mm for 18, 20.

According to microfacies data 3 main depositional environments are determined. These environments are open marine, bioclastic shoal or bank, and tidal flat environments. Although 12 major microfacies types were interpreted, they are grouped under 3 major facies belt because these microfacies may displace through time and they are named by the name of depositional belts such as, open marine facies, bioclastic shoal facies, and tidal flat and associated facies (Table 3.1 and Table 3.2).

3.1.1 Open Marine Facies

3.1.1.1 Bioclastic Packstone (BP)

This microfacies is composed of 3 sub-microfacies namely, bioclastic packstone with equally distributed skeletal grains, crinoidal foraminiferal pelloidal packstone and crinoidal pelloidal packstone with current oriented grains (Table 3.2). Since the main components of these 3 sub-microfacies are bioclasts and all of them represent the depositional environment below wave base, they are assembled under one microfacies. All 3 sub microfacies are grain supported but they contain micritic matrix, therefore, they are named as packstone.

This facies is similar to RMF 7 (bioclastic packstone, abundant echinoderms) defined by Flügel (2004) which characterize mid-ramp and seaward side of inner ramp depositional environments.

Skeletal packstone microfacies points out slightly deeper water, open ramp facies which is deposited above storm wave base (Al-Tawil and Read, 2003).

Table 3. 1: Microfacies types defined in the measured section and corresponding depositional environments

No	Microfacies type	Allochem composition	Depositional environment
1	Bioclastic packstone	Crinoid fragments, foraminifers, bivalves, gastropods, echinoderms, algae, pelloids, ostacods	Open Marine
2	Bioclastic packstone to grainstone	Crinoid fragments, foraminifers, bivalves, algae, micritized skeletal grains, cortoids,pelloids, intraclasts	Open Marine to shoal
3	Bioclastic grainstone	Foraminifers, crinoids, bivalves, echinoids, pelloids, algae, gastropods, ostracods	Shoal
4	Skeletal intraclast grainstone	Intraclasts, micritized grains, coated grains, foraminifers, crinoids, bivalve, algae,echinoids, pelloids	Shoal
5	Intraclastic grainstone	Intraclasts, algae, crinoids and echinoids	Shoal
6	Sandy bioclastic grainstone	Quartz grains, echinoids, crinoids, algae, foraminifers, bivalves	Shoal
7	Pelloidal packstone to wackestone	Pelloids, ostracods, foraminifers, clotted fabric	Restricted lagoon
8	Wackestone -mudstone	Ostracods, dark clasts, intraclasts, algae, pellets,foraminifers fenestral fabric, geopetal fabric	Restricted lagoon and tidal flat pond
9	Shale	Silt and clay sized siliciclastic particles	Restricted lagoon
10	Pelloidal grainstone or pelloidal packstone to grainstone including dark clasts	Pelloids, dark clasts, algae, foraminifers	Tidal channel
11	Pelloidal packstone to grainstone with fenestral fabric	Pelloids, ostracods, foraminifers, dark clasts,fenestral fabric	Tidal flat
12	Sandstone	Quartz grains	Tidal flat

Table 3. 2: Microfacies and sub microfacies types and major facies belts defined in the studied section

Facies		Microfacies		Sub microfacies	Position within the cycle
Open Marine Facies		Bioclastic packstone(BP)	BP1	Bioclastic packstone with equally distributed skeletal grains	Base-middle
			BP2	Crinoidal - foraminiferal - pelloidal packstone	Base-middle
			BP3	Crinoidal - pelloidal packstone with current oriented grains	Base-middle
Shoal Facies		Bioclastic packstone to grainstone (BPG)		-	Base-middle
		Bioclastic grainstone (BG)	BG1	Crinoidal - foraminiferal - pelloidal grainstone	Base-top
			BG2	Bioclastic grainstone with equally distributed skeletal grains	Base-top
		Skeletal intraclast grainstone (SIG)	SIG1	Skeletal intraclast grainstone with some micritized skeletal grains	Base-top
			SIG2	Skeletal intraclast grainstone with abundant micritized skeletal grains and dark clasts	Middle-top
			SIG3	Intraclast-crinoidal-pelloidal grainstone	Base-middle-top
		Intraclastic grainstone (IG)		-	Top
		Sandy bioclastic grainstone (SBG)		-	top
Tidal Flat and Associated Facies	Restricted Lagoon and Tidal Flat Pond Facies	Pelloidal packstone to wackestone (PPW)		-	middle
		Wackestone -mudstone (WM)	IOW	Intraclastic wackestone with ostracods	Middle-base
			MF	Mudstone with fenestral fabric	Middle-top
			IWF	Intraclastic (dark clast) wackestone with fenestral fabric	Middle
		Shale(Sh)		-	Top
	Channel Facies	Pelloidal grainstone or packstone to grainstone including dark clasts (PPG)		-	Base-Top
		Pelloidal packstone to grainstone with fenestral fabric (PPGF)		-	Top
		Quartz arenitic sandstone(S)		-	Top

3.1.1.1.1 Bioclastic Packstone with Equally Distributed Skeletal Grains(BP1)

None of the bioclastic components in this microfacies is dominant. Constituents of bioclastic packstone are foraminifera, crinoids, echinoids, algae and pelloids (Figure 3.7- A and B). Size of bioclasts, especially echinoids and crinoids is much larger than that of the crinoidal foraminiferal pelloidal packstone sub-microfacies.

SC-54, SC-84, SC-86a, SC-88, SC-91 and SC-92 thin sections display this microfacies. Grains are oriented in some thin sections like SC-88 and SC-84. Quartz grains are

present in all thin sections; however, some samples like SC-92, SC-88, and SC-84 contain more quartz grains.

Stylolites are present in thin section SC-84 (Figure 3.7-B).

This microfacies is considered to be deposited in an open marine setting below wave base just like crinoidal – foraminiferal - pelloidal packstone microfacies.

Proposed depositional environments for bioclastic packstone and bioclastic wackestone facies described in Hüneke et al. (1991) is in an open marine, low energy environment occurring below fair-weather wave base. Skeletal facies having wackestone and packstone texture described by Védrine and Strasser (2009) characterizes normal marine conditions.

4.1.1.1.2 Crinoidal – Foraminiferal - Pelloidal Packstone (BP2)

Crinoids, foraminifera and pelloids are main components of this microfacies. Crinoids are fragmented. Besides main components, bivalves, echinoid fragments, gastopoda, algae (*Koninckopora*), ostracoda present in the microfacies (Figure 3.7-C and D). All samples belonging to this microfacies include small amount of angular quartz grains and in some samples euhedral and unhedral dolomite crystals are observed. This

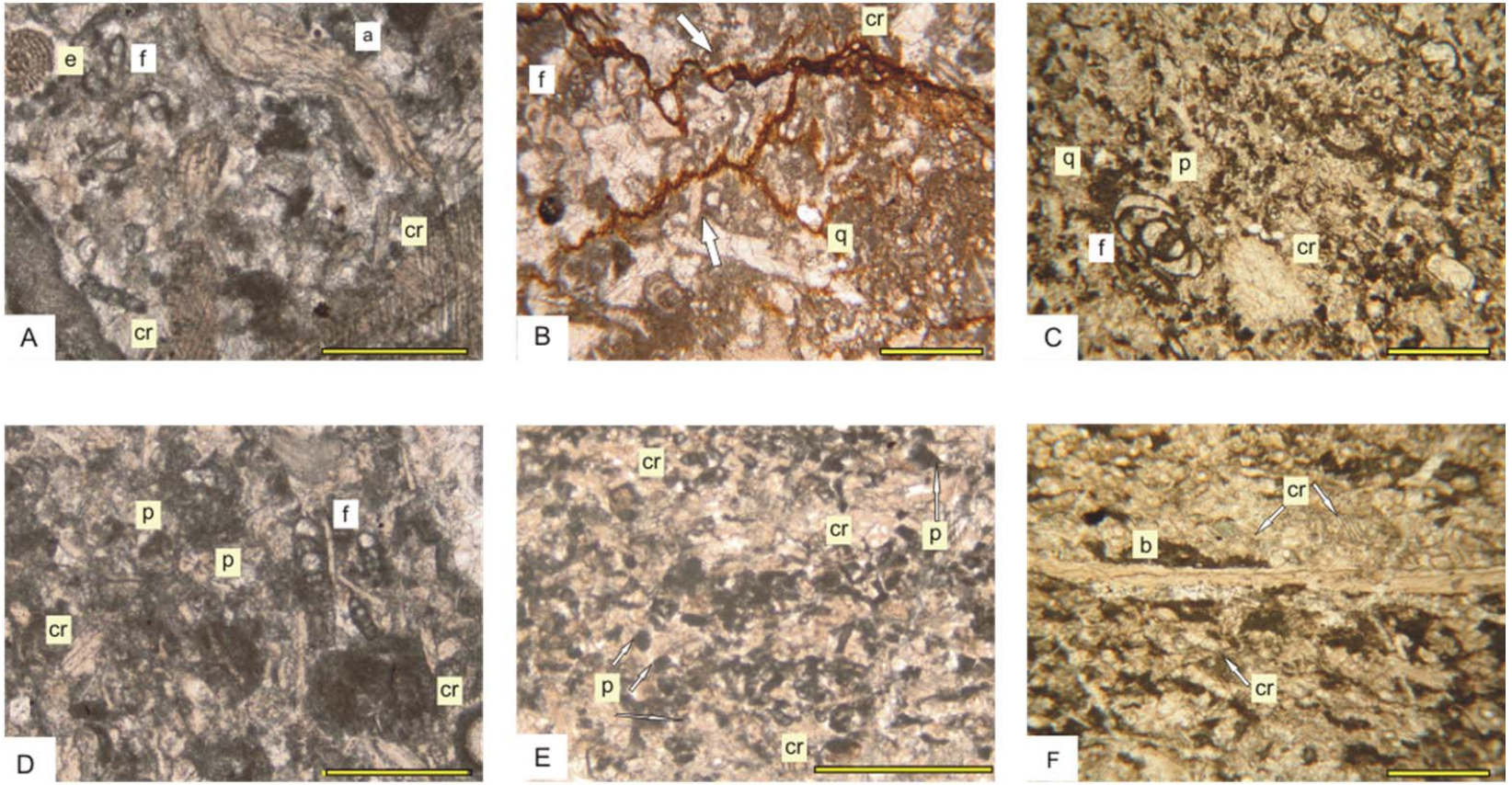

Figure 3.7: Photomicrographs of bioclastic packstone. **A:** Bioclastic packstone with equally distributed skeletal grains (SC-92). **B:** Bioclastic packstone with equally distributed skeletal grains (SC-84). **C:** Crinoidal – foraminiferal - pelloidal packstone (SC-3). **D:** Crinoidal – foraminiferal - pelloidal packstone (SC-67). **E:** Crinoidal – pelloidal packstone with current oriented grains (SC-26). **F:** Crinoidal – pelloidal packstone with current oriented grains (SC-11). (e: echinoderm spine, f: foraminifera, a: algae, cr: crinoid fragments, p: pelloids, b: bivalve fragment, q: quartz grain, white arrow: stylolite development). Scale bar: 500 μ for B, C, D, F; 1 mm for A, E.

microfacies is observed in SC-1, SC-2, SC-3, SC-4, SC-10, SC-57, SC-58, SC-59, SC-60, SC-67 thin sections.

Based on textural and compositional criteria, this microfacies is proposed to be deposited in an open marine setting below wave base (Hüneke at al., 2001; Colombié and Strasser, 2005). According to Flügel, (2004), crinoid concentrations are common in mid-ramp settings. However, autochthonous crinoid concentrations are also present in open sea shelf, foreslope and mounds while allochtonous ones occur in deep shelf margin and foreslope settings.

3.1.1.1.3 Crinoidal - Pelloidal Packstone with Current Oriented Grains (BP3)

This facies is characterized by mainly crinoids, pelloids and few amounts of bivalves, algae and foraminifers. Quartz grains are observed in all thin sections, however, the amount of quartz grains is variable in thin sections. Grains are oriented and this is the most marked characteristic of this microfacies (Figure 3.7-E and F). Mainly, hydrodynamic variables such as tidal currents and wave movements account for the oriented grains (Flügel, 2004).

SC-11, SC-13, SC-14, SC-15, SC-19, SC-25, SC-26 show the characteristics of this microfacies.

This microfacies is interpreted to be deposited in an open marine environment very close to wave base (Chamley et al., 1997).
Crinoids are probably derived from the bioclastic shoal since crinoids in bioclastic bars may be mechanically distributed through basin (Ahmad et al., 2006).

3.1.2 Shoal Facies

3.1.2.1 Bioclastic Packstone to Grainstone (BPG)

Main constituents of this microfacies are skeletal grains such as crinoids, foraminifers, echinoids, pelecypods and algae. Besides, pelloids and intraclasts are present in this microfacies (Table 3.1 and Figure 3.8). Some of the intraclasts formed as a result of micritization of skeletal grains. Activity of microbes, algae and fungi is considered to be the result of micritization (Flügel, 2004). Micritic and algal coatings may be developed in environments in which sedimentation rate is relatively low and shallow marine environments with moderate to constant agitation favors the deposition of such micritized grains (Chamley et al., 1997). Most of the skeletal grains are cortoids. Cortoids are defined by Flügel (2004) as; "carbonate grains (frequently bioclasts) exhibiting thin micrite envelopes" and he stated that shallow marine shelf and platform carbonates are suitable for cortoids although they can also be found in non-marine environments. They are especieally found in current washed sand shoals of inner ramps.

In some thin sections, for example, SC-17, SC-22 and SC-23, orientation of grains is evident. Bioclasts in this high energy zone are oriented due to the activity of tidal currents (Fürsich et al., 2007). Most of these skeletal grains are fragmented and high amount of fragmented skeletal grains indicate the presence of storm intervals (Armella et al., 2007; Schulze et al., 2005).

This facies may correspond to RMF 27 or RMF 14 of Flügel (2004) based on the changes in the wave base and FZ 6 and FZ 7 of Wilson (1975) are suitable for the environment of deposition.

Thin sections showing the characteristic features of the of bioclastic packstone to grainstone microfacies are SC-17, SC-22, SC-23, SC-49, SC-55, SC-72, and SC-73.

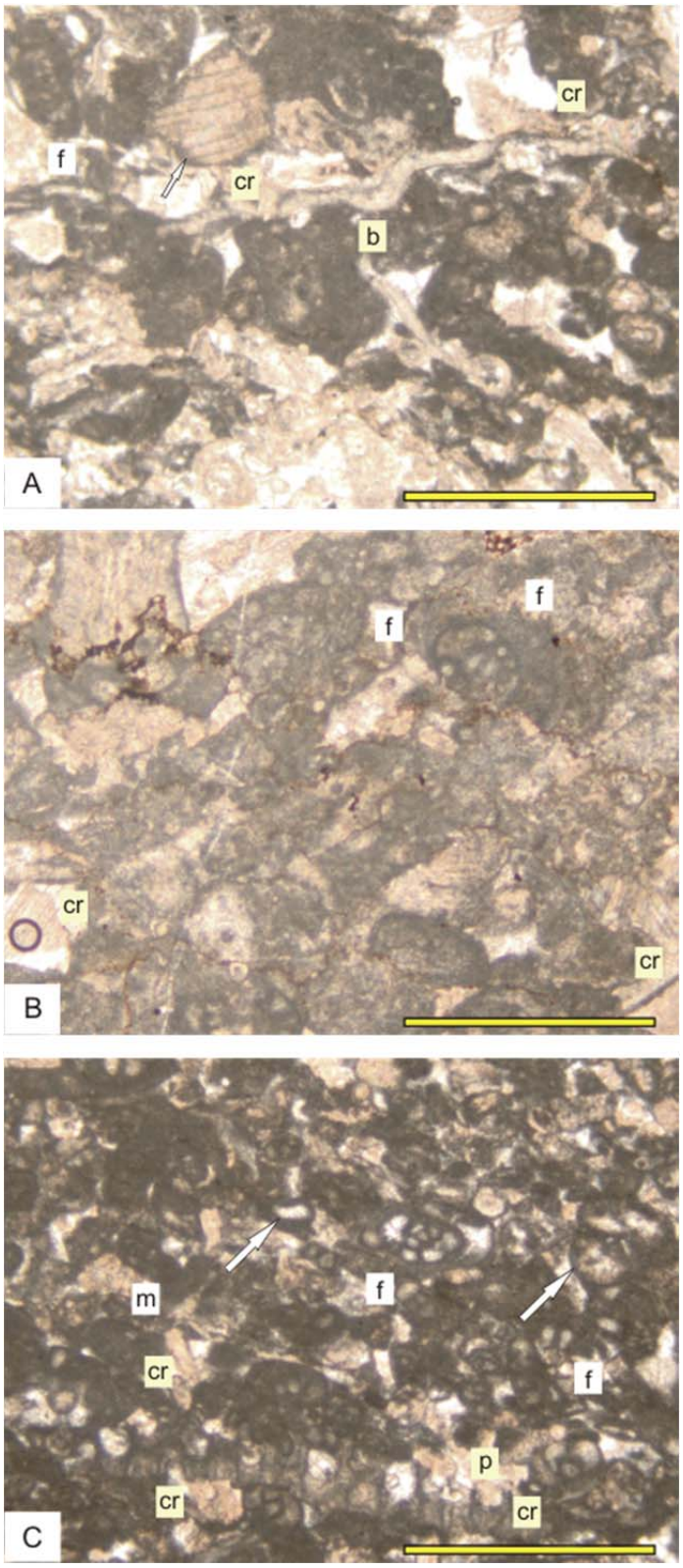

Figure 3.8: Photomicrographs of bioclastic packstone to grainstone. **A:** SC-17. **B:** SC-72. **C:** SC-23. (f: foraminifera, cr: crinoid fragments, b: bivalve fragment, p: pelloids, m: micritized skeletal grain, white arrow: micrite envelope). Scale bar: 1mm.

3.1.2.2 Bioclastic Grainstone (BG)

Bioclastic grainstone microfacies composed mainly of skeletal grains bounded by sparry calcite cement. This microfacies is the major element of bioclastic shoals or bars. Bioclastic bars forms barriers and they represent high energy shallow water conditions.

This microfacies is subdivided into 2 submicrofacies in such a way that crinoids and foraminifers are very high in abundance regarding to other skeletal grains in crinoidal - pelloidal - foraminiferal grainstone, but, relative abundance of different skeletal grains in bioclastic grainstone with equally distributed skeletal grains is nearly equal (Table 3.2). This microfacies corresponds to FZ 6 of Wilson model and similar to RMF 26 and SMF 12-S of Flügel (2004).

3.1.2.2.1 Crinoidal – Pelloidal - Foraminiferal Grainstone (BG1)

As the name of the microfacies indicates, main components of this microfacies are crinoids, pelloids and foraminifers. Algae, bivalves, gastropods and ostracods are other bioclasts (Figure 3.9-A, B and C). However, gastropods and ostracods are not present in all beds. Quartz grains are found in all thin sections, but their abundance is variable.

In all bioclastic grainstone microfacies crinoids are the great contributors. They are observed in all facies representing the bioclastic shoal. Such a widespread spatial distribution of crinoids indicates high energy conditions (Ahmad et al., 2006). Fecal pellets may be found in basinward proximal lagoonal setting which is below the low tide limit (Ahmad et al., 2006). This fact can be interpreted such that this microfacies (BG1) could be deposited more basinward than bioclastic grainstone microfacies (BG2), but they represent the same depositional belt which is a high energy shallow marine environment located in an open marine setting (Wilson, 1975).

This microfacies is observed in SC-5, SC-6, SC-7, SC-8, SC-9, SC-12, SC-69, SC-70, SC-71 samples.

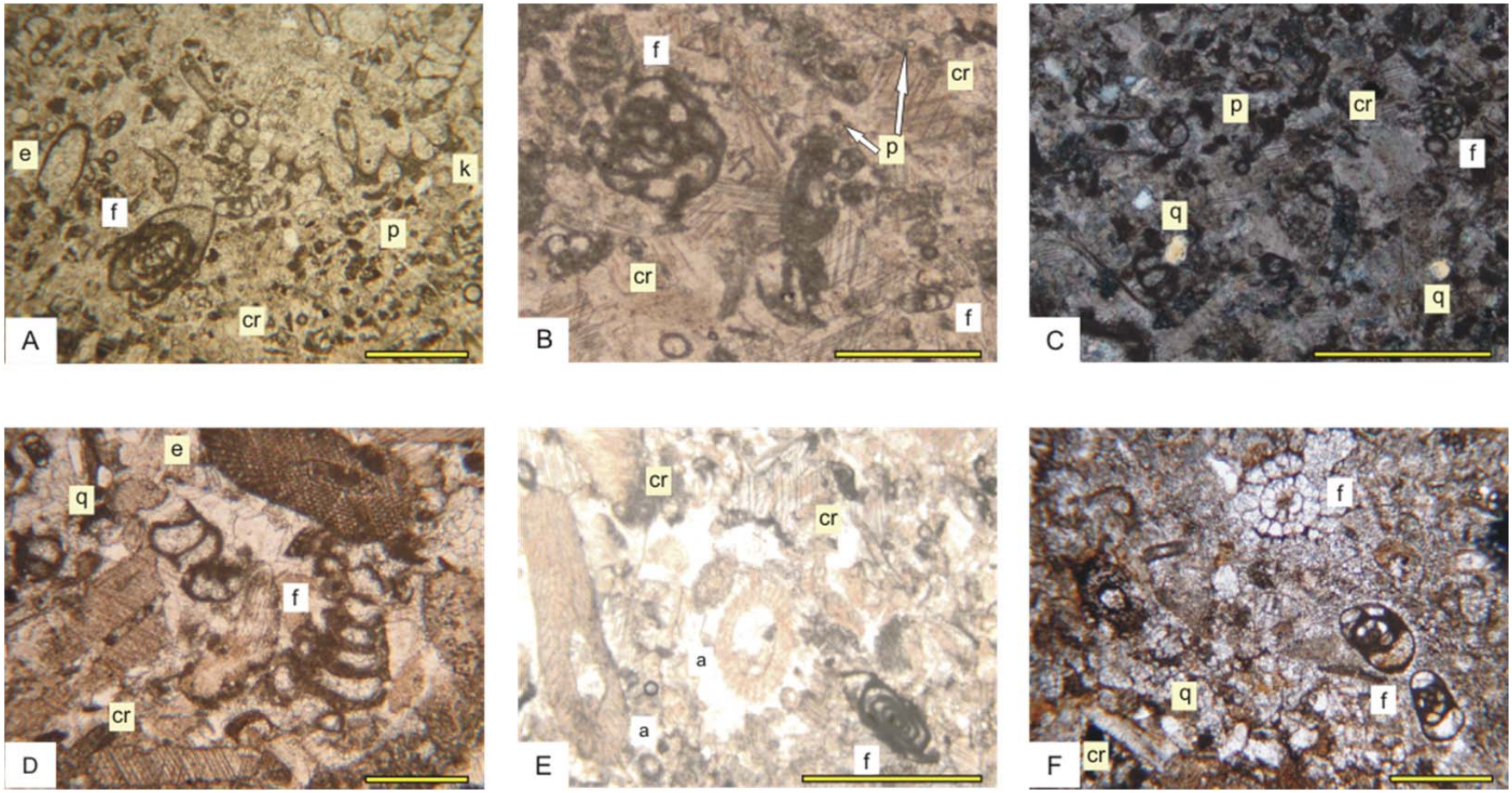

Figure 3.9: Photomicrographs of bioclastic grainstone. **A:** Crinoidal – pelloidal - foraminiferal grainstone (SC-5). **B:** Crinoidal – pelloidal - foraminiferal grainstone (SC-70). **C:** Crinoidal – pelloidal - foraminiferal grainstone (Analyzer in), (SC-12). **D:** Bioclastic grainstone with equally distributed skeletal grains (SC-83). **E:** Bioclastic grainstone with equally distributed skeletal grains (SC-90). **F:** Bioclastic grainstone with equally distributed skeletal grains (SC-79). (e: echinoderm spine, f: foraminifera, cr: crinoid fragments, p: pelloids, k: *Koninckopora*, q: quartz grain, a: algae). Scale bar: 500 μ for A, B, D, F; 1mm for C, F.

3.1.2.2.2 Bioclastic Grainstone with Equally Distributed Skeletal Grains (BG2)

The major elements characterizing this microfacies are bioclasts, namely, foraminifers, crinoids, bivalves and echinoids which are nearly equal in abundance.

Calcareous algae are low in amount. All these allochems are cemented by a sparry calcite cement (Figure 3.9-D, E and F). Grains are oriented in some thin sections (e.i., SC-86) but, this is not a representative phenomenon for the described microfacies. This orientation should be related to the effect of tidal currents during the time of deposition of bed SC-86.

Mainly uppermost Brigantian-Lower Serpukhovian beds are composed of this microfacies. These beds are SC-72, SC-74, SC-82, SC-83, SC-85, SC-86, SC-86A and SC-90. Samples SC-78 and SC-79 are represented by this microfacies however, they are different from the other samples. Composition and diversity of skeletal grains are similar to the other samples. However, whether the matrix of samples SC-78 and SC-79 is micrite or sparite cannot be certinly determined due to the recrystallization (Figure 3.9-F). Nevertheless, similarity of the constituents and abundance of crinoids lead us determine the microfacies of samples SC-78 and SC-79 as bioclastic grainstone. In addition, formation of microspar is seen as the evidence for meteoric diagenesis, for influence of low salinity or for subaerial exposure (Flügel, 2004). So this case explains the close proximity of this level to the sequence boundary which is located just below the bed SC-78.

This microfacies characterizes shoal environment occurring in shallow water setting with high wave and current action (Hüneke et al., 2001; Amirshahkarami et al., 2007).

3.1.2.3 Skeletal - Intraclast Grainstone (SIG)

Skeletal grains and intraclasts cemented by sparry calcite is the characteristic feature of this microfacies . Deposition probably occurred in high energy conditions above

wave base, so it is interpreted to be deposited in a high energy shoal environment. Although both this microfacies and bioclastic grainstone are deposited in shoal environment, this microfacies is likely to be deposited in lagoonward side of the bioclastic shoal (Amirshahkarami et al., 2007) and it equates the FZ 6 of Flügel (2004).

This microfacies is divided into 2 sub-microfacies, namely skeletal - intraclast grainstone with micritized skeletal grains and intraclast – crinoidal – pelloidal grainstone, both of which represent the same depositional belt (Table 3.2).

3.1.2.3.1 Skeletal - Intraclast Grainstone with Micritized Skeletal Grains (SIG1-SIG2)

Skeletal grains recognized in this microfacies are foraminifers, crinoids, bivalves, algae (*Koninckopora*) and echinoids. Most of the skeletal grains are current-oriented. Pelloids are non-skeletal grains observed in this microfacies but they are minor in amount. On the other hand, intraclasts which are also non skeletal grains are one of the major constituents of this microfacies (Figure 3.10-A, B, C and D). Most of the intraclasts are interpreted to be micritized skeletal grains and some of them are dark clasts. According to Ünal et al. (2003), presence of dark clasts indicates shallowing in subtidal cycles since they were probably winnowed from zones above wave base.

Dark clasts may be transported by tidal currents and deposited in high energy banks together with skeletal grains (Armella et al., 2007). So, the environment of deposition of this microfacies is a high energy shoal environment.

Careful observation of this microfacies showed that some representatives of it contains significant amount of micritized skeletal grains and dark clasts. For this reason, beds SC-27, SC-49, SC-55, SC-56, SC-61, SC-62, SC-63, and SC-68 are named as skeletal - intraclast grainstone with abundant micritized skeletal grains and dark clasts and abbreviation SIG2 is used (Figure 3.10-A and B). Other beds formed by this microfacies are SC-16, SC-17, SC-18, SC-20, SC-24, SC-53, SC-66, SC-84, SC-87

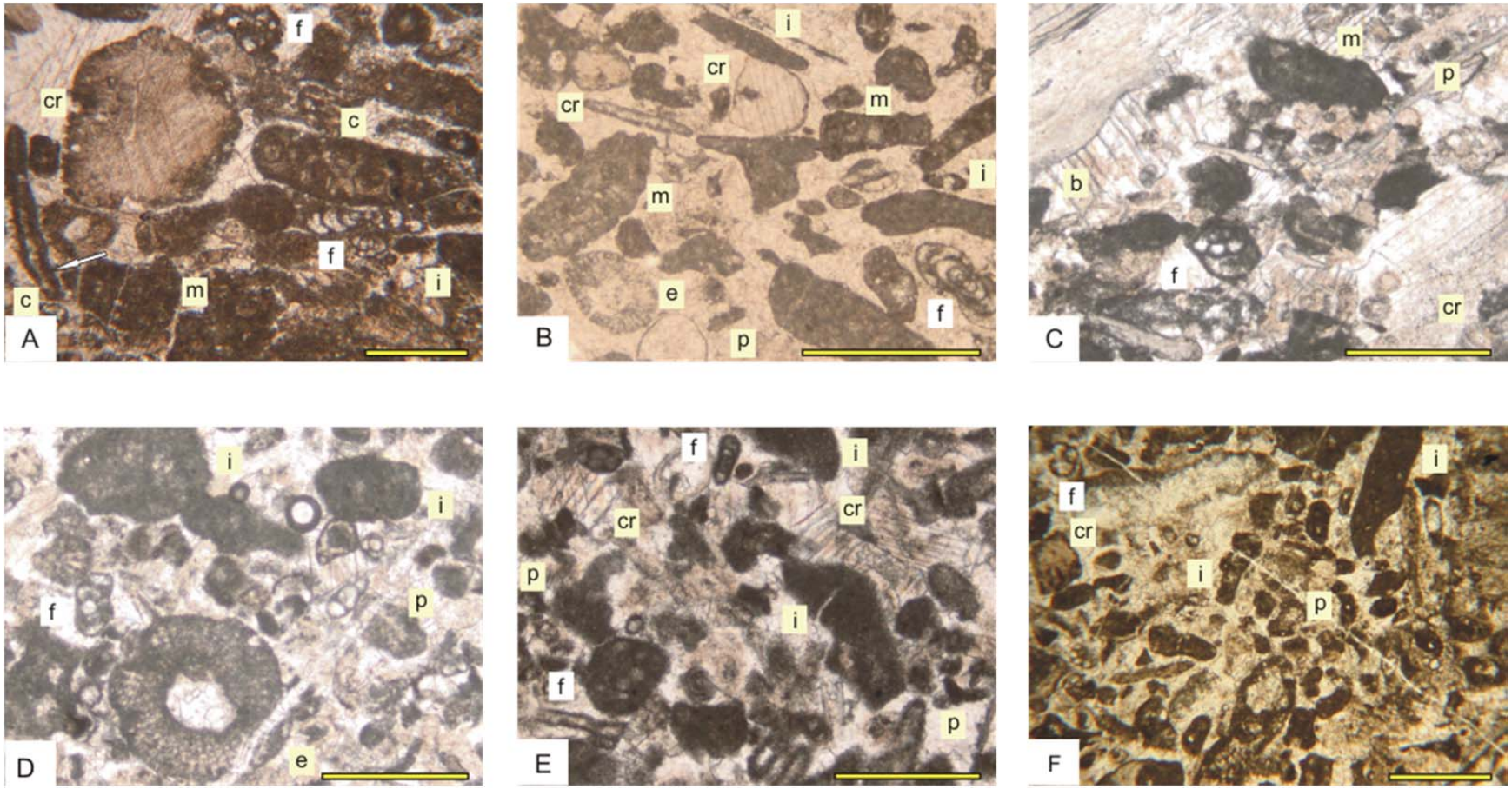

Figure 3. 10: Photomicrographs of skeletal - intraclast grainstone. **A:** SGI2 (SC-68). **B:** SGI2 (SC-49). **C:** SGI1 (SC-17). D: SGI1 (SC-18). E: SGI3 (SC-21). **F:** SGI3 (SC-51). (f: foraminifera, cr: crinoid fragments, c: cortoid, i: intraclast, m: micritized skeletal grain

and they are named as skeletal - intraclast grainstone with some micritized skeletal grains and are abbreviated as SIG1 (Figure 3.10-C and D).

3.1.2.3.2 Intraclast-Crinoidal-Pelloidal Grainstone (SIG3)

The relative abundance of main constituents which are intraclasts, crinoids and pelloids are nearly equal to each other. Apart from these major constituents, foraminifers, pelecypods, algae (*Koninckopora*) and echinoderms are found in the microfacies. There are also micritized or coated grains and some dark clasts (Figure 3.10-E and F).

This microfacies is a member of shoal facies and represents high energy, shallow, agitated water conditions.

SC-21, SC-42, SC-44, SC-45, SC-46, SC-47, SC-48, SC-50, SC-51 are the samples composed of this microfacies.

3.1.2.4 Intraclastic Grainstone (IG)

The characterizing allochems of this microfacies are intraclasts. However, their abundance may change from bed to bed. Other constituents of this microfacies are algae, crinoids and echinoids (Table 3.1 and Figure 3.11-A, B, C and D). Some intraclasts are micritized grains and dark clasts. These dark clasts are probably derived from supratidal ponds. Armella et al. (2007) defines these dark clasts or black pebbles as supratidal material.

This microfacies is a component of shoal facies (Atakul et al., 2011). A similar facies described by Armella et al. (2007) is located in high energy intertidal bars where constant wave action takes place. Considering the constituents, especially the presence of dark clasts, and the texture, this microfacies is interpreted to be deposited in a landward side of the bioclastic shoal environment. This microfacies close to SMF 17 defined by Flügel (2004) and indicate FZ 8 and FZ 7 facies belts.

This microfacies is seen in the samples SC-45, SC-48, SC-52, SC-64 and SC-65.

3.1.2.5 Sandy Bioclastic Grainstone (SBG)

Since dominant allochems are bioclasts and cement is sparry calcite, this facies can be called as bioclastic grainstone (Table 3.1). However, although the amount of quartz grains does not exceed the amount of carbonate grains, they are also very abundant in this microfacies. (Figure 3.11-E and F). Echinoids, crinoids, algae, foraminifers and bivalves are the main bio-constituents of this microfacies. The amount of foraminifers and bivalves are less than the other bio-constituents. Some bioclasts are coated. There are large dark micritic clasts deposited outside of the depositional area in the basin and transported. Algae are interpreted as *Kamaenella* or *Ungdarella*. This microfacies is similar in terms of some bio-constituents and texture to biofacies 2 of Gallagher and Somerville (2003) which contains *Pseudoendthyra*, paleotextularids, *Ungdarella* and paleoberesellid algal meadow.

Algae are good environmental indicator. For example, optimum depth for the development of *Kamaenella*, considered as a paleoberesellid, is 10 m which is approximately corresponding to fair weather wave base (Horbury and Adams, 1996) and Adams et al. (1992 in Rodríguez-Martínez et al., 2010) already stated that paleoberesellids generally occur in shallow subtidal environments. *Ungdarella* which can be called as pseudoalgea or microproblemetica is located intermound and flank areas of mud mounds in Rodríguez-Martínez et al. (2010); however, Della Porta et al. (2005) observed them in grainstone and packstone facies representing high energy shoal environments above wave base and moderate energy environments adjacent to the shoal below wave base relatively.

This microfacies is a chaotic mixture of diversified bioclasts, quartz grains and large, abraded micritic clasts and interpreted to be the result of storms since it is a densely packed grainstone consisting of skeletal debris and milimeter size micrite clasts (Flügel, 2004). *Kamaenella* is only observed in these micritic clasts so, it is interpreted to be deposited another environment where micrite was deposited and transported to this environment by storms. Evidences of transportation can be observed by the

abrasion of micritic clasts. Algal bioclasts can be transported easily by storms from open marine platform to near coastal environments (Flügel, 2004).

The environment of deposition corresponding to this microfacies should be a high energy shoal environment considering all the information above. Relative sea level fall causes the sea ward migration of backshore sand and continental sandy input and this siliciclastic input shows us that shoal should be developed close to the shore (Armella et al., 2007). Although Flügel (2004) model is not designed for mixed silicilastic and carbonate environments, this facies should be deposited in the environment corresponding to FZ 6.

The evidence of dissolution and compaction is reflected by stylolite development and probably iron minerals filled the stylolite contacts giving a red color to the facies.

Only sample SC-89 belongs to this microfacies.

3.1.3 Tidal Flat and Associated Facies

3.1.3.1 Pelloidal Packstone to Wackestone (PPW)

This microfacies is characterized by abundant pelloids and scarce biota (Table 3.1). Only a few ostracods and foraminifera present in this facies. In fact, this microfacies is composed of pelloidal micrite showing clotted fabric (Figure 3.12). Clotted fabric is associated with the microbial activity such that microbes and organic substances trigger biochemical precipitation (Flügel, 2004).

Due to lack of fossils and presence of micritic matrix, this microfacies defines low energy and restricted conditions that can form in a restricted lagoon environment at the back of a bioclastic bar. Pelloidal facies are generally formed in moderate to low energy settings and although this is not a general rule, they mostly characterize semi-restricted environments (Hüneke et al., 2001; Védrine and Strasser, 2009). Armella et al. (2007) placed a subtidal low energy environment corresponding to a

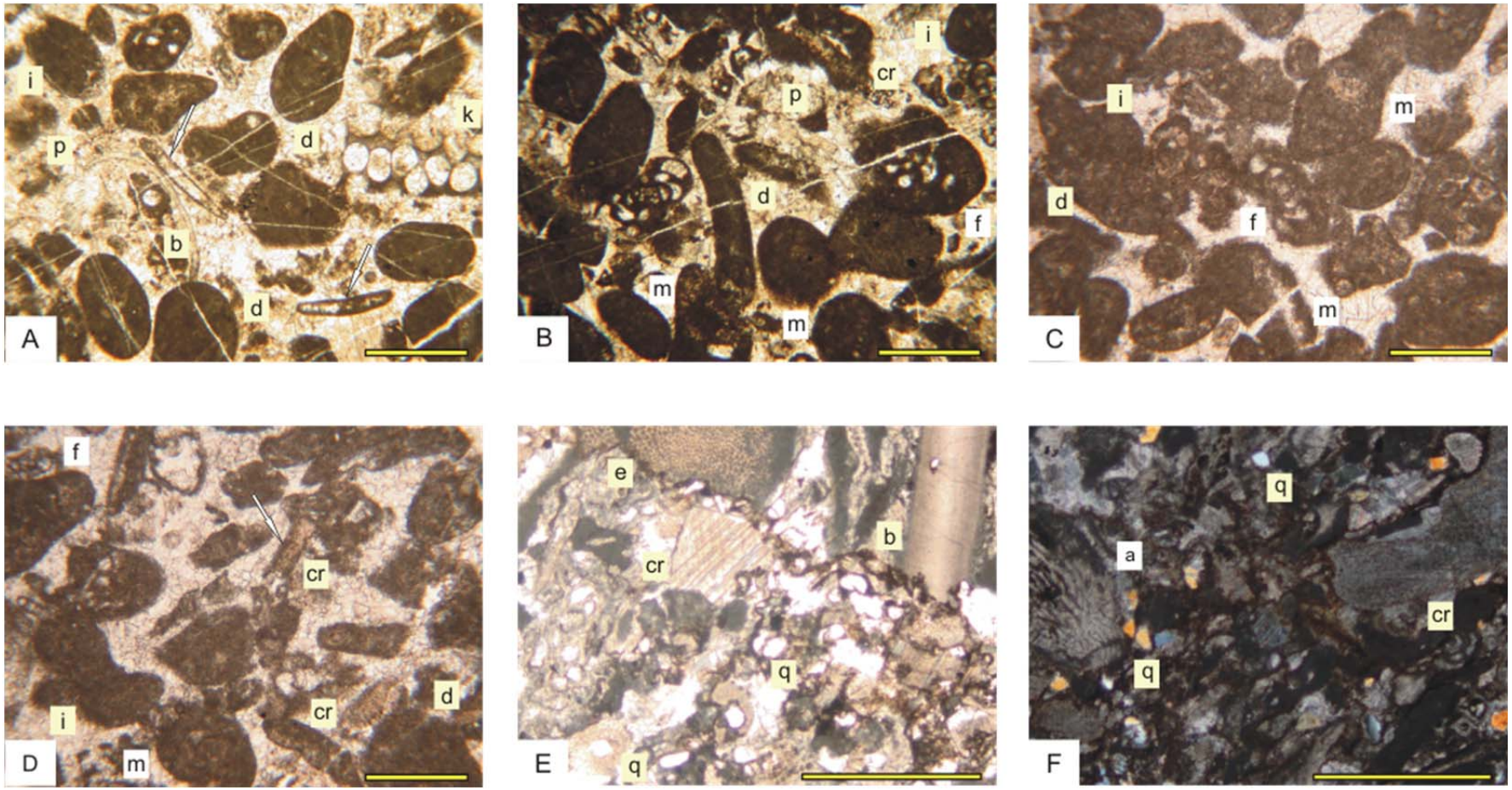

Figure 3. 11: Photomicrographs of intraclastic grainstone and sandy bioclastic grainstone. **A:** Intraclastic grainstone (SC-52). **B:** Intraclastic grainstone (SC-65). **C-D:** Intraclastic grainstone (SC-64). **E-F:** Sandy bioclastic grainstone (SC-89). (b: bivalve, k: *Koninckopora*, d: dark clast, i: intraclasts, p: pelloids, cr: crinoid fragments, f: foraminifera , m: micritized skeletal grain, e: echinoderm spine, q: quartz grain, a: algae, white arrow: micrite envelope). Scale bar: 500 μ for A, B, C D,; 1mm for E, F.

semi protected inner shelf at the back of a bar and suggest deposition of pelloidal intraclast wackestone or packstone in this environment. This facies can be

interpreted with fine grained lime wackestone and mudstone in tidal flat and lagoon environment (Al-Tawil et al., 2003). Wilson (1975) defines similar facies in FZ 8 in its model.

The only sample containing this microfacies is SC-28.

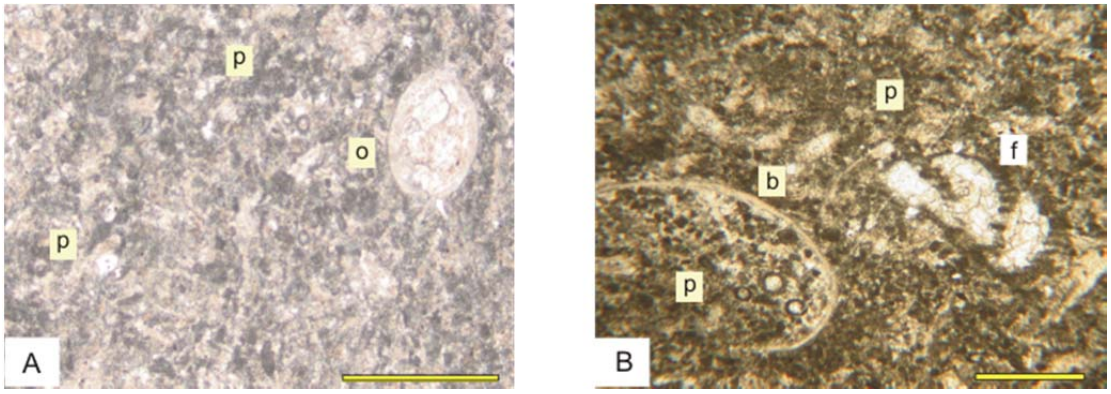

Figure 3. 12: Photomicrographs of pelloidal packstone to wackestone. **A-B:** SC-28. (p: pelloid, o: ostracod, b: bivalve, f: foraminifer). Scale bar: 500 μ for B and 1mm for A.

3.1.3.2 Wackestone Mudstone (WM)

Intraclastic wackestone with ostracods, mudstone with fenestral fabric and intraclastic (dark clast) wackestone with fenestral fabric are the major facies types which could be included under this group (Table 3.2). Due to high abundance of micrite and paucity of allochems this microfacies is named as wackestone mudstone microfacies.

Mud supported texture and scarce fauna characterize a restricted lagoonal setting (Raspini, 2001; Colombié and Strasser, 2005). This microfacies is comparable with SMF 23 and represents FZ 9 or FZ 8 (Flügel, 2004).

3.1.3.2.1 Intraclastic Wackestone with Ostracods (IOW)

Intraclasts consisting mostly of small sized dark clasts or black pebbles and ostracods in micritic matrix are the characteristic allochems of this microfacies (Figure 3.13- A, B and C). Sparitic texture is also present in patches (Figure 3.13–A). This may be the result of changes in the position of the wave base possibly related to storms (Kakizaki and Kano, 2009) or episodic high energy events (Colombié and Strasser, 2005; Joachimski, 1994). A few fenestral voids are observed in samples. One of the remarkable cases in the samples is that most of the cavities formed by the internal parts of ostracods were filled with micrite however; infilling micrite is not the same with the one forming the matrix. Infilling micrite is darker and denser than the matrix. In Figure 3.13-B infilling micrite is indicated by a blue arrow. So, this situation is interpreted such that ostracods and dense, darker micrite which should be a post storm in filling (Flügel, 2004) deposited in a different environment, which has also restricted conditions, or in different time but, transported to this environment probably by storm events. Presence of high amount of monotypic ostracods indicates very shallow water conditions and probably the fresh water input from time to time (Schulze et al., 2005).

Samples SC-38 and SC-39 show the characteristics of this microfacies. The only difference between them is that SC- 38 contains more ostracods. Sample SC-75 has also wackestone texture but it does not contain dark clasts. The most abundant allochems in sample SC-75 are totally micritized foraminifers (Figure 3.13-C). This may indicate their transportation before deposition (Hüneke et al., 2001). Moreover, this microfacies is seen after a transgressive period. Cateneau (2006) stated that shallow subtidal depozones or lagoons can be created as a result of excess of accommodation formed by slow transgression. In such a case sea connection may be established. Then, lagoon becomes more semi-restricted rather than restricted. Because restricted lagoons contain low diverse fauna however, fauna in semiresticed lagoons have moderate diversity (Bauer et al., 2002; Colombié and Strasser, 2005). Crinoids, which may sometimes be found in a restricted environment by deposition mechanically after death, are also observed in fewer

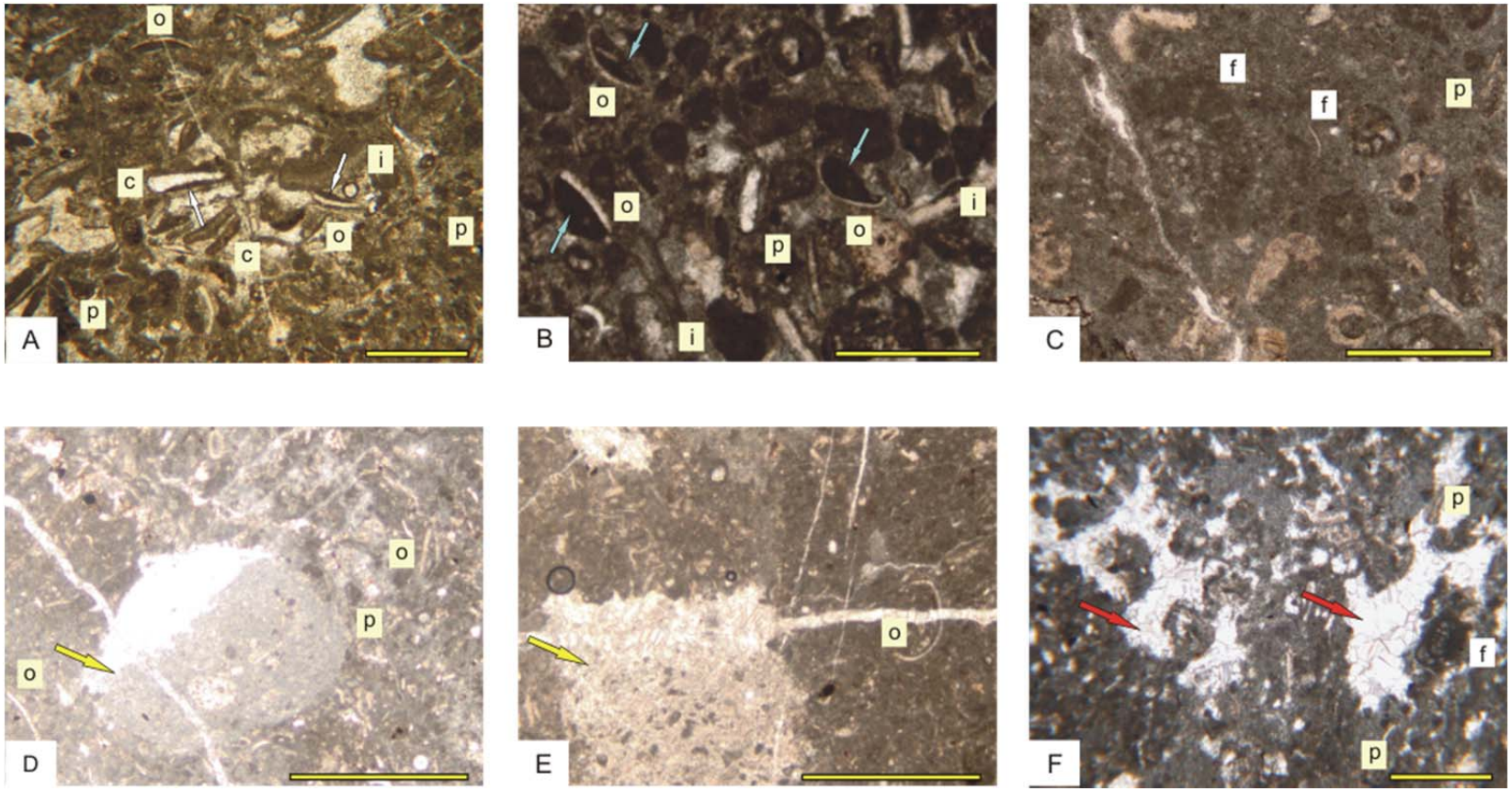

Figure 3. 13: Photomicrographs of wackestone-mudstone. **A:** Intraclastic wackestone with ostracods (SC-38). **B:** Intraclastic wackestone with ostracods (SC-39). **C:** Intraclastic wackestone with ostracods (SC-75). **D-E:** Mudstone with fenestral fabric , showing geopetal filling (in D geopetals fills in a dissolved shell) (SC- 40). **F:** Mudstone with fenestral fabric (SC-80). (o: ostracod, c: coated grain, p: pelloid, i: intraclasts, f: foraminifer, white arrow: micrite envelope, blue arrow: micrite infilling in ostracod shell, yellow arrow: geopetal filling, red arrow: fenestral fabric). Scale bar: 500 μ for A, F; 1mm for B, C, D, E.

amounts (Ahmadat et al., 2006). This microfacies belongs to shallow water, low energy environment. It is deposited in a lagoonal setting (Armella et al., 2007) in the shallow subtidal zone (Atakul et al., 2011). However, it should be affected by storm events.

3.2.3.2.2 Mudstone with Fenestral Fabric (MF)

Lime mud containing fenestral cavities is the essential component of this microfacies. It is observed in the samples SC-40, SC-41 and SC-80. Samples showing the characteristics of this microfacies include ostracods and pellets but their abundance changes in different samples (Figure 3.13-D, E and F). While SC-41 and SC-40 contains numerous ostracods, in SC-80 their number decreases dramatically. On the other hand, SC-80 includes a few foraminifera while SC-40 and SC-41 do not contain any. Common trait of all these samples is the lime mud and fenestral fabric that is very significant in the interpretation of paleoenvironments. For example, similar deposits in Colombié and Strasser (2005) are shown to be deposited in tidal flat and marsh subenvironments and pelloid and bioclast deposition is explained as spring or storm tide deposition in upper intertidal and supratidal environment.

Variously sized open spaced structures resembling blind windows in limestones are called as fenestral fabric (Flügel, 2004) (Figure 3.13-F). Shrinkage and expansion, gas bubble formation, escape of air during flooding or even burrowing may cause the formation of birdseye or fenestral structures (Shin, 1983, in Amirshahkarami et al., 2007). Fenestral fabrics are good environmental indicators and they characterize shallow near coast supratidal and upper intertidal environments (Flügel, 2004; Hüneke et al., 1991).

Additionally, in the samples SC-40 and SC-41 geopetal fabric is observed (Figure 3.13-D and F). Flügel (2004) defines geopetal fabric as “particles and mud trapped in bottom reliefs or in intra- or interskeletal cavities, grains deposited on flat surfaces and normal grading with coarse particles at the bottom and fine grains at the top”. Geopetal filling observed in the samples SC-40 and SC-41 are interpreted as internal geopetals filling the fenestral cavities. Low sedimentation rates like in peritidal

environments generate suitable conditions for intraskeletal geopetal filling (Flügel, 2004).

Vadose silt which indicates intermittent subareal exposure of tidal platform interior carbonates (Flügel, 2004) is seen in the sample SC-40.

Since calm conditions are needed for deposition of carbonate mudstones, they can represent peritidal conditions and this microfacies characterizes low energy environment in a shallow water setting (Armella et al., 2007).

A similar facies which is fenestrate mudstone, in the study of Amirshahkarami et al. (2007), is interpreted to indicate a tidal flat environment due to fine grained nature, lack of fauna and presence of fenestral fabric.

Consequently this microfacies was deposited in a tidal flat setting.

3.1.3.2.3 Intraclastic (Dark Clast) Wackestone with Fenestral Fabric (IWF)

Dioristic feature of this microfacies is dark clasts in a micritic matrix. Some parts between grains are filled with pelloidal micrite. Additionally, algae (*Koninckopora*) and ostracods are present (Figure 3.14).

Dark intraclasts may be formed in such a way that thalli of allochthonous algea is eroded and filled with dark micrite (Noe, 1987 in Ünal et al., 2003). Strasser (1983) call these dark clasts as black pebbles and suggest that; if dark organic substances are available and if suitable geochemical and mineralogical conditions exist for preservation and fixation, blackening occur and while reworking takes place by waves, currents and storms on the exposed surface of blackened consolidated layer, black pebbles are formed. Local ponds are favorable environments for the deposition of this facies. These ponds provide shallow and calm conditions. Such ponds may be created by vertical accretion of bars in a shallow intertidal environment (Armella et al., 2007).

Samples SC-29 and SC-32 are composed of this facies.

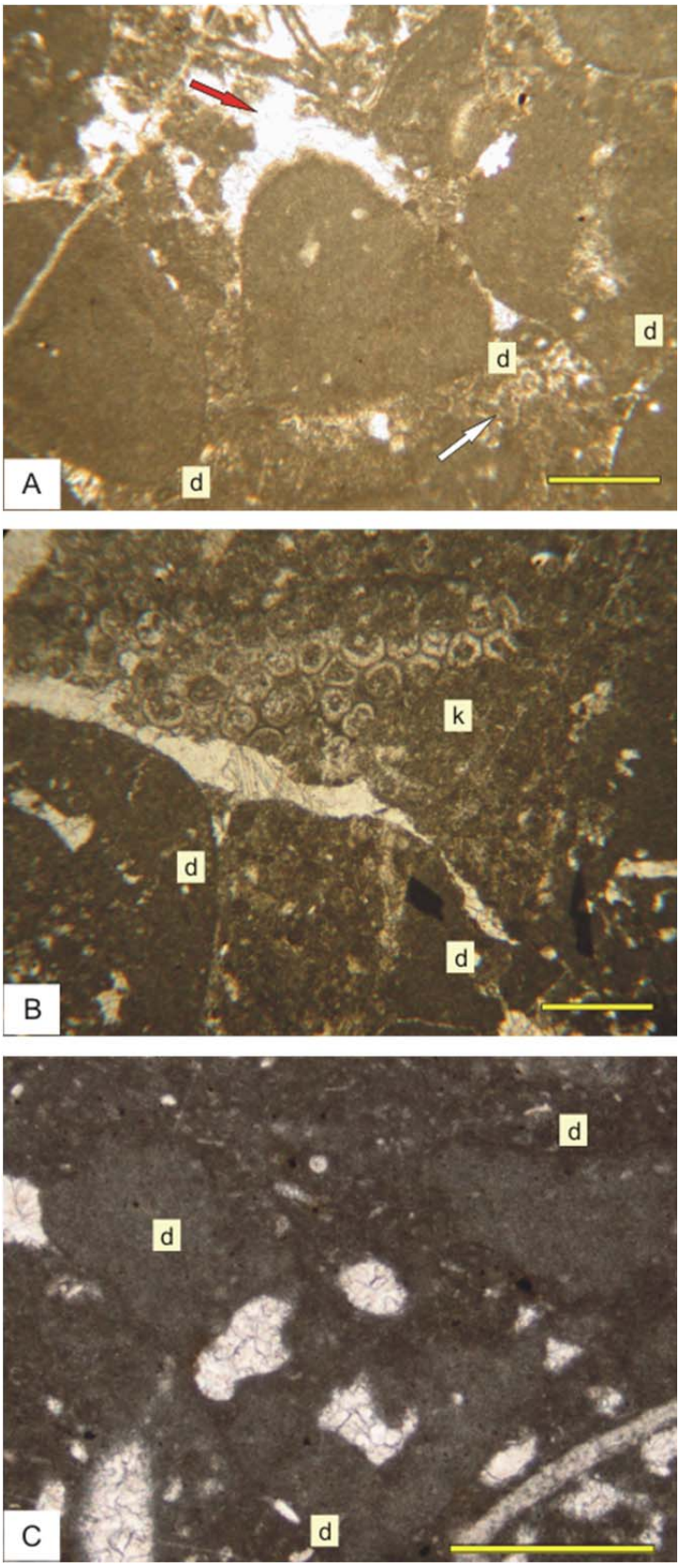

Figure 3. 14: Photomicrographs of intraclastic (dark clast) wackestone with fenestral fabric. **A-B:** SC-29. **C:** SC-32. (d: dark clast, k: konickopora,white arrow: pelloidal micrite, red arrow: fenestral fabric). Scale bar: 500μ for A, B; 1 mm for C.

3.1.3.3 Shale (Sh)

This microfacies is composed of silt and clay sized siliciclastic particles. It consists only of quartz minerals (Figure 3.15). It occurs in the sample SC-81. 50 g of this sample has waited for 3 days in 50% diluted hidrojen peroksit (H_2O_2) in order to

extract foraminifers if they exist. However, neither in thin section nor in the washing sample foraminifers were observed. So, this microfacies is completely unfossiliferous.

This microfacies is formed in a lagoonal setting because, lagoons which are shoreward of sandstone, siltstone units offer appropriate conditions for the formation of poorly fossiliferous thin shales (Ettensohn et al., 1984). Shale microfacies is seen above fenestral mudstone microfacies. This case favors that it is deposited in a very shallow water environment because; close association of shale with peritidal mudstone and ooid grainstone facies supports its shallow water setting (Al Tawil and Read, 2003). In addition any pelagic fauna have not been observed in the studied section. So, pelagic environment does not take into account as the possible environment of deposition.

Sample SC-81 is composed of shale microfacies.

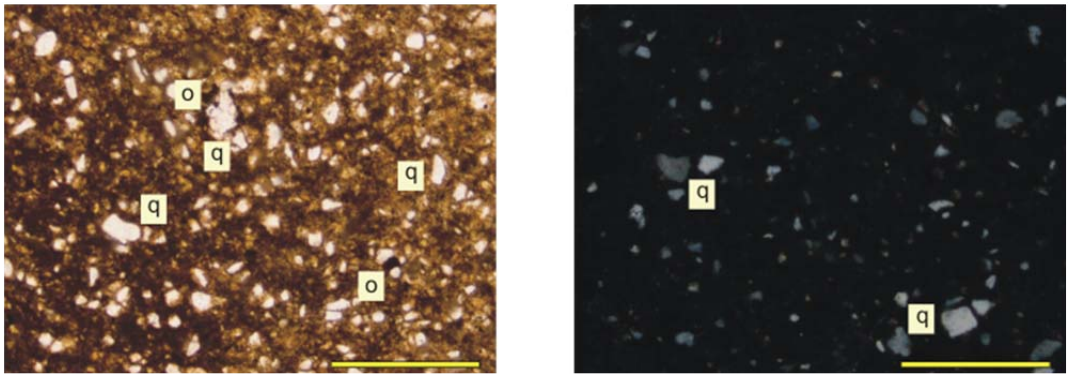

Figure 3. 15: Shale. **A:** SC-81. **B:** Analayzer in view (SC-81). (q: quartz, o: opaq mineral). Scale bar: 1mm.

4.1.3.4 Pelloidal Grainstone or Pelloidal Packstone to Grainstone Including Dark Clasts (PPG)

Pelloids in sparitic cement define this facies. Other allochems are dark intraclasts, foraminifera and algae (*Koninckopora*) (Table 3.1 and Figure 3.16-A, B and C). However, abundance of allochems is very variable. For example, in samples SC-34, SC-36 (Figure 3.16- C) abundance of foraminifers is lesser than samples SC-33, SC-35 (Figure 3.16-A-B) while dark clasts, which are considered to be derived from pond environment, is much higher than the other constituents. This may be the result of resistance of dark clasts to disintegration due to their early cementation and stable mineralogy so that they are preserved while unconsolidated sediment is washed away (Strasser, 1983). Micrite content of samples also changes from sample to sample. To illustrate, samples SC-33 and SC-36 lacks of micrite so they are named as grainstone however, in some parts of thin sections SC-34 and SC-35 micritic matrix can be seen and they are named as packstone to grainstone. This is considered to be the result of changing energy conditions.

This microfacies is interpreted to be a tidal channel facies (Joaschimski, 1994). Chamley et al. (1997) have described a similar microfacies in a channel and shallow pool environment and Colombié and Strasser (2005) located tidal channels in a back barrier setting or tidal flat environment. Ahmad et al. (2006) suggest the place of deposition as the lagoonward side of the shoal due to abrasion and lagoonward transportation of allochems (Ahmad et al., 2006).

It is similar to SMF 16 defined by Flügel (2004) which represents FZ 8.

Samples SC-31, SC-33, SC-34, SC-35, SC-36 and SC-43 are composed of this microfacies.

3.1.3.5 Pelloidal Packstone to Grainstone with Fenestral Fabric (PPGF)

This microfacies is composed of pelloids and large fenestral cavities. Skeletal grains in this microfacies are ostracods and a few foraminifera. Dark clasts can also be recognized (Table 3.1, Figure 3.16-D, E and F).

Samples SC-30 and SC-37 show the characteristic features of this microfacies. Sample SC-30 shows alteration with mudstone with fenestral fabric.

Fenestral fabric is commonly associated with pelleted sediment and generally best develop in tidal flats (Wilson, 1975). Wilson (1975) exemplified that "Fenestral fabric in pelloidal grainstone-packstone and wackestone with varying amounts of micrite matrix; some mud cracks; occurs commonly at top of sedimentary cycles in Pillara Limestone of Australia."

Pelloidal facies of tidal flat sequences occur in protected coastal lagoon which is seaward side of the intertidal zone where pelleted mud readily stirred with suspension and transported to the flats during storm events (Hüneke et al., 2001).

This facies is interpreted to be deposited in a tidal flat environment. It represent most landward position and forms at the cycle tops. This microfacies is comparable with SMF 21 and FZ 8, FZ 9 (Flügel, 2004).

3.1.3.6 Quartz Arenitic Sandstone (S)

Since more than 90% of the grains are quartz, this microfacies is named as quartz arenitic sandstone (Figure 3.17). This microfacies is observed in the samples SC-75A, SC-76 and SC-77. Except for SC-76, other samples do not contain any grain rather than quartz. However, in sample SC-76 a few crinoids and one bivalve shell are observed.

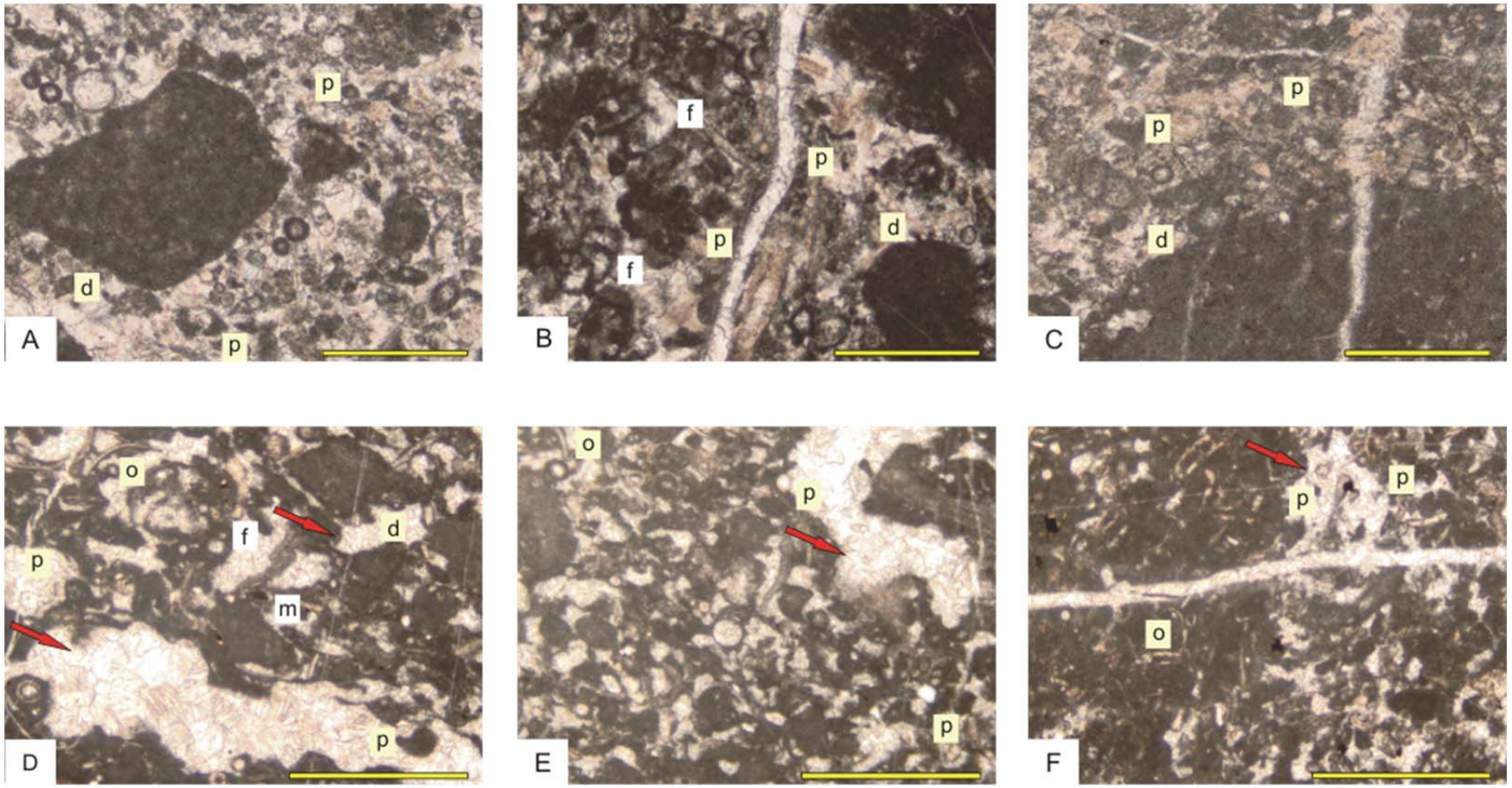

Figure 3. 16: Photomicrographs of pelloidal grainstone or pelloidal packstone to grainstone including dark clasts (PPG) and pelloidal packstone to grainstone with fenestral fabric (PPGF). **3. 1: A:** PPG (SC-33). **B:** PPG (SC-35). **C:** PPG (SC-36). **D-E:** PPGF (SC-30). **F:** PPGF (SC-37). (p: pelloid, d: dark clast, , f: foraminifer, o: ostracod, m: micritized skeletal grains, red arrow: fenestral fabric). Scale bar: 500 μ for A, B, C; 1mm for D, E, F.

This microfacies is only seen once in the whole succession. It represents a major fall in sea level. It was deposited in peritidal zone (Atakul et al., 2011). The depositional environment corresponds to FZ 10 of Flügel (2004).

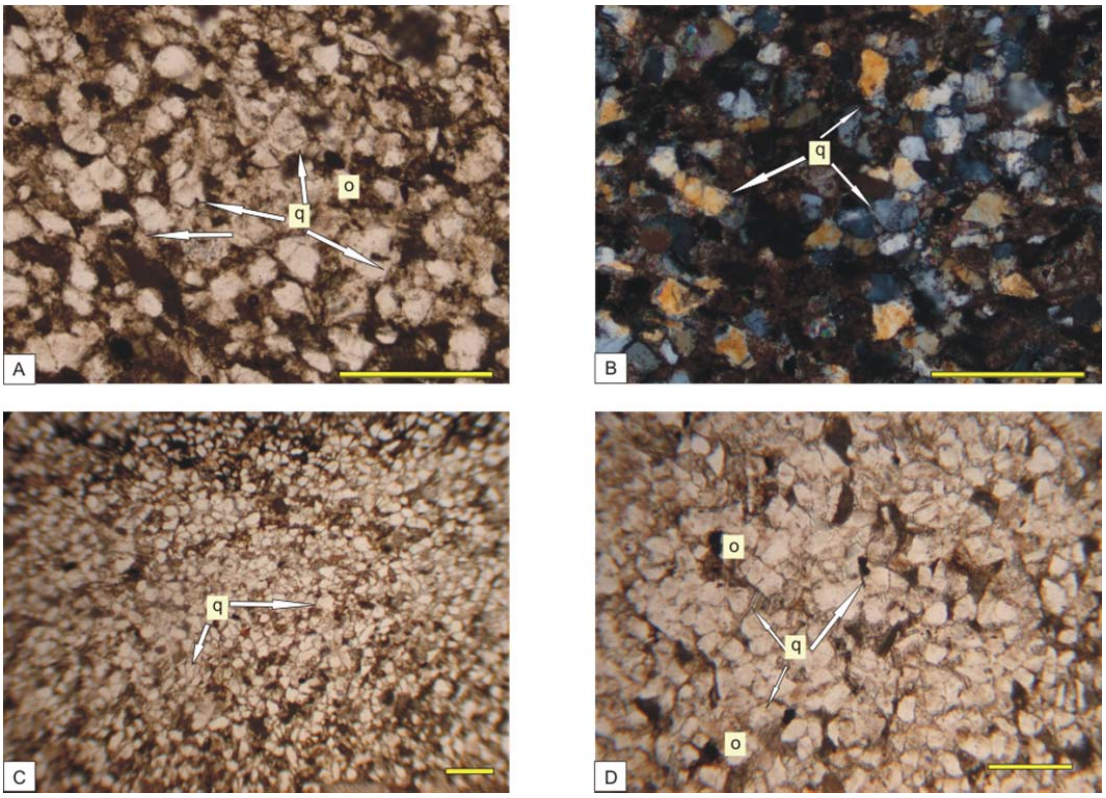

Figure 3. 17: Photomicrograps of quartz arenitic sandstone. **A:** SC-75A. **B:** SC-75A (Analyzer in). **C:** SC-76. D: SC-77. (q: quartz, o: opaq minerals). Scale bar: 500 μ for C, D; 1mm for A, B.

3.2.3 Composite Depositional Model and Facies Distribution

Since most carbonate sediments are naturally autochthonous, they offer a great advantage in interpretation of depositional environments (Wilson, 1975).

Using especially platform type carbonate deposition models proposed by Wilson (1975) and Flügel (2004) and referring also works of various authors a two dimensional time independent depositional model illustrating lateral changes of depositional environments is proposed. According to this model, 12 main microfacies were attributed to 3 main facies belts namely, open marine, bioclastic shoal and tidal flat that include restricted lagoon, pond and tidal channel subenvironments (Figure 3.18).

Open marine facies belt in this model is only represented by bioclastic packstone microfacies (Figure 3.18). Despite bioclastic wackestone and mudstone are important elements of this facies belt, they were not observed in the measured section since the studied section does not cross the basinward side of the open marine facies. Many researchers (Hüneke et al., 1991; Chamley et al., 1997; Colombié and Strasser, 2005; Al – Tawil and Read, 2003; Védrine and Strasser 2009) agreed that skeletal or bioclastic packstones indicate open marine conditions below wave base.

Bioclastic packstone to grainstone, bioclastic packstone and intraclastic grainstone are the major components of bioclastic shoal environment, because they are suitable to be deposited in a shallow water high-energy setting (Raspini, 2001; Ahmad et al., 2006; Colombié and Strasser, 2005; Amirshahkarami et al., 2007) (Figure 3.18).
During significant falls in sea level, sandy bioclastic grainstone is deposited on the shoal due to significant rise in clastic sediment influx.

"Carbonate tidal flats occur in settings which are protected from open ocean waves" (Flügel, 2004). In the proposed model tidal flat environment which indicates low energy, calm conditions, is located to the landward side of the bioclastic shoal (Figure 3.18). Tidal flat environment also comprises subenvironments in which lagoonal and tidal flat pond facies and tidal channel facies are deposited. Typically, mudstone - wackestone microfacies and pelloidal microfacies are deposited in tidal flat environment. Pelloidal packstone to wackestone and intraclastic wackestone with ostracods characterize restricted lagoonal environment (Hüneke et al., 2001; Al-Tawil et

al., 2003; Védrine and Strasser, 2009). However, slow transgressive periods create excess accommodation and forms lagoons (Cateneau, 2006) and tidal inlets sometimes may cut the barrier (shoal) and allow the connection of lagoon and open sea (Védrine, S., Strasser, A., 2009) such that lagoon gains a semi-restricted character and more diverse fauna can be observed in wackestone microfacies. As relative sea level falls significantly and siliciclastic input increases, shale may develop in a lagoonal setting. In tidal flats, changes of the tide line may cause developments of local ponds. In this model these ponds are represented by intraclastic (dark clast) wackestone with fenestral fabric and mudstone with fenestral fabric microfacies (Bauer et al., 2002; Colombié and Strasser, 2005; Amirshahkarami et al., 2007) (Figure 3.18).

Tidal channels may develop in intertidal flat, near local ponds or just at the back of the barrier (bioclastic shoal) (Colombié and Strasser, 2005; Ahmad et al., 2006) and they are represented by pelloidal grainstone or packstone to grainstone including dark clasts microfacies.

The most landward side of the tidal flat environment is occupied by pelloidal packstone to grainstone with fenestral fabric microfacies (Wilson, 1975) and quartz arenitic sandstone (Atakul et al., 2011) (Figure 3.18).

Ahmad et al. (2006) suggest that these distinct and irrelevant associations of microfacies are the result of high frequency dynamic environmental changes.

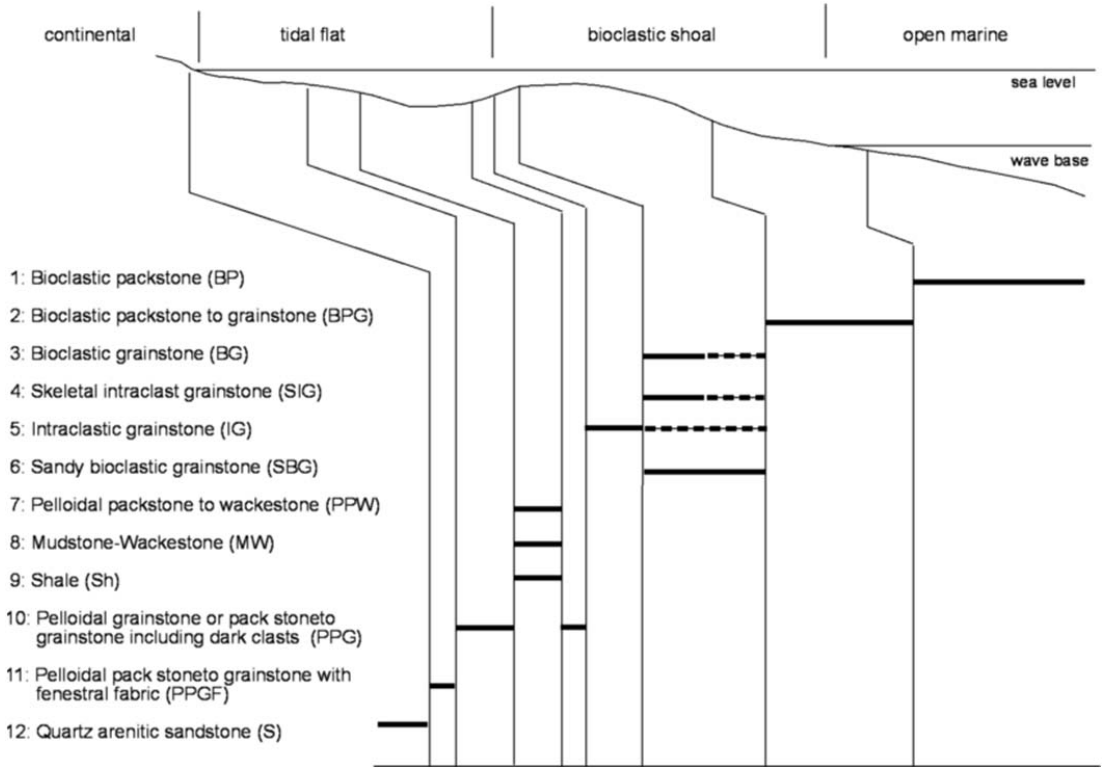

Figure 3. 18: Conceptual depositional model and associated facies distribution. (Solid line shows the most likely expected location, dashed line shows all possible locations)

CHAPTER 4

SEQUENCE STRATIGRAPHY

4.1 Background on Sequence Stratigraphy

One of the most important concepts that controls marine deposition is relative sea level changes. Sequence stratigraphic models were constructed to understand better eustatic fluctuations since; sequence stratigraphy is a very useful tool to exhibit the relationship between coastal and marine successions.

Sequence stratigraphy is a new technique that emerged during second half of the 20th century and developed by seismic and outcrop stratigraphy. Although since 1910's many researchers have recognized the relations between sea level fluctuations, sedimentation and unconformities, the relation of these parameters with depositional sequences has clearly revealed by the study of Vail et al. (1977). In addition, the work of Sloss (1963) should not be ignored since he is the one who first described the term sequence and a depositional sequence is the backbone of seismic stratigraphy. Sloss have considered sequences as major rock stratigraphic units of interregional scope, separated and delimited by interregional unconformities (Sloss, 1963). Nevertheless, depositional sequence concept has redefined by Mitchum et al. (1977) as "a stratigraphic unit composed of a relatively conformable succession of genetically related strata and bounded at its top and base by unconformities or their correlative conformities".

Since for deposition of sediments a space, which is called an accommodation space, is needed and the volume of this space can only be changed by a change of relative sea level, the relation between depositional sequence, sequence development and relative sea level fluctuations became important and accentuated in the studies of Vail et al. (1984). Strasser and Samankasou (2003) have stated that ''If sediment accumulation is controlled by sea level fluctuations, the concepts of sequence stratigraphy can be applied to describe and interpret the resulting sedimentary sequences''. Eustatic sea level fluctuations were documented for Mesozoic and Cenozoic on a global sea level chart prepared by Haq et al. (1987), for Paleozoic by Haq and Schutter (2008) and eustatic sea level changes have started to be used as global predictive tool for exploration (Emery, 1996).

While in 1970's physical relations are the most important criteria in a depositional sequence, in the late 1980's outcrop and well data came into prominence with the work of Posamentier et al. (1988) and Van Wagoner et al. (1988) such that sequence stratigraphy is defined as "the study of rock relationships within a chronostratigraphic framework of repetitive, genetically related strata bounded by surfaces of erosion or nondeposition, or their correlative conformities" (Van Wagoner et al., 1988). In the same study, a sequence is proposed as the fundamental unit of sequence stratigraphy and a sequence is subdivided into sytems tracts. System tracts are formed by depositional systems, which are three-dimensional assemblages of lithofacies, and they are defined by stacking patterns of parasequence sets or cycles that is relatively conformable succession of genetically related beds or bed sets bounded by marine flooding surfaces and their correlative surfaces (Van Wagoner et al., 1988).

In 1990's sequence stratigraphy has been regarded as a tool and Posamentier and James (1993) stated, "Sequence stratigraphy should be considered as a way of looking at and ordering geological data, rather than an end itself."

Sequence stratigraphy was first applied on siliciclastic depositional environments however, its application on carbonate systems did not take long time and Sarg discussed it in 1988. After this very significant work of Sarg on carbonate sequence stratigraphy other prominent publications on carbonate sequence stratigraphy belong to Hunt and Tucker (1993), Loucks and Sarg (1993), Tucker et al. (1993) and Schlager (2005).

According to Sarg (1988), relative sea level change is the most important and major control on carbonate productivity and platform or bank growth and therefore, on the resultant facies distribution. As a result, high-resolution sequence stratigraphic analysis requires interpretation of facies and gathers essential facies information to interpret depositional environments (Tresch and Strasser, 2010). In this study, a detailed microfacies analysis was carried out in order to detect the cyclic pattern of carbonate successions of Upper Visean and Lower Serpukhovian deposits of Aziziye Gediği Formation and to construct the sequence stratigraphic framework of these deposits.

4.2 Meter Scale Cycles

Deposition of various kinds of sediments within a repeated succession is known as cyclic sedimentation (Einsele et al., 1991) and eustatic sea level changes cause the formation of systematic cycles in the accommodation space created by tectonism and rise and fall of eustasy (Vail et al., 1991). Shallowing upward cycles are named as parasequences and the parasequence is defined as relatively conformable succession of bed or bedsets bounded by marine flooding surfaces and their correlative surfaces (Van Wagoner et al., 1988). Parasequences and parasequence sets are the building block of system tracts (Van Wagoner et al., 1990).

4.2.1 Types of Cycles

Types of cycles were determined based on the vertical stacking patterns of microfacies; eleven type, and nineteen sub-types of cycles were identified in the measured section. Cycles are mainly subtidal and intertidal character and composed of tidal flat, bioclastic shoal and open marine facies. Cycle tops were determined based on the presence of fenestral fabric or geopetal fabric, presence of dark clasts and clastic deposits like shale and sandstone. Except from one type of cycle, all of them are shallowing throughout. One of them shows deepening stage at first then it shallows upward.

In the present study a 59,61 m thick stratigraphic section is measured. 26 cycles were determined which have an average thickness 2,3 m. The thickness of individual cycles changes between 0,32 m and 10,45 m.

4.2.1.1 A Type Cycles

A type cycles are mainly characterized by the alternation of packstones and grainstones. All A type cycles start with bioclastic packstone and according to the variations in microfacies sub types are determined. There are five sub types within the cycle A. Cycle A1 (Figure 4.1) is capped by bioclastic grainstone whereas cycle A2 (Figure 4.1) is capped by skeletal intraclast grainstone. Cycle A3 (Figure 4.2) is one of the cycles characterized by a clear shallowing trend. It is similar to Cycle A2 in the lower part such that bioclastic packstone is followed by skeletal intraclast grainstone. Cycle A3 continues in its development in the following order: Pelloidal packstone to wackestone, intraclastic (dark clast) wackestone with fenestral fabric and pelloidal packstone to grainstone with fenestral fabric. Fenestral fabric indicates most landward position of the relative sea level and shows a significant fall in relative sea level. In cycle A4 (Figure 4.3) bioclastic packstone is followed by skeletal intraclast grainstone and it is capped by intraclastic grainstone and differs from the A2 type of cycle. In A5 (Figure 4.4) type cycle sandy bioclastic grainstone is deposited on top of bioclastic packstone

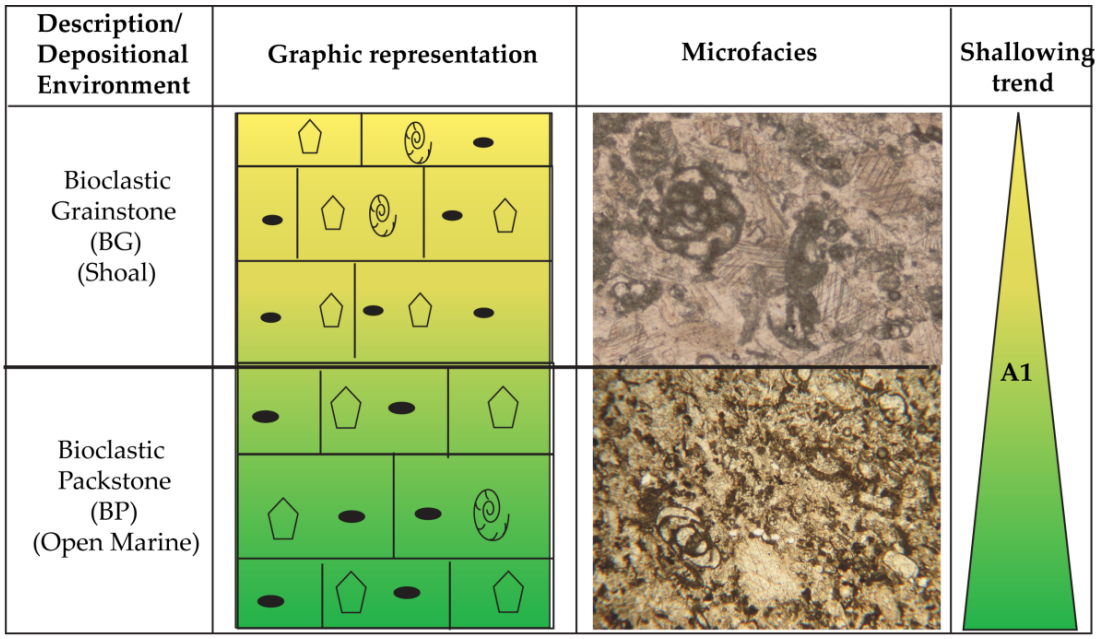

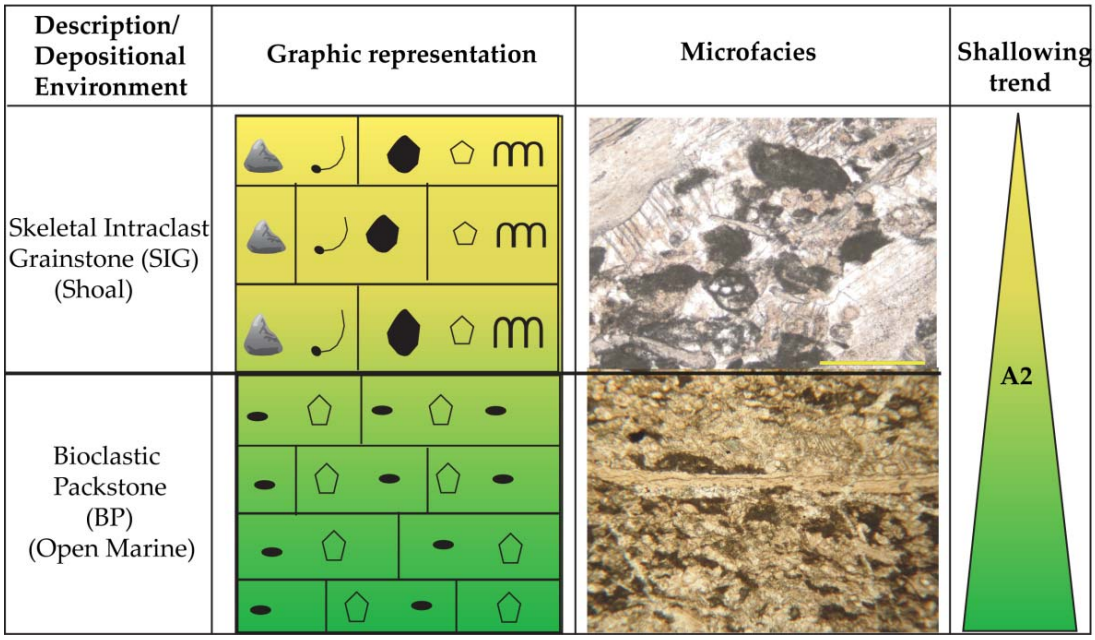

Figure 4. 1: A1 (Cycle 1) and A2 (Cycle 3) type cycles. For legend, see figure 5.15.

and this situation indicates a fall in relative sea level. A type cycles are periodically seen in the whole measured section.

4.2.1.2 B Type Cycles

These type of cycles are characterized by bioclastic packstone to grainstone at their base and divided into three subtypes namely B1, B2 and B3 based on the internal variations. B1 (Figure 4.4) type of cycle is capped by skeletal intraclast grainstone. B2 (Figure 4.5) type of cycle is similar to B1 type of cycle in terms of the two microfacies at the bottom, however, it is capped by intraclastic grainstone. In cycle type B3 (Figure 4.6), bioclastic grainstone is deposited on top of the bioclastic packstone to grainstone, and followed upwards by intraclastic wackestone with octracods. The cycle is capped by quartz arenitic sandstone. The appearance of quartz arenitic sandstone at the top of the cycle is an indicator of relative sea level fall. B type cycles are seen in the lower and middle part of the measured section.

4.2.1.3 C Type Cycles

There are three subtypes in the C types cycles namely C1, C2 and C3. All three types of cycles are observed in the middle part of the section after the first sequence boundary and they are consecutive. C type cycles are mainly characterized by pelloidal grainstone or pelloidal packstone to grainstone including dark clasts and subtypes are formed by the abundance of dark clasts since dark clasts are considered to be derived from supratidal or intertidal ponds and represent the sea level fall. The presence and abundance of dark clasts or black pebbles may indicate subareal exposure and/or shoaling in cycles.

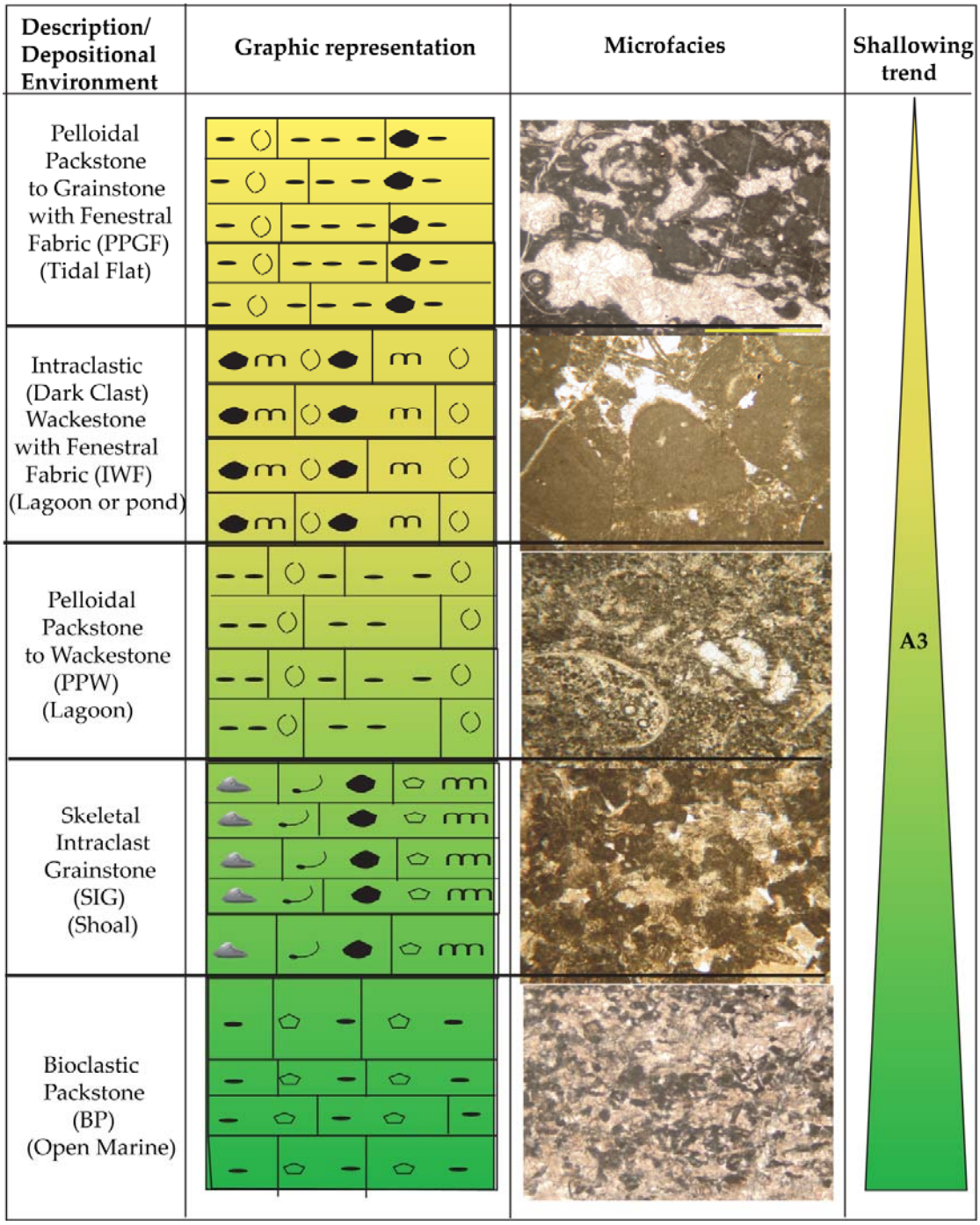

Figure 4. 2: A3 (Cycle 7) type cycle. For legend, see figure 5.15.

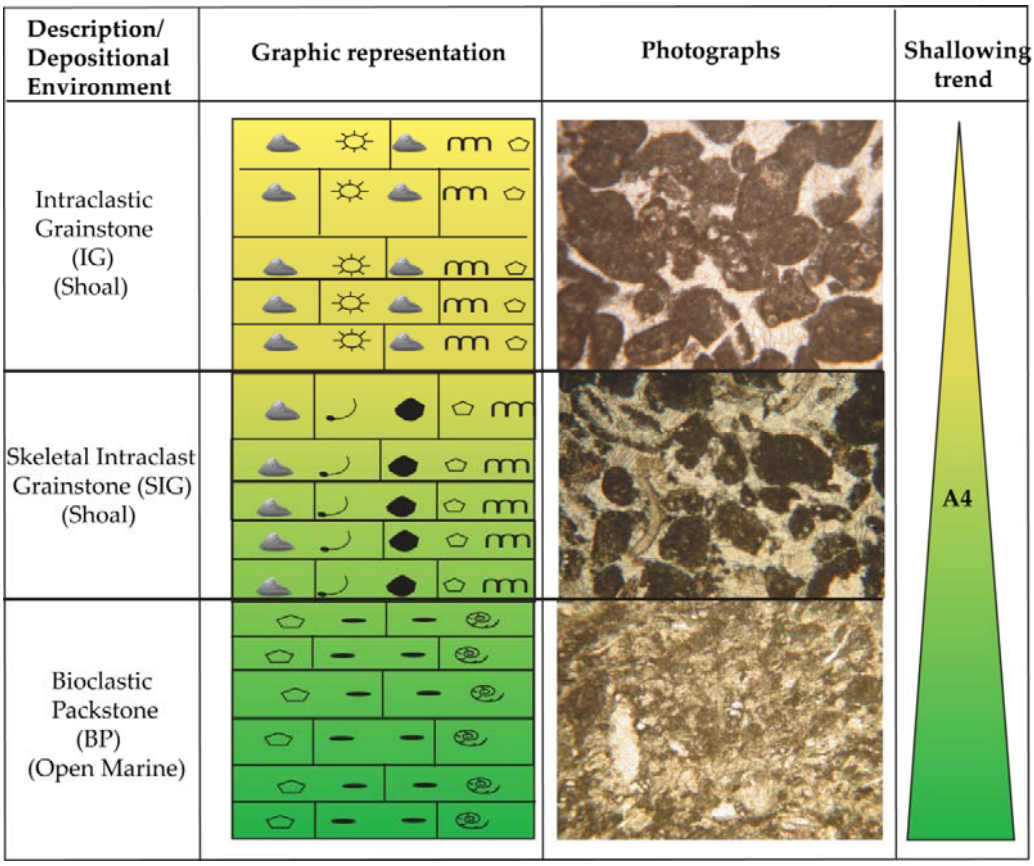

Figure 4. 3: A4 (Cycle 17) type cycle. For legend, see figure 5.15.

C1 type cycle (Figure 4.7) starts with pelloidal grainstone including dark clasts and capped by intraclastic (dark clast) wackestone with fenestral fabric. C2 type cycle (Figure 4.7) is characterized by the variation between pelloidal grainstone and pelloidal packsone to grainstone including dark clasts such that the microfacies made up of less dark clast is at the bottom, more dark clast is at the top. In the cycle type C3 (Figure 4.8) the first microfacies is composed of pelloidal packstone including dark clasts and capped by pelloidal packstone to grainstone with fenestral fabric. C types cycles are observed in the middle part of the section, above the first sequence boundary.

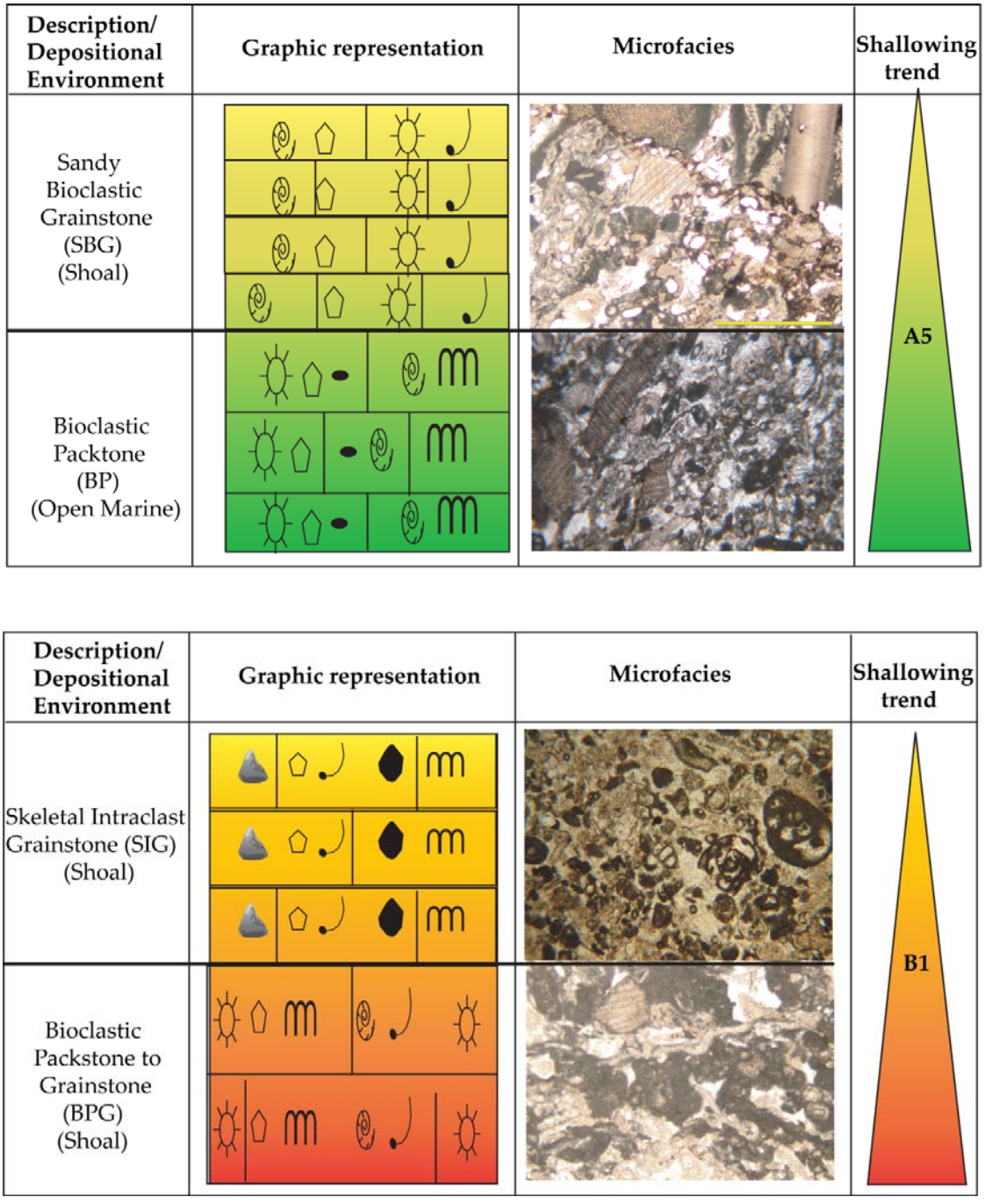

Figure 4. 4: A5 (Cycle 25) and B1 (Cycle 4) type cycles. For legend, see figure 5.15.

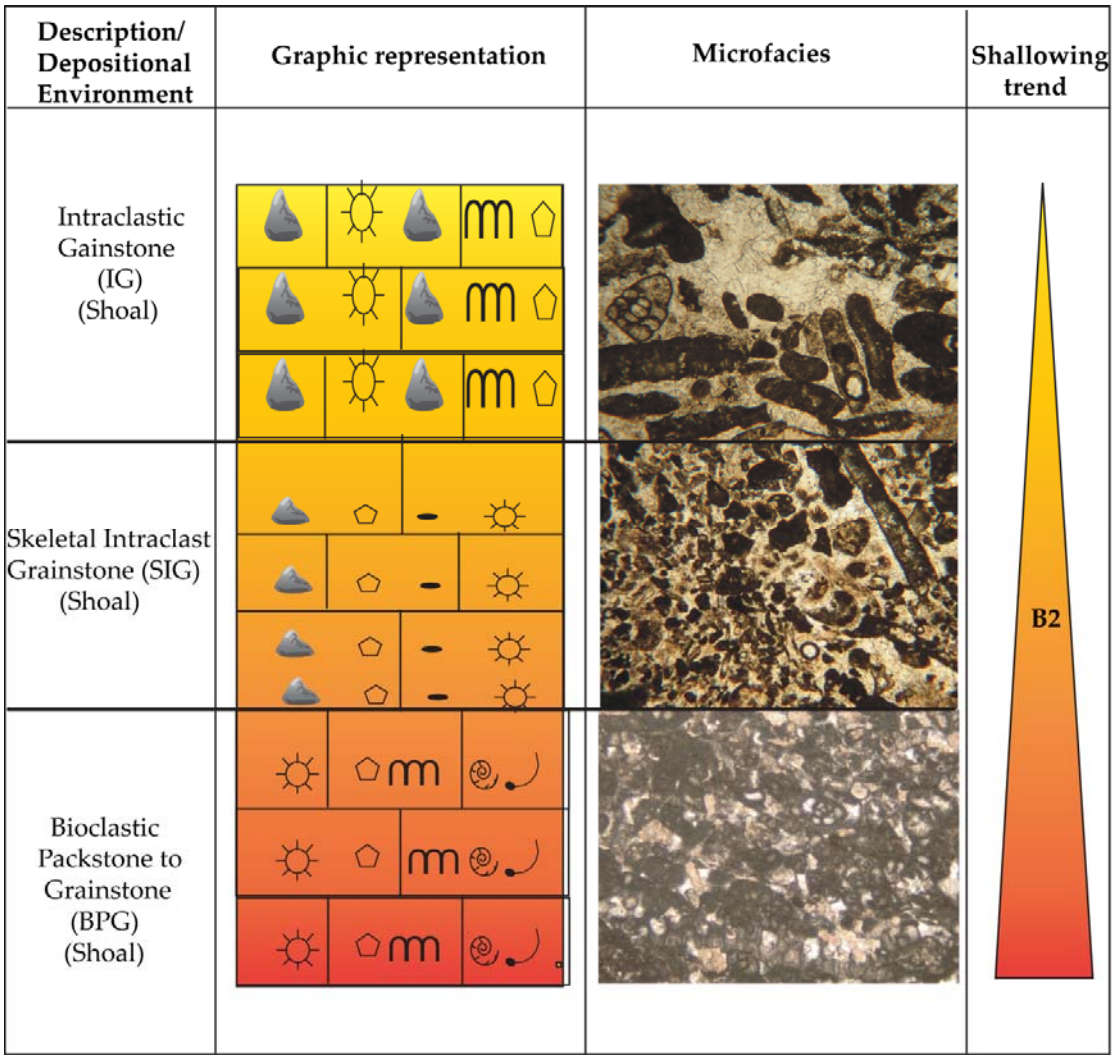

Figure 4. 5: B2 (Cycle 15) type cycle. For legend, see figure 5.15.

4.2.1.4 D Type Cycles

D type cycles (Figure 4.9) are mainly represented by wackestone and mudstone microfacies. It starts with intraclast ostracod wackestone microfacies and capped by mudstone with fenestral fabric microfacies. The shallowing trend is represented with the fenestral fabric. This microfacies is found in the middle part of the section.

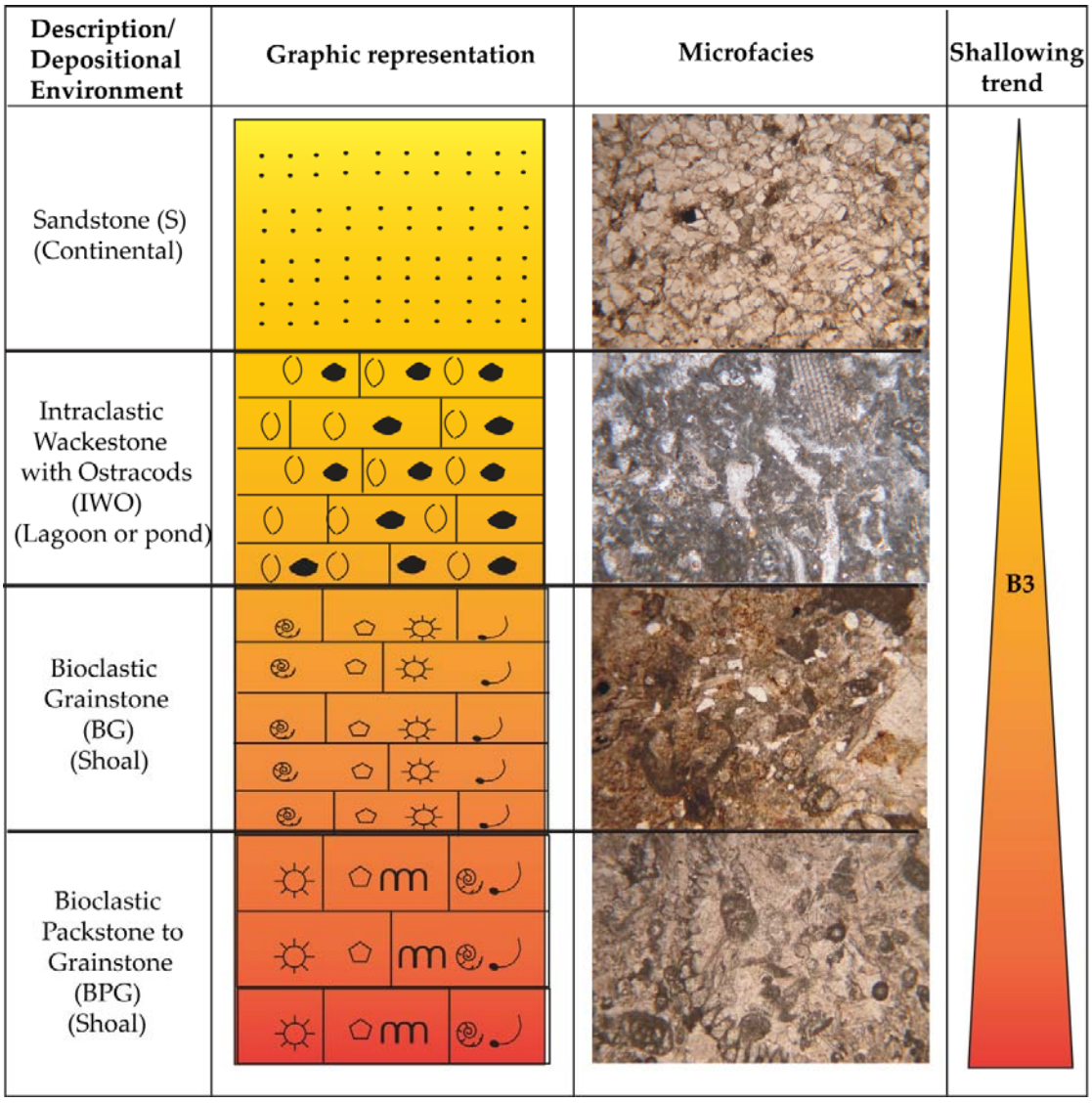

Figure 4. 6: B3 (Cycle 20) type cycle. For legend, see figure 5.15.

4.2.1.5 E Type Cycles

E type cycles are composed of two subtypes both of which start with skeletal intraclast grainstone. E1 type cycle (Figure 4.9) is followed and capped by pelloidal grainstone whereas E2 type cycle (Figure 4.10) is followed and capped by intraclastic grainstone. E type cycles are consecutive and they follow D type cycles in the measured section.

4.2.1.6 F Type Cycles

These type cycles are mainly characterized by grainstones. In F1 type cycle (Figure 4.10) bioclastic grainstone with equally distributed skeletal grains is deposited on top of crinoidal – pelloidal - foraminiferal grainstone. Both of these sub-microfacies belong to bioclastic grainstone microfacies. Although the two sub-microfacies represent the shoal environment, bioclastic grainstone with equally distributed skeletal grains is considered to be deposited landwardside of the crinoidal –pelloidal - foraminiferal grainstone. F2 type cycle (Figure 4.11) is a mixture of siliciclastic and carbonate system. It starts with bioclastic grainstone and is followed by mudstone with fenestral fabric and shale. In F3 type cycle (Figure 4.12) skeletal intraclast grainstone is deposited on top of bioclastic grainstone.

4.2.1.7 G Type Cycles

G type cycles are different from all types of cycles mentioned above because G type of cycles show a deepening trend first then they shallow upward. The important feature of G type cycles is that they start with grainstones, deepen with packstones or packstones to grainstones and they shallow with grainstones. However, depending on the internal variation and the type of grainstone 3 subtypes are defined G1 type cycle (Figure 4.13) starts with skeletal intraclast grainstone, and is followed by bioclastic packstone and bioclastic packstone to grainstone and capped by skeletal intraclast grainstone. G2 type cycle (Figure 4. 14) starts and ends with skeletal intraclast

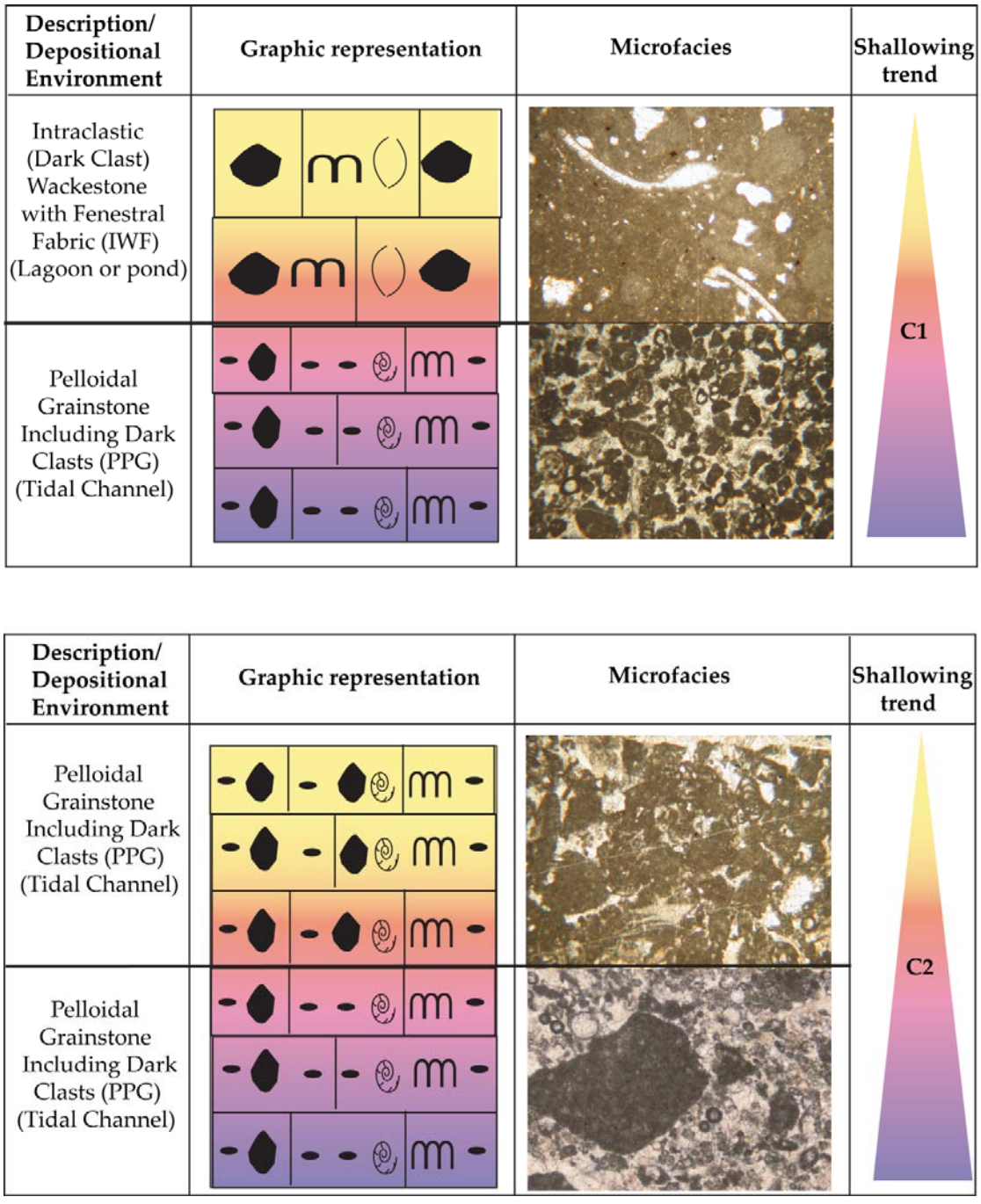

Figure 4. 7: C1 (Cycle 8) and C2 (Cycle 9) type cycles. For legend, see figure 5.15.

grainstone but in the middle, bioclastic packstone microfacies is intercalated. G3 type cycle (Figure 4. 14) does not show shallowing trend since the measured section ends within this cycle and bioclastic packstone is deposited on top of bioclastic grainstone.

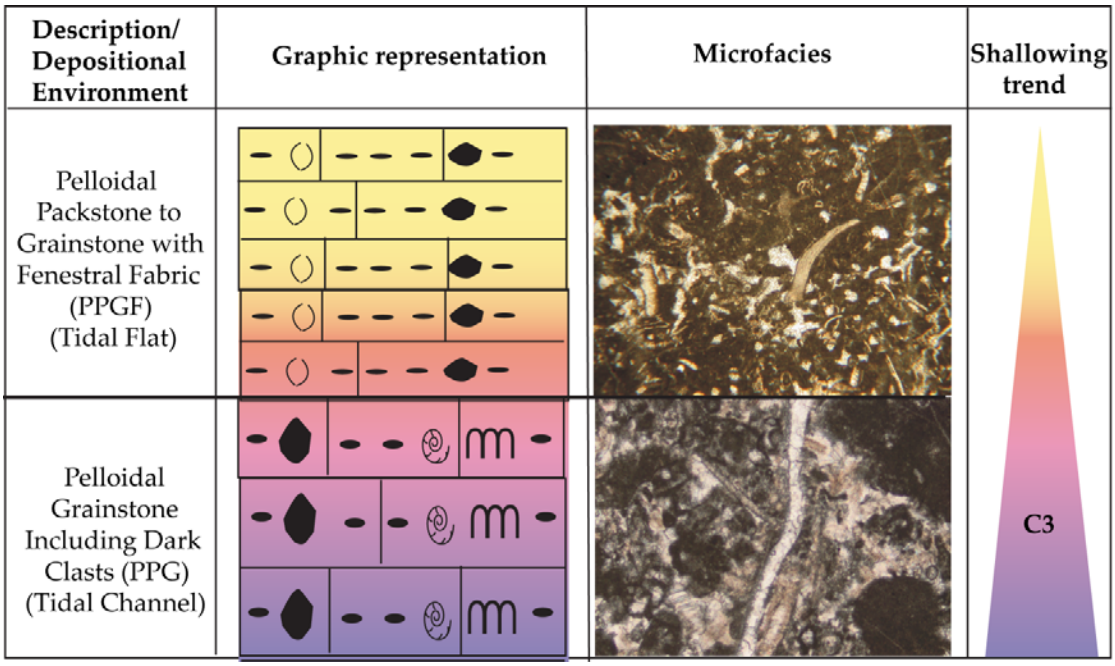

Figure 4. 8: C3 (Cycle 10) type cycle. For legend, see figure 5.15.

4.3 Sequence Stratigraphic Interpretation

In order to set the measured section in a sequence stratigraphic framework, a detailed microfacies analysis is needed because, system tracts are determined based on the vertical associations of microfacies forming cycles. Sequences are identified by vertical configuration of system tracts and by bounding surfaces, which are sequence boundaries.

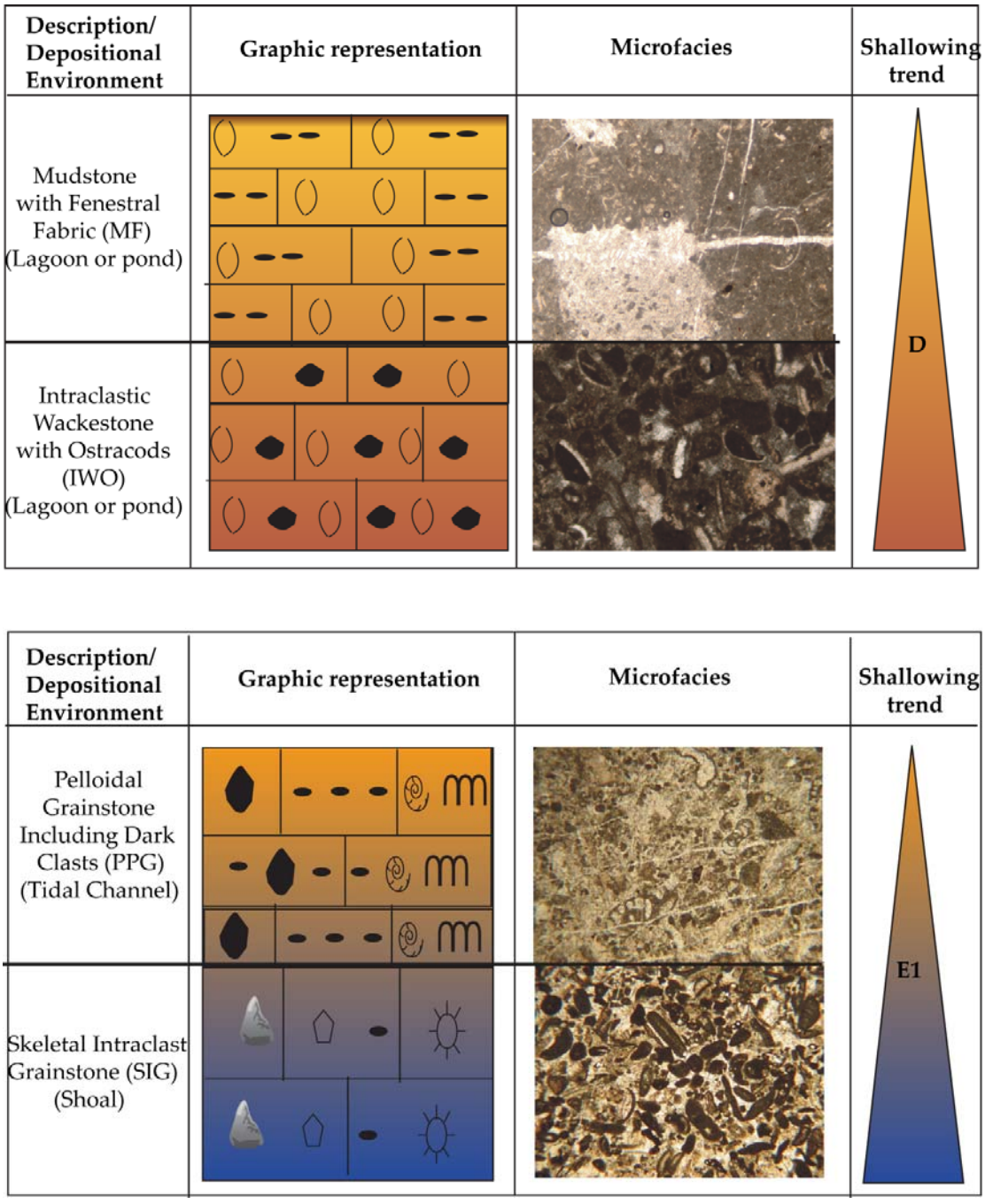

Figure 4. 9: D (Cycle 11) and E1 (Cycle 12) type cycles. For legend, see figure 5.15.

Three sequences and two sequence boundaries were detected in the measured section. In the first sequence only highstand system tract that forms during the late stage of base-level rise, is observed and the sequence boundary is determined by a significant change from grainstones of shoal environment to intraclastic (dark clast) wackestone with fenestral fabric of pond environment and pelloidal packstone to grainstone with fenestral fabric microfacies representing the most landward part of the tidal flat environment (Figure 5.15). The type of the first sequence boundary is probably a type 2 sequence boundary. "Type 2 sequence boundary is formed when the eustatic sea level is less than or equal to the rate of basin subsidence at the platform/ bank margin" so that only the inner platform area is exposed (Sarg, 1988).

Second package includes a transgressive system tract that is formed by the early rise of base level, high stand system tract and falling stage system tract formed by the early fall of sea level. Second sequence boundary is positioned just above the sandstone deposited resulted from the forced regression. The type of the second sequence boundary is a type 1 sequence boundary which forms when relative sea level falls just below the bank /platform margin causing peritidal rocks sharply overly the subtidal rocks (Sarg, 1988). Measured section ends with the transgressive system tract of the third sequence (Figure 4.15).

The high stand system tract of the first sequence ranges from the first sample SC-1 to the sample SC-30. It is composed of the alternation of A and B type cycles namely A1, A2, A3 and B1. In the lower part of this systems tract bioclastic packstones and grainstones alternate and exhibit an aggradational pattern. With the entry of the B type cycles to the system, which are composed of bioclastic packstone to grainstone and skeletal intraclast grainstone, the stacking pattern becomes progradational. Thus this system tract is determined as a high stand system tract because, relatively thick aggradational to progradational stratal patterns characterize the highstand system tract and this system tract is bounded below and above by the top of the transgressive system tract and a sequence boundary, respectively (Sarg, 1988) (Figure 4.15).

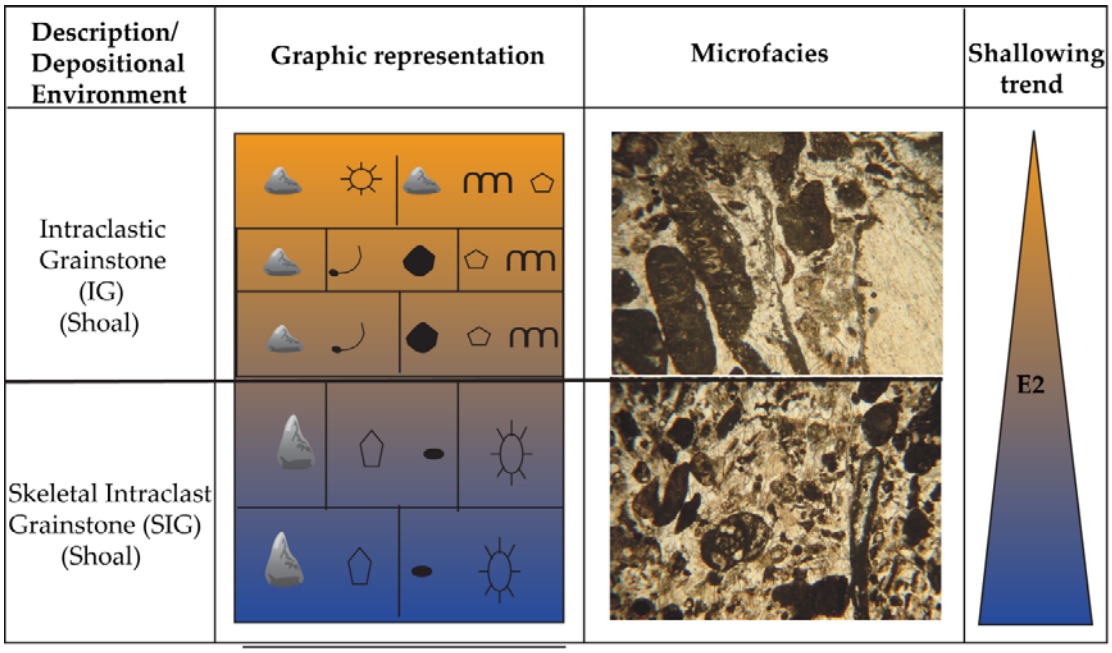

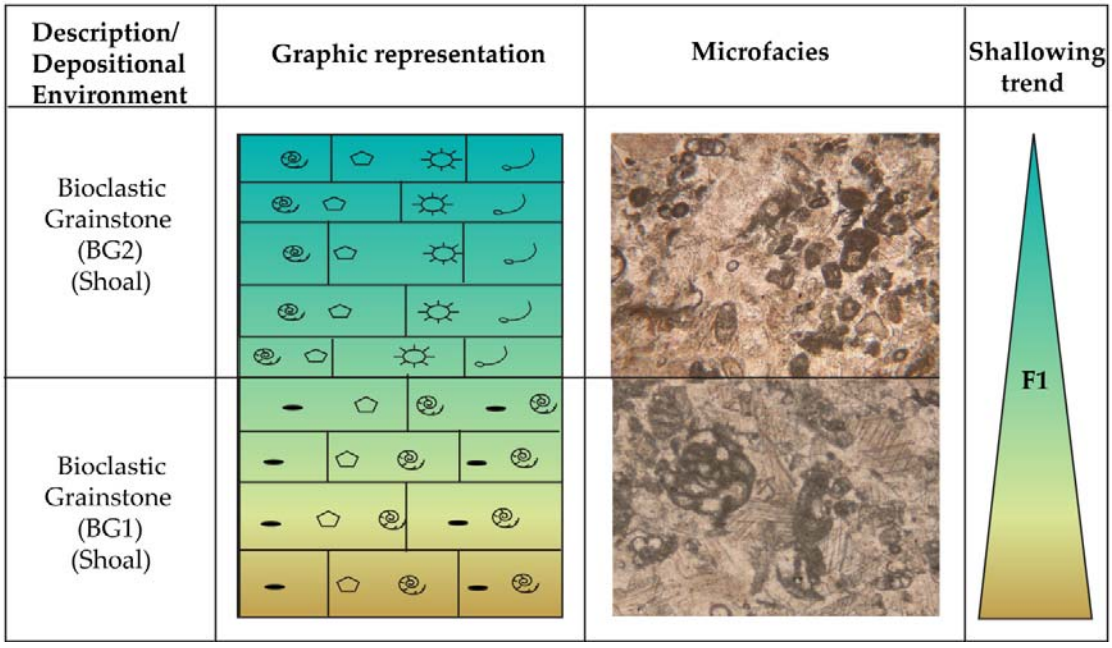

Figure 4. 10: E2 (Cycle 14) and F1 (Cycle 19) type cycles. For legend, see figure 5.15.

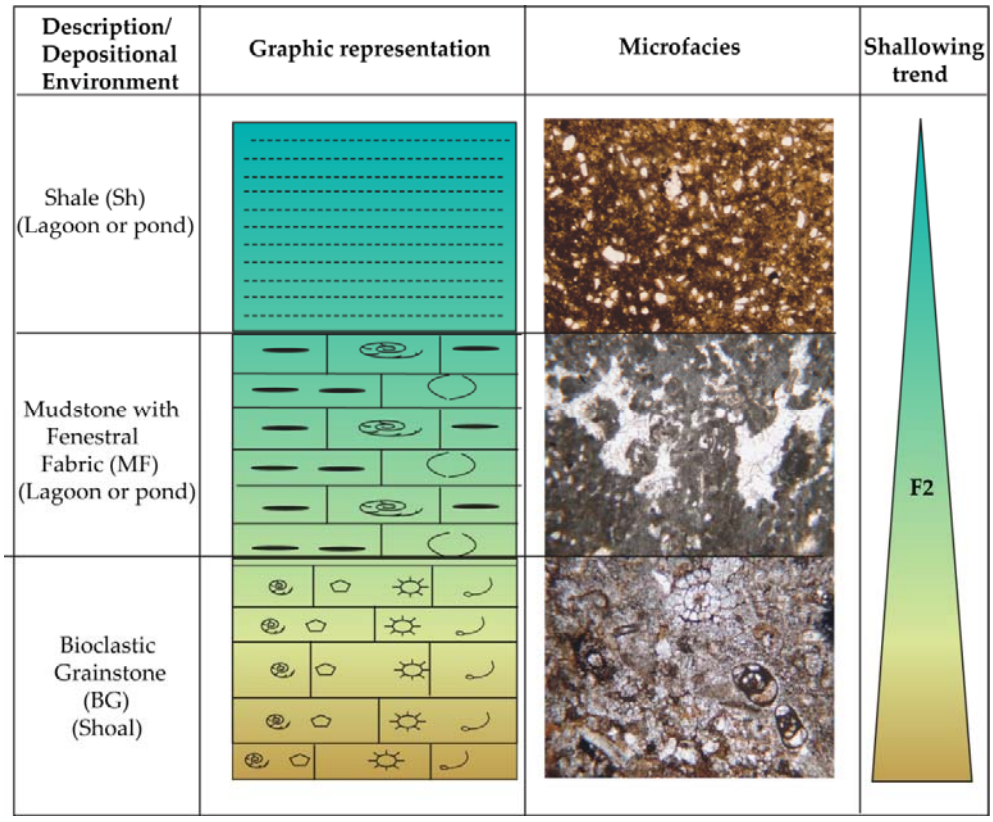

Figure 4. 11: F2 (Cycle 21) type cycle. For legend, see figure 5.15.

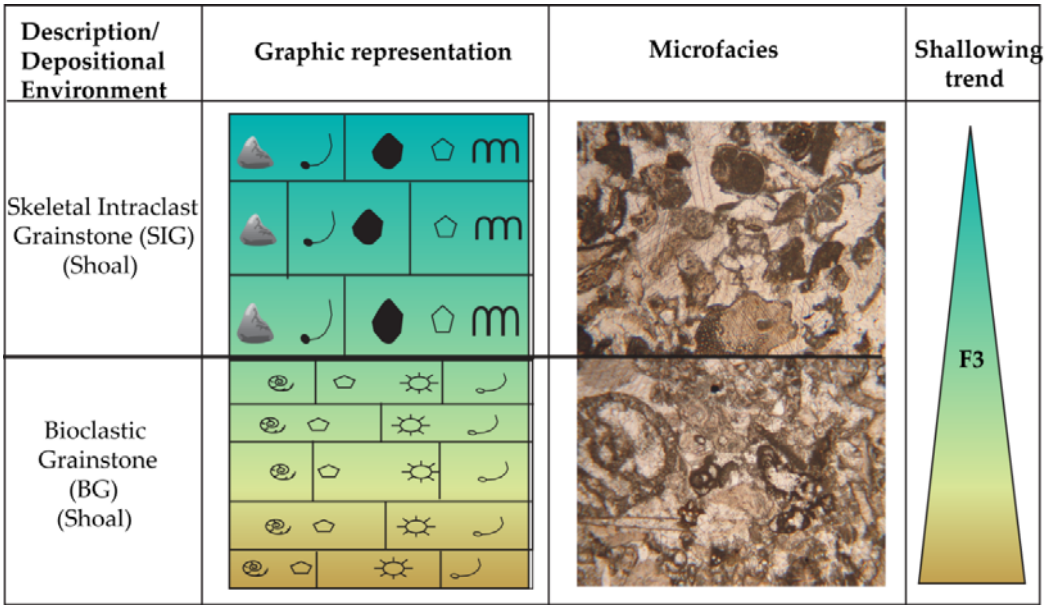

Figure 4. 12: F3 (Cycle 23) type cycle. For legend, see figure 5.15.

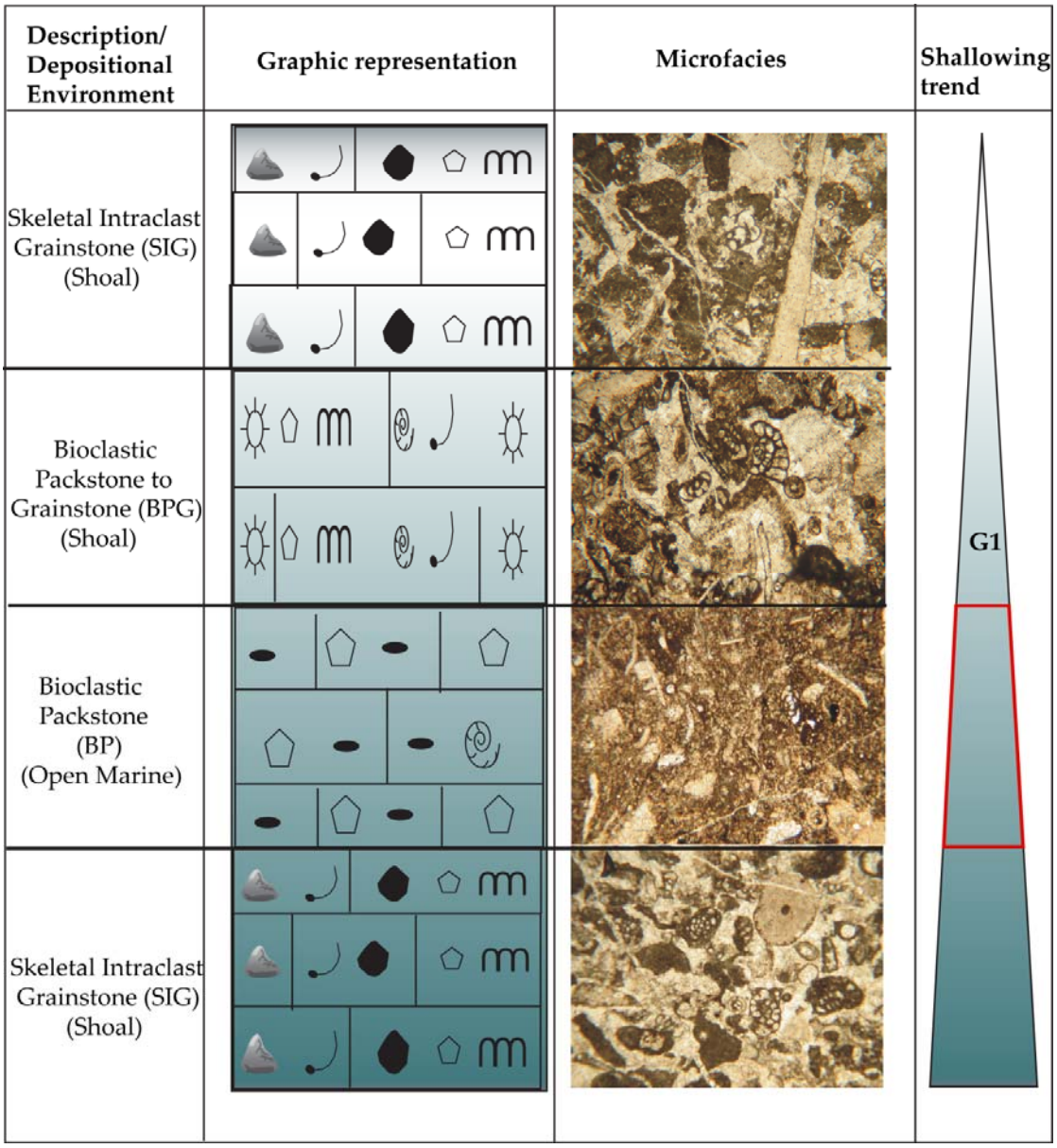

Figure 4. 13: G1 (Cycle 16) type cycle. (Red line shows deepening stage)For legend, see figure 5.15.

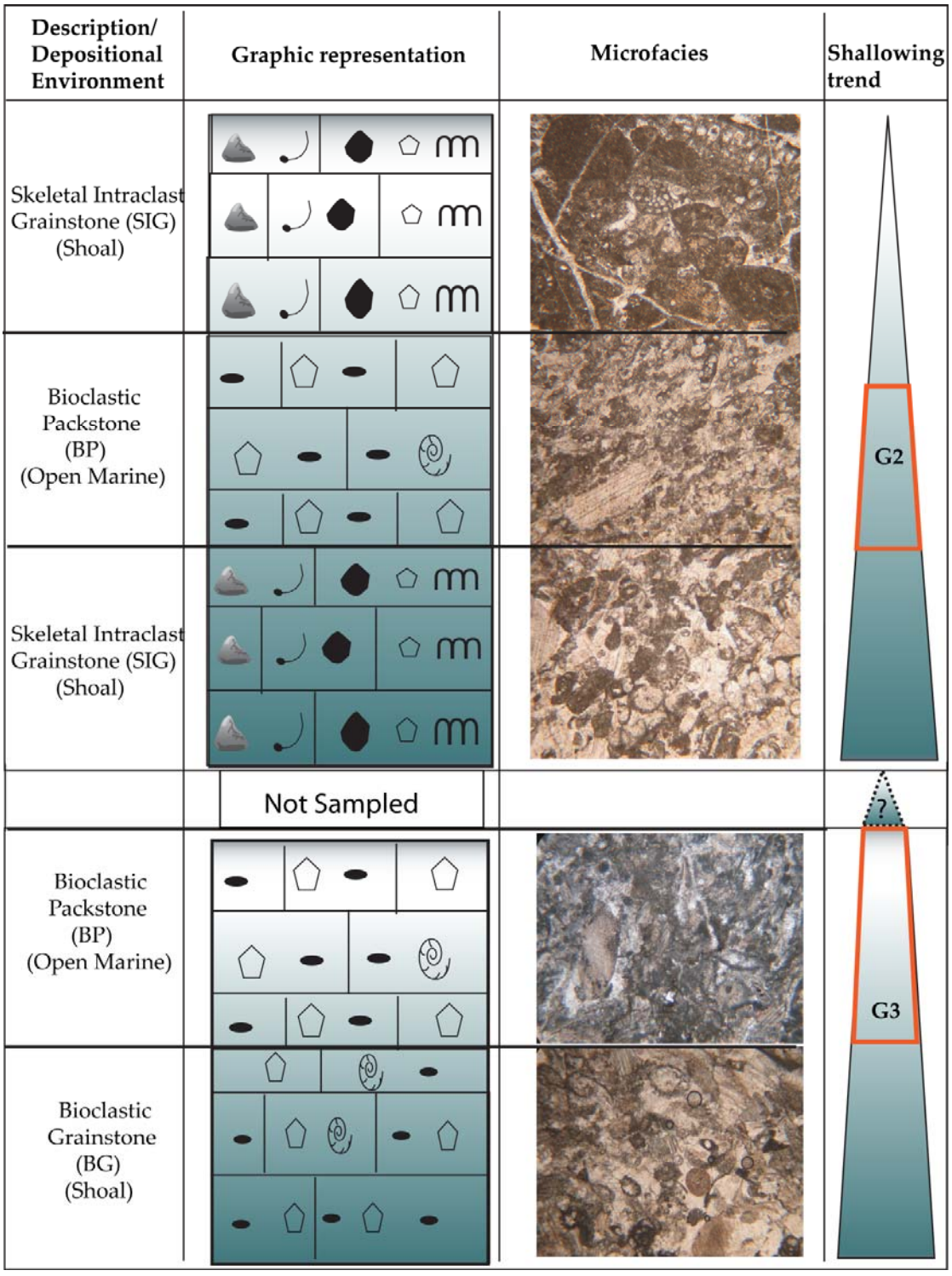

Figure 4. 14: G2 (Cycle 18) and G3 (Cycle 26) type cycles. (Red line shows deepening stage). For legend, see figure 5.15.

Second sequence starts with sample SC-31 with transgressive systems tract and continues till the sample SC-77. The lower part of the transgressive system tract is composed of C1, C2 and C3 type cycles, which are formed by the alternation of tidal flat deposits. Retrogradation continues with lagoonal deposits of D type cycle and shoal deposits of all E, B2 and G1 type cycles. This system tract is composed of retrogradational parasequence sets (Figure 4.15). Highstand system tract of second sequence is formed by A4, G2 and F1 types of cycles that are composed of shoal and open marine deposits. The following system tract is a falling stage systems tract that is composed of B3 type cycle which is capped by sandstone and the falling stage system tract can be understood from the presence of sharp-based shoreface sandbodies in wave-dominated nearshore areas (Figure 4.15).

On the contrary of the standard model proposing sea-level falls are not likely to produce a sediment record, retreating sea may cause an important sediment accumulation that records downward shift of the shoreline and shelf surface (Schlager, 2005). Sediment accumulation during forced regression is a significant example for this situation. "Forced regressions occur during stages of base-level fall, when the shoreline is forced to regress by the falling base level irrespective of sediment supply" (Cateneau, 2004) and all sediment accumulation during forced regression of the shoreline is included in the falling-stage systems tract (Plint and Nummedal, 2000).

The second sequence boundary is located the sandstones of the falling stage system tract. The third sequence starts with shale and limestones of F type cycles. Retrogradation continues with the bioclastic shoal and open marine deposits of the A and G type cycles. This system tract is in between sample SC-78 and sample SC-92 (Figure 4.15).

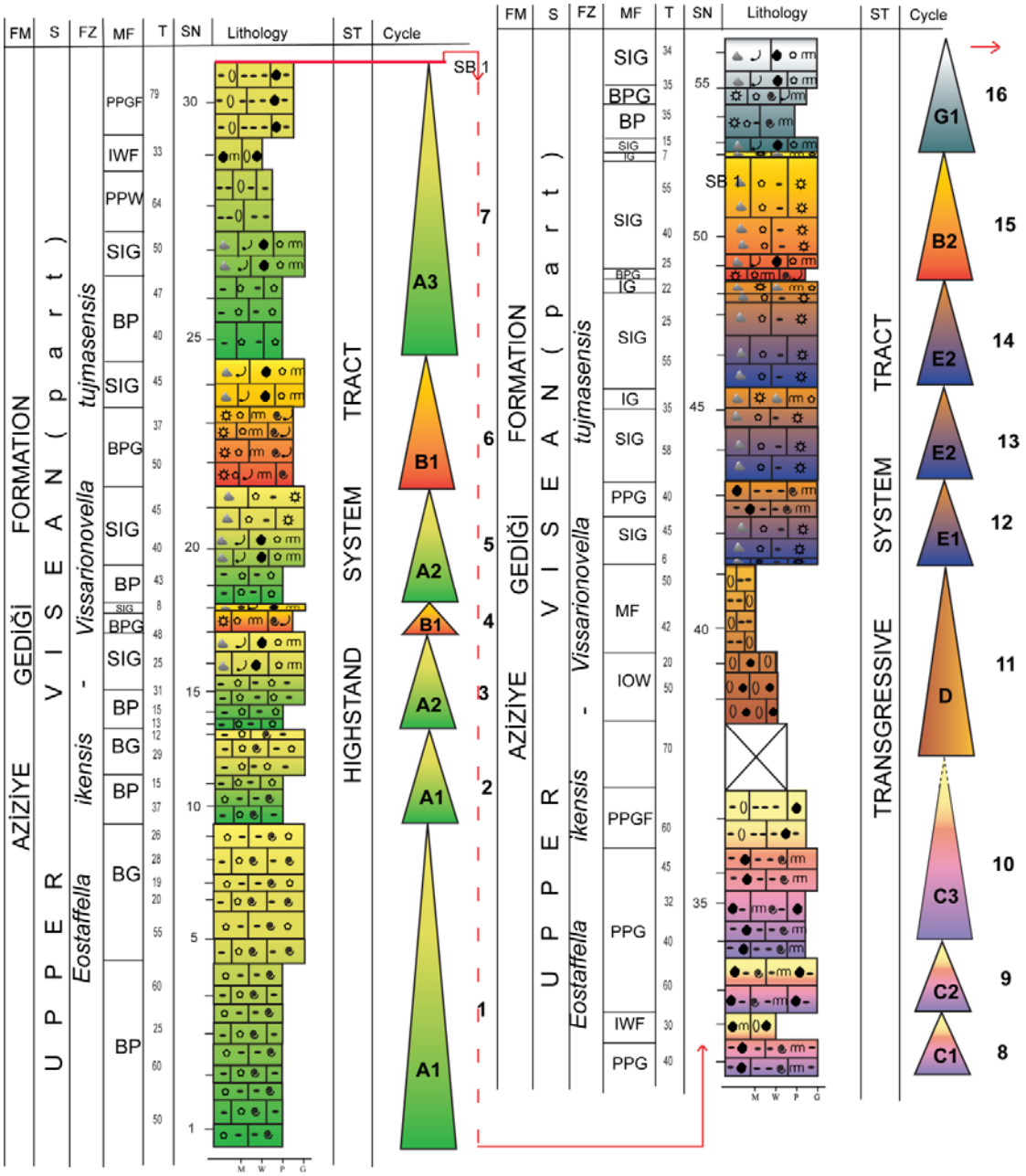

Figure 4. 15: Columnar section of the studied section showing meter scale cycles and its position in the sequence stratigraphic construction

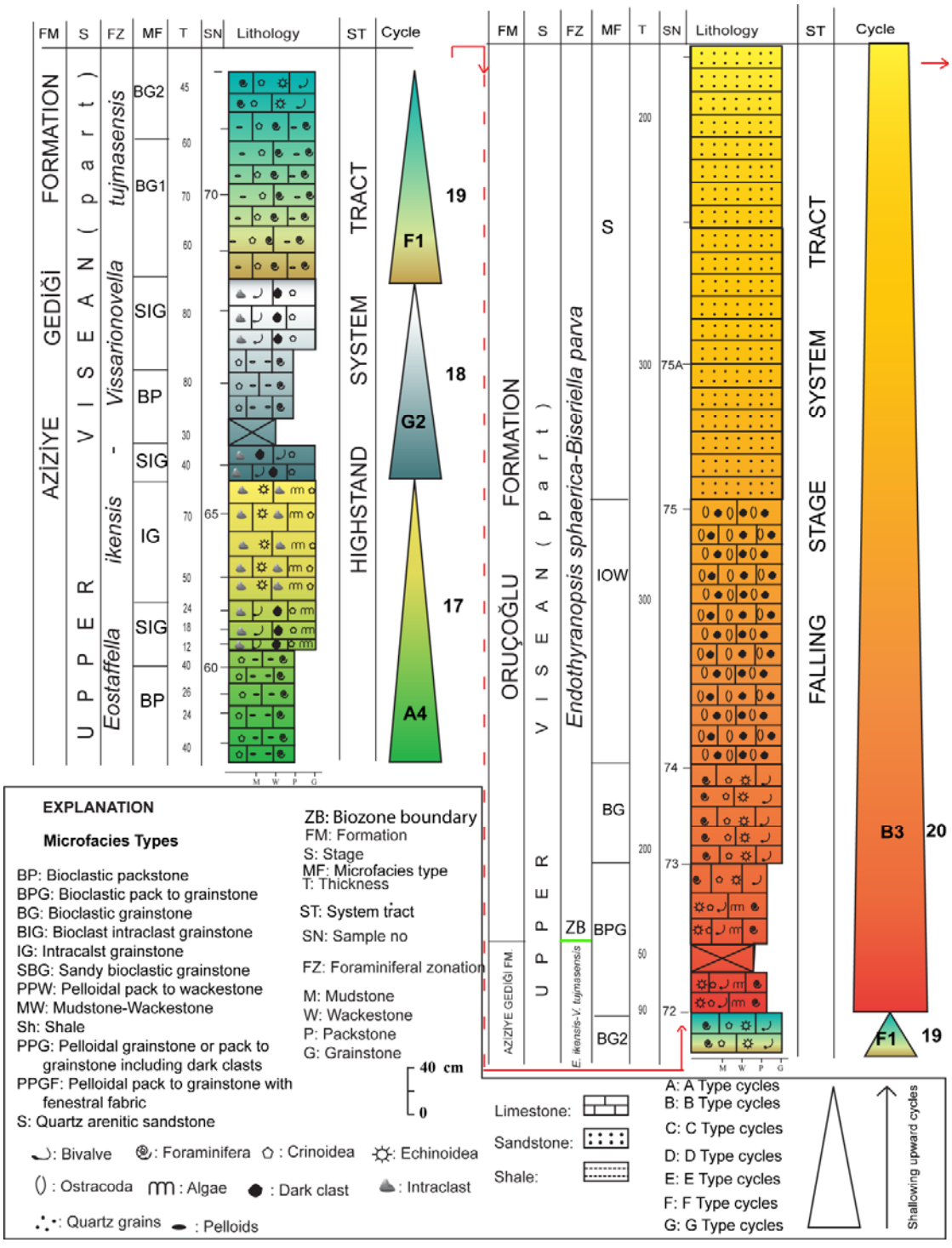

Figure 4.15: Continued.

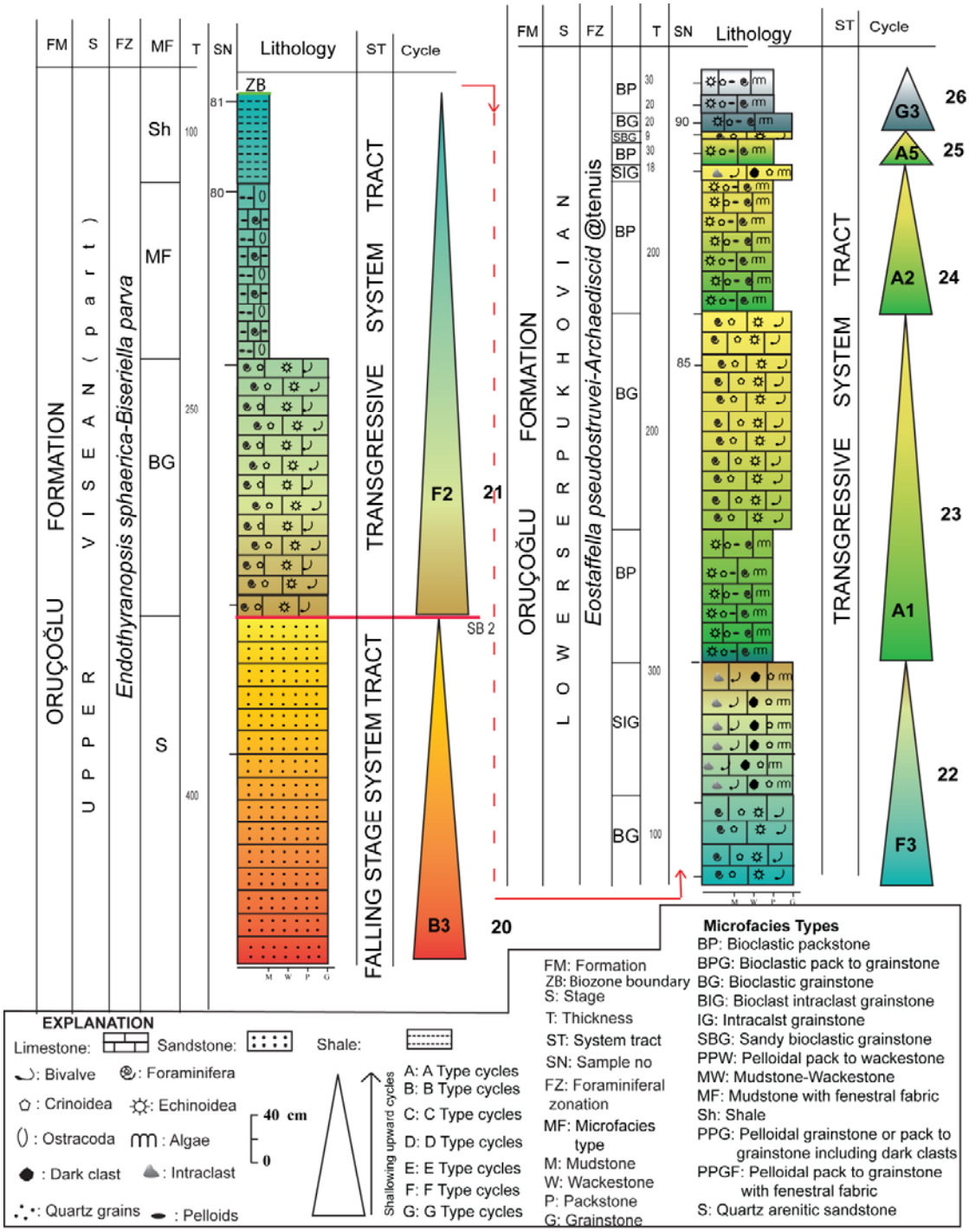

Figure 4.15: Continued

4.4 Eustatic Sea Level Fluctuations and Glaciation in Late Visean and Serpukhovian

Global sea level chart for Paleozoic is published in 2008 by Haq and Schutter. According to Haq and Schutter (2008) (Figure. 4.16), a significant fall near Carboniferous – Devonian boundary followed by a short recovery period and a subsequent long-term decrease started in the mid-Mississippian (mid Visean), reaching a low in the late Mississippian (near the Mississippian/Pennsylvanian boundary). Until the end of the Carboniferous, a period of eustatic rise is experienced. The position of sea level during Visean and Serpukhovian stages, particularly its position near the Visean - Serpukhovian boundary, is important for our study since significant eustatic falls and rises cause changes in deposition systems globally.

Global sea level chart of Haq and Schutter (2008) (Figure. 4.16), indicate sea level fall in the latest Visean and a relative rise between the latest Visean and earliest Serpukhovian. This trend is also observed in our measured section such that the sequence boundary corresponds to the uppermost part of the Venevsky Horizon (corresponds to the appearance of *Biseriella parva*) and deposits of the rest of the Venevsky Horizon and Serpukhovian stage in the measured section belongs to the transgressive stand system tract. Thus, the second sequence boundary in our study can be correlated with the one in the southern West Virginia (Haq and Schutter, 2008).

The study of Ross and Ross (1985) discuss the Late Paleozoic depositional sequences and correlate eustatic sea level curves of NW Europe, Russian Platform and Mississippi Valley. They do not particularly study Visean and Serpukhovian deposits but in general, they show a worldwide rise in sea level in the Late Brigantian but an eustatic fall just at the Visean - Serpukhovian boundary while Haq and Schutter (2008) show rises below and above the boundary.

Makhlina (1996) recognized 4 sixth order transgressive –regressive cycles in the Dinantian of Russian Platform. Mikhailovsky horizon together with Aleksinsky

Horizon is within a fourth transgression which is the maximum transgression of Dinantian and Venevsky horizon shows regressive phase of transgression and shallower water conditions. It is stated that pre-Serpukhovian karst is the characteristic event for the upper parts of this unit. Our study yields similar results such that Mikhailovsky Horizon is reflected by highstand and transgressive system tracts and in the Venevsky horizon shallowing trend begins and in the upper part sandstone is laid down by forced regression.

During the Late Paleozoic, eustatic sea level fluctuations are expressed by glacioeustasy. There are many studies on the nature of glaciation on Gondwana. Isbell et al. (2003) carried out the widely used work that can be summarized such that on the contrary the view advocating the Late Paleozoic as an uninterrupted glacial period, it in fact, includes glacial and non-glacial intervals. First glaciation starts from Frasnian, ends possibly at the end of Tournasian; second glaciation continues from Serpukhovian to late Bashkarian and the final glaciation starts in Gzhalian and ends at the middle of the Sakhmarian. Therefore, according to Isbell et al. (2003), our studied interval Late Visean is within an interglacial period and Serpukhovian is in a glacial period (Figure 4.17).

Rygel et al. (2008) agree on the findings of Isbell et al. (2003) and draw a similar correlation chart however, they argue that between non-glacial period of Early Visean and glacial period of mid-Carboniferous there is a transitional period from Asbian to middle Brigantian (Figure 4.17). In addition, latest Visean and Serpukhovian is proposed as a glacial period in this study.

Another recent study (Fielding et al., 2008) considers the eastern Australia in Late Paleozoic ice age and compares his study with previous ones. They found glaciation from the latest Serpukhovian to the Early Moscovian but this glaciation is also interrupted and divided into four intervals (Figure 4.17).

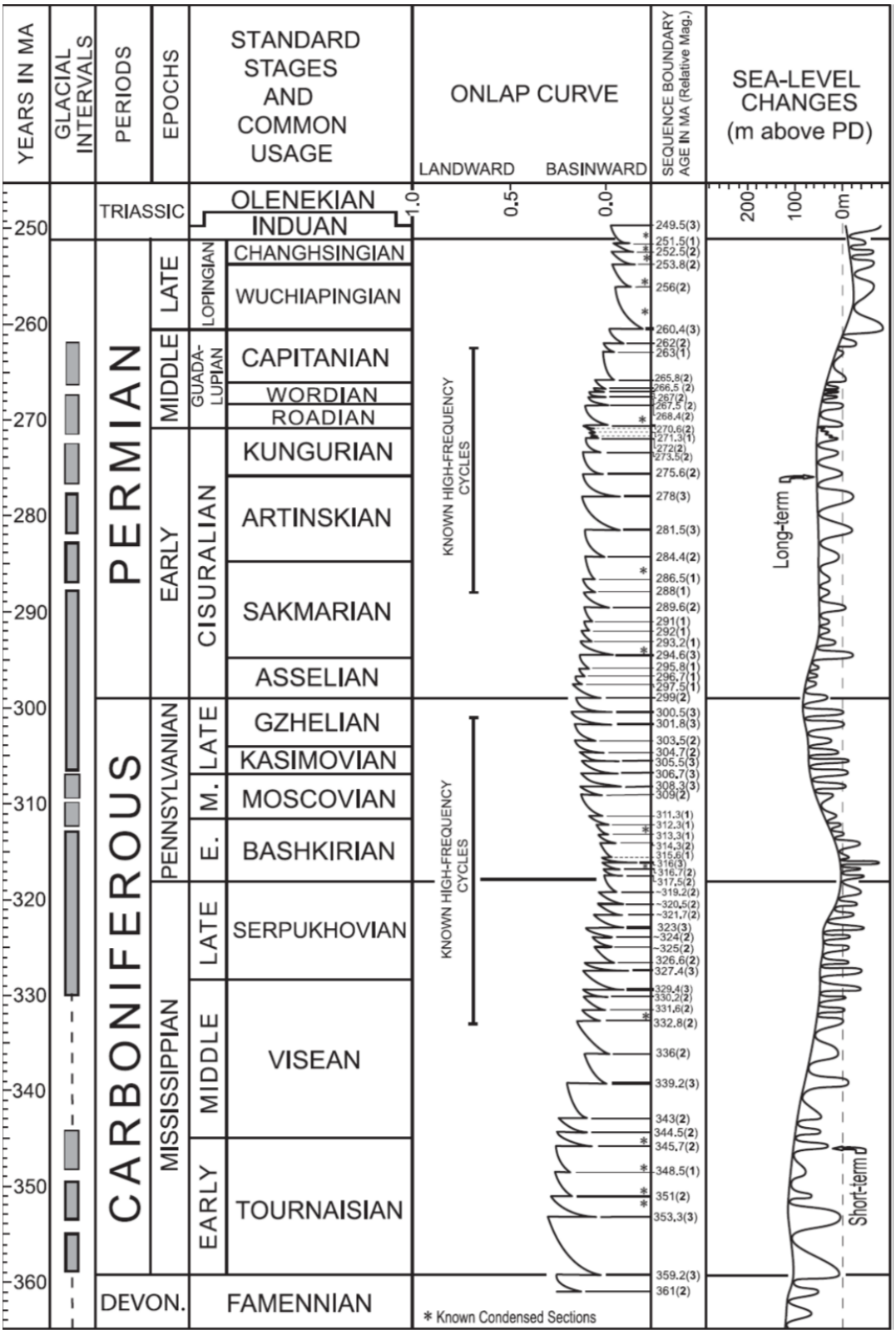

Figure 4. 16: Carboniferous-Permian sea-level changes (Haq and Schutter, 2008).

4.5 Origin and Duration of Cycles

Vail et al. (1977), Vail et al. (1991) and Haq et al. (1987) propose the subdivision of depositional sequences based on duration of cycles. They divided the stratigraphic record into global cycles of relative sea level change from first order to the sixth order. First, second, third, fourth, fifth and sixth order cycles have duration of more than 50 Ma, 3-50 Ma, 0.5 - 3 Ma, of 0.08-0.5 Ma, 0.03 to 0.08 Ma and of 0.01 – 0.03 Ma, respectively (Vail et al, in 1991). The first and second order cycles have very long time durations to observe in the field and they are thought to be derived from geotectonic mechanisms (Vail et al., 1977). Third order cycles are better observed on the field and most probably derived from glacioeustatic fluctuations. Forth order cycles represent eustatic variations around the larger eccentricity cycles. Fifth order cycles represent the periodicities of the Milankovitch frequency band such as glacio-eustatic cycles. Sea level changes with a higher frequency as the Milankovitch variations are denoted as the sixth order cycles (Einsele, 1991).

Carboniferous is well known with cyclic sedimentation and high frequency cycles are the result of both glacioeustasy and changes of the Earth's orbital parameters known as eccentricity, obliquity and precession. The relationship between regular changes in orbital parameters and climate is used to explain the origin of ice ages in Milankovitch theory and Milankovich cycles are identified as the 21 ky precession cycle, the 41 ky obliquity cycle and the 100 ky eccentricity cycle (Schwarzacher, 1991). However, according to Schwarzacher (1993) direct evidence for Milankovitch cyclicity is poor for Carboniferous and he stated that identification of Milankovitch cycles is always uncertain. According to Ruddiman and Wrigth (1987 in Wrigth and Vandstone, 2001) eccentricity is dominant only in Pleistocene ice house world and before Pleistocene shorter rhythm obliquity cycles are important. On the contrary, Wrigth and Vandstone (2001) defines Brigantian cycles of British Isles as 100 ky eccentricity cycles. The results of this thesis also support the argument of Wrigth and Vandstone (2001). Because the duration of the Upper Visean cycles interpreted in the present study are 117ky and this

value is very close to the Milankoitch eccentricity cycles. Thus, this study also show that Milankovitch cyclicity is also valid for Carboniferous.

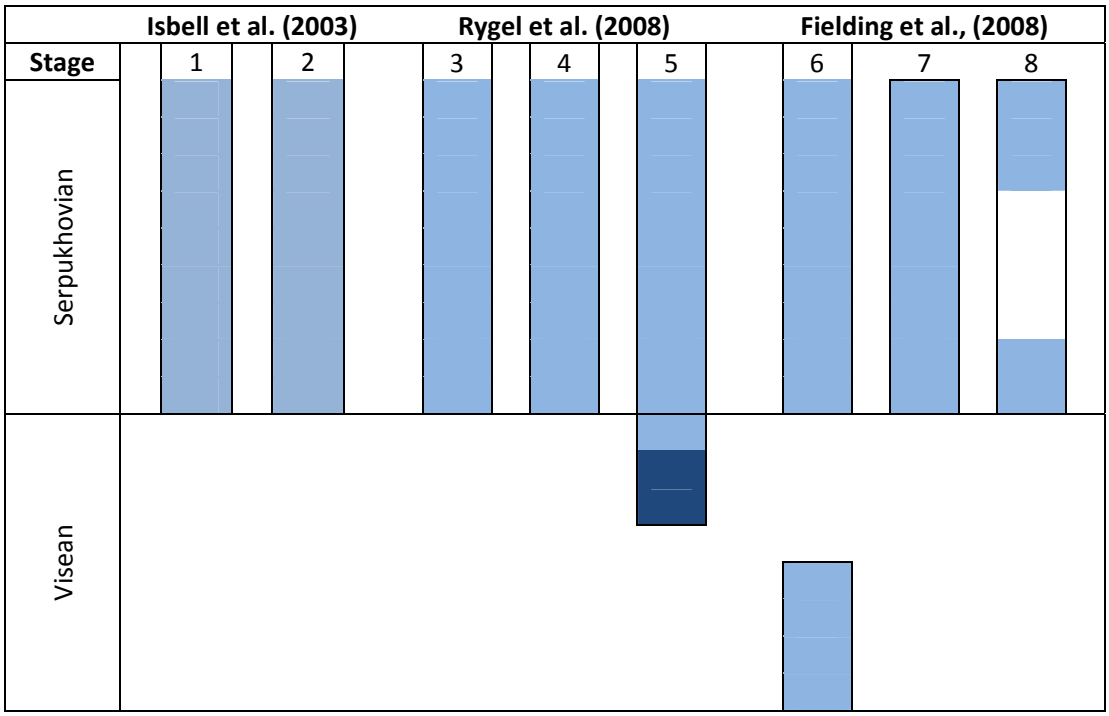

Figure 4. 17: Correlation of glacial periods in different studies. **1:** Northern Gonwana Basins. **2:** Panthallassan Margin Basins. **3:** Overall Gondwana. **4:** Eastern Australia. **5:** Transitional interval from non-glacial period to glacial period in British Isles (Wright and Vanstone, 2001) is shown by dark blue. **6:** Local Alpine glaciation proposed by Veevers and Powell (1987). **7:** Duration of glaciation proposed by Frakes et al. (1992). **8:** Eastern Australia glacial intervals.

Haq and Schutter (2008) correlate the eustatic sea level changes and sequence boundaries according to the "Concise Geologic Time Scale" (2008). In this time scale the boundary between Mikhailovsky and Venevsky horizons is approximately 330.2 my. Before this boundary a sea level fall which causes a sequence boundary is observed at 331.6 my. This sequence boundary is thought to be coincided with the first sequence boundary in our measured section. Duration between these two levels is 1.4 my and 12 cycles are determined in the measured section. So, the average duration of one cycle is

117 ky. In addition, the Mikhailovsky-Venevsky boundary in "Geological Time Scale" (2004) is 328.8 my. The first sequence boundary before this level is in 330.2 my. According to this scale, the average duration of one cycle is 116 ky. This is close to the eccentricity cycles.

The reason why duration of cycles in this study is not exactly 100 ky can be related with the nature of cycles described in the present study. There may be hidden cycles beyond the resolution of the study and they may not mistakenly be noticed. In fact, Late Paleozoic Glaciation is sensitive to the changes in Milankovitch insolation variations. However, other mechanisms may also trigger the extensive glaciation causing the changes of the duration of eccentricity cycles interpreted in this study. The mechanisms triggering the glaciation are proposed by other workers as the changes in CO_2 content of the atmosphere, the closure of the equatorial sea way, namely Rheic Ocean, during Mid-Late Visean which causes significant changes in oceanic circulation (Wright and Vandstone, 2001).

CHAPTER 5

SYSTEMATIC PALEONTOLOGY

Study for systematic micropaleontology has been carried out on calcarerous foraminifera by the analysis of thin sections of systematically collected samples along the measured section. The classification of calcareous foraminifera was determined by some taxonomical criteria namely, wall structure, diameter, width and form ratio (Width/ diameter) of test, shape of the umbilical region and periphery, type of coiling, number of volutions and chambers, presence of secondary deposits, shape of chambers, septa and secondary deposits.

In suprageneric and generic classification mainly Conil et al. (1979) was used. Loeblich and Tappan (1988) was also helpful. In the classification of Tournayelids Conil and Lys (1964) was followed. In the classification of Archaediscids Brenckle and Marchant (1987) is utilized.

It should be noted that the present taxonomic study given in this chapter includes short descriptions of available forms instead of detailed explanations and complete synonym lists and remarks reflecting the writer's observations on the important identification criteria of the forms and comparison with similar forms. Synonym list was prepared considering particularly the recent studies.

SUPERFAMILY PARATHURAMMINACEA BYKOVA, 1955

FAMILY ARCHAESPHAERIDAE Malakhova, 1956

SUBFAMILY ARCHAESPHERINAE Malakhova, 1956

Genus *Diplosphearina* Derville, 1952

Type species: *Diplosphaerina inequalis* Derville, 1931

Diplosphaerina inequalis Derville, 1931

Pl. I, figs. 1-5, 10-11

1931. *Diplosphaerina inequalis* Derville; pl. 18, figs. 77-80.

1973. *Diplosphaerina inequalis* Derville; Mamet, p. 111, pl. 3, figs. 26-27.

1979. *Diplosphaerina inequalis* Derville; Conil, Longerstaey and Ramsbottom, p. 186, pl. 30, fig. 8.

1982. *Diplosphaerina inequalis* Derville; Rich, p. 245, pl.1, figs. 2, 3?, 4? 5?.

1987. *Diplosphaerina inequalis* Derville; Brenckle and Marchant, p. 85, pl. 4, figs. 19?, 20.

1995. *Diplosphaerina inequalis* Derville; Altıner and Savini, p. 445, pl. 4, figs. 4-5.

1995. *Diplosphaerina inequalis* Derville; Hoare and Skipp, p. 619, text fig. 3, figs. 1-7.

2004. *Diplosphaerina inequalis* Derville; Brenckle, p. 154, pl. 5, fig. 17.

2005. *Diplosphaerina inequalis* Derville; Zhijun et al., p. 342, pl. 1, fig. 13

Description:

Test is bilocular or unilocular. Chambers are spherical or hemispherical. In bilocular forms, one sphere is enveloped by a much larger sphere. Wall is microgranular or finely granular.

Dimensions:

Diameter first chamber: 0.05 mm

Diameter of the second chamber: 0.13 mm

Height: 0.07-0.33

Basal diameter: 0.09-0.22

Wall thickness: 6-20 μm

Stratigraphic distribution:

The stratigraphic range of this form in our samples is from Upper Visean to Serpukhovian.

FAMILY CALCISPHARERIDAE Willamson, 1880

Genus *Calcisphaera* Willamson, 1880

Type species: *Calcisphaera cancellata* Willamson, 1880

Calcisphaera sp.

Pl. I, figs. 6-7

Description:

Test is unilocular and spherical. Wall is hyaline-radial.

Dimensions:

Diameter of the chamber: 0.09-0.13

Wall thickness: 11-29 μm

Stratigraphic distribution:

The stratigraphic range of *Calcisphaera* sp. in the studied section is Upper Visean.

FAMILY PARATHURAMMINIDAE Bykova, 1955

SUBFAMILY PARATHURAMMININAE Bykova, 1955

Genus *Parathurammina* Suleymanov, 1945

Type species: *Parathuramina dagmarae* Suleymanov, 1945

Parathurammina sp.

Pl. I, figs. 8-9

Description:

Test is unilocular and spherical. There are radiating projections and many apertures. Wall is dark and microgranular.

Dimensions:

Diameter of the chamber: 0.06-0.09 mm

Wall thickness: 8-12 μm

Stratigraphic distribution:

The stratigraphic range of *Parathurammina* sp. in our samples is from Upper Visean to the lower part of the Serpukhovian.

FAMILY TUBERITINIDAE Miklukho-Maklay, 1958

Genus *Hemithurammina* Mamet, 1973

Type species: *Webbina fimbriata* Howchin, 1888

Hemithurammina fimbriata (Howchin, 1888)

Pl. I, figs. 14?, 15-16

1888. *Webbina fimbriata* Howchin, p. 538-539, pl. 8, fig. 8-9.

1973. *Hemithurammina fimbriata* Howchin; Mamet, p. 111, pl. 3, figs. 14-17.

1981. *Hemithurammina fimbriata* Howchin; Altıner, p. 431, ol. 1, figs. 26-29.

2006. *Hemithurammina fimbriata* Howchin; Okuyucu and Vachard, p. 544, text fig 7, figs. 8-10?.

Description:

Test is convex or hemispherical. It is formed by one or two chambers. Wall is microgranular and dark.

Dimensions:

Height: 0.05-0.06 mm

Basal diameter: 0.15-0.18 mm

Wall thickness: 21-23 μm

Stratigraphic distribution:

The stratigraphic distribution of *Hemithurammina fimbriata* is from Devonian to uppermost Visean (Mamet, 1973). This form ranges in our samples from Upper Visean to Serpukhovian.

Genus *Tuberitina* Galloway and Harlton, 1928

Type species: *Tuberitina bulbacea* Galloway and Harlton, 1928

Tuberitina ? sp.

Pl. I, figs. 15

Description:

Test is formed by two hemispherical chambers which are attached to a basal disc. Wall is microgranular.

Dimensions:

Basal diameter of two chambers: 0.16 mm

Wall thickness: 12 μm

Stratigraphic distribution:

The stratigraphic range of this form in the studied section is Asbian and Serpukhovian?

SUPERFAMILY EARLANDIACEA Cummings, 1955

FAMILY EARLANDIIDAE Cummings, 1955

Genus *Earlandia* Plummer, 1930

Type species: *Earlandia pervarva* Plummer, 1930

Earlandia elegans (Rauzer-Chernoussova and Reitlinger in Rauzer-Chernoussova and Fursenko, 1937)

Pl. I, figs. 11-12

1937. *Hyperammina elegans* Rauzer-Chernoussova and Reitlinger in Rauzer-Chernoussova and Fursenko, p. 256-257, fig. 191.

1960. *Earlandia elegans* Rauzer-Chernoussova and Reitlinger; Grozdilova and Lebedeva, p. 38, pl. 1, fig.2.

1981. *Earlandia elegans* Rauzer-Chernoussova and Reitlinger; Altıner, p. 431, pl. 2, figs. 4-10.

1982. *Earlandia elegans* Rauzer-Chernoussova and Reitlinger; Rich, p. 245, pl.1, figs. 6-25.

1987. *Earlandia* of the group *elegans* Rauzer-Chernoussova and Reitlinger; Brenckle and Marchant, p. 85, pl. 4, figs. 4-5.

1993. *Earlandia* of the group *elegans* Rauzer-Chernoussova and Reitlinger; Mamet et al., pl. 1, figs. 1-2.

1993. *Earlandia elegans* Rauzer-Chernoussova and Reitlinger; Ueno and Nakazawa, p. 10,text fig. 3, figs. 4-8.

2004. Earlandia of the group *E. elegans* Rauzer-Chernoussova and Reitlinger; Brenckle, p. 150, pl. 3, fig. 27.

2005. *Earlandia elegans* Rauzer-Chernoussova and Reitlinger; Zhijun et al., p. 342, pl. 1, figs. 18-19.

Description:

Test is rectilinear and bilocular. Spherical proloculus is followed by an undivided rectilinear second chamber. Wall is microgranular.

Dimensions:

Length of the tubular chamber: 0.18-0.45 mm

Diameter of the tubular chamber: 0.07-0.05 mm

Diameter of the proloculus: 0.11-0.13 mm

Wall thickness: 13-14 μm

Remarks:

This species has smaller dimensions than *Earlandia minor* and *Earlandia vulgaris*.

Stratigraphic distribution:

The stratigraphic range of this form is from Tournaisian to Lower Bashkirian (Grozdilova and Lebedeva, 1960). Our specimens belong to Upper Visean to Serpukhovian interval.

FAMILY PSEUDOAMMODISCIDAE Conil and Lys in Conil and Pirlet, 1970

Genus *Brunsia* Mikhailov, 1939

Type species: *Spirillina irregularis* Moeller, 1879

Brunsia pulchra Mikhailov, 1939

Pl. II, figs. 3-4

1939. *Brunsia pulchra* Mikhailov, p. 64, tf. 1a-b.

1973. *Brunsia pulchra Mikhailov*; Mamet, p. 115, pl. 5, fig.4.

1981. *Brunsia pulchra Mikhailov*; Altıner, p. 431, pl. 2, figs. 20-21.

2009. *Brunsia pulchra* Mikhailov; Ueno and Miyazaki, p. 85, text fig. 4, fig. 19.

Description:

Test is discoidal and laterally compressed. It is composed of an undivided tubular chamber that coils glomospirally in initial tours and planispirally in later tours. Inner volutions inflate in the umbilical region. Volutions do not increase their heights

through the ontogenesis. There are approximately 6 tours and the number of the tours after the skewed part is 3. Wall is microgranular or finely granular.

Dimensions:

Diameter: 0.38-0.44 mm

Width: 0.15-0.18 mm

Height of the last tour: 0.03-0.04 mm

Wall thickness: 13-15 μm

Remarks:

Inflated umbilical region in axial section due to highly skewed coiling and nearly permanent height of volution in all tours differs *Brunsia pulchra* from *Brunsia spirillinoides.* Planispiral final 3 volutions and inflation in the umbilicus differs the former from *Brunsia sygmoidalis*.

Stratigraphic distribution:

The stratigraphic distribution of *Brunsia pulchra* is Lower Visean to Upper Visean (V1a to V3b) (Altıner, 1981). Specimens of *Brunsia pulchra* in this study have been recovered from the Upper Visean (Mikhailovsky).

Brunsia spirillinoides (Grozdilova and Glebovskaia, 1948)

Pl. II, figs. 1-2

1948. *Glomospira spirillinoides* Grozdilova and Glebovskaia, p. 147, pl. 1, figs. 2-4.

1963. *Glomospirella spirillinoides* Grozdilova and Glebovskaia; Conil, pl. 1, fig. 12.

1973. *Brunsia spirillinoides* Grozdilova and Glebovskaia Phillips; Austin et al., p. 183, pl. 1, fig. 16.

1973. *Brunsia spirillinoides* Grozdilova and Glebovskaia; Mamet, p. 115, pl. 5, figs. 1-3.

1981. *Brunsia spirillinoides* Grozdilova and Glebovskaia; Altıner, p. 431, pl. 2, figs. 13-15.

1982. *Brunsia spirillinoides* Grozdilova and Glebovskaia; Strank, p. 106, pl. 10, fig. 5.

2005. *Brunsia spirillinoides* Grozdilova and Glebovskaia; Zhijun et al., p. 345, pl. 4, fig. 13

Description:

Test is discoidal and large. Undivided second tubular chamber slightly oscillates in the initial 2-3 volutions but it is planispiral in the final 4-5 volutions. There are nearly 6-8 volutions. Height of the volutions increases progressively through the spire. Wall is microgranular or finely granular.

Dimensions:

Diameter: 0.6-0.7 mm

Width: 0,12 mm

Height of the last tour: 0.06 mm

Wall thickness: 33-24 μm

Remarks:

Brunsia spirillinoides has more regular coiling than *Brunsia pulchra* and *Brunsia sygmoidslis*. It lacks an umbilical protuberance like *Brunsia pulchra* and the height of volution increases on the contrary of *Brunsia pulchra*.

Stratigraphic distribution:

The stratigraphic distribution of *Brunsia spirillinoides* is Lower Visean to Upper Visean (V1a to V3b) (Altıner, 1981). Specimens of *Brunsia spirillinoides* have been recovered from the Upper Visean (Mikhailovsky) in the studied section.

Brunsia sygmoidalis Rauser-Chernoussova, 1948

Pl. II, fig. 10

1948. *Brunsia sygmoidalis* Rause-Chernoussova, p. 241, pl. 17, fig. 13.

1981. *Brunsia sygmoidalis* Grozdilova and Glebovskaia; Altıner, p. 431, pl. 2, figs. 13-15.

Description:

Test is discoidal. It is formed by a proloculus and an undivided second tubular chamber. Coiling strongly oscillates but aligned. Number of volutions is 6 or 7. Spire expands gradually through the ontogenesis.

Dimensions:

Diameter: 0.37 mm

Width: 0.11 mm

Height of the last tour: 0.04 mm

Wall thickness: 17 μm

Remarks:

Brunsia sygmoidalis has a highly oscillatory coiling that the same feature cannot be observed in other species of this genus. It lacks of the prominent inflation in umbilical region that is seen in *Brunsia pulchra*.

Stratigraphic distribution:

The stratigraphic distribution of *Brunsia sygmoidalis* is Lower Visean in Taurides however it is observed from Lower Visean and Upper Visean (Aleksinsky horizon) (Altıner, 1981). Only one single specimen of *Brunsia sygmoidalis* in this study is found in the Upper Visean (Mikhailovsky).

Brunsia spp.

Pl. II, figs. 6-9

Description:

All forms having a discoidal test, undivided tubular chamber, microgranular or finely granular wall and oscillatory to planispiral coiling have been grouped under *Brunsia* spp.

Stratigraphic distribution:

The stratigraphic distribution of *Brunsia* spp. in this study is Upper Visean (Mikhailovsky).

Genus *Pseudoammodiscus* Conil and Lys in Conil and Pirlet, 1970

Type species: *Ammodiscus priscus* Rauser-Chernoussova, 1948

Pseudoammodiscus sp.

Pl. II, figs. 11-14

Description:

Test is discoidal composed of 5-6 tours. Umbilical region is wide and shallow. Coiling is planispiral evolute. Volutions are convex in axial section and they increase their height progressively. The wall is dark, thin and microgranular.

Dimensions:

Diameter (d): 0.22-0.60 mm

Width (w): 0.06-0.17 mm

w/d: 0.27-0.28

Wall thickness: 10-43 μm

Remarks:

The genus *Pseudoammodiscus* differs from the genus A*mmodiscus* by its microgranular and thin wall. In our material non of the specimens are well-oriented sections.

Stratigraphic distribution:

The stratigraphic distribution of *Pseudoammodiscus* sp. in the studied section is Upper Visean (Mikhailovsky).

Genus *Pseudoglomospira* Bykova in Bykova and Polenova,1955

Type species: *Pseudoglomospira devonica,* Bykova, 1955

Pseudoglomospira sp.1

Pl. III, figs. 1-8

Description:

Small spherical proloculus is followed by undivided tubular chamber. Coiling tends to be planispiral or skewed to planispiral in initial tours, but it is skewed in the

last tour or last two tours. There are nearly 6 whorls. Wall is dark, thin and microgranular.

Dimensions:

Diameter (d): 0.19-0.29 mm

Wall thickness: 5-14 μm

Remarks:

Pseudoglomospira sp.1 is different form *Pseudoglomospira* sp. 2 by its more regular coiling.

Stratigraphic distribution:

The stratigraphic distribution of *Pseudoglomospira* sp.1 is Serpukhovian in the studied section.

Pseudoglomospira sp.2

Pl. III, figs. 9-10

Description:

Test is bilocular. Second tubular chamber is highly skewed coiled and irregular. Test is compressed and its shape is slightly rectangular. Wall is dark, thin and microgranular.

Dimensions:

Diameter (d): 0.19-0.21 mm

Wall thickness: 8-10 μm

Remarks:

Pseudoglomospira sp.2 differs from *Pseudogolospira* sp.1 by its highly irregular coiling and more compressed test.

Stratigraphic distribution:

The stratigraphic distribution of *Pseudoglomospira* sp.2 is (83-91) Serpukhovian in the studied section.

Pseudoglomospira sp. 3

Pl. III, figs. 11-15

Description:

Test is bilocular. Second chamber is tubular, undivided. Coiling is skewed in the initial volutions and tends to be planispiral in the final or final two volutions. Wall is dark, thin and microgranular.

Dimensions:

Diameter (d): 0.22-0.32 mm

Wall thickness: 10-14 μm

Remarks:

Pseudoglomospira sp. 3 is differentiated from other species of *Pseudoglomospira* sp. 2 by its more regular coiling and larger dimensions. It is differentiated from *Pseudoglomospira* sp. 1 by initially skewed finally planispiral coiling.

Stratigraphic distribution:

The stratigraphic distribution of *Pseudoglomospira* sp. 3 is Sepukhovian in the studied section.

Pseudoglomospira spp.

Pl. III, figs. 16-18, 19?-21?

Description:

Several forms of this genus that cannot be identified in a particular species have been grouped under *Pseudoglomospira* spp. This form is composed of one proloculus and one undivided tubular chamber that coils glomospirally ot streptospirally. Their wall is dark, thin and microgranular.

Remarks:

Conil and Lys (1964) have used the genus *Warnantella* instead of *Pseudoglomospira* for most of Visean forms. However both genera define the same character. Due to the priority of the genus *Pseudoglomospira* we prefer to use it. Some of the specimens have been given here with a question mark since their wall structure and coiling type cannot be identified definitely.

Stratigraphic distribution:

The stratigraphic distribution of the genus *Pseudoglomospira* is from Devonian to Carboniferous (Loeblich and Tappan, 1988). The stratigraphic distribution of *Pseudoglomospira* spp. is from Upper Visean to Serpukhovian in the studied section.

SUPERFAMILY ARCHAEDISCACEA Cushman, 1928

FAMILY ARCHAEDISCIDAE Cushman, 1928

SUBFAMILY PLANOARCHAEDISCINAE Mamet, 1975

Genus *Viseidiscus* Mamet, 1975

Type species: *Permosdiscus* (?) *primaevus* Pronina, 1963

Viseidiscus monstratus (Grozdilova and Lebedeva, 1954)

Pl. IV, fig. 1

1954. *Archaediscus monstratus* Grozdilova and Lebedeva, p. 61, pl. 7, figs. 17-18.

1987. *Viseidiscus monstratus* Grozdilova and Lebedeva; Brenckle and Marchant, p. 80. pl. 2, figs. 1-7.

Description:

Test is narrowly discoidal. Planispirally coiled second tubular chamber expands rapidly. Chamber floor is convex. Wall is microgranular and pseudofibrous hyaline

layer is developed on sides. In the late stages of ontogenesis this hyaline layer is absent and the wall is microgranular.

Dimensions:

Diameter (d): 0.19 mm

Width (w): 0.04 mm

w/d: 0.21

Remarks:

Its narrowly discoidal test, rapid expansion of the tours and poorly developed pseudo-fibrous layer are the features that distinguish this species from others.

Stratigraphic distribution:

The stratigraphic range of this form is from Lower and Upper Visean (Brenckle, 1987). The only specimen found in this study belongs to Upper Visean (Mikhailovsky).

Viseidiscus umbogmaensis (Omara and Conil, 1965)

Pl. IV, figs. 2-3, 5, 4?

1965. *Permodiscus umbogmaensis* Omara and Conil, p. 227-228, pl. 2, fig. 5.

1987. *Viseidiscus umbomaensis* Omara and Conil; Brenckle and Marchant, p. 79, pl. 1, figs. 20-31, 32?

Description:

Test is discoidal. Coiling is planispiral or slightly oscillating. Volutions expand progressively. Chamber floor is convex. There is a hyaline fibrous layer on the sides and inner microgranular laye is visible in all tours. Hyaline layer thickens around umbilicus. Final half or one and a half volutions contain only microgranular wall and they are evolute.

Dimensions:

Diameter (d): 0.13-0.17 mm

Width (w): 0.06-0.04 mm

w/d: 0.25-0.41

Remarks:

The hyaline pseudofibrious layer of this form is well developed but do not cover the final volution. Coiling expands more rapidly in *Viseidiscus monstratus*.

Stratigraphic distribution:

The stratigraphic range of this form is from Lower Visean to Namurian (Brenckle, 1987). Our specimens belong to Upper Visean (Mikhailovsky).

Viseidiscus spp.

Pl. IV, figs. 6-7

Description:

Test is discoidal. Coiling is oscillatory to planispiral. Chamber floor is convex or flat. Hyaline fibrous layer occurs only on the sides of the form and inner microgranular layer is present in all tours. All volutions are involute except for the volutions that are not covered with hyaline layer.

Remarks:

Since hyaline layer does not cover all volutions this form is assigned to the genus *Viseidiscus*.

Stratigraphic distribution:

Samples belonging to *Viseidiscus* spp. were recovered from Upper Visean (Mikhailovsky).

FAMILY ARCHAEDISCIDAE Cushman, 1928

SUBFAMILY ARCHAEDISCINAE Cushman, 1928

Genus *Archaediscus* Brady, 1873

Type species: *Archaediscus karreri* Brady, 1873

Archaediscus karreri Brady, 1873

Pl. V, fig. 15

1873. *Archaediscus karreri* Brady, p. 113, pl. 4, figs. 32-34.

? 1963. *Archaediscus karreri* Brady; Conil and Pirlet, pl. 2, fig. 14.

1979. *Archaediscus* ex gr. *karreri* Brady; Brazhnikova, pl. 9, fig. 16.

1988. *Archaediscus karreri* Brady; Vachard, p. 121, pl. 1, figs. 19-21; pl. 2, fig. 4.

1993. *Archaediscus karreri* Brady; Brenckle and Grelecki, p. 47, pl. 1, fig.1-4.

2004. *Archaediscus* ex gr. *karreri* Brady; Cózar and Somerville, p. 50, text fig. 10, figs. 9-14; p. 56, text fig. 14, figs. 5-7, 10-11.

2008. *Archaediscus* ex gr. *karreri* Brady; Cózar et al., p. 473, text fig. 8, fig. 1.

Description:

Test is large and lenticular. Second tubular chamber coils sigmoidally but oscillations do not continue till the final tour. Coiling is involute. There are 5 volutions. Chamber floors are flat. The wall is thick, hyaline, radial.

Dimensions:

Diameter (d): 0.66 mm

Width (w): 0.30 mm

w/d: 0.45

Remarks:

This species is differentiated from *Archaediscus karreriformis* by the presence of distinct radial structure in the wall. It is more sigmoidal than *Archaediscus chernoussovensis*. It differs from *Archaediscus nanus* by its larger dimensions.

Stratigraphic distribution:

The stratigraphic range of this form is given as Lower Carboniferous by Brady, 1873). Our specimens belong to Serpukhovian.

Archaediscus moelleri Rauser-Chernousova, 1948.

Pl. VI, fig. 16

1948. *Archaediscus moelleri* Rauser-Chernousova; p. 231, pl. 15, figs. 14, 15.

1979. *Archaediscus moelleri* Rauser-Chernousova; Brazhnikova, pl. 2, fig.17.

1982. *Archaediscus moelleri* Rauser-Chernousova; Rich, p. 257, pl. 6, figs. 6-7.

1993. *Archaediscus moelleri* Rauser-Chernousova; Brenckle and Grelecki, p. 51, pl.3, fig.3, 4, 9.

2011. *Archaediscus moelleri* Rauser-Chernousova; Atakul-Özdemir et al., p. 715, text fig. 6, fig. q.

Description:

Test is lenticular. Periphery of the final half tour is angular. Coiling is sigmoidal however, second tubular chamber coils circularly around proloculus at first then, rate of oscillation diminishes and the tubular chamber becomes aligned. Coiling is involute in initial tours but it is evolute in the final tour. There are 4-5 volutions. Chambers have flat floors. The wall is hyaline, radial.

Dimensions:

Diameter (d): 0.27 mm

Width (w): 0.18 mm

w/d: 0.64

Remarks:

It differs from *Archaediscus gigas* and *Archaediscus karreri* by its smaller dimensions. In addition, the circular coiling in the axial section of the inner tours and lenticular but inflated test differ this form from the others. The periphery of *Archaediscus moelleri* is much more angular than the periphery of *Archaediscus convexus*.

Stratigraphic distribution:

The stratigraphic distribution is from Upper Visean to Lower Serpukhovian (Dain and Grozdiliova, 1953). The specimen found in this study is from Serpukhovian.

FAMILY ARCHAEDISCIDAE Cushman, 1928

SUBFAMILY ARCHAEDISCINAE Cushman, 1928

Genus *Betpakodiscus* Marfenkova, 1983

Type species: *Propermodiscus*? *attenuatus* Marfenkova 1978

Betpakodiscus attenuatus (Marfenkova, 1978)

Pl. VI, fig. 6

1967. *Archaediscus krestovnikovi* Rauser-Chernoussova var. *compressa* Vdovenko in Brazhnikova et al. , p. 160-161, pl. 54, figs. 1-7

1993. *Betpakodiscus attenuatus* Marfenkova; Brenckle and Grelecki, p. 59, pl. 7, figs. 9-10.

2008. *Tubispirodiscus attenuatus* Marfenkova; Cózar et al., p. 914, text fig. 6, figs. 1-5.

Description:

Test is narrowly discoidal. Coiling is skewed and involute in the first 2 or 3 whorls; evolute and planispiral in the preceding whorls. Sides are flat. There are 6-7 volutions. Chamber floors are convex in the initial tours, flat in the final tours. Sutures are well marked. The wall is hyaline, radial.

Dimensions:

Diameter (d): 0.32 mm

Width (w): 0.07 mm

w/d: 0.21

Remarks:

Presence of prominent sutures, excessive number of evolute whorls and absence of microgranular wall differ *Betpakodiscus attenuatus* from *Paraarchaediscus koktjubensis*.

Stratigraphic distribution:

Stratigraphic distribution of *Betpakodiscus attenuatus* is Upper Visean (Brenckle and Grelecki, 1993). Samples in this study have been recorded from Mikhailovsky horizon.

FAMILY ARCHAEDISCIDAE Cushman, 1928

SUBFAMILY KASACHSTANODISCINAE Marfenkova, 1983

Genus Paraarchaediscus Orlova, 1955

Type species: *Paraarchaediscus dubitabilis*, Orlova, 1955

Paraarchaediscus convexus (Grozdilova and Lebedeva, 1953)

Pl. VI, figs. 1-5

1953. *Archaediscus convexus* Grozdilova and Lebedeva in Dain and Grozdilova, p. 91-92, pl. 2, fig.11

1963. *Archaediscus convexus* Grozdilova and Lebedeva; Conil and Pirlet, pl. 2, fig. 18.

1979. *Archaediscus convexus* Grozdilova and Lebedeva; Vdovenko, pl. 3, fig. 25.

1988. *Archaediscus convexus* Grozdilova and Lebedeva; Vachard, p. 123, pl. 2, fig. 6.

1981. *Archaediscus* ex gr. *convexus* Grozdilova and Lebedeva; Altıner, p. 432, pl. 4, figs. 34-37; pl. 5 figs. 1-3; pl. 11, figs. 1-12, 13? 14?.

1993. *Paraarchaediscus convexus* Grozdilova and Lebedeva; Brenckle and Grelecki, p. 57, pl. 6, figs. 7-8.

1999. *Archaediscus convexus* Grozdilova and Lebedeva; Özkan, p. 201, pl. 2, fıg. 14.

2003. *Paraarchaediscus* ex gr. *convexus* Grozdilova and Lebedeva; Groves et al., p. 384, text fig. 5, figs. 6-10.

2004. *Paraarchaediscus convexus* Grozdilova and Lebedeva; Brenckle, p. 152, pl. 4, figs. 13-18?.

2005. *Paraarchaediscus convexus* Grozdilova and Lebedeva; Zhijun et al., p. 345, pl. 4, fig. 30.

Description:

Test is lenticular with a rounded periphery. Coiling is sigmoidal. Third volution changes the plane of coiling axis and makes a circle around the previous tours in axial section. After the third volution, rate of oscillation decreases. Coiling is involute. There are 5.5- 6 tours. Chambers floors are flat to convex. The outer wall is hyaline, radial and inner wall is microgranular.

Dimensions:

Diameter (d): 0.22-0.38 mm

Width (w): 0.18-0.20 mm

w/d: 0.53-0.55

Remarks:

Since microgranular wall maintains its existence this species is assigned to the genus *Paraarchaediscus*. Its coiling is similar to *Archaediscus moelleri*. But, *Paraarchaediscus convexus* makes a circle in its coiling in the third tour whereas *Archaediscus moelleri* makes it around the proloculus and their wall structure is different.

Stratigraphic distribution:

The stratigraphic range is from Upper Visean (Aleksinsky) to Lower Serpukhovian (Lys, 1988). The specimens found in this study have been recorded from Upper Visean (Venevsky) and Serpukhovian.

Paraarchaediscus koktjubensis (Rauser-Chernousova, 1948)

Pl. IV, figs. 8-24; Pl. V, fig. 1?

1948. *Archaediscus krestovnikovi* var. *koktjubensis* Rauser-Chernousova, p. 10-11, pl. 3, figs. 1-3.

? 1963. *Archaediscus koktjubensis* Rauser-Chernousova; Conil and Pirlet, pl. 2, fig. 16.

1973. A*rchaediscus koktjubensis* Rauser-Chernousova; Mamet, p. 113, pl. 4, figs. 1-7, 16.

1993. *Paraarchaediscus koktjubensis* Rauser-Chernousova; Brenckle and Grelecki, p. 47, pl. 1, figs. 10-11; p. 49, pl. 2, figs. 18-19.

1993. A*rchaediscus koktjubensis* Rauser-Chernousova; Mamet et al., pl. 14, figs. 2-12, 15, 29, 30.

1993. *Paraarchaediscus koktjubensis* Rauser-Chernousova; Ueno and Nakazawa, p. 12, text fig. 4, figs. 1-5.

1995. *Paraarchaediscus* cf. *P. koktjubensis* Rauser-Chernousova; Hoare and Skipp, p. 619, text fig. 3, figs. 27-28.

2004. *Paraarchaediscus koktjubensis* Rauser-Chernousova; Brenckle, p. 152, pl. 4, figs. 20-22.

2005. *Paraarchaediscus koktjubensis* Rauser-Chernousova; Zhijun et al., p. 345, pl. 4, figs. 23?,25, 26

2011. *Paraarchaediscus koktjubensis* Rauser-Chernousova; Atakul-Özdemir et al., p. 715, text fig. 6, figs. g-h.

Description:

Test is discoidal. Sigmoidally coiled initial volutions continue their development as oscillatory to planispiral. Initially involute coiling can be evolute in the final or final 2 tours. Number of volutions is 5-6. Chamber floors are slightly convex. The outer wall is hyaline, radial and inner wall is microgranular.

Dimensions:

Diameter (d): 0.25-0.42 mm

Width (w): 0.11-0.29 mm

w/d: 0.44-0.45

Remarks:

This form is very similar to *Archaediscus krestovnikovi.* In fact it was firstly described as a variety of this form. However, their wall structure is different.

Archaediscus krestovnikovi does not contain an inner microgranular layer. Its coiling pattern is also similar to *Archaediscus karreri* but, *Archaediscus karreri* has larger dimensions and the height of volutions do not increase too much while the rate of expansion rapidly increases in *Paraarchaediscus koktjubensis.* In addition, their wall structure is different.

Stratigraphic distribution:

The stratigraphic range was assigned to the Visean but it is considered as Serpukhovian by Brenckle ans Grelecki (1993). However many authors report this species from Visean. Specimens of this study have been encountered from the Upper Visean and Serpukhovian.

Paraarchaediscus stilus (Grozdilova and Lebedeva in Grozdilova, 1953)

Pl. VI, figs. 7-9

1953. A*rchaediscus stilus* Grozdilova and Lebedeva in Grozdilova, p. 110-111, pl. 4, figs. 19, 20.

1979. A*rchaediscus (Archaediscus) stilus* Grozdilova and Lebedeva; stade *angulatus* Conil, Longerstaey and Ramsbottom, p. 148, pl.14, figs. 29-30; p. 186, pl. 30, fig.5.

1979. A*rchaediscus (Archaediscus) stilus*, Grozdilova and Lebedeva; Conil, Longerstaey and Ramsbottom, p. 180, pl.28, fig. 46.

1982. *Archaediscus stilus* Grozdilova and Lebedeva; Rich, p. 257, pl. 6, figs. 8-10.

1982. *Archaediscus* ex gr. *stilus* Grozdilova and Lebedeva; Strank, p. 105, pl. 9, fig. 5.

1993. *Paraarchaediscus stilus* Grozdilova and Lebedeva; Brenckle and Grelecki, p. 56, pl. 6, figs. 3, 4.

2003. *Paraarchaediscus stilus* Grozdilova and Lebedeva; Groves et al., p. 384, text fig. 5, figs. 1-5.

2006. *Paraarchaediscus* ex gr. *stilus* Grozdilova and Lebedeva; Vachard et al., p. 774, text fig. 5, fig. 9.

2011. *Paraarchaediscus stilus* Grozdilova and Lebedeva; Atakul-Özdemir et al., p. 715,

text fig. 6, figs. l-m.

Description:

Test is discoidal and compressed. Initially, coiling is sigmoidal and involute; finally it is planispiral and evolute. There are 5 whorls. Chamber floors are convex. The outer wall is hyaline, radial and inner wall is microgranular.

Dimensions:

Diameter (d): 0.41-0.27 mm

Width (w): 0.09-0.13 mm

w/d: 0.29-0.35

Remarks:

There is a similarity between *Paraarchaediscus koktjubensis* and *Paraarchaediscus stilus.* The former has more complete sigmoidal coiling around the proloculus and the test of the latter is more compressed.

Stratigraphic distribution:

Although the stratigraphic range was given as Bashkirian, this species also occurs in the Visean (Brenckle and Grelecki, 1993). Samples in this study has been encountered in the Upper Visean and Serpukhovian.

Paraarchaediscus ex.gr. *stillus* Grozdilova and Lebedeva in Grozdilova, 1953

Pl. VI, figs. 10-15

Dimensions:

Diameter (d): 0.24-0.41 mm

Width (w): 0.08-0.14 mm

w/d: 0.35-0.36

Remarks:

These forms named as *Paraarchaediscus* ex.gr. *stillus* have lesser number of volutions and some of them have smaller dimensions. In addition, in the absence of well-oriented specimens inner volutions are not well defined.

Stratigraphic distribution:

Specimens of *Paraarchaediscus* ex.gr. *stillus* have been encountered in the Upper Visean and Serpukhovian interval.

Paraarchaediscus sp. 1

Pl. VI, figs. 17-20

Description:

Test is discoidal and very small. Coiling is sigmoidal and involute through. There are 3-4 volutions. Chamber floors are convex. The outer wall is hyaline, radial and inner wall is microgranular.

Dimensions:

Diameter (d): 0.15-0.18 mm

Width (w): 0.09-0.07 mm

w/d: 0.51

Remarks:

The main characteristic feature of this form is its very small dimension. Due to the maintenance of microgranular wall it is assigned to the genus *Pararchaediscus. Neoarchaediscus parvus* has also small dimensions but, its chambers are occluded and it lacks from the microgranular wall. *Paraarchaediscus* sp. 1 is different from *Paraarchaediscus pauxilus* such that it has a totally involute coiling and sutures of *Paraarchaediscus pauxilus* are prominent.

Stratigraphic distribution:

Specimena of *Paraarchaediscus* sp.1 in this study have been encountered in the Upper Visean – Serpukhovian interval.

Paraarchaediscus spp.

Pl. V, figs. 2-14; Pl. VI, figs. 21-22

Description:

All forms having lenticular or discoidal shape, composed of inner microgranular and outer hyaline wall with an not occluded chamber were grouped as *Paraarchaediscus* spp.

Stratigraphic distribution:

Specimens of *Paraarchaediscus* spp. in this study have been encountered in the Upper Visean – Serpukhovian interval.

FAMILY ASTEROARHAEDISCIDAE Miklukho-Maklai, 1957

SUBFAMILY ASTEROARCHAEDISCINAE Miklukho-Maklai, 1957

Genus Asteroarchaediscus Miklukho-Maklai, 1957

Type species: *Archaediscus baschkiricus* Krestovnikov-Theodorovitch, 1936

Asteroarchaediscus rugosus (Rauser-Chernousova, 1948)

Pl. VII, figs. 1-4

1948. *Archaediscus rugosus* Rauser – Chernousova, p. 11, pl. 3, figs. 4-6.

1979. *Asteroarchaediscus* ex gr. *rugosus* Rauser-Chernousova; Brazhnikova, pl. 4, figs. 6-7.

1989. *Nodosarchaediscus* (Asteroarchaediscus) ex gr. *rugosus* Rauser – Chernousova; Skompski et al., p. 470, pl. 6, fig. 19.

1993. *Asteroarchaediscus rugosus* Rauser - Chernousova; Brenckle and Grelecki, p. 49, pl. 2, figs. 3-5.

1999. *Asteroarchaediscus rugosus* Rauser - Chernousova; Özkan, p. 205, pl. 3, figs. 8-9.

2003. *Asteroarchaediscus rugosus* Rauser-Chernousova; Cózar, p. 162, text fig. 5, fig. J.

2004. *Asteroarchaediscus rugosus* Rauser-Chernousova; Cózar and Rodriguez, p. 41, text fig. 9, fig. 3.

2005. *Asteroarchaediscus rugosus* Rauser-Chernousova; Somerville and Cózar, p. 134, pl. 1, fig.19.

2005. *Asteroarchaediscus rugosus* Rauser-Chernousova; Zhijun et al., p. 345, pl. 4, fig. 11,20.

2006. *Asteroarchaediscus rugosus* Rauser-Chernousova; Groves and Beason, p. 384, pl. 1, figs. 1-9.

2008. *Asteroarchaediscus rugosus* Rauser-Chernousova; Cózar, et al., p. 473, text fig. 8, fig. 4.

2011. *Archaediscus rugosus* Rauser-Chernousova; Atakul-Özdemir et al., p. 715, text fig. 6, figs. ak-am.

Description:

Test is broadly discoidal with oscillations in the coiling. Final tours are evolute and sutures are prominent. Initial tours are involute. There are 5-6 whorls. Volutions are occluded. In some specimens final half volution is not occluded. The wall is hyaline, radial.

Dimensions:

Diameter (d): 0.61-0.21mm

Width (w): 0.08-0.12 mm

w/d: 0.49-0.56

Remarks:

There is a resemblance between *Asteroarchaediscus rugosus* and *Neoarchaediscus parvus* but, the latter has smaller dimensions and last volution is definitely not occluded.

Stratigraphic distribution:

This form originally assigned to Visean but now it is considered to be Serpukhovian and also Bashkirian. (Brenckle and Grelecki, 1993). Specimens in this study have been encountered in the Serpukhovian.

Asteroarchaediscus spp.

Pl. VII, figs. 5-6

Description:

This group is characterized by occlusion of the chambers except for the final one or the final half whorl. All members of this group have stellate appearance around proloculus. Despite their dimensions are different from each other, they are small. Their wall is hyaline-radial.

Stratigraphic distribution:

Specimens of *Asteroarchaediscus* spp. have been identified in the Serpukhovian.

Genus Neoarchaediscus Miklukho-Maklai, 1957

Type species: *Archaediscus incertus* (Grozdilova and Lebedeva, 1954)

Neoarchaediscus incertus (Grozdilova and Lebedeva, 1954)

Pl. VII, figs. 7-8

1954. *Archaediscus incertus* Grozdilova and Lebedeva, p. 60, pl. 7, figs. 14-15.

1963. *Neoarchaediscus incertus* Grozdilova and Lebedeva; Conil and Pirlet, pl. 2, fig. 29.

1979. *Neoarchaediscus incertus* Grozdilova and Lebedeva; Reitlinger, pl. 10, fig. 14.

1982. *Neoarchaediscus incertus* Grozdilova and Lebedeva; Rich, p. 257, pl. 6, figs. 11-12.

1989. *Nodosarchaediscus* (*Neoarchaediscus*) *incertus* Grozdilova and Lebedeva; Skompski et al., p. 470, pl. 6, fig. 12; pl. 7, fig. 26.

2003. *Neoarchaediscus incertus* Grozdilova and Lebedeva; Cózar, p. 162, text fig. 5, fig. B.

2004. *Neoarchaediscus incertus* Grozdilova and Lebedeva; Cózar, p. 375, pl. 1, fig. 15.

2004. *Neoarchaediscus incertus* Grozdilova and Lebedeva; Cózar and Rodriguez, p. 41, text fig. 9, fig. 2.

2004. *Neoarchaediscus* cf. *incertus* Grozdilova and Lebedeva; Cózar and Somerville, p. 50, text fig. 10, fig. 18.

2005. *Neoarchaediscus incertus* Grozdilova and Lebedeva; Somerville and Cózar, p. 134, pl. 1, fig.22.

2006. *Neoarchaediscus incertus* Grozdilova and Lebedeva; Gallagher et al., p. 80, text fig. 14, figs. 25-26.

Description:

Test is small, discoidal. Periphery is broadly rounded. Sides are nearly parallel to each other. Inner whorls coils glomospirally and are involute. They form a stellate outline. Preceding whorls coils oscillatory to planispiral and increase their heights considerably. Final 2 or 3 whorls are evolute and sutures are prominent. The number of volutions is 5. The wall is thin and hyaline.

Dimensions:

Diameter (d): 0.24-0.25 mm

Width (w): 0.08-0.10 mm

w/d: 0.34-0.40

Remarks:

This form is differentiated from *Neoarchaediscus probatus* and *Neoarchaediscus gregorii* by its thinner wall and smaller dimensions. The latter also lacks a sharp transition from glomospiral to planispiral coiling in inner whorls.

Stratigraphic distribution:

The stratigraphic distribution ranges from the Upper Visean to Bashkirian stage (Grozdilova and Lbedeva, 1954). Specimens in this study have been found in the Serpukhovian.

*Neoarchaediscus parvus (*Rauser-Chernousova), 1948

Pl. VII, figs. 9-11

1948. A*rchaediscus parvus* Rauser-Chernoussova, p. 233, pl. 16, figs. 9-12.

1973. *Neoarchaediscus parvus* Rauser-Chernousova; Mamet, p. 113, pl. 4, figs. 20-21.

1979. *Neoarchaediscus parvus* Rauser-Chernousova; Potievskaya, pl. 12, fig. 20.

1982. *Neoarchaediscus parvus* Rauser-Chernousova, Grozdilova and Lebedeva; Rich, p. 257, pl. 6, figs. 14-16.

1993. *Neoarchaediscus parvus* Rauser-Chernousova; Mamet et al., pl. 15, figs. 5-6.

1993. *Neoarchaediscus parvus* Rauser-Chernousova; Ueno and Nakazawa, p. 12, text fig. 4, figs. 13-17.

1999. *Neoarchaediscus parvus* Rauser-Chernousova; Vdovenko et al., p. 188, text fig. 1, fig. 22.

2003. *Neoarchaediscus parvus* Rauser-Chernousova; Cózar, p. 162, text fig. 5, fig. D.

2004. *Neoarchaediscus* cf. *parvus* Rauser-Chernousova; Cózar and Somerville, p. 56, text fig. 14, fig. 20.

2005. *Neoarchaediscus parvus* Rauser-Chernousova; Cózar et al., p. 294, text fig. 8, fig.8.

2005. *Neoarchaediscus parvus* Rauser-Chernousova; Somerville and Cózar, p. 134, pl. 1, fig.14.

2011. *Archaediscus parvus* Rauser-Chernousova; Atakul-Özdemir et al., p. 715, text fig. 6, figs. af-ag.

Description:

Test is very small, discoidal. Periphery is rounded. Sides are nearly parallel to each other. Although spire starts its expansion with oscillations, it continues nearly planispirally. Final tour is obviously evolute and sutures are well marked. There are 4 volutions. Except for the final two volutions, others are occluded. Inner volutions form a stellate appearance. The wall is thick and hyaline.

Dimensions:

Diameter (d): 0.17-0.19 mm

Width (w): 0.08-0.10 mm

w/d: 0.48-0.53

Remarks:

This form is differentiated from *Neoarchaediscus baschkiricus* by its smaller dimensions and flattened form. *Neoarchaediscus parvus* is also smaller than *Asteroarchaediscus rugosus* and the last 2 volutions are not occluded.

Stratigraphic distribution:

This form is stratigraphicaly distributed in the Upper Visean and Serpukhovian stages (Ueno and Nakazawa, 1993). Specimens in this study have been encountered in the lowermost Serpukhovian.

*Neoarchaediscus probatus (*Reitlinger, 1950)

Pl. VII, figs. 12-13

1950. *Archaediscus probatus* Reitlinger, p. 83, pl. 18, fig.9.

1993. *Neoarchaediscus probatus* Reitlinger; Brenckle and Grelecki, p. 53, pl. 4, figs. 1, 2, 14, 15; p. 57, pl.6, figs. 5, 6.

1999. *Neoarchaediscus probatus* Reitlinger; Özkan, p. 205, pl. 3, figs. 18-19

2011. *Neoarchaediscus probatus* Reitlinger; Atakul-Özdemir et al., p. 715, text fig. 6, figs. w-y.

Description:

Test is discoidal. Coiling starts sigmoidally but continues its development planispirally in the final 2 volutions. First 2 or 3 volutions are occluded and show a stellate outline. Last 3-3.5 volutions are open and they are evolute with prominent sutures. Number of volutions is 6. The wall is formed by a thick hyaline layer.

Dimensions:

Diameter (d): 0.290 mm

Width (w): 0.105 mm

w/d: 0.36

Remarks:

Trend of coiling is similar to *Neoarchaediscus koktjubensis* but, *Archaediscus probatus* differs by its occluded chambers and do not contain a microgranular layer. *Neoarchaediscus incertus* has thinner wall and smaller dimensions than *Neoarchaediscus probatus*.

Stratigraphic distribution:

The stratigraphic range of this form is reported as upper Namurian (Brenckle and Grelecki, 1993). Specimens in this study have been encountered in the Serpukhovian.

Neoarchaediscus ex gr. *subbashckiricus* (Reitlinger, 1949)

Pl. VII, figs. 14-15

1949. *Asteroarchaediscus subbaschkiricus* Reitlinger, pl. 1, figs. 8a-b.

1973. *Neoarchaediscus* aff. *N. subbashckiricus* Reitlinger; Mamet, p. 113, pl. 4, figs. 30-31.

1979. *Asteroarchaediscus subbaschkiricus* Reitlinger; Brazhnikova, pl. 2, figs.18-19.

1979. *Asteroarchaediscus subbaschkiricus* Reitlinger; Potievskaya, pl. 12, fig. 23.

1988. *Asteroarchaediscus subbashckiricus* Reitlinger; Vachard, p. 123, pl. 2, fig. 24.

1993. *Neoarchaediscus subbaschkiricus* Reitlinger; Mamet et al., pl. 15, figs. 7-12.

1993. *Neoarchaediscus* cf. *subbashckiricus* Reitlinger; Ueno and Nakazawa, p. 12, text fig. 4, figs. 6-8

1999. *Neoarchaediscus subbaschkiricus* Reitlinger; Özkan, p. 205, pl. 3, figs. 5-7.

2003. *Neoarchaediscus subbashckiricus* Reitlinger; Cozar, p. 162, text fig. 5, fig. C.

2005. *Neoarchaediscus subbashckiricus* Reitlinger; Somerville and Cózar, p. 134, pl. 1, fig.18.

2011. *Archaediscus . subbashckiricus* Reitlinger,; Atakul-Özdemir et al., p. 715, text fig. 6,

figs. z-ab.

Description:

Test is small, lenticular. Periphery is rounded to acute. Central region is prominent. Coiling is skewed in initial volutions and oscillatory to planispiral in the outer volutions. The height of the lumen increases through the coiling. Initial tours are occluded with a stellate appearance. Last or last one and a half tour is evolute and sutures are prominent. There are approximately 5 whorls. The wall is formed by thick a hyaline layer.

Dimensions:

Diameter (d): 0.265-0.288 mm

Width (w): 0.138-0.145 mm

w/d: 0.48-0.52

Remarks:

In some specimens characteristic shape of outline could not be observed however all other features are present. So, all these specimens are named as *Neoarchaediscus* ex gr. *subbashckiricus.*

Stratigraphic distribution:

The stratigraphic range of *Neoarchaediscus subbaschkiricus* is uppermost Serpukhovian through Lower Bashkirian (Dain and Grozdilova, 1953). However, many autors observed this from also in the Lower Serpukhovian . Samples in this study have been encountered from the Serpukhovian.

Neoarchaediscus? sp.

Pl. VII, fig. 20

Description:

Test is discoidal. Periphery is slightly rounded. The height of the lumen increases gradually in each volution. Coiling is skewed in initial volutions and

oscillatory to planispiral in the outer volutions. Last one and a half volution is evolute with well-marked sutures. The number of volutions is 5. The wall is formed by a thick hyaline-radial layer.

Dimensions:

Diameter (d): 0.279 mm

Width (w): 0.145 mm

w/d: 0.52

Remarks:

Since the occlusion of chambers is not obvious this formed is named with a question mark. In fact occlusion starts in the initial tours so that it disturbs the chamber floor but it does not totally fill even the first chamber.

Stratigraphic distribution:

The only specimen belonging to *Neoarchaediscus*? sp. has been encountered from uppermost part of Mikhailovsky horizon.

Neoarchaediscus sp. (@tenuis stage)

Pl. VII, figs. 19

Description:

Test is discoidal. Chamber floors are flat or concave. Coiling is oscillatory, involute in the initial tours and evolute in the final tours. Sutures are pronounced. Initial two or more chambers are occluded. There are 4-5 chambers. The wall is formed by thick hyaline layer.

Remarks:

This species is particularly explained separately because tenuis morphology is the last step of the archaediscid evolution. It is biostratigraphically very important because Arhaedicids @ tenuis stage can be observed at the beginning of Serpukhovian stage.

Stratigraphic distribution:

Specimens in this study have been encountered in the Serpukhovian.

Neoarchaediscus spp.

Pl. VII, figs. 16-18, 21-23

Description:

Specimens that cannot be assigned to a particular species of the genus *Neoarchaediscus* were grouped as *Neoarchaediscus* spp. Their common features are the occlusion of initial chambers. They can be discoidal or lenticular in shape. They coil mostly streptospiral in the initial tours, oscillatory to planispiral in final tours.

Stratigraphic distribution:

Specimens in this study have been encountered in the Upper Visean and Serpukhovian interval.

SUPERFAMILY BISERIAMMINACEA Chernysheva, 1941

FAMILY BISERIAMMINIDAE Chernysheva, 1941

SUBFAMILY BISERIAMMININAE Chernysheva, 1941

Genus *Biseriella* Mamet, 1974

Type species: *Globivalvulina parva*, Chernysheva, 1948

Biseriella parva (Chernysheva, 1948)

Pl. VIII, figs. 1-11, 12?

1948. *Globivalvulina parva* Chernysheva, p. 249, pl. 13, figs. 1-4.

1979. *Globivalvulina parva* Chernysheva; Brazhnikova, pl. 3, figs. 13-14.

1979. *Biseriella* cf. p*arva* Chernysheva; Conil, Longerstaey and Ramsbottom, p. 170, pl. 24, figs. 2-4; p. 178, pl. 28, figs. 40-41

1981. *Globivalvulina parva* Chernysheva; Altıner, p. 439, pl. 23, figs. 18-23

1988. *Biseriella parva* Chernysheva; Groves, p. 382, text fig. 14, figs. 1-9.

1993. *Biseriella* of the group *B. parva* Chernysheva; Mamet et al., pl. 13, figs. 1-3, 5-6.

1995. *Biseriella parva* Chernysheva; Altıner and Savini, p. 447, pl. 5, figs. 26-29

1999. *Biseriella parva* Chernysheva; Özkan, p. 210, pl. 5, figs.1-11.

2004. *Biseriella parva* Chernysheva; Cózar and Somerville, p. 50, text fig. 10, figs. 23-24.

2005. *Biseriella parva* Chernysheva; Cózar et al., p. 294, text fig. 8, figs. 18-20.

2006. *Biseriella* aff. p*arva* Chernysheva; Okuyucu and Vachard, p. 540, text fig 5, figs 17-19.

2006. *Globivalvulina parva* Chernysheva; Vachard et al., p. 459, text fig. 4, fig. 3; p. 461, text fig. 6, figs. 8-12, 14-15, 17.

2008. *Biseriella* aff. p*arva* Chernysheva; Cozar et al., p. 473, text fig. 8, fig. 28.

Description:

Test is small and biserially enrolled. It trochospirally coils in initial portion. Chambers are spherical and expand rapidly through coiling. Wall is microgranular and dark.

Dimensions:

Diameter (d): 0.140-0.223mm

Width (w): 0.177-0.211 mm

Wall thickness: 7-13 μm

Remarks:

This form resembles morphologically to *Globivalvulina bulloides* but, *Globivalvulina bulloides* has greater dimensions and its wall definitely contains luminotheca. The genus *Biseriella* is questioned here because some specimens of *Biseriella parva* contain lighter layer in its wall but this genus should have a dark microgranular wall. In addition, the validity of the genus *Biseriella* is still controversial. Some authors (Vachard and Beckary, 1991; Perret, 1993 in Cozar 1992) do not agree with the generic significance of differentiation in the wall and they synonymized the genus G*lobivalvulina* and *Biseriella*. On the other hand other authors; (Mamet, 1974;

Mamet and Pinard, 1998 in Cozar, 2002) use this differentiation on the generic classification and also consider that the stratigraphic distribution of G*lobivalvulina* and *Biseriella* are different (Cozar, 2002).

Stratigraphic distribution:

The stratigraphic range of this form corresponds to the latest Brigantian (Upper Visean) - Serpukhovian (Vachard et al., 2006). The samples of this study were recovered Upper Visean (Venevsky) and Serpukhovian.

Genus *Globivalvulina* Schubert, 1921

Type species: *Valvulina bulloides* Brady, 1876

Globivalvulina bulloides Brady, 1876

Pl. VIII, figs. 13-14, 15?

1876. *Valvulina bulloides* Brady, pl. 4, figs. 12-15.

1995. *Globivalvulina bulloides* Brady; Altiner and Savini, p. 448, pl. 4, figs. 1-3.

1999. *Globivalvulina bulloides* Brady; Özkan, p. 210, pl. 5, figs.12-19.

2011. *Globivalvulina bulloides* Brady; Atakul-Özdemir et al., p. 717, text fig. 7, figs. g-m.

Description:

Test is large and biserially enrolled. Chambers expand rapidly through coiling. Wall is microgranular but includes a clear layer particularly observed in the final chambers.

Dimensions:

Width (w): 301-447 mm

Wall thickness: 10-16 μm

Remarks:

Globivalvulina bulloides is distinguished from *Biseriella parva* by its larger size, clear layer in its wall and greater number of chambers.

Stratigraphic distribution:

The stratigraphic range of this form is in Upper Serpukhovian (Zapaltyubinsky Horizon) through latest Carboniferous (Groves, 1988). The specimens of this study were recovered from Serpukhovian.

Globivalvulina sp. 1

Pl. VIII, figs. 16-20

Description:

Coiling is planispiral and biserial. Chambers are globular and they increase their height very rapidly. Particularly, last 2 chambers expand approximately two times more than the preceding ones. Last one or 2 chambers tend to uncoil. Wall is microgranular and in some specimens, clear layer can be observed.

Remarks:

The main feature that characterizes *Globivalvulina* sp. 1 is its uncoiling trend of the final chambers and rapid expansion of the final 2 chambers. *Biseriella parva* is smaller than *Globivalvulina* sp. 1 and it coils throughout the ontogenesis. *Globivalvulina bulloides* is larger and does not show an uncoiling trend.

Stratigraphic distribution:

Specimens of *Globivalvulina* sp. 1 have been recovered from the Serpukhovian of the measured section.

Globivalvulina spp.

Pl. IX, figs. 1-6, 7?, 8-9

Description:

A broad range of morphologies is represented in this group. All forms are biserially enrolled. Some of them have uncoiling trend at the end. In some specimens

final chambers expand rapidly. Mainly chambers are globular. Wall is microgranular and inner clear layer is present.

Stratigraphic distribution:

Specimens of *Globivalvulina* spp. have been recovered from Mikhailovsky horizn and Serpukhovian.

SUPERFAMILY BISERIAMMINACEA Chernysheva, 1941

FAMILY KOKTJUBINIDAE Marfenkova, 1991

Pl. IX, figs. 10-13

Description:

These forms consist of two parts. In the first part coiling is trochospiral and initial one or two whorls planispiral. Chambers are convex and *Chernyshinella* type in the first part. Second part is in the form of rectilinear conical. This part is wider. Wall is microgranular, agglutinated and dark.

Remarks:

Specimens that cannot be identified generically but show the characteristics of the family Koktjubinidae were grouped under this family.

Stratigraphic distribution:

This family occupies Upper Visean and Serpukhovian (Marfenkova, 2007). Our samples have been recovered from Serpukhovian.

SUPERFAMILY ENDOTHYRACEA Brady, 1884

FAMILY BRADYINIDAE Reitlinger, 1950

Genus *Bradyina* Moeller, 1878

Type species: *Bradyina nautiliformis* Moeller,1878

Bradyina spp.

Pl. X, figs. 1-10

Description:

Specimens that cannot be assigned to a particular species of the genus *Bradyina* were grouped as *Bradyina* spp. Nautiloid test, planispiral and involute coiling, thick, short and straight septa and keriothecal wall structure are the common features of specimens included in this zone. Periphery is broadly rounded in axial sections of some specimens and there are secondary sutural apertures in equatorial sections of some specimens. Last tour of some specimens rapidly increases their height and width but, in some other forms height and width increase progressively.

Dimensions:

Diameter (d): 0.563-1.765mm

Width (w): 0.365-1.298 mm

Wall thickness: 31-107μm

Stratigraphic distribution:

The stratigraphic distribution of the genus *Bradyina* is from Late Asbian (Cózar and Somerville, 2006) to Late Permian (Loeblich and Tappan, 1988). The specimens of this study were recovered from Upper Visean (Mikhailovsky? and Venevsky) and Serpukhovian.

Genus *Bibradya* Strank, 1983

Type species: *Bibradya inflata* Strank, 1983

Bibradya? sp.

Pl. X, figs. 11-12

Description:

Coiling is irregular and endothyroid. Wall is microgranular and dark. It increases its thickness through the coiling. There are 2.5-3 volutions. Initial volutions are very tight. In the final volution the whorl increases its height and becomes highly inflated. Septa are thick and bluntly pointed.

Dimensions:

Diameter (d): 0.527-1.210mm

Height of the final chamber: 0.745 mm

Wall thickness: 26-37μm

Remarks:

Since the bifurcation od septa cannot be well observed this species is defined here with a question mark. This genus is differentiated from *Plectogyranopsis* by its microgranular wall and bifurcating septa. It is distinguished from *Janischewskina* by its thicker wall and inflated final whorl.

Stratigraphic distribution:

The stratigraphic range of *Bibradya* is Upper Visean (Asbian) (Strank, 1983). The specimens of this study were recovered the Mikhailovsky Horizon.

SUPERFAMILY ENDOTHYRACEA Brady, 1884

FAMILY ENDOTHYRIIDAE Brady, 1884

SUBFAMILY ENDOTHYRINAE Brady, 1884

Genus *Banffella* Mamet, 1970

Type sepcies: *Endothyra*? *baffensis*

Banffella sp.1

Pl. XI, figs. 11-12

Description:

Test is discoidal and compressed laterally. Coiling is oscillatory to planispiral and oscillation is well marked in the initial volutions. There are 4 volutions. Secondary deposits are obreved in axial section, at the bottom of each volution and in the form of rectangular shape basal coverings. Wall is granular and has a peusdofibrous layer but not observed in all whorls of the form.

Dimensions:

Diameter (d): 0.666-0.812mm

Width if the unbilical region (w): 0.114-0.127 mm

Height of the last tour: 0.121-0.133

Wall thickness: 24-29μm

Remarks:

This form is differentiated from *Banffella*? sp.2 by the wall structure, oscillatory to planispiral coiling, less number of volutions and shape of the secondary deposits.

Stratigraphic distribution:

The stratigraphic distribution of the genus *Banffella* is Lower to Upper Visean (Loeblich and Tappan, 1988). The speciemns of this study were recovered Upper Visean (Mikhailovsky).

Banffella? sp.2

Pl. XI, figs. 13-15

Description:

Test is discoidal and compressed laterally. Coiling is endothyroid in the first tour and planispiral in the preceding tours. Slight oscillations can be observed. Slight salience can be observed in umbilical region of some speciemens. There are 5 volutions. Secondary deposits can be developed as pseudochomata or rectangular shaped floor coverings. Wall is granular to microgranular and pseudofibrous layer can be observed only in some specimens.

Dimensions:

Diameter (d): 0.496-0.630mm

Width if the unbilical region (w): 0.63-0.119 mm

Height of the last tour: 0.085-0.092

Wall thickness: 12-14μm

Remarks:

The generic attribution is questioned here because, the pseudofibrious layer can not be observed in all specimens. On the contrary some forms are composed of microgranular and dark layer. This form is differentiated from *Banffella* sp. 1 by endothyroid coiling in the first volution, higher number of volutions and shape of secondary deposits.

Stratigraphic distribution:

The specimens of *Banffella*? sp. 2 in this study were recovered the Upper Visean (Mikhailovsky).

Genus *Endospiroplectammina* Lipina, 1970

Type species: *Spiroplectammina venusta*

Endospiroplectammina sp.1

Pl. XII, figs. 13-15

Description:

Test is small and aligned. Chambers are probably arranged spirally in the initial stage but immediately after, biserially. Sides of the test are parallel to each other. There are 4-6 biserially arranged chambers. Shape of chambers is rectangular. They are separated by long and straight septa. The points of septa are nodular. Wall is microgranular.

Dimensions:

Height: 0.339-0.216mm

Width: 0.105-0.095 mm

Wall thickness: 3-4μm

Remarks:

This form is differentiated from *Endospiroplectammina* sp. 2 by parallel sides of the test and nodular shaped pointed septa.

Stratigraphic distribution:

The specimens of this study were recovered from the Upper Visean (Mikhailovsky).

Endospiroplectammina sp.2

Pl. XII, fig. 16

2005. *Endospiroplectammina* sp.1, Somerville and Cózar, p. 136, pl. 2, fig. 17.

Description:

Test is small and aligned. The shape of the overall form is triangular. Initial chambers are probably arranged spirally. After this spiral part there are 6 pairs of biserially arranged chambers. They are separated by long and slightly curved septa. Wall is microgranular.

Dimensions:

Height: 0.279 mm

Width: 0.069 mm

Wall thickness: 7μm

Remarks:

This form is differentiated from *Endospiroplectammina* sp.1 by its triangular shape in longitidunal section. Although the sections of our specimens are not well-oriented, triangularity of the form is obvious.

Stratigraphic distribution:

The specimens of this study were recovered from the Upper Visean (Mikhailovsky).

Genus *Endothyra* Phillips, 1846

Type species: *Endothyra bowmani* Phillips, 1846

Endothyra archerbecki Conil and Longerstaey, 1979

Pl. XIII, figs. 10-11

1979. *Endothyra archerbecki* Conil and Longerstaey in Conil, Longerstaey and Ramsbottom, p. 158, pl. 19, figs. 9-10; p. 176, pl. 27, fig. 4

Description:

Test is small. Spire coils tightly in the initial tours but it expands very rapidly in the final 1 or 1.5 tours. Chambers are generally flattened and they are slightly convex divided by straight septa which are slightly inclined towards the aperture. Sutures are moderately marked. There are 3.5 volutions and 7 chambers in the final volution. Supplementary deposits are moderately developed in the last tours. They are in the form of small crusta and they form a thin layer on the lower surface of the cambers of the inner volutions. Spine-like outgrows can be observed in the terminal part. Wall is dark, microgranular.

Dimensions:

Diameter: 0.404-0.425 mm

Height of the last chamber: 0.116-0.117 mm

Wall thickness: 7-10μm

Remarks:

This form is similar to *Endothyra phrissa* and it is differentiated from it by its less globular chambers and less developed secondary deposits.

Stratigraphic distribution:

The stratigraphic range of *Endothyra archerbecki* is Upper Visean (Upper Asbian-Brigantian) (Conil et al., 1979). The specimens of this study were recovered the Upper Brigantian (Venevsky).

Endothyra bowmani Phillips, 1846

Pl. XIII, figs. 17-19

1846. *Endothyra bowmani* Phillips, p. 277-279, pl. 7, fig. 1.

1973. *Endothyra bowmani* Phillips; Austin et al., p. 185, pl. 2, fig. 28.

1973. *Endothyra* ex gr. *bowmani* Phillips; Austin et al., p. 183, pl. 1, fig. 12.

1979. *Endothyra bowmani* Phillips; Conil, Longerstaey and Ramsbottom, p. 132, pl. 7, fig. 9.

1981. *Endothyra bowmani* Phillips; Altıner, p. 436, pl. 16, figs. 8-13.

1982. *Endothyra bowmani* Phillips; Rich, p. 247, pl. 2, figs. 11, 12?, 14.

1987. *Endothyra bowmani* Phillips; Brenckle and Marchant, p. 80, pl. 2, figs. 8-11.

1993. *Endothyra bowmani* Phillips; Mamet et al., pl. 3, fig. 17.

1995. *Endothyra bowmani* Phillips; Hoare and Skipp, p. 621, text fig. 4, figs. 5-10.

2005. *Endothyra bowmani* Phillips; Zhijun et al., p. 344, pl. 3, figs. 23-24.

2006. *Endothyra* ex gr. *bowmani* Phillips; Groves and Beason, p. 384, pl. 1, figs. 33-36.

Description:

Test is small. Tightly and evenly coiled initial whorls make oscillations. In the final whorls coiling became planispiral and spire expands more rapidly with a broadly rounded periphery. Chambers are convex and septa separating them are curved and slightly inclined towards the aperture. The number of volutions is 2.5-3 and there are 7.5 chambers in the final volution. Supplementary deposits are not well developed but if it exists it is in the form of nodes. Wall is dark, microgranular.

Dimensions:

Diameter (d): 0.293-0.375 mm

Height of the last chamber: 0.081 mm

Width (w): 0,197 mm

w/d: 0,67

Wall thickness: 13-14µm

Remarks:

Endothyra bowmani resembles to *Endothyra obseleta* to some extent. It is distinguished from the latter by less convex chambers and less curved septa.

Stratigraphic distribution:

The stratigraphic range of *Endothyra bowmani* is from the Lower Visean to Moscovian (Altıner, 1981). The specimens of this study were recovered from the Upper Visean and Serpukhovian.

Endothyra cuneispeta (Conil and Lys, 1964)

Pl. XIII, fig. 15

1964. *Plectogyra cuneispeta* Conil and Lys, p. 182, pl. 27, figs. 541-544.

1981. *Endothyra cuneispeta* Conil and Lys; Altıner, p. 436, pl. 16, figs.1-2.

Description:

Test is very small. 1.5-2 tours are planispirally coiled. Progressively developed spire does not increase too much its height through the ontogenesis. Chambers are not convex. Septa are very short and triangular so that its larger edge is attached to the base of the wall of upper volution and it points towards the lower volution. Sutures are not marked. There are 5-6 chambers in the final volution. Supplementary deposits are not developed. Wall is dark, microgranular.

Dimensions:

Diameter: 0.183 mm

Height of the last chamber: 0.30 mm

Wall thickness: 8μm

Remarks:

The shape of the septa is very characteristic in *Endothyra cuneisepta*. This feature also differentiates *Endothyra cuneisepta* from *Priscella prisca* .

Stratigraphic distribution:

The stratigraphic distribution of *Endothyra cuneispeta* ranges between Lower Visean (V1b) and Upper Visean (Asbian, V3b) (Altıner, 1981). Only one specimen in this study has been found from the Mikhailovsky Horizon (Upper Visean).

Endothyra excellens (Zeller, 1953)

Pl. XIII, fig. 14

1953. *Plectogyra excellens* Zeller, p. 198, pl. 28, figs. 8-9

1973. *Endothyra excellens* Zeller; Mamet, p. 117, pl. 6, fig. 2.

1979. *Endothyra excellens* Zeller; Conil, Longerstaey and Ramsbottom, p. 176, pl. 27, figs. 2-3.

1979. *Endothyra* aff. *excellens* Conil, Longerstaey and Ramsbottom, p. 154, pl. 17, fig. 1.

1982. *Endothyra excellens* Zeller; Rich, p. 247, pl. 2, figs. 16-17.

1993. *Endothyra excellens* Zeller; Mamet et al., pl. 3, fig. 13.

1995. *Endothyra excellens* Zeller; Hoare and Skipp, p. 621, text fig. 4, figs. 11-15.

2004. Endothyra if the group *E. excellens* Zeller; Brenkle, p. 148, pl. 2, fig. 15.

Description:

Test is large. Coiling is planispiral but distortions exist in the initial tours. There are 3.5-4 volutions. Spire expands very rapidly in the final tour so that chambers are very large and high. Globular chambers are divided by curved and short septa. Sutures

are well depressed. There are 6.5 chambers in the final tour. Supplementary deposits are very well developed and they are in the form of hook like projections in the last volution and they are in the form of nodes in the initial volutions. Wall is very finely granular.

Dimensions:

Diameter: 0.610 mm

Height of the last chamber: 0.167 mm

Wall thickness: 20μm

Remarks:

Endothyra excellens differs from *Endothyra phrissa* by its larger diameter, more convex chambers, and more massive secondary deposits. *Endothyra* sp. 2 resembles to *Endothyra excellens* but, the last tour of the former increases in height and width much more rapidly.

Stratigraphic distribution:

Illustrated specimen has been recovered from the Serpukhovian.

Endothyra obsoleta Rauser-Chernoussova, 1948

Pl. XIII, fig. 16

1973. *Endothyra obsoleta* Rauser-Chernoussova; Mamet, p. 117, pl. 6, figs. 6-7.

1974. *Endothyra* of the group *E. obsoleta* Rauser-Chernoussova; Brenckle et al., p. 435, text fig. 3, figs. 11-12.

1979. *Endothyra* cf. *obsoleta* Rauser-Chernoussova; Conil, Longerstaey and Ramsbottom, p. 154, pl. 17, fig. 7

1981. *Endothyra obsoleta* Rauser-Chernoussova; Altıner, p. 436, pl. 16, figs. 18-20.

1993. *Endothyra* of the group *E. obsoleta* Rauser-Chernoussova; Mamet et al., pl. 3, figs. 1-5.

Description:

Test is small and planispirally coiled with a slight oscillation in the initial volution. Chambers enlarge progressively through the coiling but, the final 2 chambers are much larger than the previous ones. There are 2.5 tours and the last tour contains 6.5 chambers. Chambers are globular and inflated. Septa are curved and inclined towards the floor. Sutures are depressed. Secondary deposits are in the form nodes. Wall is dark, microgranular.

Dimensions:

Diameter: 0.307 mm

Height of the last chamber: 0.086 mm

Wall thickness: 13μm

Remarks:

Chambers are globular and septa are more curved than the septa of *Endothyra bowmani* and *Endothyra similis*. Dimensions are smaller than the former and *Endothra excellens*. In addition it has less obvious secondary deposits and less distorted initial tours.

Stratigraphic distribution:

The stratigraphic range of *Endothyra obsoleta* is from Middle Visean (Livian) to Upper Visean (Altıner, 1981). The specimens of this study were recovered from the Upper Visean (Mikhailovsky).

Endothyra phrissa (Zeller, 1953)

Pl. XIII, fig. 9

1953. *Plectogyra phrissa* Zeller, p. 198, pl. 28, figs. 1,4,6.

1979. *Endothyra phrissa* Zeller; Conil, Longerstaey and Ramsbottom, p. 156, pl. 18, fig. 14; p. 176, pl.27, figs. 5-8; p.176, pl. 27, fig. 25

1979. *Endothyra* ex gr. *phrissa* Conil, Longerstaey and Ramsbottom, p. 146, pl. 13, fig. 15; p. 176, pl. 27, fig. 9

1979. *Endothyra* cf. *phrissa* Conil, Longerstaey and Ramsbottom, p. 174, pl. 26, fig. 10.

1989. *Endothyra phrissa* Zeller; Skompski et al., p. 473, pl. 7, fig. 32.

2004. *Endothyra phrissa* Zeller; Cózar and Somerville, p. 52, text fig. 11, fig. 3.

Description:

Coiling is planispiral with highly distorted initial tours. Chambers in the final tour are much larger than the previous ones due to the rapid expansion in coiling of the last tour. There are 3 volutions and 6 chambers in the final tour. Chambers are globular and they are divided by slightly curved septa. Sutures are depressed. Secondary deposits are very well developed as crusta and hook like projection is obvious in the last chamber. Wall is very finely granular.

Dimensions:

Diameter: 0.414 mm

Height of the last chamber: 0.134 mm

Wall thickness: 8μm

Remarks:

Endothyra phrissa is differentiated from *Endothyra archerbecki* by its more convex chambers and more curved septa. In addition its supplementary deposits are better developed but less developed than *Endothyra excellens*.

Stratigraphic distribution:

The stratigraphic range of *Endothyra phrissa* is Upper Chesteran (Zeller, 1953), but it is a typical Brigantian marker (Cózar and Somerville, 2004). Specimens have been recovered from the Upper Brigantian.

Endothyra similis Rauser-Chernoussova and Reitlinger, 1936

Pl. XIII, figs. 1-3

1936. *Endothyra similis* Rauser-Chernoussova and Reitlinger, p. 211, pl. 6, figs. 5-6.

1981. *Endothyra similis* Rauser and Reitlinger; Altıner, p. 437, pl. 17, figs. 1-7.

1982. *Endothyra similis* Rauser and Reitlinger; Rich, p. 249, pl. 3, figs. 9, 10, 13, 14?, 16?, 17?.

Description:

Test is small. Strongly distorted coiling becomes planispiral through the ontogenesis. Spire expands progressively but rather rapidly in the final tour. The number of tours is 2.5-3.5 and the number of chambers in the final tour is 6.5 and 8. Chambers are subraunded. Septa are long and straight. Sutures are less marked. Secondary deposits are developed in the form of nodes. Wall is dark and microgranular.

Dimensions:

Diameter: 0.201-0.248 mm

Height of the last chamber: 0.050-0.054 mm

Wall thickness: 7-10μm

Remarks:

The most distinguishing feature of this form is its highly distorted coiling in the initial volutions.

Stratigraphic distribution:

The stratigraphic range of *Endothyra similis* is from Lower Visean to Lower Serpukhovian (Altıner, 1981). Specimens in this study has been found in the Upper Visean.

Endothyra sp. 1

Pl. XIII, figs. 12-13

Description:

Test is small. Coiling is endothyroid but highly distorted till the last tour. Initial tours are tightly coiled, final ones are loosely coiled and they expand very rapidly relative to the initial volutions. There are 3-3.5 volutions. Chambers are slightly convex

and septa are curved. Supplementary deposits are well developed as small crusta. Wall is microgranular and differentiated.

Dimensions:

Diameter (d): 0.331-0.336 mm

Width (w): 0.191-0.198 mm

w/d: 0.59

Wall thickness: 1-17μm

Remarks:

The morphology of the outline and initially tight finally loose coiling is characteristic for *Endothyra* sp.1.

Stratigraphic distribution:

Specimens of *Endothyra* sp.1 have been found in the Serpukhovian.

Endothyra sp. 2

Pl. XIII, figs. 23-24

Description:

Test is large. Coiling axis changes its plane in the last tour. There are 2.5-3 volutions. The height and width of the chambers in the first 2 volution increase gradually however, chambers of the last half volution expand very rapidly. Chambers are strongly convex and septa are curved. Supplementary deposits are developed as crusta or nodes. Wall is finely granular.

Dimensions:

Diameter: 0.438-0.497 mm

Height of the last chamber: 0.105-0.084 mm

Wall thickness: 13-15μm

Remarks:

Dimensions are large like dimensions of *Endothyra excellens*. *Endothyra* sp. 2 is differentiated from it by its more distorted coiling and less developed basal deposits.

The most prominent feature of *Endothyra* sp. 2 is its extremely large chambers in the final half volution.

Stratigraphic distribution:

Specimens of *Endothyra* sp.2 have been found in the Venevsky to Early Serpukhovian interval.

Endothyra spp.

Pl. XIII, figs. 20-22

Description:

A variety of specimens that cannot be assigned to a particular species but share characteristic morphological features of the genus *Endothyra*, are grouped in *Endothyra* spp. These features are spiral coiling (generally, oscillated at first then planispiral at the end), supplementary basal deposits and microgranular wall that can include a tectum.

Stratigraphic distribution:

Specimens of *Endothyra* spp. have been observed through the columnar section Upper Visean and Serpukhovian.

Priscella prisca (Rauser-Chernoussova and Reitlinger, 1936)

Pl. XIII, figs. 4-8

1936. *Endothyra prisca* Rauser-Chernoussova and Reitlinger, p. 213, pl. 6, fig. 7-8.

1974. *Endothyra* of the group *E. prisca* Rauser-Chernoussova and Reitlinger; Brenckle et al., p. 435, text fig. 3, figs. 7-10.

1981. *Endothyra prisca prisca* Rauser-Chernoussova and Reitlinger; Altıner, p. 436, pl. 16, figs. 3-4.

1982. *Priscella prisca* Rauser-Chernoussova and Reitlinger; Rich, p. 249, pl. 5, figs. 6, 13, 14?.

1993. *Priscella* of the group *P.prisca* Rauser-Chernoussova and Reitlinger; Mamet et al., pl. 3, fig. 13.

? 2005. *Priscella prisca* Rauser-Chernoussova and Reitlinger; Zhijun et al., p. 344, pl. 3, figs. 5-6.

Description:

Test is very small and is composed of planispirally coiled 2 tours. Spire expands gradually though coiling. The number of chambers in the final tour is 6-7. Chambers are not convex and they are divided by slightly inclined straight septa. Sutures are not obvious. Secondary deposits are less developed. Wall is dark and granular.

Dimensions:

Diameter: 0.132-0.200 mm

Height of the last chamber: 0.030-0.038 mm

Wall thickness: 7-8μm

Remarks:

This form resembles to *Endothyra cuneisepta*. They differ from each other in the morphology of their septa. *Endothyra cuneisepta* has triangular septa and its chambers are more convex. In addition, wall structure is more granular than the wall structure of the members of the genus *Endothyra*.

Stratigraphic distribution:

The stratigraphic distribution of *Priscella prisca* is Visean (Altıner, 1981). Specimens in this study has been found in the Upper Visean (Mikhailovsky).

Genus *Globoendothyra* Reitlinger, 1959

Type species: *Globoendothyra pseudoglobulus* Bogush and Yuferev, 1962

Globoendothyra spp.

Pl. XI, figs. 1-10

Description:

Test is very large and nautiloid. Coiling is skewed through ontogenesis, but tends to be planispiral finally. The height and width of chambers increases rapidly but progressively. Chambers are divided by blunt pointed and short septa. In some specimens septa are thicker than the wall. Sutures are not marked. Secondary deposits are developed as nodes or thickenings at the base of the chambers. Wall is granular.

Dimensions:

Diameter: 0.492-0.990 mm

Wall thickness: 20-28μm

Remarks:

Various morphologies showing the characters mentioned in the description are grouped under *Globoendothyra* spp. The granular wall structure and shape of septa are characteristic features for this genus.

Stratigraphic distribution:

Specimens of *Globoendothyra* spp. in this study has been encountered in Upper Visean and Serpukhovian.

Genus *Omphalotis* Schlykova, 1969

Type species: *Endothyra omphalota* Rauser-Chernoussova and Reitlinger, 1937

Omphalotis minima (Rauser-Chernoussova and Reitlinger in Rauser-Chernoussova, Beliaev and Reitlinger, 1936)

Pl. XII, figs. 1-7

1936. *Omphalotis omphalota* var. *minima* Rauser-Chernoussova and Reitlinger in Rauser-Chernoussova, Beliaev and Reitlinger, p. 210, tf. 5

1963. *Plectogyra omphalota minima* Rauser-Chernoussova and Reitlinger; Conil and Pirlet, pl. 3, figs. 35?-36.

1979. *Omphalotis minima* Rauser-Chernoussova and Reitlinger; Conil, Longerstaey and

Ramsbottom, p. 156, pl. 18, figs. 1-5, 15; p. 170, pl. 24, fig. 8

1981. *Omphalotis minima* Rauser-Chernoussova and Reitlinger; Altiner, p. 437, pl. 19, figs. 1-7.

1982. *Omphalotis minima* Rauser-Chernoussova and Reitlinger; Strank, p. 105, pl. 9, fig. 10.

1989. *Omphalotis minima* Rauser-Chernoussova and Reitlinger; Athersuch and Strank, p. 11, pl. 1, fig. 2.

1998. *Omphalotis minima* Rauser-Chernoussova and Reitlinger; Gallagher, p. 200, pl. 1, fig. 4.

1999. *Omphalotis minima* Rauser-Chernoussova and Reitlinger; Özkan, p. 212, pl. 6, figs. 6-8.

2004. *Omphalotis omphalota* Rauser-Chernoussova and Reitlinger; Cózar and Somerville, p. 52, text fig. 11, fig. 4.

2005. *Omphalotis omphalota* Rauser-Chernoussova and Reitlinger; Zhijun et al., p. 344, pl. 3, figs.27-29.

Description:

Test is large and nautiloid. Coiling is skewed initially and in the final tour it is planispiral. Spire expands progressively. There are 3-3.5 volutions. Chambers are globular, large and high and they are divided by curved, short septa inclined towards the aperture. Sutures are not well marked. Secondary deposits are well developed as crusta and nodes. In addition a hook like projection is present in the final chamber. Wall is microgranular with a tectum and a pseudofibrous inner layer or it is finely granular.

Dimensions:

Diameter (d): 0.525-0.772 mm

Width (w): 0.357-0.474 mm

w/d: 0.540-0.647

Wall thickness: 11-25μm

Remarks:

Omphalotis minima is distinguished from O*mphalotis samarica* by its involute coiling in the last tour. It is generally synonymized with *Omphalotis omphalota*. One specimen is questionably identified because of its smaller dimensions.

Stratigraphic distribution:

The stratigraphic range of *Omphalotis minima* is from Lower Visean to Serpukhovian (Altıner, 1981). Our specimens have been recovered from the Upper Visean (Mikhailovsky).

Omphalotis sp.

Pl. XII, figs. 8-9, 10?-11?, 12

Description:

Test is large. Chambers are planispirally coiled but slight oscillations are present in the initial tours. Spire expands progressively except for the final tour. There are 2.5-3 volutions. Chambers are globular and large. Septa are short, straight and thick. Sutures are not marked. Secondary deposits are in the form of crusta, nodes or hook. Wall is microgranular with a tectum and a finely granular layer.

Dimensions:

Diameter: 0.387-0.918 mm

Height of the last chamber: 0.116-0.117 mm

Wall thickness: 11-32μm

Remarks:

Omphalotis sp. is distinguished from *Omphalotis minima* by its straight septa, more regular coiling and smaller dimensions. In addition, hook like secondary deposits can form in the initial tours of *Omphalotis* sp.

Stratigraphic distribution:

The stratigraphic range of *Omphalotis* sp. is the Visean (Mikhailovsky and Venevsky).

SUPERFAMILY ENDOTHYRACEA Brady, 1884

FAMILY ENDOTHYRIIDAE Brady, 1884

SUBFAMILY HAPLOPHRAGMELLINAE Reitlinger, 1959

Genus *Haplophragmella* Rauser-Chernoussova and Reitlinger, 1936

Type species: *Endothyra panderi* Moeller, 1879

Haplophragmella fallax Rauser-Chernoussova and Reitlinger in Rauser-Chernoussova et al., 1936

Pl. XIV, fig. 1

1936. *Haplophragmella fallax* Rauser-Chernoussova and Reitlinger in Rauser-Chernoussova et al., p. 215, 228, pl. 6, figs. 10-11.

1977. *Georgella dytica* Conil and Lys, p. 49, pl. 6, figs. 92-95

1993. *Haplophragmella fallax* Rauser-Chernoussova and Reitlinger; Ueno and Nakazava, p. 33, text fig. 12, figs. 11-14.

1998. *Nevillella dytica* Conil and Lys; Gallagher, p. 200, pl. 1, fig. 6.

2004. *Nevillea dytica* Conil and Lys; Cózar and Somerville, p. 52, text fig. 11, fig. 1.

2005. *Nevillea dytica* Conil and Lys; Somerville and Cózar, p. 136, pl. 2, fig. 9.

2006. *Nevillea dytica* Conil and Lys; Gallagher et al., p. 80, text fig. 14, fig. 16.

Description:

Test is large and composed of a spirally coiled part and a rectilinear part. There are rapidly expanding two volutions in the coiled part with an endothyroid type coiling. Septa are very short and thick. In the uncoiled part there are 2 rectangular chambers. The height and width of the chambers increases rapidly. Cribrate aperture at the end of the spiral part is not well defined in our specimen. Wall is very thick and agglutinated.

Dimensions:

Diameter of the coiled part: 0.393 mm

Height: 0.850 mm

Wall thickness: 52μm

Remarks:

Various names have been attributed to this form by Conil and Lys. It was named as *Georgella dyctia* and *Nevillea dyctia*. Since the genus properties of *Haplophragmella* and these genera are the same, *Haplophragmella fallax* is the valid name.

Stratigraphic distribution:

The stratigraphic distribution of this form is Visean (Rauser-Chernoussova and Reitlinger in Rauser-Chernoussova et al., 1936). The only specimen of this species in this study has been identified from the Upper Visean (Mikhailovsky).

Genus *Mikhaiolovella* Ganelina, 1956

Type species: *Mikhailovella gracilis* (Rauser-Chernoussova)=*Endothyrina*? *gracilis* Rauser-Chernoussova, 1948

Mikhailovella gracilis (Rauser-Chernoussova, 1948)

Pl. XIV, fig. 2

1948. *Endothyrina* (?) *gracilis* Rauser-Chernoussova, p. 18, pl. 7, fig. 6.

1979. *Mikhailovella gracilis* Rauser-Chernoussova; Conil, Longerstaey and Ramsbottom, p. 156, pl. 18, fig. 6.

1989. *Mikhailovella gracilis* Rauser-Chernoussova; Skompski et al., p. 473, pl. 7, figs. 33-34.

2004. *Mikhailovella gracilis* Rauser-Chernoussova; Cózar, p. 381, pl. 2, fig. 4.

2004. *Mikhailovella gracilis* Rauser-Chernoussova; Cózar and Somerville, p. 52, text fig. 11, fig. 10.

2005. *Mikhailovella gracilis* Rauser-Chernoussova; Somerville and Cózar, p. 136, pl. 2, fig. 11.

Description:

Test is composed of 2 parts, a spirally coiled initial part and an uncoiled part. Coiling is endothyroid, involute. Septa are slightly curved, inclined and in the same thickness of the wall. There are 2 volutions in the spire. Uncoiled part is composed of subcylindrical chambers. Chambers in this part do not increase their height. Wall is microgranular and dark.

Dimensions:

Diameter of the coiled part: 0.374 mm

Height: 0.615 mm

Width of the uncoiled part: 0.279 mm

Wall thickness: 23μm

Remarks:

This form has greater dimensions and more convex chambers than *Mikhailovella* mica.

Stratigraphic distribution:

The stratigraphic distribution of this form is from Lower Visean to Lower Brigantian (Upper Visean) (Rauser-Chernoussova, 1948). The only specimen of this species in this study has been identified from the Mikhailovsky Horizon (Upper Visean).

Mikhailovella sp.

Pl. XIV, fig. 3

Description:

Test is spirally coiled in early stage and uncoiled in the final stage. Coiling is endothyroid and involute. There are 2-3 volutions in this part. Chambers are convex and divided by curved septa. The uncoiled part is uniserial and formed by globular chambers. There is a cribrate aperture at the end of the uniserial par. Wall is dark and microgranular.

Dimensions:

Diameter of the coiled part: 0.211 mm

Height: 0.309 mm

Width of the uncoiled part: 0.199 mm

Wall thickness: 10μm

Stratigraphic distribution:

The only specimen of this species in this study has been identified from the Upper Visean (Mikhailovsky).

SUPERFAMILY ENDOTHYRACEA Brady, 1884

FAMILY ENDOTHYRIIDAE Brady, 1884

SUBFAMILY ENDOTHYRANOPSINAE Reitlinger, 1958

Genus *Endothyranopsis* Cummings, 1955

Type species: *Involutina crassa* (Brady, 1876)

Endothyranopsis hirosei Okimura, 1965?

Pl. XIV, fig. 13

1973. *Endothyranopsis* du group *hirosei* Okimura; Mamet, p. 119, pl. 7, figs. 25-26.

1993. *Endothyranopsis hirosei* Okimura; Mamet et al., pl. 7, figs. 5-9.

Description:

Test is large. Coiling is planispiral and involute but shows some oscillations. There are 2-2.5 volutions and volutions increase their height very rapidly immediately

after the first tour. Chambers are slightly convex. Septa are very thick, short and bluntly pointed. Sutures are well marked. Wall is agglutinated and thick.

Dimensions:

Diameter: 0,867 mm

Wall thickness: 34 μm

Remarks:

Septa of this form are significantly thick. They are nearly two or three times thicker than the wall. In addition well marked sutures are another distinguishing criterion of this form.

Stratigraphic distribution:

The stratigraphic distribution is in Asbian (Upper Visean) (Mamet, 1973). The samples of *Endothyranopsis hirosei* have been recovered in Upper Visean (Mikhailovsky).

Endothyranopsis cf. *sphaerica* (Rauser-Chernoussova and Reitlinger, 1936)

Pl. XIV, fig. 9

1936. *Endothyra crassa* var. *sphaerica* Rauser-Chernoussova and Reitlinger, p. 209, pl. 6, fig. 4

1979. *Endothyranopsis sphaerica* Rauser-Chernoussova and Reitlinger; Brazhnikova, pl. 2, fig. 1.

1979. *Endothyranopsis sphaerica* Rauser-Chernoussova and Reitlinger ; Rozovskaya, pl. 3, fig. 1.

1979. *Endothyranopsis sphaerica* Rauser-Chernoussova and Reitlinger; Conil, Longerstaey and Ramsbottom, p. 184, pl. 29, fig. 23.

1999. *Endothyranopsis sphaerica* Rauser-Chernoussova and Reitlinger; Vdovenko et al., p. 188, text fig. 1, fig. 24.

2004. *Endothyranopsis sphaerica* Rauser-Chernoussova and Reitlinger; Cózar and Rodriguez, p. 41, text fig. 9, fig. 6.

2004. *Endothyranopsis sphaerica* Rauser-Chernoussova and Reitlinger; Cózar and Somerville, p. 52, text fig. 11, figs. 12, 15-17.

2005. *Endothyranopsis sphaerica* Rauser-Chernoussova and Reitlinger; Cózar et al., p. 294, text fig. 8, fig. 23.

2005. *Endothyranopsis* cf. *Sphaerica* Rauser-Chernoussova and Reitlinger; Zhijun et al., p. 345, pl. 4, fig. 1.

2005. *Endothyranopsis sphaerica* Rauser-Chernoussova and Reitlinger; Somerville and Cózar, p. 138, pl. 3, fig. 5.

Description:

Test is large. Coiling is nearly planispiral and involute but shows some oscillations. Volutions increases their height very rapidly. Chambers are slightly convex. Septa are very thick, short and bluntly pointed. Wall is agglutinated and thick.

Remarks:

Septa of this form are very thick. They are nearly two or three times as much thicker as the wall.

Stratigraphic distribution:

The stratigraphic distribution of *Endothyranopsis sphaerica* is between Brigantian (Upper Visean) (Cózar and Somerville, 2004) and Lower Serpukhovian (Rauser-Chernoussova, 1948). The two specimens of this species in this study have been identified from the Brigantian and Lower Serpukhovian.

"Endothyranopsis" sp.

Pl. XIV, figs. 4-8

Description:

Test is large. Coiling is planispiral throught but, in some froms slight oscillations are observe. The height of the chambers increases gradually. There are 2.5-

3.5 volutions. There are numerous subquadratic chambers divided by short, bluntly pointed septa which are inclined towards the aperture. Wall is agglutinated.

Dimensions:

Diameter: 0,318-0.556 mm

Wall thickness: 12-19 μm

Remarks:

This form has smaller dimensions than *Endothyranopsis sphaerica*. In this group there are some specimens that the agglutinated structure of the wall can not be well identified (Pl. XIV, figs. 4-5) and their dimensions are smaller.

Stratigraphic distribution:

Specimens of *"Endothyranopsis"* sp. in this study has been identified from Upper Visean to Serpukhovian.

Endothyranopsis spp.

Pl. XIV, figs. 10-12, 14?

Description:

Test is nautiloid. Coiling is planispiral, involute and with oscillations. Spire expands gradually but more rapidly in the final tour. Septa are short and thick. Chambers may be convex or subquadratic. Sutures are well developed in some froms but absent in others. Wall is agglutinated and thick.

Remarks:

Various morphologies having thick agglutinated wall, planispiral coiling and divided by thick and short septa were grouped under *Endothyranopsis* spp. Shape of chambers and more regular coiling differ this form from *Plectogyranopsis* spp. One of the specimens is questioned because the septa seem to be different than the typical septa of the genus *Endothyranopsis*.

Stratigraphic distribution:

Specimens of *Endothyranopsis* spp. in this study have been identified from the Upper Visean.

Genus *Plectogyranopsis* Vachard, 1977

Type species: *Endothyra convexa* (Rauser-Chernoussova, 1948)

Plectogyranopsis ampla (Conil and Lys, 1964)

Pl. XIV, figs. 18-19

1964. *Plectogyra exelicta* var. *ampla* Conil and Lys, p. 184, pl. 28, figs. 553-554.

1979. *Plectogyranopsis ampla* Conil and Lys; Conil, Longerstaey and Ramsbottom, p. 136, pl. 8, fig. 1; p. 142, pl. 11, fig. 2; p. 144, pl. 12, fig. 4.

1981. *Plectogyranopsis* cf. *ampla* Conil and Lys; Altıner, p. 437, pl. 20, fig. 14.

1989. *Plectogyranopsis* cf. *ampla* Conil and Lys; Athersuch and Strank, p. 11, pl. 1, fig. 4.

1982. *Plectogyranopsis ampla* Conil and Lys; Strank, p. 105, pl. 9, fig. 11.

Description:

Test is large. Coiling is initially skewed then nearly planispiral. Spire expands rapidly in the initial tours and much more rapidly in the final tour so that it is very large and high. There are 2-3 volutions. Chambers are globular and spacious and they are divided by short, bluntly pointed septa which are inclined towards the aperture. The wall of the septa is thicker than the wall of the form. Wall is agglutinated and thick.

Dimensions:

Diameter: 0.594-0,577 mm

Width: 0.429

w/d: 0.72

Wall thickness: 19-22 μm

Remarks:

This form has greater dimensions than *Plectogyranopsis convexa* and smaller than *Plectogyranopsis moraviae*.

Stratigraphic distribution:

The stratigraphic distribution of this form is from Middle Visean (V2b) to Upper Visean (V3b) (Altıner, 1981). Specimens of this species in this study have been identified from the Upper Visean (Mikhailovsky).

Plectogyranopsis convexa (Rauser-Chernoussova, 1948)

Pl. XIV, figs. 15-17

1948. *Endothyra convexa* Rauser-Chernoussova, p. 169, pl. 4, fig. 8-10.

1979. *Plectogyranopsis convexa* Rauser-Chernoussova; Conil, Longerstaey and Ramsbottom, p. 156, pl. 18, fig. 13; p. 172, pl. 25, fig. 9.

1981. *Plectogyranopsis convexa convexa* Rauser-Chernoussova; Altıner, p. 437, pl. 20, figs. 4-6.

2004. *Plectogyranopsis convexa* Rauser-Chernoussova; Brenkle, p. 148, pl. 2, fig. 18; p. 150, pl 3, figs. 1-2.

Description:

Test is small. Umbilical depression is well marked. Initially skewed coiling becomes oscillant and then planispiral. Chambers increase their height rapidly after the first tour. Chambers are very convex and divided by short, thick and inclined septa. There are 2.5-3 volutions. Wall is agglutinated and thick. Thickness of the wall increases though the ontogenesis.

Dimensions:

Diameter: 0.409-0,469 mm

Width: 0.307-0.366

w/d: 0.75-0.78

Wall thickness: 10-28 μm

Remarks:

Plectogyranopsis convexa is smaller than *Plectogyranopsis ampla* and its chambers are more globular. In addition, septa of the former are thinner.

Stratigraphic distribution:

The stratigraphic distribution of this form is from Lower Visean (V1a) to (Upper Visean (V3b) (Altıner, 1981). Specimens of *Plectogyranopsis convexa* in this study have been identified from the Upper Visean (Mikhailovsky).

Plectogyrnopsis? sp.1

Pl. XIV, fig. 20

Description:

Test is large. Coiling is skewed in the first tour but planispiral in the final tours. Spire expands progressively. Chambers are very convex and divided by short, thick and inclined septa. Number of volutions is 3.5. There are 8 chambers in the final volution. Wall is coarsely agglutinated and thick.

Dimensions:

Diameter: 0.526 mm

Wall thickness: 17 μm

Remarks:

This genus is questionably identified here because it has more chambers and more regular coiling than the genus *Plectogyranopsis.* Sutures are also more marked. However, the wall structure and morphology of septa is the same with the typical specimens of the genus *Plectogyranopsis*. This form is differentiated from *Plectogyranopsis ampla* and *Plectogyranopsis convexa* by its more regular coiling and higher number of chambers. In addition, it is different from the latter by its greater dimensions.

Stratigraphic distribution:

The stratigraphic distribution of this form is Upper Visean(Mikhailovsky).

Plectogyranopsis spp.

Pl. XIV, figs. 21-22

Description:

Various morphologies sharing the characteristic features of the genus *Plectogyranopsis* and can not be assigned to a a particular species of this genus were grouped under *Plectogyranopsis* spp. The common criteria are less number of convex chambers divided by short and thick septa, initially skewed, finally planispiral coiling and agglutinated wall structure.

Stratigraphic distribution:

The stratigraphic distribution of *Plectogyranopsis* spp. in this study is Mikhailovsky (Upper Visean)

FAMILY LOEBLICHIIDAE Cummings, 1955 emend. Rauser-Chernoussova et al., 1996

SUBFAMILY LOEBLICHIINAE Cummings, 1955 emend. Cózar and Vachard, 2001

Genus *Endostaffella* Rozovskaya, 1961

Type species: *Endothyra parva* Moeller, 1879

Endostaffella delicata Rozovskaya, 1963?

Pl. XV, figs. 1-2

1963. *Endostaffella delicata* Rozovskaya, p. 68, pl.12, figs. 11-17.

1979. *Endostaffella delicata* Rozovskaya; Conil, Longerstaey and Ramsbottom, p. 164, pl. 22, fig. 37; p. 178, pl. 28, fig. 18

1981. *Endostaffella delicata* Rozovskaya; Altıner, p. 440, pl. 26, figs. 15-20.

1982. *Endostaffella delicata* Rozovskaya; Rich, p. 245, pl.1, figs. 21-22, 23?, 24?.

1982. *Endostaffella delicata* Rozovskaya; Strank, p. 105, pl. 9, fig. 15.

2006. *Endostaffella* cf. *delicata* Rozovskaya; Okuyucu and Vachard, p. 544, text fig 7, fig. 18.

Description:

Test is lenticular with a rounded periphery. Umbilical region is deep and wide. There are 3-4 tours. Volutions are progressively developed and evolute. Coiling is endothyroid but its axis changes its plane about 90 . Initial tours make oscillations. Chomata are absent. Wall is microgranular.

Dimensions:

Diameter (d): 0.270-0,278 mm

Width (w): 0.139-0.141 mm

w/d: 0.50-0,51

Wall thickness: 8-10 μm

Remarks:

The most significant features of this species are a remarkable umbilical depression and oscillating inner tours. It is discriminated form *Endostaffella fucoides* and *Endostaffella rozovskayae* by these features. Despite in the original description of *Endostaffella delicata*, pseudochomata are absent or poorly developed Conil et al. (1979) have indicated the presence of well developed pseudochomata. In our specimens pseudochomata are not observed. For this reason, this species is defined with a question mark in this study.

Stratigraphic distribution:

The stratigraphic distribution of *Endostaffella delicata* is Upper Visean to Serpukhovian (Altıner, 1981). In this study this species has been encountered from the Upper Visean (Mikhailovsky).

Endostaffella fucoides Rozovskaya, 1963

Pl. XV, figs. 3,5, 4?

1963. *Endostaffella fucoides* Rozovskaya, pl. 11, figs. 30-34.

1979. *Endostaffella fucoides* Rozovskaya; Conil, Longerstaey and Ramsbottom, p. 164, pl. 22, figs. 11, 29-31, 33-36; p. 178, pl. 28, figs. 14-17; p. 182, pl. 29, fig. 7.

? 2008. *Endostaffella fucoides* Rozovskaya; Cozar et al., p. 473, text fig. 8, fig. 17.

Description:

Test is discoidal with a rounded periphery and compressed. Number of volutions is 2.5-3. Last 1.5-2 tours are planispiral and they are perpendicular to the previous tours. The height of tours gradually increases. Coiling is evolute. Initial tours make oscillations. Pseudochomata is very small and poorly developed if it exists. Wall is microgranular, undifferentiated.

Dimensions:

Diameter (d): 0.225-0,262 mm

Width (w): 0.101-0.108 mm

w/d: 0.41-0,45

Wall thickness: 9-11 μm

Remarks:

This specie resemble to *Endostaffela shamordini*. However, *Endostaffela shamordini* has oscillating inner tours and depressed central part.

Stratigraphic distribution:

The stratigraphic distribution is Upper Visean (Aleksin and Mikhaylov horizons) (Rozovskaya, 1963). In this study this species has been encountered from the Upper Visean (Mikhailov horizon).

Endostaffella rozovskayae Conil and Longerstaey, 1979

Pl. XV, figs. 6-7

1979. *Endostaffella rozovskayae* Conil and Longerstaey in Conil, Longerstaey and Ramsbottom, p. 164, pl. 22, figs. 25-28

Description:

Test is small with a rounded periphery. Number of tours is in between 3-3.5. Development of the tour and chambers is progressive; however, the increase of the height of the last tour is remarkable. There are numerous chambers and they are so dense that they form a salience around the umbilical area. Chambers are globular and dense and septa are inclined and long. Coiling axis changes its plane in the final tour about 90 and it is evolute. Chomata can be poorly developed. Wall is microgranular.

Dimensions:

Diameter (d): 0.276-0,278 mm

Width (w): 0.117-0.152 mm

w/d: 0.42-0,55

Wall thickness: 8-13 μm

Remarks:

This species is much wider than the other species of the genus. Initial dense coiling is obvious. It changes its coiling axis in the last tour.

Stratigraphic distribution:

The stratigraphic distribution of *Endostaffella rozovskayae* is the Upper Visean (Brigantian) (Conil et al., 1979). In this study this species has been encountered from the Upper Visean (Mikhailovsky).

Endostaffella sp. 1

Pl. XV, figs. 8-9

Description:

Test is small with a rounded periphery. Initial coiling is highly skewed and in the last tour or half of the last tour the plane of coiling axis changes 90° and the last

volution become planispiral and evolute. There are numerous chambers divided by long and oblique septa inclined towards the aperture. Chomata is poorly developed. Wall is microgranular.

Dimensions:

Diameter (d): 0.285-0,288 mm

Width (w): 0.140-0.175 mm

w/d: 0.49-0,61

Height of the last tour: 0.066-0.050 mm

Wall thickness: 9-10 μm

Remarks:

The most distinguishable feature of this form is that the initial coiling is so skew and dense that it causes a salience in the umbilical region.

Stratigraphic distribution:

Samples were recovered from Upper Visean (Brigantian).

Endostaffella sp.

Pl. XV, figs. 10-21

Description:

Test is small. Periphery is rounded. Number of tours ranges between 2-3. After an endothyroid coiling, plane of coiling axis changes about 90° and preceding tours are planispiral and evolute. Chambers are globular and they are not much dense. Chomata is poorly developed or absent. Wall is microgranular and undifferentiated.

Remarks:

Some species of *Endostaffella* can be confused with some representatives of *Praeplectostaffella*. However, *Endostaffella* changes the axis of coiling about 90° and continue its coiling as planispiral, generally it does not oscillate in coiling as much as *praeplectostaffella*.

Stratigraphic distribution:

In this study this species has been encountered from Upper Visean and Serpukhovian.

Genus *Planoendothyra* Reitlinger in Rauser-Chernousova and Fursenko, 1959

Type species: *Endothyra aljutovica*, Reitlinger, 1950

Planoendothyra spp.

Pl. XVI, figs. 1-6

Description:

Several forms that cannot be grouped under different species were assigned to *Planoendothyra* spp. Their common features are as follows: Test is discoidal and compressed. Periphery is broadly rounded in all tours. Coiling is endothyroid in the initial tours, then plane of coiling axis changes and final tours are nearly perpendicular to the initial ones. Last tour is rapidly developed and becomes more spacious, planispiral and evolute but with slight oscillations. In addition the last tour is very convex in axial section. Chomata can be observed in some specimens or are absent. Wall is microgranular and dark.

Dimensions:

Diameter (d): 0.472-0,602 mm

Width (w): 0.233-0.298 mm

w/d: 0.49

Height of the last tour: 0.150-0.128 mm

Wall thickness: 19-24 μm

Remarks:

Stratigraphic distribution:

Our speciemens are found in Upper Visean and Lower Serpukhovian.

FAMILY LOEBLICHIIDAE Cummings, 1955 emend. Rauser-Chernoussova et al., 1996

SUBFAMILY LOEBLICHIINAE Cummings, 1955 emend. Cózar and Vachard, 2001

Genus *Euxinita* Conil and Dîl, 1979

Type species: *Dainella*? *efremovi* Vdovenko and Rostovtseva in Brazhnikova et al., 1967

Euxinita efremovi (Vdovenko and Rostovtseva, 1967)

Pl. XVI, figs. 7, 8?

1967. *Dainella*? *efremovi* Vdovenko and Rostovtseva in Brazhnikova et al., p. 148-149, pl. 47, figs. 1-5.

1981. *Euxinita efremovi* Vdovenko and Rostovtseva; Altıner, p. 439, pl. 25, figs. 7-8.

2004. *Pojarkovella efremovi* Vdovenko and Rostovtseva; Cózar, p. 381, pl.2, fig. 9.

2004. *Pojarkovella efremovi* Vdovenko and Rostovtseva; Cózar and Somerville, p. 52, text fig. 11, figs. 24-26, 28-30.

2008. *Euxinita efremovi* Vdovenko and Rostovtseva; Cózar et al., p. 437, text fig. 8, fig. 18.

Description:

Test is small, lenticular or nautiloid. Periphery is rounded. Test is composed of 4 volutions. Coiling is planispiral and involute. Volutions developed progressively except for the last tour. Width and height of the last tour increase very rapidly. There are numerous septa and chambers. Chambers are subquadratic and septa are long and inclined. Sutures are less developed. Secondary deposits are in the form of chomata. Wall is microgranular or granular.

Dimensions:

Diameter (d): 0.458-0,663 mm

Width (w): 0.259-0.357 mm

w/d: 0.54-0,56

Height of the last tour: 0.104-0.128 mm

Wall thickness: 19-22 μm

Remarks:

Cózar (2002) prefers to use the name *Pojarkovella efremovi* for this species. He considers that the wall structure has not genetic importance. We prefer to keep the name *Euxinita efremovi* due to different wall structure of two genus.

Stratigraphic distribution:

The stratigraphic range of this species is from Brigantian to Lower Serpukhovian (Altıner, 1981). Samples were recovered from Brigantian.

Genus *Loeblichia* Cummings, 1955

Type species: *Endothyra ammonoides* (Brady, 1873)

Loeblichia minima Brazhnikova, 1962

Pl. XVI, fig. 9

1962. *Loeblichia minima* Brazhnikova, p. 36-37, pl. 14, figs. 1-8.

Description:

Test is small discoidal, strongly compressed. Periphery is rounded. Umbilical region is flat. There are 3.5 volutions. Coiling is planispiral and evolute. Chomata is absent. Wall is microgranular.

Dimensions:

Diameter (d): 0.256 mm

Wall thickness: 7 μm

Remarks:

This species is differentiated from other species of the genus *Loeblichia* by its smaller dimensions. It differs from *Loeblichia ukranica* by non-oscillatory, planispiral coiling. *Loeblichia paraammonoides* is different from *Loeblichia minima* such that it has

larger dimension and higher number of tours and chambers, broader coiling and distinct umbilici.

Stratigraphic distribution:

The stratigraphic range of *Loeblichia minima* is Upper Visean (Brazhnikova, 1962). Specimens were recovered from Upper Visean (Asbian).

Loeblichia ?sp.

Pl. XVI, fig. 10

Description:

Test is discoidal. Coiling is planispiral and evolute. Slight oscillations can be seen during growth. There are progressively expanding five volutions. Chomata is absent. Wall is thick and microgranular.

Dimensions:

Diameter (d): 0.433 mm

Wall thickness: 14 μm

Remarks:

Only two specimens are found in the study area. It is questioned here because, the wall structure seem to be granular instead microgranular.

Stratigraphic distribution:

The stratigraphic range of *Loeblichia* is Visean (Loeblich and Tappan, 1988). The samples were recovered from Upper Visean (Asbian).

Genus *Pojarkovella* Simonova and Zub, 1975 emend. Cózar 2002

Type species: *Quasiendothyra nibelis* Durkina, 1959

Pojarkovella guadiatensis Cózar, 2002

Pl. XVII, figs. 1-4

2002. *Pojarkovella guadiatensis* Cózar, p. 286, text fig. 2, figs. 1-12.

2004. *Pojarkovella guadiatensis* Cózar, p. 381, pl.2, fig. 6.

Description:

Test is small and flattened. Periphery is rounded in the initial tours and acute in the final whorl causing the form to be rhombic or square shape. Umbilical region is wide and deep. There are 2.5-3 volutions. Axis of coiling progressively changes, most of the specimens do not show a change in plane of about 90°. The height and width of the last volution is larger than previous ones and the last tour is evolute. Chambers of the final volutions are quadrate but in initial volutions they are more rounded. Final volution in equatorial section consists of 13-14 chambers. Sutures are well marked. Chomata is well developed. Wall microgranular and luminotheca is observed.

Dimensions:

Diameter (d): 0.466-0,498 mm

Width (w): 0.191-0.207 mm

w/d: 0.41-0,42

Height of the last tour: 0.112-0.126 mm

Wall thickness: 11-13 μm

Remarks:

This species is differentiated from *Pojarkovella nibelis* by its well marked sutures, less deviation in the coiling axis and thinner wall. Uncoiling trend of the later is less marked. Its test is more flattened other species of this genus defined in this study.

Stratigraphic distribution:

The stratigraphic range is the whole Brigantian (Upper Visean) (Cózar, 2002). Our specimens were recovered Mikhailovsky.

Pojarkovella cf. *guadiatensis* Cózar, 2002

Pl. XVII, fig. 5

2002. *Pojarkovella guadiatensis* Cózar, p. 286, text fig. 2, figs. 1-12.

Remarks:

In this form the last half of the tour cannot be observed. However, dimensions, rounded initial volutions, flattened test characterizes *Pojarkovella guadiatensis*.

Stratigraphic distribution:

The only specimen of *Pojarkovella* cf. *guadiatensis* was recovered from Mikhailovsky.

Pojarkovella ex gr. *guadiatensis* Cózar, 2002

Pl. XVII, figs. 6-7

2002. *Pojarkovella guadiatensis* Cózar, p. 286, text fig. 2, figs. 1-12.

Remarks:

Specimens assigned to *Pojarkovella* ex gr. *guadiatensis* have smaller dimensions and lesser number of chambers in their last whorl and chambers are some what more convex.

Stratigraphic distribution:

Our specimens were recovered form Asbian.

Pojarkovella nibelis (Durkina, 1959)

Pl. XVIII, figs. 1-9

1959. *Quasiendothyra nibelis* Durkina, p. 152, pl. 5, figs. 9-13.

? 1973. *Quasiendothyra* (?) *nibelis* Durkina; Austin et al., p. 185, pl. 2, fig. 27

? 1973. *Urbanella nibelis* Durkina; Mamet, p. 117, pl. 6, fig.10

1981. *Urbanella nibelis* Durkina; Altıner, p. 440, pl. 26, figs. 26-34.

? 1982. *Nibelia nibelis* Durkina; Strank, p. 106, pl. 10, figs. 3-4.

1993. *Pojarkovella* aff. *nibelis* Durkina; Ueno and Nakazawa, p. 21, text fig. 7, figs. 1-5.

Description:

Test is discoidal. Acute periphery is especially distinct in axial sections. Umbilical region is wide. This form is composed of 3-3.5 volutions. Coiling is planispiral but coiling axis change in plane of about 90°. The last tour rapidly increases its height and becames evolute. In equatorial sections, chambers of the initial volutions are rounded and convex but they are narrow and rectangular in the final volutions. Chambers in the last whorl ranges between 13-18. Septa are perpendicular to the wall. Sutures are less marked. Secondary deposits are in the form of chomata and they are very well developed. Wall is microgranular but well developed luminotheca is observed in many speciemens.

Dimensions:

Diameter (d): 0.430-0,644 mm

Width (w): 0.259-0.357 mm

w/d: 0.43-0,46

Height of the last tour: 0.088-0.172 mm

Wall thickness: 12-30 μm

Remarks:

This species shows an uncoiling trend which is in fact a property of its genus. However, this trend is much more remarkable in *Pojarkovella nibelis* than in *Pojarkovella guadiatensis*. Sutures of *Pojarkovella nibelis* are less marked than sutures of *Pojarkovella guadiatensis* and the changes in the coiling axis of the former is much clearer. This form has larger dimensions than other *Pojarkovella* species described in this study. In 1980, Conil described a new genus *Nibelia* and type species of this genus is accepted as *Quasiendothyra nibelis* and he named this species as *Nibelia nibelis* but he did not show

the figures of this new genus in its article. Today, instead *Nibelia nibelis*, *Pojorkovella nibelis* is used as the name of this species.

Stratigraphic distribution:

The stratigraphic range is from Middle Visean through Upper Visean (Asbian) (Altıner, 1981). Samples were recovered from Upper Visean (Mikhailovsky).

Pojarkovella sp. 1

Pl. XVIII, figs. 10-11

Description:

Test is small. The periphery of the last tour is strongly angular with convex sides. Umbilical region is shallow and due to the coiling of initial volutions a salience is observed in this region. Number of tours is in between 2.5-3.5. The height of tour increases progressively till the last whorl. The height of the last whorl is much greater than the initial ones. Coiling axis changes its plane in the final or final half tour as 90°. Secondary deposits are developed in the form of massif chomata. Wall is microgranular, luminotheca is obvious.

Dimensions:

Diameter (d): 0.298-0,380 mm

Width (w): 0.176-0.179 mm

w/d: 0.60-0.47

Height of the last tour: 0.077-0.094 mm

Wall thickness: 11-14 μm

Remarks:

It is differentiated from *Pojarkovella* sp. 2 by a salience in the umbilical region, smaller dimensions and well developed massive chomata.

Stratigraphic distribution:

Specimens were recovered from Upper Visean (Mikhailovsky).

Pojarkovella sp. 2

Pl. XVIII, figs. 12-13

Description:

Test is lenticular,with a wide and deep umbilicus and angular periphery in all tours. It is formed by 2.5-3 volutions developing gradually however, the height of the last volution increases rapidly. After an endothyroid coiling in the first or one and a half tour, coiling axis changes 90°. Coiling is evolute. Chomata are well developed. Wall is microgranular, light colored luminotheca can be observed.

Dimensions:

Diameter (d): 0.446-0,465 mm

Width (w): 0.277-0.281 mm

w/d: 0.60-0.63

Height of the last tour: 0.109-0.130 mm

Wall thickness: 12-17 μm

Remarks:

The form ratio (w/d) of this form is greater than all other species of *Pojarkovella* described here. Its dimensions are smaller than *Pojarkovella nibelis* and *Pojarkovella guadiatensis.* The width is much larger than the latter. It is differentiated from *Pojarkovella* sp. 1 by its greater dimensions and coiling of the initial tours.

Stratigraphic distribution:

Samples were recovered from Upper Visean (Mikhailovsky).

Pojarkovella spp.

Pl. XVII, figs. 8-17

Description:

Several specimens that cannot be grouped with a definite species are assembled as *Pojarkovella spp*. All members of this group show a change in the axis of coiling, in most of them this change is 90 . All of them contain chomata and in their microgranular wall luminotheca can be observed. Their dimensions are different from each other.

Stratigraphic distribution:

Specimens belong to Upper Visean (Mikhaolovsky).

FAMILY LOEBLICHIIDAE Cummings, 1955 emend. Rauser-Chernoussova et al., 1996

SUBFAMILY DAINELLINAE Cózar and Vachard, 2001

Genus *Vissarionovella* Cózar and Vachard, 2001

Type species: *Eostaffella tujmasensis* Vissarionova, 1948

Vissarionovella tujmasensis (Vissarionova, 1948)

Pl. XIX, figs. 1-7

1948. *Eostaffella tujmasensis* Vissarionova, p. 224-225, pl. 14, figs. 12-14.

1981. *Dainella tujmasensis* Vissarionova; Altıner, p. 439, pl. 25, figs. 4-6.

2003. *Vissarionovella tujmasensis* Vissarionova; Cozar,p. 161, text fig. 4, fig. D.

2005. *Vissarionovella tujmasensis* Vissarionova; Somerville and Cózar, p. 136, pl. 2, figs. 14-15.

Description:

Test is nautiloid. Periphery is rounded. Umbilicus is shallow and wide. Number of volutions is 3.5-4.5. Development of ontogenesis is progressive. Coiling is endothyroid and distorted in the initial tours but it is nearly planispiral in the final tours although it can show slight oscillation. There are numerous chambers that are

divided by short and inclined septa. Secondary deposits can be poorly developed in the form of pseudochomata and also they are observed in equatorial section on the bottom wall of a volution. Wall is microgranular, containing a tectum and in some specimens lighter appearance in the wall can be observed.

Dimensions:

Diameter (d): 0.534-0,697 mm

Width (w): 0.293-0.463 mm

w/d: 0.55-0.66

Wall thickness: 20-28 μm

Remarks:

Dimensions of our specimens assigned to *Vissarionovella tujmasensis* are smaller. In our examples, chambers of the first volution are globular whereas they are subquadratic and more spacious in the preceding tours.

Stratigraphic distribution:

The stratigraphic distribution of is in Upper Visean (Asbian) (Cózar and Vachar, 2001) In this study this species has been encountered from the Upper Visean (Mikhailovsky).

Vissarionovella sp.1

Pl. XIX, figs. 9-12

Description:

Test is nautiloid. There are 3.5-4.5 volutions. After the first volution, height of the tours rapidly increases. Coiling is endothyroid and distorted in the initial tours but, it continues its development with slight oscillations. Chambers are very large, subquadratic and divided by short and inclined septa. Septa have blunt points. Secondary deposits can be observed in equatorial section above the septa. Wall is microgranular.

Dimensions:

Diameter (d): 0.704-0,627 mm

Wall thickness: 13-20 μm

Remarks:

Vissarionovella sp.1 is differentiated from *Vissarionovella tujmasensis* by its larger dimensions, very rapid increase of the tours, lesser number of chambers, especially in the final tour, more oscillated coiling and well developed secondary deposits. In addition, blunt points of septa in *Vissarionovella* sp.1 are distinct.

Stratigraphic distribution:

In this study this species has been encountered from the Upper Visean (Mikhailovsky).

Vissarionovella spp.

Pl. XIX, figs. 8, 13-15

Description:

Specimens which cannot be designated to a particular species of *Vissarionovella* are grouped under the name of *Vissarionovella* spp. Their common criteria are the trend of coiling, shape of the septa and the wall structure.

Stratigraphic distribution:

In this study it has been onserved in the Upper Visean (Mikhailovsky).

SUPERFAMILY ENDOTHYRACEA Brady, 1884

FAMILY TOURNAYELLIDAE Dain, 1953 emend

SUBFAMILY CHERNYSHINELLINAE Reitlinger, 1958

Genus *Condrustella* Conil and Longerstaey, 1977 in Conil and Lys, 1977

Type species: *"Mistinia" modavensis* Conil and Lys, 1967

Condrustella sp.

Pl. XX, figs. 1-4

Description:

Nearly planispiral coiling consists of 1 tour. There are 3 chambers in this tour and proloculus is large. Chambers are in the form of a tear drop which is the characteristic feature of chernyshinellids. Septa are thick, very short and inclined. The wall is formed by two layers. Inner layer is microgranular and thin, outer layer is thick and coarsely granular.

Dimensions:

Diameter (d): 0.315-0,668 mm

Wall thickness: 40-74 μm

Remarks:

Condrustella sp. differs from the representatives of the genus *Tournayella* and *Septatournayella* by its differentiated wall and the shape of its chambers which are in the form of tear a drop. In addition, the former does not have real septa, it includes pseudosepta.

Stratigraphic distribution:

Stratigraphic distirbution of genus *Condrustella* is from Upper Tournaisian to Lower Visean, but it can be observed also in the Upper Visean (Conil and Lys, 1977). In this study this species has been encountered from the Upper Visean (Mikhailovsky).

Genus *Mistinia* Dain, 1953

Type species: *Mstinia bulloides* Dain, 1953

Mistinia sp.

Pl. XX, figs. 5-6

Description:

Coiling is nearly planispiral and oscillatory. Chambers are in the form of a tear drop. Septa are short and inclined. Aperture is cribrate. The wall is differentiated into two layers. Inner layer is microgranular and thin, outer layer is thick and coarsely granular.

Dimensions:

Diameter (d): 0.484-0,565 mm

Wall thickness: 22-25 μm

Remarks:

Mistinia sp. is differentiated from *Condrustella* sp. by its cribrate aperture. Cribrate aperture is obvious only in one specimen. In addition, septa of the former is thinner.

Stratigraphic distribution:

The stratigraphic range of the genus *Mistinia* is Upper Visean (Conil and Lys, 1977). In this study specimens of *Mstinia* has been recovered from the Upper Visean (Mikhailovsky).

FAMILY TOURNAYELLIDAE Dain, 1953 emend.

SUBFAMILY FORSCHIINAE Dain, 1953

Genus *Forschia* Mikhailov, 1939

Type species: *Forschia mikhailovi* Dain, 1953

Foschia parvula Rauser-Chernoussova, 1948

Pl. XX, fig. 7

1948. *Foschia parvula* Rauser-Chernoussova, p. 241, pl. 17, figs. 9-10.

1981. *Foschia parvula* Rauser-Chernoussova; Altıner, p. 436, p. 15, figs. 3-6.

Description:

Test is small and laterally compressed. It is bilocular. Tubular chamber planispirally coils and evolute. Spire expands gradually but rapidly in the final tour. Number of volutions is 3-4. Wall is differentiated into 2 layers. Inner layer is thin and microgranular, outer layer is very thick and agglutinated.

Dimensions:

Diameter (d): 0.370 mm

Width (w): 0.133 mm

w/d: 0.36

Wall thickness: 22μm

Remarks:

Foschia parvula resembles to *Forschia subangulata*. Its dimensions is smaller than Forschia *subangulata* and generally it has less number of whorls.

Stratigraphic distribution:

The stratigraphic distribution of *Forschia parvula* is from Middle Visean to Upper Visean (V3b) (Altıner, 1981). In this study this species has been encountered from the Upper Visean (Mikhailovsky).

Forschia subangulata (Moeller, 1880)

Pl. XX, figs. 8-10

1880. *Spirillina subangulata* Moeller, p. 38-39, pl. 5, figs. 3.

1977. *Forschia*(?) *subangulata* Moeller; Conil and Lys, p. 39, pl. 1, fig. 17.

1981. *Forschia subangulata* Moeller; Altıner, p. 436, p. 15, figs. 1-2.

1999. *Forschia subangulata* Moeller; Özkan, p. 210, pl. 5, fig. 23.

Description:

Test is large and compressed. It is formed by 2 chambers which are proloculus and 2. tubular chamber. Coiling is planispiral, evolute and may show some oscillations. Spire expands very rapidly. The last tour is considerably high and large. There are 3.5-5 volutions. In axial section, volutions are angular. Wall is very thick and composed of 2 layers. Inner layer is thin and microgranular, outer layer is very thick and agglutinated. It contains foreign particles.

Dimensions:

Diameter (d): 0.874-970 mm

Width (w): 0.313-0.329 mm

w/d: 0.33-0.38

Wall thickness: 41-50μm

Remarks:

This form is synonymized with *Forschia mikhailovi* by Altıner (1981). *Forschia subangulata* is differentiated from *Forschia parvula* and by its larger dimensions.

Stratigraphic distribution:

The stratigraphic distribution of *Forschia subangulata* is from Middle Visean to Upper Visean (V3b) (Altıner, 1981). In this study this species has been encountered from the Upper Visean (Mikhailovsky).

Forschia sp.

Pl. XX, figs. 11-13

Description:

Test is bilocular. 2. tubular chamber planispirally coils around the prolocus. Coiling is evolute. Second chamber is undivided but in some forms pseudopartitions can be developed. Expansion of the spire is gradual and the final tour may be more larger. There are 3 volutions. Wall includes an inner microgranular and thin layer and an outer agglutinated thick layer.

Dimensions:

Diameter (d): 0.529-0.877 mm

Width (w): 0.182-0.320 mm

w/d: 0.34-0.37

Wall thickness: 39-50 μm

Remarks:

This form is differentiated from *Forschia subangulata* by the shape of volutions which are not angular and from *Forschia parvula* by its larger dimensions.

Stratigraphic distribution:

The stratigraphic distribution of *Forschia* sp. is Upper Visean and Lower Serpukhovian.

Genus Forschiella Mikhailov, 1935

Type species *Forschiella prisca* Mikhailov, 1935

Forschiella sp. 1

Pl. XX, figs. 14-15

Description:

Test is laterally compressed. Second tubular chamber coils approximately 3 times planispirally around the prolocus then it continues its development uniserially. Coiled part is evolute. Volutions are angular in axial section. Wall includes an inner microgranular and thin layer and an outer agglutinated thick layer.

Dimensions:

Diameter : 0.794-0.818 mm

Height: 0.893-1.042 mm

Wall thickness: 42-39 μm

Remarks:

This form is differentiated from *Forschiella prisca* by less number of volutions and smaller dimensions. It is differentiated from *Forscia subangulata* by the final uniserial part.

Stratigraphic distribution:

The stratigraphic distribution of *Forschiella* sp 1. is Upper Visean (Mikhailovsky).

Forschiella sp. 2

Pl. XX, fig. 16

Description:

Test is large. Umbilical region is depressed. It consist of two parts in the test morphology. One is the coiling part and the other is uncoiled, rectilinear part. Coiled part is formed by an undivided chamber which makes 3 tours around the procolulus. Coiling is planispiral and evolute. Uncoiled part is formed by two pseudochambers. Volutions have globular appearance in the axial section and expand very rapidly in the final tour and the uncoiled part. Wall includes an inner microgranular and thin layer and an outer agglutinated thick layer.

Dimensions:

Diameter : 0.449 mm

Height: 0.673 mm

Wall thickness: 27 μm

Remarks:

The important distinguishing feature of this form is its umbilical depression and convex volutions. *Forschiella* sp. 1 has greater dimensions and angular volutions. In addition, its umbilical region is wide.

Stratigraphic distribution:

The only specimen belonging to this species has been encountered from the Upper Visean (Mikhailovsky).

Forschiella sp.

Pl. XX, fig. 17

Description:

Specimens including a coiling part formed by a non septate chamber and an uncoiled rectilinear part is assigned to *Forschiella* sp. The wall is formed by an agglutinated, thick outer layer and a microgranular, thin inner layer.

Stratigraphic distribution:

The stratigraphic distribution of *Forschiella* spp. is Upper Visean (Mikhailovsky).

SUPERFAMILY FUSULINACEA Moeller, 1878

FAMILY EOSTAFFELLIDAE Mamet in Mamet, Mikhailoff and Mortelmans, 1970

Genus Eostaffella Rauser-Chernoussova, 1948

Type species: *Staffella* (*Eostaffella*) *parastruvei* Rauser-Chernoussova, 1948

Eostaffella ikensis Vissarionova, 1948

Pl. XXI, figs. 1-7

1948. *Eostaffella ikensis* Vissarionova, p. 219, pl. 13, figs. 8-10; pl. 14, fig. 1.

1981. *Eostaffella* sp. aff. *Eostaffella ikensis* Vissarionova; Altıner, p. 440, pl. 27, fig. 8.

1999. *Eostaffella ikensis* Vissarionova; Vdovenko et al., p. 188, text fig. 1, fig. 23.

1999. *Eostaffella ikensis* Vissarionova; Özkan, p. 225, pl. 11, figs. 4-5.

2004. *Eostaffella* aff. *ikensis* Cózar, p.381, pl.2, fig.16.

? 2005. *Eostaffella* ex.gr. *ikensis* Vissarionova; Somerville and Cózar, p. 138, pl. 3, fig. 24.

2006. *Eostaffella* ex.gr. *ikensis* Vissarionova; Okuyucu and Vachard, p. 540, text fig 5, figs. 15-16.

2011. *Eostaffella* ex.gr. *ikensis* Vissarionova; Atakul-Özdemir et al., p. 713, text fig. 5, figs. v-x

Description:

Test is lenticular. The periphery is angular in axial section. Flanks on the sides are convex. There is no umbilical depression. The number of volutions is 4 in the present specimens. Coiling is planispiral and involute and spire expands gradually. There are numerous chambers. Septa are straight and sutures were not observed. Secondary deposits can be seen as pseudochomata. Wall is dark, microgranular, undifferentiated.

Dimensions:

Diameter (d): 0.552-0.820 mm

Width (w): 0.340-0.440 mm

Height of the last tour: 0.079-0.137 mm

w/d: 0.54-0.62

Wall thickness: 20-22 μm

Remarks:

Sides are convex. However, in axial section, towards the tips of the form slight depressions are observed on both sides of the test. This species is one of the largest forms distinguished in this work. It is differentiated from *Eostaffella tenebrosa* by its convex flanks, less remarkable pseudochomata and larger w/d ratio and from *Eostaffella mosquensis* by its larger dimensions and absence of umbilici.

Stratigraphic distribution:

The stratigraphic range of this form is in from Mikhailovsky horizon (Upper Visean) to Upper Serpukhovian (Vdovenko et al., 1990). Our samples belong to Upper Visean and Lower Serpukhovian.

Eostaffella mosquensis Vissarionova, 1948

Pl. XXII, fig. 12

1979. *Eostaffella mosquensis* Vissarionova; Conil, Longerstaey and Ramsbottom, p. 154, pl. 17, fig. 13; p. 160, pl. 20, figs. 14, 21; p. 176, pl. 27, fig. 21

1979. *Eostaffella* aff. *Mosquensis* Vissarionova; Conil, Longerstaey and Ramsbottom, p. 160, pl. 20, fig. 10.

1989. *Eostaffella* cf. *mosquensis* Vissarionova; Skompski et al., p. 473, pl. 7, fig. 40.

1999. *Eostaffella mosquensis* Vissarionova; Özkan, p. 225, pl. 11, figs. 13-15.

2004. *Eostaffella mosquensis* Vissarionova; Cozar, p.381, pl.2, fig.15.

2005. *Eostaffella mosquensis* Vissarionova; Somerville and Cózar, p. 138, pl. 3, fig. 27.

? 2006. *Eostaffella mosquensis* Vissarionova; Okuyucu and Vachard, p. 542, text fig 6, fig. 7.

2006. *Eostaffella ex gr. mosquensis* Vissarionova; Vachard et al., p. 774, text fig. 5, fig. 1.

Description:

Test is lenticular and laterally compressed. Umbilical depression is shallow and small. The periphery is rounded particularly in the initial tours, it is rounded to acute in the final 2 tours. There are 4 volutions expanding rapidly but progressively. Coiling is planispiral and involute throughout. Secondary deposits can be seen as pseudochomata. Wall is dark, microgranular, undifferentiated.

Dimensions:

Diameter (d): 0.499 mm

Width (w): 0.216 mm

Height of the last tour: 0.079 mm

w/d: 0.433

Wall thickness: 12 μm

Remarks:

This form differentiated from *Eostafella parastruvei* by its more compressed test and rounded to acute periphery in the final 2 volutions. It is differentiated from *Eostafella ikensis* by its smaller dimensions, compressed test and presence of small umbilici.

Stratigraphic distribution:

The stratigraphic range of this form is from Aleksinsky Horizon (Upper Visean) through Lower Bashkirian (Maslo and Vachard, 1997). Our specimens were found in Upper Visean (Mikhailovsky).

Eostaffella ovesa Ganelina, 1956?

Pl. XXIII, fig. 7

1956. *Eostaffella ovesa* Ganelina, p. 110, pl. 11, figs. 10-11.

Description:

Test is small and oval. The periphery is broadly rounded. Umbilical depression is absent. Lateral flanks are slightly convex. Number of volutions is 3. Coiling is planispiral and involute and it is developed gradually. Chomata is not observed. Wall is dark, microgranular.

Dimensions:

Diameter (d): 0.184 mm

Width (w): 0.112 mm

Height of the last tour: 0.036 mm

w/d: 0.608

Wall thickness: 11 μm

Remarks:

This form is used with a question mark in this study. Because of its very small dimensions the form may be deceptive and this identification might be completely

erroneous. However, small dimensions are characteristic for this species. In addition, oval test, convex lateral sides, tight spire and the thin wall are other distinguishing features. *Eostaffella pseudostruvei* has also oval test but, its umbilicus is well defined and dimensions are larger.

Stratigraphic distribution:

The stratigraphic range of this form is in Lower Carboniferous (Ganelina, 1956). The only specimen was recovered from the Lower Serpukhovian.

Eostaffella ovoidea (Rauser- Chernoussova, 1948)

Pl. XXIII, figs. 1-3

1948. S*taffella* (*Eostafella*) *prisca* var. *ovoidea* Rauser- Chernoussova, p. 16, pl. 3, figs. 21-22.

1981. *Eostaffella ovoidea* Rauser- Chernoussova; Altıner, p. 440, pl.27, figs. 31-32.

Description:

Test is lenticular and small. The periphery is rounded in initial tours and slightly angular in the final tour. Umbilical depression is not well defined and it is shallow. There are 4 volutions. In the first tour coiling is endothyroid and some oscillation is obvious, the preceding tours are planispiral and involute and spire expands gradually except for the first volution which is smaller in height and width. Pseudochomata are well developed. Wall is dark, microgranular, undifferentiated.

Dimensions:

Diameter (d): 0.348-0,419 mm

Width (w): 0.163-0.197 mm

Height of the last tour: 0.072-0.105 mm

w/d: 0.608

Wall thickness: 9-14 μm

Remarks:

The angularity of the final tour resembles to *Eostaffella* sp. 1, but it is differentiated by its deeper umbilici. The test of *Millerella angusta* is much more compressed than the test of *Eostaffella ovoidea*.

Stratigraphic distribution:

The stratigraphic range of this form is from Upper Visean (V3c) to Lower Serpukhovian (Altıner, 1981). Our samples were recovered from Upper Visean (Venevsky) and Lower Serpukhovian.

Eostaffella cf. *ovoidea* Rauser- Chernoussova, 1948

Pl. XXIII, figs. 4-6

Remarks:

Well preserved axial sections cannot be found and this name is given by observing tangentil sections that do not pass from the initial tours. So, the endothyroid coiling in the first tour cannot be observed and dimensions of the form are smaller than the dimensions of *Eostaffella ovoidea*. Due to the morphology of the periphery and umbilical region and the expansion of the tours this form is assigned to *Eostaffella* cf. *ovoidea*.

Stratigraphic distribution:

Our samples were recovered from Upper Visean.

Eostafella parastruvei (Rauser- Chernoussova, 1948)

Pl. XXII, figs. 1-11

1948. *Staffella* (*Eostaffella*) *parastruvei* Rauser- Chernoussova, p. 15, pl. 3, figs. 16-18.

1963. *Eostafella parastruvei* Rauser- Chernoussova; Conil and Pirlet, pl. 3, fig. 41.

1979. *Eostafella parastruvei* Rauser- Chernoussova; Conil, Longerstaey and Ramsbottom, p. 143, pl. 11, figs. 9-10; p. 144, pl. 12, fig. 11; p. 161, pl. 20, fig. 11; p. 171, pl. 24,

fig. 15; p. 174, pl. 25, fig. 15; p. 177, pl. 27, figs. 18-20; p. 160, pl. 20, fig. 11; p. 170, pl. 24, fig. 15; p. 172, pl. 25, fig. 15, p. 176, pl. 27, figs. 18-20; p. 182, pl. 29, fig. 6

1981. *Eostafella parastruvei* Rauser- Chernoussova; Altıner, p. 440, pl.27, figs. 1-5.

1982. *Eostafella parastruvei* Rauser- Chernoussova Rozovskaya; Strank, p. 106, pl. 10, fig. 1.

1989. *Eostafella parastruvei* Rauser- Chernoussova; Athersuch and Strank, p. 17, pl. 4, fig. 11.

1989. *Eostafella* cf. *parastruvei* Rauser- Chernoussova; Skompski et al., p. 473, pl. 7, fig. 24.

1998. *Eostafella parastruvei* Rauser- Chernoussova; Gallagher, p. 202, pl. 2, fig. 2.

2004. *Eostafella parastruvei* Rauser- Chernoussova; Cózar, p. 381, pl. 2, fig. 14.

2004. *Eostafella parastruvei* Rauser- Chernoussova; Cózar and Somerville, p. 56, text fig. 14,fig. 30.

2005. *Eostafella parastruvei* Rauser- Chernoussova; Somerville and Cózar, p. 138, pl. 3, fig. 28.

Description:

Test is lenticular. Umbilical region is moderately shallow and deep. Sides of the form are moderately compressed. Periphery of the inner whorls is rounded while it is angular in the final one or two tours. It has 3-5 volutions. Coiling is planispiral and involute. The height of the initial tours increases progressively but, the height and width the final tour significantly increases. Secondary deposits are in the form of massif chomata. Wall is dark, microgranular, undifferentiated.

Dimensions:

Diameter (d): 0.435-0.711 mm

Width (w): 0.223-0.342 mm

Height of the last tour: 0.80-0.177 mm

w/d: 0.422-0.480

Wall thickness: 12-18 μm

Remarks:

The periphery of the last volution of *Eostafella parastruvei* is more angular than *Eostafella mosquensis* and umbilicus of the former is deeper than the latter. The general morphology of *Eostaffella* sp. 5 resembles to the present form however, *Eostafella parastruvei* has larger dimensions and larger number of tours.

Stratigraphic distribution:

The stratigraphic range of this form is from Upper Visean and Serpukhovian (Altıner, 1981). Our specimens also belong to the Upper Visean and Lower Serpukhovian.

Eostaffella pseudostruvei (Rauser-Chernousova and Beliaev in Rauser-Chernousova, Beliaev and Reitlinger, 1936)

Pl. XXIII, figs. 8-10

1936. *Staffella pseudostruvei* Rauser-Chernousova and Beliaev in Rauser-Chernousova, Beliaev and Reitlinger, p. 79, pl. 1, fig. 7.

1979. *Eostaffella* (*Eostaffella*) *pseudostruvei* Rauser-Chernousova and Beliaev; Potievskaya, pl. 13, fig. 3.

1979. *Eostaffella pseudostruvei* Rauser-Chernousova and Beliaev; Vdovenko, pl. 3, fig. 4, pl. 5, fig. 25.

1981. *Eostaffella pseudostruvei* Rauser-Chernousova and Beliaev; Altıner, p. 440, pl. 27, figs. 18-20.

2008. *Eostaffella pseudostruvei* Rauser-Chernousova and Beliaev; Cozar et al., p. 473, text fig. 8, fig. 22.

2011. *Eostaffella pseudostruvei* Rauser-Chernousova and Beliaev; Atakul-Özdemir et al., p. 713, text fig. 5, figs. j-r.

Description:

Test is small, discoidal and umbilical region is narrow and deep. Periphery is rounded in all tours. In some specimens found in the present study, the periphery of the final tour is angular. Slight oscillations are observed in the initial voulutions. There are 3- 4 volutions. Coiling is planispiral and involute throughout. Spire expands gradually except for the last volution which is higher and wider than the previous ones. Pseudochomata can be developed. Wall is dark, microgranular.

Dimensions:

Diameter (d): 0.199-0.264 mm

Width (w): 0.069-0.114 mm

Height of the last tour: 0.031-0.051 mm

w/d: 0.35-0.531

Wall thickness: 8-17 μm

Remarks:

This form differs from *Millerella angusta* by its more rounded periphery and involute coiling.

Stratigraphic distribution:

Our samples were recovered from Lower Serpukhovian.

Eostaffella tenebrosa Vissarionova, 1948

Pl. XXI, fig. 8

1948. *Eostaffella ikensis* var. *tenebrosa* Vissarionova, pl. 13, figs. 11-13.

1999. *Eostaffella tenebrosa* Vissarionova; Vdovenko et al., p. 188, text fig. 1, fig. 29.

1999. *Eostaffella tenebrosa* Vissarionova; Özkan, p. 225, pl. 11, figs. 6-9.

2011. *Eostaffella tenebrosa* Vissarionova; Atakul-Özdemir et al., p. 713, text fig. 5, figs. y-z.

Description:

Test is lenticular and sharply keeled in the last two whorls. Periphery is angular in the final tours but rounded in the initial tours. Umbilical region is slightly depressed. Sides of the form are moderately compressed. It has 4 volutions. Coiling is planispiral and involute and it is developed progressively in the initial tours but, rapidly in the final tour. Pseudochomata is obvious. Wall is dark, microgranular, undifferentiated.

Dimensions:

Diameter (d): 0.689 mm

Width (w): 0.322 mm

Height of the last tour: 0.159 mm

w/d: 0.47

Wall thickness: 0,021 μm

Remarks:

This form differs from *Eostaffella ikensis* by its keel and angular periphery, more compressed sides, well developed pseudochomata. In addition, convexity of flanks seen in *Eostaffella ikensis* cannot be observed in this species.

Stratigraphic distribution:

The stratigraphic range is from Upper Visean (Venevsky horizon) through Upper Serpukhovian (Vdovenko et al., 1990). Only one specimen is observed in this study and it belongs to the Lower Serpukhovian.

Eostaffella compacta Rozovskaya, 1963

Pl. XXII, figs. 13-14

1963. *Eostaffella versabilis* Orlova subsp. *Compacta* Rozovskaya, p. 92-93, pl. 16, figs. 13-15.

Description:

Test is lenticular and umbilical region is depressed. Periphery is rounded in all volutions. There are 3-4 volutions. Coiling is planispiral and involute and the height of the tours increases gradually. Chomata may be developed. Wall is dark, microgranular, undifferentiated.

Dimensions:

Diameter (d): 0.414-0.490 mm

Width (w): 0.219-0.221 mm

Height of the last tour: 0.088-0.099 mm

w/d: 0.448-0.534

Wall thickness: 11-13 μm

Remarks:

This form has been raised to a species level and considered independent from "*E. versabilis*". It differs from the others with a more rounded periphery and progressive development of the whorls. Although both *Eostaffella compacta* and *Eostaffella pseudostruvei* has rounded periphery the former is much larger than the latter.

Stratigraphic distribution:

The stratigraphic range of this form is Mikhailov horizon (Rozovskaya, 1963). Our specimens also belong to the Mikhailovsky Horizon.

Eostaffella sp. 1

Pl. XXIII, figs. 11-14

Description:

Test is lenticular and umbilical region is deep and narrow. Periphery is rounded in the initial tours, strongly angular in the final 2 tours. Flanks of the last tour are convex sided but, the tip is pointed. There are 3-4 volutions. Coiling is planispiral, involute and slight oscillations can be seen in the initial tours. Spire gradually expands

except for the last whorl. Chomata is well developed. Wall is dark, microgranular, undifferentiated.

Dimensions:

Diameter (d): 0.306-0.385 mm

Width (w): 0.145-0.174 mm

Height of the last tour: 0.060-0.092 mm

w/d: 0.45-0.47

Wall thickness: 9-17 μm

Remarks:

This form differs from *Eostaffella ovoidea* by its deeper umbilicus, more compressed test and angularity of the last 2 volutions. *Millerella angusta* has a more compressed test and its coiling is more evolute. It is differentiated from *Eostaffella* sp. 4 by its smaller dimensions, oscillations in its initial tours and convex sides of the flanks.

Stratigraphic distribution:

Our samples belong to the Upper Visean.

Eostaffella sp. 2

Pl. XXIII, figs. 15-16

Description:

Test is small, inflated with a well-rounded periphery in all volutions. There are 3 volutions. Coiling is planispiral, involute throughout. The height of the last tour rapidly increases. Chomata can be observed. Wall is dark, microgranular, undifferentiated.

Dimensions:

Diameter (d): 0.332-0.342 mm

Width (w): 0.194-0.199 mm

Height of the last tour: 0.068-0.080 mm

w/d: 0.35-0.40

Wall thickness: 13-16 μm

Remarks:

The most characteristic feature of this form that differentiates it from other species of this genus is its distinct rounded and inflated periphery.

Stratigraphic distribution:

Our samples were recovered from Upper Visean (Mikhailovsky).

Eostaffella sp. 3

Pl. XXIII, fig. 17

Description:

Test is small and nautiloid. Periphery is rounded in initial tours. In the last tour periphery is angular with pointed tips and sides are convex so that the shape of the form is rhombic. Umbilical region is shallow and wide. There are 3-3.5 volutions. Coiling is planispiral, involute through. Spire gradually expands. Chomata can be observed. Wall is dark, microgranular.

Dimensions:

Diameter (d): 0.277 mm

Width (w): 0.189 mm

Height of the last tour: 0.065 mm

w/d: 0.68

Wall thickness: 17 μm

Remarks:

The pointed tips of this form resemble to those of *Eostaffella tenebrosa*. However, the latter has greater dimensions and more compressed test. The most characteristic features of *Eostaffella* sp. 3 are greater w/d ratio, obviously pointed tip periphery and large and shallow umbilical area.

Stratigraphic distribution:

In this study the only specimen has been observed in the Upper Visean (Mikhailovsky).

Eostaffella sp. 4

Pl. XXIV, figs. 1-5

Description:

Test is small and lenticular. Umbilical region is shallow and slightly deeper. Periphery is well rounded in the initial tours but, it is slightly angular in the last tour. There are 3 volutions. Coiling is planispiral and involute through. Spire expands rapidly in all tours. Chomata are developed but not observed in all specimens. Wall is dark, microgranular.

Dimensions:

Diameter (d): 0.333-0.433 mm

Width (w): 0.153-0.188 mm

Height of the last tour: 0.060-0.092 mm

w/d: 0.43-0.46

Wall thickness: 8-10 μm

Remarks:

This species resembles to *Eostaffella* sp. 5. It is discriminated from it by its smaller w/d ratio and slightly deeper umbilical region. Its dimensions and number of tours are smaller than *Eostaffella parastruvei*.

Stratigraphic distribution:

Our specimens were recovered from Upper Visean (Mikhailovsky).

Eostaffella sp. 5

Pl. XXIV, figs. 6-11

Description:

Test is small, lenticular. Umbilical region is not well defined. Periphery is rounded in initial tours. It is strongly angular in the final. Coiling is planispiral,

involute through. It consists of progressively developed 3 or 3.5 tours. Only the last volution is developed rapidly. The presence of chomata is eventual. Test is microgranular, dark and undifferentiated.

Dimensions:

Diameter (d): 0.354-0.413 mm

Width (w): 0.92-0.198 mm

Height of the last tour: 0.054-0.080 mm

w/d: 0.48-0.54

Wall thickness: 10-14 μm

Remarks:

The number of tours is smaller than *Eostaffella parastruvei* and the initial endothyroid coiling of the latter is not observed in *Eostaffella* sp. 5. Dimensions and number of volutions are smaller than *Eostaffella mosquensis* and *Eostaffella mosquensis* has more compressed test than the present one. w/d ratio of *Eostaffella* sp. 5 is larger than w/d ratio of *Eostaffella* sp. 1.

Stratigraphic distribution:

In this study the samples of *Eostaffella* sp. 5 has been encountered from the Upper Visean and Serpukhovian.

Eostaffella sp. 6

Pl. XXIV, figs. 12-15; Pl. XXV, 1-2

Description:

Test is large with a broad and well-rounded periphery. Umbilical region is not well defined, it is shallow and wide. Coiling is planispiral, involute but, in some specimens semi-evolute last half tour was observed. There are 4-5 volutions. The height of the tours progressively increases except for the final one. The last volution is developed very rapidly and it is much higher and wider than the initial ones.

Development of pseudochomata especially in the final tours is eventual. Test is microgranular, dark and undifferentiated.

Dimensions:

Diameter (d): 0.627-0.699 mm

Width (w): 0.286-0.376 mm

Height of the last tour: 0.116-0.147 mm

w/d: 0.45-0.47

Wall thickness: 16-32 μm

Remarks:

The most characteristic features of this form are its very large dimensions and broadly rounded periphery. It is differentiated from *Eostaffella ikensis* by its broadly rounded periphery. Although umbilicus is not well defined in both of the species, it is more marked in *Eostaffella* sp. 6.

Stratigraphic distribution:

In this study the samples of *Eostaffella* sp. 6 has been encountered from the Upper Visean (Mikhailovsky).

Eostaffella? sp. 7

Pl. XXV, 3-5

Description:

Test is small with a rounded periphery. Umbilical region is not marked. Coiling is planispiral, involute till the last tour. In the last tour, the plane of coiling axis changes at about 10-30°. There are 2-5 tours. In the last tour the height markedly increases. Previous tours expand gradually. Chomata or pseudochomata are absent. At the sides of the initial volutions darkness is eventual. This darker region may be the result of the secondary deposits or wall thickening. Test is microgranular, dark and undifferentiated.

Dimensions:

Diameter (d): 0.292-0.367 mm

Width (w): 0.156-0.174 mm

Height of the last tour: 0.073-0.097 mm

w/d: 0.47-0.53

Wall thickness: 11-12 μm

Remarks:

The most characteristic feature of this form is the shift in the coiling axis and this is the reason why this form is named with a question mark.

Stratigraphic distribution:

In this study the samples of *Eostaffella*? sp. 7 has been found in the Upper Visean (Mikhailovsky).

Eostaffella spp.

Pl. XXIII, fig. 18?-19?, 20-26; Pl. XXV, figs. 6-11

Description:

Many forms that cannot be assigned to a particular species of *eostaffella* are grouped under the name of *Eostaffella* spp. Their common criteria is their wall structure, planispiral and involute coiling and numerous and straight septa.

Remarks:

The validity of the name *Eostaffella* for some specimens in this study (Appendix A, Plate XXIII, figs. 18-19) is suspicious because, the last volutions of these specimns are tend to be evolute.

Stratigraphic distribution:

In this study the samples of *Eostaffella* spp. were identified in Upper Visean and Lower Serpukhovian.

Genus *Chomatamediocris* Vdovenko, 1973

Type species: *Mediocris brevisculiformis* Vdovenko, 1973

Chomatamediocris ? sp.

Pl. XXVI, fig. 16

Description:

Test is discoidal with a rounded periphery in all tours. There are gradually expanding 4.5 volutions, however, the last tour is more spacious. Coiling is planispiral and involute except for the last half tour which is evolute. Secondary deposits exist on lateral sides of the test and also in form of chomata. Wall is dark, microgranular.

Dimensions:

Diameter (d): 0.443 mm

Width (w): 0.204 mm

Height of the last tour: 0.057 mm

w/d: 0.46

Wall thickness: 14 μm

Remarks:

This form differs from the genus *Mediocris* by the presence of chomata. Chomata is present but not massive and very well marked. Therefore, the genus is questionably identified.

Stratigraphic distribution:

The stratigraphic range of the genus *Chomatamediocris* is from Middle to Upper Visean (Loeblich and Tappan, 1988). Our specimen belongs to the Upper Visean (Mikhailovsky).

Genus Mediocris Rozovskaya, 1961

Type species: *Eostaffella mediocris* Vissarionova, 1948

*Mediocris breviscula (*Ganelina, 1951)

Pl. XXVI, figs. 11-15

1951. *Eostaffella mediocris* var. *breviscula* Ganelina, p. 197-198, pl. 3, figs. 1-3.

1954. *Eostaffella breviscula* Ganelina; Grozdilova and Lebedeva, p. 121-122, pl. 13, figs. 12, 13.

1963. *Mediocris breviscula* Ganelina; Rozovskaya, p. 108, pl. 19, figs. 14-17.

1969. *Mediocris mediocris* var. *breviscula* Ganelina; Manukalova-Grebeniuk et al., p. 24-25, pl. 6, figs. 3-4.

1973. *Mediocris breviscula* Ganelina; Mamet, p. 119, pl. 7, figs.15-16.

1979. *Mediocris breviscula* Ganelina; Conil, Longerstaey and Ramsbottom, p. 160, pl. 20, fig. 17.

1981. *Mediocris breviscula* Ganelina; Altıner, p. 440, pl. 28, figs. 20-25.

1993. *Mediocris breviscula* Ganelina; Mamet et al., pl. 10, figs. 19-22.

1993. *Mediocris breviscula* Ganelina; Ueno and Nakazawa, p. 42, text fig. 15, figs. 6-26.

1999. *Mediocris breviscula* Ganelina; Özkan, p. 222, pl. 10, figs. 9-20.

2005. *Mediocris breviscula* Ganelina; Zhijun et al., p. 343, pl. 2, figs. 16-21.

2009. *Mediocris breviscula* Ganelina; Ueno and Miyazaki, p. 85, text fig. 4, fig. 13.

2011. *Mediocris breviscula* Ganelina; Atakul-Özdemir et al., p. 717, text fig. 7, fig. w.

Description:

Test is small, discoidal with a rounded periphery in all tours. Sides of the form are narrow. It has 2-3 volutions. The last tour expands rapidly and occupies larger places. Coiling is planispiral throughout. Secondary deposits exist on lateral sides of the test. It does not contain chomata. Wall is thin, microgranular.

Dimensions:

Diameter (d): 0.172-0.271 mm

Width (w): 0.064-0.109 mm

Height of the last tour: 0.050-0.028 mm

w/d: 0.37-0.40

Wall thickness: 7-8 μm

Remarks:

This form differs from *Mediocris mediocris* by more compressed test and smaller w/d ratio. Also, no initially skewed coiling is observed in *Mediocris breviscula*. In our examples number of tours is also less than the ones in *Mediocris mediocris*.

Stratigraphic distribution:

The stratigraphic range of this form is from Lower Visean to Bashkirian (Altıner, 1981). Our specimens belong to Upper Visean (Mikhailovsky).

Mediocris mediocris (Vissarionova, 1948)

Pl. XXVI, figs. 1-4, 5?, 6-10

1948. *Eostaffella mediocris* Vissarionova; p. 222-223, pl. 14, figs. 7-9.

1956. *Eostaffella mediocris* Vissarionova; pl. 15, fig. 12.

1960. *Eostaffella mediocris* Vissarionova; Grozdilova and Lebedeva, p. 109, pl. 13, fig.13

1963. *Eostafella mediocris* Vissarionova; Conil and Pirlet, pl. 3, fig. 42.

1963. *Mediocris mediocris* Vissarionova; Rozovskaya, p. 103-104, pl. 18, figs. 26-33.

1979. *Mediocris mediocris* Vissarionova; Conil, Longerstaey and Ramsbottom, p. 160, pl. 20, fig 23; p. 168, pl. 23, fig. 14.

1973. *Mediocris mediocris* Vissarionova; Mamet, p. 119, pl. 7, figs.17-18.

1979. *Mediocris mediocris* Vissarionova; Brazhnikova, pl. 9, fig. 7.

1981. *Mediocris mediocris* Vissarionova; Altıner, p. 440, pl. 28, figs. 15-18.

1982. *Mediocris mediocris* Vissarionova; Strank, p. 105, pl. 9, fig. 14.

1993. *Mediocris mediocris* Vissarionova; Ueno and Nakazawa, p. 42, text fig. 15, figs. 1-5

1999. *Mediocris breviscula* Ganelina; Özkan, p. 222, pl. 10, figs. 21-27.

2005. *Mediocris mediocris* Vissarionova; Zhijun et al., p. 343, pl. 2, figs. 22-26.

2011. *Mediocris breviscula* Ganelina; Atakul-Özdemir et al., p. 717, text fig. 7, figs. x-y.

Description:

Test is lenticular with a rounded periphery in all tours. It consists of progressively developed 3 or 4 tours. Only the last whorl is wider and longer than the others. Coiling is generally skewed in the initial voultions, then it becomes planispiral. Secondary deposits concentrate on the lateral parts of the the test and form dense,dark layers on the sides, especially around umbilicus. Wall is dark and microgranular.

Dimensions:

Diameter (d): 0.327-0.469 mm

Width (w): 0.158-0.233 mm

Height of the last tour: 0.057-0.104 mm

w/d: 0.38-0.48

Wall thickness: 9-17 μm

Remarks:

This form shows some morphologic variations. Since the stratigraphic distribution of the *Mediocris mediocris* and the morphotypes are the same, no subspecies is created in the present study. For example, the last tours of the forms in fig 6 and 7 (Appendix A, pl. XXVI) are much more spacious and these forms have narrower umbilical regions. Coiling of specimens illustrated in figures 8, 9, 10 (Appendix A, pl. XXVI) starts to be evolute and these forms have smaller w/d ratio. *Mediocris mediocris* differs from *Mediocris breviscula* and *Mediocris minima* by greater w/d ratio.

Stratigraphic distribution:

The stratigraphic range of this form is from Middle Visean to Bashkirian (Altıner, 1981). Our specimens belong to the Upper Visean (Mikhailovsky).

Mediocris spp.

Pl. XXVII, figs. 1-13

Description:

Several specimens that cannot be grouped with in a definite species are assambled as *Mediocris* spp. All members of this group have secondary deposits on lateral parts of their tests and have a dark microgranular layer. All of them are planispiral. For these reasons, they are grouped under the genus name *Mediocris*.

Remarks:

They differ from *Mediocris mediocris* such that they do not show initial skewed coiling. The compressed test and smaller w/d ratio of *Mediocris breviscula* can not be observed in the members of this group.

Stratigraphic distribution:

Specimens belongs to Upper Visean and Lower Serpukhovian.

Genus *Millerella* Thompson, 1942

Type species: *Millerella marblensis* Thompson, 1942

Millerella spp.

Pl. XXVII, figs. 17-19

Description:

Test is lenticular with a rounded periphery in all tour. Umbilicus is deep and wide. There 3-4 volutions. Expansion rapidly increases in the last 2 volutions. Coiling is planispiral and evolute in most of the tours. Chomata is eventual. Wall is dark, microgranular.

Dimensions:

Diameter (d): 0.195-0.455 mm

Width (w): 0.099-0.181 mm

Height of the last tour: 0.036-0.040 mm

w/d: 0.26-0.40

Wall thickness: 7-11 μm

Remarks:

Individulas share the characteristics mentioned in the descripton part but their dimensions and w/d ratio are different from each other. As a result they were grouped as *Millerella* spp.

Stratigraphic distribution:

Our specimens belong to the Upper Visean and Serpukhovian.

Genus *Praeostaffellina* Cózar, Sommerville and Burges, 2008

Type species: *Praeostaffellina macdonaldensis* Cózar, Sommerville and Burges

Praeostaffellina macdonaldensis Cózar, Sommerville and Burges, 2008

Pl. XXVIII, fig. 1

1979. *Endostaffella parva*, Moeller; Conil, Longerstaey and Ramsbottom, p. 167, pl. 22, figs. 19- 22.

2008. *Praeostaffellina macdonaldensis* Cózar, Sommerville and Burges, p. 915, text fig. 7, figs. 14-19.

Description:

Test is small and subglobose. Umbilical region is narrow. Coiling is skewed. Periphery of all whorls is rounded. Final whorl is evolute. In the last 1.5 whorl pseudochomata is developed. Chambers are narrow and divided by straight septa. Wall is microgranular and composed of a tectum and a dense layer.

Dimensions:

Diameter (d): 0.481 mm

Width in the umbilicate area (w): 0.226 mm

Wall thickness: 13 μm

Remarks:

This form may be confused with *Endostaffella parva*, but the wall of *Praeostaffellina macdonaldensis* is differentiated as two layers namely a tectum and a dense layer and it contains pseudochomata. In addition all volutions of the former are involute while the last volution of the latter is evolute. In our examples coiling starts to be skewed but ends as planispiral. This trend was not discussed in the original description but, it was shown in the figures.

Stratigraphic distribution:

The stratigraphic range is Upper Visean (Brigantian) – Serpukhovian (Cózar et al., 2008). Specimens were recovered only Mikhailovsky (Upper Visean).

Genus *Praeplectostaffella* Cózar, Sommerville and Burges, 2008

Type species: *Endostaffella asymmetrica* Rozovskaya, 1963

Praeplectostaffella ex gr. *anvilensis* Cózar, Sommerville and Burges, 2008

Pl. XXVIII, figs. 2-9, 10?, 11-12

1979. *Endostaffella stella* Ganelina; Conil, Longerstaey and Ramsbottom, p. 185, pl. 29, fig. 2.

2007. *Endostaffella asymmetrica* Rozovskaya; Gibshman and Baranova, p. 275, text fig. 7, figs. 14-16.

2008. *Praeplectostaffella anvilensis* Cózar, Sommerville and Burges, p. 915, text fig. 7, figs. 1-9.

Description:

Test is small, with wide and shallow umbilicus. Periphery of the initial tours is rounded but, in the final half tour it is angular. Number of volutions is in between 2.5 to 3.5. Coiling is highly skewed but in the final tour coiling is planispiral. Final whorl is semievolute. Secondary deposits are in the form of pseudochomata and they are

observed in the last or last 2 tours. Wall is microgranular and composed of a tectum and a dence layer.

Dimensions:

Diameter (d): 0.226-0.470 mm

Width in the umbilicate area (w): 0.184-0.126 mm

Wall thickness: 11-14 μm

Remarks:

Wide umbilicate area and well developed pseudochomata in the last 1-2 tour is typical for this species. Initial coiling is skewed but last tour is planispiral. However some of the specimens in our samples change coiling axis 90° just after the first tour and make planispiral coiling in the last 1.5 tour which can be observed in some members of the genus *Endostaffella*. But these specimens were not considered as *Endostaffella* species because pseudocomata in the last 1 or 2 tour is very well developed and wall is composed of two layers. Considering these differences all specimens were assigned to *Praeplectostaffella* ex gr. *anvilensis.* One of the specimens of this species (Plate XXVIII, fig. 10) is questioned because the periphery of its final tour is not angular.

Stratigraphic distribution:

The stratigraphic range is Upper Visean – Serpukhovian (Cózar et al., 2008). Our specimens were recovered form the Upper Visean- Lower Serpukhovian.

Praeplectostaffella sp.

Pl. XXVIII, figs. 13-14

Description:

Test is small. Coiling is highly skewed and periphery is rounded in the initial tours, wheras the final tour is planispiral and periphery of the final tour is subangular. Final whorl is semievolute. Pseudochomata is present. Wall is microgranular and differentiated.

Dimensions:

Diameter (d): 0.329-0.442 mm

Width in the umbilicate area (w): 0.170-0.227 mm

Wall thickness: 9-13 μm

Remarks:

This form resembles some representatives of endostaffella. However, pseudochomata and angular to subangular periphery of the final tour is not typical for *Endostaffella*. Also the wall structure of *Endostaffella* is microgranular and undifferentiated.

Stratigraphic distribution:

The representatives of this form were recovered from Upper Visean.

FAMILY PSEUDOENDOTHYRIDAE Mamet in Mamet, Mikhailoff and Mortelmans, 1970

Genus *Pseudoendothyra* Mikhailov, 1939

Type species: *Fusulinella struvei* Möller, 1879

Pseudoendothyra ex gr.*bona* Rozovskaya, 1963

Pl. XXIX, figs. 11-13

1963. *Pseudoendothyra bona* subsp. *bona* Rozovskaya, pl. 14, figs. 9-12

2003. *Pseudoendothyra bona* Rozovskaya; Cozar, p. 161, text fig. 4, fig. R.

2005. *Pseudoendothyra bona* Rozovskaya; Somerville and Cózar, p. 138, pl. 3, fig. 34.

Description:

Test is large, lenticular with an angular periphery nearly in all volutions. In the last or last one and a half tour, the periphery is strongly acute due to development of the keel. Umbilicus is marked. Coiling is planispiral and evenly developed till the last

volution. The height of the last volution is markedly high. There are 4.5 volutions. Chomata are well developed. The wall is microgranular, lighter colored diaphonatheca is obvious.

Dimensions:

Diameter (d): 0.649-0.814 mm

Width (w): 0.309-0.436 mm

Height of the last tour: 0.088-0.139 mm

w/d: 0.48-0.53

Wall thickness: 12-32 μm

Remarks:

In the original description, depressions on both sides of the keeled and inflated last half whorl are indicated. However, in the members of *Pseudoendothyra* ex gr. *bona*. these depressions can not be observed or they can be identified only in one side of the keel. In addition umbilical depression is not very well defined in all representatives.

Stratigraphic distribution:

The stratigraphic range of *Pseudoendothyra bona* is Upper Visean (Rozovskaya, 1963). The samples of this study are from Upper Visean (Mikhailovsky).

Pseudoendothyra concinna (Schlykova, 1951)

Pl. XXX, fig. 2

1951. *Parastaffella concinna* Schlykova, p. 150-151, pl. 2, figs. 1-3.

1973. *Pseudoendothyra* aff. *P. concinna* Schlykova; Mamet, p. 119, pl. 7, fig.9.

1979. *Pseudoendothyra concinna* Schlykova; Conil, Longerstaey and Ramsbottom, p. 160, pl.20, fig. 12

1981. *Pseudoendothyra concinna* Schlykova; Altıner, p. 441, pl. 29, fig. 5.

1989. *Pseudoendothyra concinna* Schlykova; Skompski et al., p. 473, pl. 7, fig. 37.

Description:

Test is large with a deep and narrow umbilicus. Periphery of initial tours is subangular to rounded but, it is perfectly subangular in the final tour. Coiling is planispiral and involute in the initial tours, semi evolute in the final tour. Coiling is developed progressively but rapidly. There are 4.5 volutions. Chomata can be observed. The wall is microgranular and differentiated.

Dimensions:

Diameter (d): 0.676 mm

Width (w): 0.270 mm

Height of the last tour: 0.127 mm

w/d: 0.34

Wall thickness: 14 μm

Remarks:

The present form resembles to the representatives of *Pseudoendothyra* ex gr. *ornata*. However, *Pseudoendothyra concinna* has deeper and narrower umbilicus, its flanks ar inflated above the umbilical region, its periphery is more angular and it has a thicker wall.

Stratigraphic distribution:

The stratigraphic range of *Pseudoendothyra concinna* is Upper Visean (V3b to V3c) (Altıner, 1981). The samples of this study is Upper Visean (Mikhailovsky).

Pseudoendothyra ex gr. o*rnata* (Durkina, 1959)

Pl. XXX, figs. 3-5

1959. *Parastaffella luminosa* Ganelina var. *ornata* Durkina, p. 212-213, pl. 22, figs. 10.

2003. *Pseudoendothyra ornata* Durkina; Cozar, p. 161, text fig. 4, fig. S.

2004. *Pseudoendothyra* cf. *ornata* Durkina; Brenckle, p. 150, pl. 3, fig. 8.

2005. *Pseudoendothyra ornata* Durkina; Somerville and Cózar, p. 138, pl. 3, fig. 30.

Description:

Test is large with a wide and deep umbilical region. Periphery is well rounded in the initial tours, rounded to subangular and tapered in the final half tour. There are 3.5-4.5 volutions. Coiling is planispiral involute in the initial tours, evolute in the final tour. Spire expands very rapidly. In addition, the final whorl is significantly larger and higher than the previous tours. Chomata are well developed. The wall is microgranular and differentiated and thick.

Dimensions:

Diameter (d): 0.674-0.827 mm

Width (w): 0.256-0.349 mm

Height of the last tour: 0.123-0.153 mm

w/d: 0.38-0.42

Wall thickness: 15-18 μm

Remarks:

The present species may resemble to *Pseudoendothyra concinna* but, it is differentiated from *Pseudoendothyra concinna* by its more rounded peripheral margin of the inner whorls, more evolute whorls, more inflated test and less tapered periphery. It is defined under the name of *Pseudoendothyra* ex gr. *ornata* because dimensions of some specimens are smaller than the original description and they are more rounded.

Stratigraphic distribution:

The specimens of this study are from the Upper Visean (Mikhailovsky).

Pseudoendothyra struvei (Moeller, 1879)

Pl. XXIX, figs. 1-2

1879. *Fusulinella struvei* Moeller, p. 22, pl. 2, figs. 1a-c; pl. 5, figs. 4a-c.

1981. *Pseudoendothyra struvei* Moeller; Altıner, p. 441, pl. 29, figs. 1-3.

28-31.

1993. *Pseudoendothyra* cf. *struvei* Moeller; Ueno and Nakazawa, p. 42, text fig. 15, figs.

1999. *Pseudoendothyra struvei* Moeller; Özkan, p. 229, pl. 13, figs. 1-4.

2006. *Pseudoendothyra* ex gr. *struvei* Moeller; Vachard et al., p. 774, text fig. 5, fig. 14.

Description:

Test is lenticular. Umbilical region is narrow and shallow. Periphery is subrounded in the initial tours. In the final or final two tours it is subangular. There are 4 volutions. Coiling is endothyroid in the first tour and it is planispiral involute in the preceding tours. Development of pseudochomata is obvious and they can be observed in all volutions except for the first one. Wall is microgranular and differentiated.

Dimensions:

Diameter (d): 0.614-0.623 mm

Width (w): 0.293-0.375 mm

Height of the last tour: 0.129-0.142 mm

w/d: 0.48-0.60

Wall thickness: 18 μm

Remarks:

Initially endothyroid coiling and larger w/d ratio is characteristic for this species. The flanks are slightly inflated than other forms illustrated in this study. If compared to *Pseudoendothyra bona*, *Pseudoendothyra struvei* has smaller dimensions and no keel.

Stratigraphic distribution:

The stratigraphic range is Upper Visean (V3b) – Serpukhovian (Altıner., 1981). Specimens were recovered form the Upper Visean (Mikhailovsky).

Pseudoendothyra ex gr. *struvei* (Moeller, 1879)

Pl. XXIX, figs. 3-9

Dimensions:

Diameter (d): 0.314-0.512 mm

Width (w): 0.170-0.284 mm

Height of the last tour: 0.084-0.117 mm

w/d: 0.54-0.58

Wall thickness: 9-16 μm

Remarks:

Dimensions and number of whorls of the specimens that is named as *Pseudoendothyra* ex gr. *struvei* in the present study are smaller than *Pseudoendothyra struvei*. In addition, some of them have more compressed tests.

Stratigraphic distribution:

The specimens have been identified from the Upper Visean.

Pseudoendothyra sublimis (Schlykova, 1951)

Pl. XXX, figs. 6-7

1951. *Parastaffella sublimis* Schlykova, p. 149-150, pl. 1, figs. 11-13

1979. *Pseudoendothyra sublimis* Schlykova; Conil, Longerstaey and Ramsbottom, p. 160, pl. 20, fig. 20; p. 182, pl. 29, fig. 19.

1982. *Pseudoendothyra sublimis* Schlykova; Strank, p. 105, pl. 9, fig. 6.

1989. *Pseudoendothyra sublimis* Schlykova; Skompski et al., p. 473, pl. 7, fig. 23.

1998. *Pseudoendothyra sublimis* Schlykova; Gallagher, p. 202, pl. 2, fig. 1.

2004. *Pseudoendothyra sublimis* Schlykova; Cózar, p.381, pl.2, fig.17.

2004. *Pseudoendothyra sublimis* Schlykova; Cózar and Somerville, p. 56, text fig. 14, fig. 29.

2005. *Pseudoendothyra sublimis* Schlykova; Somerville and Cózar, p. 138, pl. 3, fig. 31.

Description:

Test is lenticular with a shallow umbilical region. Periphery is rounded in the initial tours, subangular last or last two tours. Coiling is planispiral and involute throughout. 3.5-4.5 volutions exist in this form and they are rapidly and progressively

developed. Pseudochomata can be observed. The wall is microgranular and differentiated, lighter layer is distinct.

Dimensions:

Diameter (d): 0.505-0.535 mm

Width (w): 0.234-0.260 mm

Height of the last tour: 0.117-0.118 mm

w/d: 0.46-0.49

Wall thickness: 16-23 μm

Remarks:

w/d ratio is smaller in *Pseudoendothyra concinna* so it is more compressed.

Stratigraphic distribution:

The stratigraphic range of *Pseudoendothyra sublimis* is Upper Visean and Serpukhovian. The specimens of this study were recovered from the Upper Visean.

Pseudoendothyra sp. 1

Pl. XXX, fig. 1

Description:

Test is small with broadly rounded periphery. Sides of the last tour are remarkably convex. Umbilical region is very wide and shallow. There are 4.5 volutions. Coiling of the first tour is endotyroid. Then, it becomes planispiral and involute till the last volution. Last volution is evolute. Inner whorls are tightly coiled whereas the last 1.5 volutions attains considerably in height in comparison with the preceding ones. Secondary deposits are absent. Wall is microgranular and diaphonatheca is distinct.

Dimensions:

Diameter (d): 0.486 mm

Width (w): 0.199 mm

Height of the last tour: 0.115 mm

w/d: 0.40

Wall thickness: 17 μm

Remarks:

This form may be considered belonging to the genus *Millerella* but, the wall structure is obviously differentiated and includes diaphonatheca. Very wide and shallow umbilicus, roundness of the periphery and strongly tightly coiled initial whorls are the characteristic features of *Pseudoendothyra* sp. 1.

Stratigraphic distribution:

Specimens were found in the Upper Visean and Serpukhovian.

Pseudoendothyra sp 2

Pl. XXX, fig. 12

Description:

Test is lenticular with a very deep and narrow umbilicus. Periphery of the initial volutions is rounded, in the final one or one and a half tour it is subangular. Sides of the last half tour are obviously convex above umbilicus and it is depressed towards the tip. There are 4 volutions. Coiling of the first tour is endothyroid and continues its development as planispiral, involute. The height and width of the final 1.5 whorls are significantly large. Chomata are well developed. Wall is microgranular but since the wall can easly recrystallize, a lighter layer in the wall is distinct.

Dimensions:

Diameter (d): 0.598 mm

Width (w): 0.299 mm

Height of the last tour: 0.129 mm

w/d: 0.500

Wall thickness: 16 μm

Remarks:

This form is distinguished from *Pseudoendothyra concinna* by the convexity of its flanks and *Pseudoendothyra concinna* has more compressed test. It is different from

Pseudoendothyra sublimis and *Pseudoendothyra struvei* by its narrower and deeper umbilicus.

Stratigraphic distribution:

Specimens were found in the Upper Visean (Mikhailovsky).

Pseudoendothyra sp. 3

Pl. XXX, figs. 13-14

Description:

Test is small, lenticular and compressed laterally. Umbilical region is wide and deep. Periphery is angular in the last volution but it is well rounded in the initial ones. There are progressively developed 3.5 volutions. Coiling is planispiral and involute in the initial tours but the final half tour is evolute. Chomata may be present. Wall is microgranular, thin and contains a lighter layer.

Dimensions:

Diameter (d): 0.384-0.474 mm

Width (w): 0.171-0.209 mm

Height of the last tour: 0.095-0.074 mm

w/d: 0.441-0.446

Wall thickness: 8-11 μm

Remarks:

This form is smaller than *Pseudoendothyra sublimis* and it has deeper umbilicus. However, its umbilicus is shallower than the one in *Pseudoendothyra* sp. 2. It has more compressed test and smaller dimensions than *Pseudoendothyra struvei*.

Stratigraphic distribution:

Our specimens were found in the Upper Visean (Mikhailovsky).

Pseudoendothyra spp.

Pl. XXIX, fig. 10; Pl. XXX, figs. 8-10

Description:

Some specimens belong to the genus *Pseudoendothyra* that cannot be designated to a particular species were grouped as *Pseudoendothyra* spp. Their common feature is their wall structure and planispiral coiling.

Stratigraphic distribution:

Samples have been recovered from Upper Visean and Serpukhovian.

SUPERFAMILY PALAEOTEXTULARIACEA Galloway, 1933

FAMILY PALEOTEXTULARIDAE Galloway, 1931

Genus *Paleotextularia* Schubert, 1921

Type species: *Paleotextularia schellwieni* Galloway and Ryniker, 1930

Paleotextularia sp. 1

Pl. XXXI, figs. 1-2

Description:

Test is biserial. Aperture is simple. There are 4-5 pairs of flattened chambers. These chambers are separated by long and relatively straight septa. Chambers are slightly quadrangular. Wall is composed of two layers namely, microgranular or finely granular layer in the outer part, hyaline fibrious layer in the inner part.

Dimensions:

Height: 0.530-0.708 mm

Width of last chamber pair: 0.446-0.479 mm

Wall thickness: 46-51 μm

Remarks:

Paleotextularia sp. 1 differs from all speciemens of *Paleotextularia* that have been defined here, by its more flattened and wider chambers.

Stratigraphic distribution:

The stratigraphic distribution of *Paleotextularia* sp. 1 is Lower Serpukhovian.

Paleotextularia sp. 2

Pl. XXXI, fig. 3

Description:

Test is composed of biserially arranged chambers. Aperture is simple. Chambers are slightly convex and they are separated by relatively short and curved septa. Wall is composed of inner hyaline, outer microgranular or granular layer.

Dimensions:

Height: 0.420 mm

Width of last chamber pair: 0.369 mm

Wall thickness: 23 μm

Remarks:

Paleotextularia sp. 2 differs from all speciemens of *Paleotextularia* that have been defined here, by its smaller dimensions. It is different from *Paleotextularia* sp. 2 by its slightly convex chambers. *Paleotextularia* sp. 1 has more flattened chambers and more straight septa than *Paleotextularia* sp. 2.

Stratigraphic distribution:

The stratigraphic distribution of *Paleotextularia* sp. 2 is Upper Visean (Venevsky) and Lower Serpukhovian.

Paleotextularia sp. 3

Pl. XXXI, fig. 4

Description:

Biserially arranged 4 pairs of chambers have a very convex and globular shape. Aperture is simple. Septa are short and curved. Wall is composed of inner hyaline, outer microgranular or granular layer.

Dimensions:

Height: 0.709mm

Width of last chamber pair: 0.651 mm

Wall thickness: 29 μm

Remarks:

Paleotextularia sp. 3 differs from *Paleotextularia* sp. 1, 2 and 5 by its globular chambers. It is differentiated from *Paleotextularia* sp. 4 by its curved septa and height and width of chambers during growth.

Stratigraphic distribution:

The stratigraphic distribution of *Paleotextularia* sp. 3 is Lower Serpukhovian.

Paleotextularia sp. 4

Pl. XXXI, fig. 5

Description:

It is composed of biserially arranged 4 pairs of chambers. Chambers are very globular and they do not increase their height and width during growth. Form does not broaden. Chambers are divided by slightly curved septa. Aperture is simple. Wall is composed of two layers. The outer one is microgranular; the inner one is hyaline and fibrous.

Dimensions:

Height: 0.711 mm

Width of last chamber pair: 0.369 mm

Wall thickness: 36 μm

Remarks:

Paleotextularia sp. 4 differs from all speciemens of *Paleotextularia* that have been defined here such that its test does not broaden during growth. It is differentiated from *Paleotextularia* sp. 1, 2 and 5 by its more globular test.

Stratigraphic distribution:

The stratigraphic distribution of *Paleotextularia* sp. 4 is Upper Visean (Venevsky).

Paleotextularia sp. 5

Pl. XXXI, figs. 6-8

Description:

Biserially arranged 5 to 6 pairs of chambers are slightly convex to quadrangular in shape. Chambers are divided by slightly straight septa. Aperture is simple. Wall is composed of inner thin hyaline layer and outer thick, granular layer.

Dimensions:

Height: 0.423-0.909 mm

Width of last chamber pair: 0.219-0.539 mm

Wall thickness: 33-43 μm

Remarks:

Paleotextularia sp. 5 differs from *Paleotextularia* sp. 1 by less flatened chambers but chambers of other species except for *Paleotextularia* sp. 1 are more convex than chambers of *Paleotextularia* sp. 5.

Stratigraphic distribution:

The stratigraphic distribution of *Paleotextularia* sp. 5 is Lowe Serpukhovian.

Genus *Climacammina* Brady in Etheridge, 1873

Type species: *Textularia antiqua* Brady in Young and Armstrong, 1871

Climacammina sp.

Pl. XXXI, figs. 11-12

Description:

Biserially arranged chambers become uniserial during growth. Aperture is cribrate. Septa short and slightly curved. Wall is composed of inner hyaline layer and outer microgranular layer.

Dimensions:

Height: 0.737-1.028 mm

Width of last chamber: 0.288-0.490

Wall thickness: 35-40 μm

Remarks:

This form differs from *Cribrostumum* by initially biserial finally uniserial growth.

Stratigraphic distribution:

The stratigraphic distribution of *Paleotextularia* sp. 1 is from Venevsky to Lower Serpukhovian.

Genus *Paleobigenerina* Galloway, 1933

Type sepcies: *Paleobigenerina geyeri* (Schellwien, 1898)

Paleobigenerina sp.

Pl. XXXI, figs. 9-10

Description:

Test is formed by biserially to uniserially arranged chambers. Aperture is simple. Chambers are convex and they are divided by long and slightly convex septa. Wall is composed of 2 layers; outer one microgranular, inner one hyaline. .

Dimensions:

Height: 0.5582-0.615 mm

Width of last chamber: 0.209

Wall thickness: 17 μm

Stratigraphic distribution:

The stratigraphic distribution of this genus in the studied section is Upper Visean (Venevsky) and Serpukhovian.

Genus *Consobrinella* Mamet and Pinard, 1990

Type species: *Paleotextularia consobrina* Lipina, 1948

Consobrinella sp. 1

Pl. XXXII, figs. 1-5

Description:

Test is composed of 3-4 pairs of biserially arranged chambers. Chambers are slightly convex and divided by long and slightly curved septa. Aperture is simple. Wall is composed of only one agglutinated layer.

Dimensions:

Height: 0.178-0.340 mm

Width of last chamber pairs: 0.117-0.341mm

Wall thickness: 9-22 μm

Remarks:

Consobrinella sp. 1 differs from *Consobrinella* sp. 2 by less convex chambers and shape of septa. It is differentiated from *Consobrinella* sp. 3 by more widening in the test.

Stratigraphic distribution:

In the studied section, the only one specimen of *Consobrinella* sp. 1 has been recovered from Upper Visean and Serpukhovian.

Consobrinella sp. 2

Pl. XXXII, fig. 6, 9

Description:

Chambers are arranged biserially arranged. They are highly convex. Septa are short, strongly curved and points are nodular. Aperture is simple. Wall is agglutinated.

Dimensions:

Height: 0.358 mm

Width of last chamber: 0.273 mm

Wall thickness: 16 μm

Remarks:

Consobrinella sp. 2 differs from *Consobrinella* sp. 3 by strongly convex chambers and nodular points of septa. Larger dimensions, less number of chambers and widening of its test are other criteria distinguishing it from *Consobrinella* sp. 3

Stratigraphic distribution:

In the studied section the specimens of *Consobrinella* sp. 2 have been recovered from Upper Visean.

Consobrinella sp. 3

Pl. XXXII, figs. 7-8

Description:

Test is small and formed by biserially arranged 3-4 pairs of chambers. Chambers are convex and they are divided by long and curved septa. Aperture is simple. Wall is agglutinated.

Dimensions:

Height: 0.245-0.256 mm

Width of last chamber: 0.162-0.163 mm

Wall thickness: 10-14 μm

Remarks:

Consobrinella sp. 3 is differentiated from *Consobrinella* sp. 1 by its convex chambers and more compressed test. It differs from *Consobrinella* sp. 2 by its smaller dimension and shape of septa.

Stratigraphic distribution:

In the studied section, specimens of *Consobrinella* sp. 3 have been recovered from the Mikhailovsky.

Consobrinella spp.

Description:

Individuals having agglutinated wall, biserially arranged chambers and simple aperture have been grouped under *Consobrinella* spp. since they cannot be assigned to a specific species of this genus.

Stratigraphic distribution:

The stratigraphic distribution of this genus is between Middle Visean to Serpukhovian (Mamet and Pinard, 1990). The specimens foud in the studied section of have been recovered from Upper Visean and Serpukhovian.

Genus *Koskinobigerina* Eickhoff, 1968

Type species: *Koskinobigerina breviseptata* Eickhoff, 1968

Koskinobigerina sp. 1

Pl. XXXII, fig. 10

Description:

Test is compressed and aligned with biserially to uniserially arranged chambers. Aperture is cribrate and they can be observed not only at the end but also in all

uniserial chambers. Chambers are slightly convex and there are 3 biserially arranged chamber pairs, 3 uniserial chambers. Chambers are convex and divided by short and curved septa. Wall is composed of an agglutinated layer.

Dimensions:

Height: 1.368 mm

Width of last chamber: 0.435 mm

Wall thickness: 39 μm

Remarks:

Koskinobigerina sp. 1 differs from other specimens of *Koskinobigerina* by its aligned test and higher number of chambers.

Stratigraphic distribution:

In the studied section, the specimen of *Koskinibigerina* sp. 1 has been recovered from Lower Serpukhovian.

Koskinobigerina? spp.

Pl. XXXII, figs. 11-13

Description:

Chambers arranged biserially first, uniserially at the end. Aperture is cribrate. Septa are short and curved. Wall is composed of only one agglutinated layer.

Remarks:

The transition from biserial part to uniserial part cannot be well defined in the specimens found in our study. So, this form is named with a question mark in the present study.

Stratigraphic distribution:

The stratigraphic distribution of *Koskinibigerina*? spp is Upper Visean and Serpukhovian.

Genus *Koskinotetktularia* Eickhoff, 1968

Type species: *Koskinotetktularia cribriformis* Eickhoff, 1968

Koskinotextularia sp.

Pl. XXXII, figs. 14-17

Description:

Test is biserial through. Aperture is cribrate. There are 2-3 visible pairs of chambers. Chambers are convex and divided by short and curved septa. Wall is composed of an agglutinated layer.

Dimensions:

Height: 0.394-0.463 mm

Width of last chamber pair: 0.216-0.305 mm

Wall thickness: 17-21 μm

Remarks:

Koskinotextularia sp differs from all specimens of *Koskinobigerina* by a biserial growth.

Stratigraphic distribution:

The stratigraphic distribution of this genus is from Middle Visean to Lower Serpukhovian. In the studied section it has been recovered from Upper Visean and Serpukhovian.

SUPERFAMILY TETRATAXACEA Galloway, 1933

FAMILY TETRAYAXIDAE Galloway, 1933

Genus *Tetrataxis* Ehrenberg, 1854

Type species: *Tetrataxis conica* Ehrenberg, 1854

Tetrataxis sp.

Pl. XXXI, fig. 13

Description:

Test is trochospiral, multilocular. Volutions are divided approximately 3-4 chambers. There is an cavity in the umbilical region. Wall is two layered. Inner one is microgranular outer one is hyaline.

Dimensions:

Height: 0.234 mm

Basal diameter: 0.441 mm

Wall thickness: 25 μm

Remarks:

The specimens of the genus *Tetrataxis* is differentiated from specimens of the genus *Valvulinella* by its double layered wall structure and absence of vertical partitions.

Stratigraphic distribution:

The stratigraphic distribution of *Tetrataxis* sp. is from Lower Carboniferous (Tournasian-Visean) to the Upper Carboniferous Namurian, Moscovian) (Loeblich and Tappan, 1988). Our specimens of this genus is from the Upper Visean.

Unidentified Genus 1

Pl. XXXIII, figs. 1-9

Description:

Test is discoidal. Umbilical depression is marked and mostly deep and wide. Coiling is initially skewed then, oscillatory to planispiral and evolute. Height of the

tours increases progressively but rapidly.There four to six volutions. Wall is thick and granular.

Remarks:

Several axial and oblique specimens were found belonging to Undentified Genus 1. This genus resembles to the genus *Eblanaia* in terms of evolute and oscillatory to planispiral coiling, development of septa and secondary deposits. However in this genus differentiation of wall can not be well identified although in some individuals a hyaline layer(?) is hardly observed. But, this may be the result of diagenesis so may not be a real hyaline wall. In addition, stratigraphic distribution of the genus *Eblanaia* is Upper Tournaisian to Lower Visean (Conil and Lys, 1977) which corresponds to a stratigraphically lower level.

Stratigraphic distribution:

The stratigraphic distribution of Unidentified Genus 1 is Upper Visean (Mikhailovsky).

Unidentified Genus 2

Pl. XXXIII, figs. 10,12

Description:

Coiling is planispiral. There four to five volutions that increase its height progressively. Septa are not well developed in the initial volutions instead, psudosepta and pseudochambers exist. In the later volutions septa are well developed and they are thicker than the wall. Secondary deposits may be present and they can be observed in equatorial section. Wall is microgranular.

Remarks:

This genus resembles to the genus *Septabrunsiina* such that it has pseudosepta and pseudochambers in the initial volutions and wall is undifferentiated and microgranular. Although in the definition of this genus the number of chambers is not mentioned, when compared to the illustrations of the specimens, Unidentified Genus 2 has much more chambers than *Septabrunsiina*. In addition, *Septabrunsiina* belongs to stratigraphically lower levels, from Fammenian to Lower Visean (Conil and Lys, 1977).

Stratigraphic distribution:

The stratigraphic distribution of Unidentified Genus 2 is Upper Visean (Mikhailovsky).

Unidentified Genus 3

Pl. XXXIII, figs. 11

Description:

Coiling is planispiral. There 2.5-3 volutions. Chambers are convex and divided by long and inclined septa. There are no supplementary deposits. Wall is granular.

Remarks:

This genus resembles to the genus *Endothyra* however, its coiling is more regular and wall is granular. In addition, this genus does not include secondary deposits. Granular wall structure is similar to that of the family Tournayellidae.

Stratigraphic distribution:

The stratigraphic distribution of Unidentified Genus 3 is Upper Visean (Mikhailovsky).

Unidentified Genus 4

Pl. XXXIII, fig. 14

Description:

Test is coiled. Cribrate aperture is obvious. Wall is microgranular.

Remarks:

Any similar form can not be found in the literature but only one specimen is found in the studied stratigraphic section.

Stratigraphic distribution:

Only one specimen of this genus can be found and it is from the Upper Visean (Mikhailovsky).

Unidentified Genus 5

Pl. XXXIII, fig. 15

Description:

Test is formed an undivided tubular chamber. Coiling is planispiral through the ontogenesis. Secondary deposits are well develop in the form of nodes. Wall is dark and microgranular.

Remarks:

This form resembles to the genus *Eotournayella* in terms of the expansion of spire however, *Eotournayella* does not have secondary deposits and sometimes pseudochambers can be developed. In the Unidentified Genus 5 basal deposits are markedly well developed and they can be observed also on the wall of the final tour. Other genera with supplementary deposits of the subfamily Tournayelidae have absolutely chambers or pseudochambers. In addition wall structure of this form is different from Tournayellids, it is microgranular.

Stratigraphic distribution:

Only one specimen is found in the stratigraphic section and it the is from Upper Visean (Mikhailovsky).

Unidentified Genus 6

Pl. XXXIII, figs. 16-17

Description:

Coiling is planispiral and involute. In the initial tours, coiling is skewed and in the last tour or last two tours it is nearly planispiral. Periphery of the test is rounded and umbilical region is wide and shallow but remarkable. In the initial tours septa can not be observed but later they are present. Wall is microgranular or granular.

Stratigraphic distribution:

The stratigraphic distribution of this genus in the studied section is from the Upper Visean (Mikhailovsky).

Unidentified Genus 7

Pl. XXXIII, fig. 18

Description:

Test is small and bilocular. is probably planispiral. Wall is microgranular.

Remarks:

This form may resemble to the genus *Pseudoammodiscus* or *Ammovertella* but, the zigzag growth of Ammovertella can not be identified.

Stratigraphic distribution:

Only one specimens can be found in the stratigraphic section and it is from the Upper Visean (Mikhailovsky).

CHAPTER 6

DISCUSSIONS AND CONCLUSIONS

In this study, Upper Visean – Serpukhovian boundary beds were examined with a micropaleontological and sequence stratigraphical approach. 59,61 m thick stratigraphic section was measured in the Aziziye Gediği and Oruçoğlu formations of the Aladağ Unit which are mainly composed of limestone and partly sandstone. With this, study foraminiferal content, biostratigraphy, microfacies, depositional environments and cyclicity of Upper Visean-Serpukhovian deposits in Pınarbaşı (Eastern Taurides) were established (Figure 6.1).

The Visean-Serpukhovian boundary is defined between the Russian Venevsky and Taurrsky Horizons and Brigantian and Pendelian or Namurian substages of the Western Europe. However, in 2008 this boundary is located within the the Brigantian substage with the first evolutionary appearance of the coodont *L. ziegleri.* But this has not been voted yet in the subcommision on Carboniferous of the International Commission of stratigraphy (Richards et al., 2010) and many workers are still accept the position of the boundary between the Brigantian and Namurian substages. Since the decision of the location of boundary has not certainly been voted, in this thesis the Visean-Serpukhovian boundary is placed between the Venevsky and Taurrsky Russian Horizons and Brigantian-Namurian substages of Western Europe.

In order to detect Visean-Serpukhovian boundary in the studied section biostratigraphy and chronostratigraphy are constructed based on the association and distribution of foraminifera.

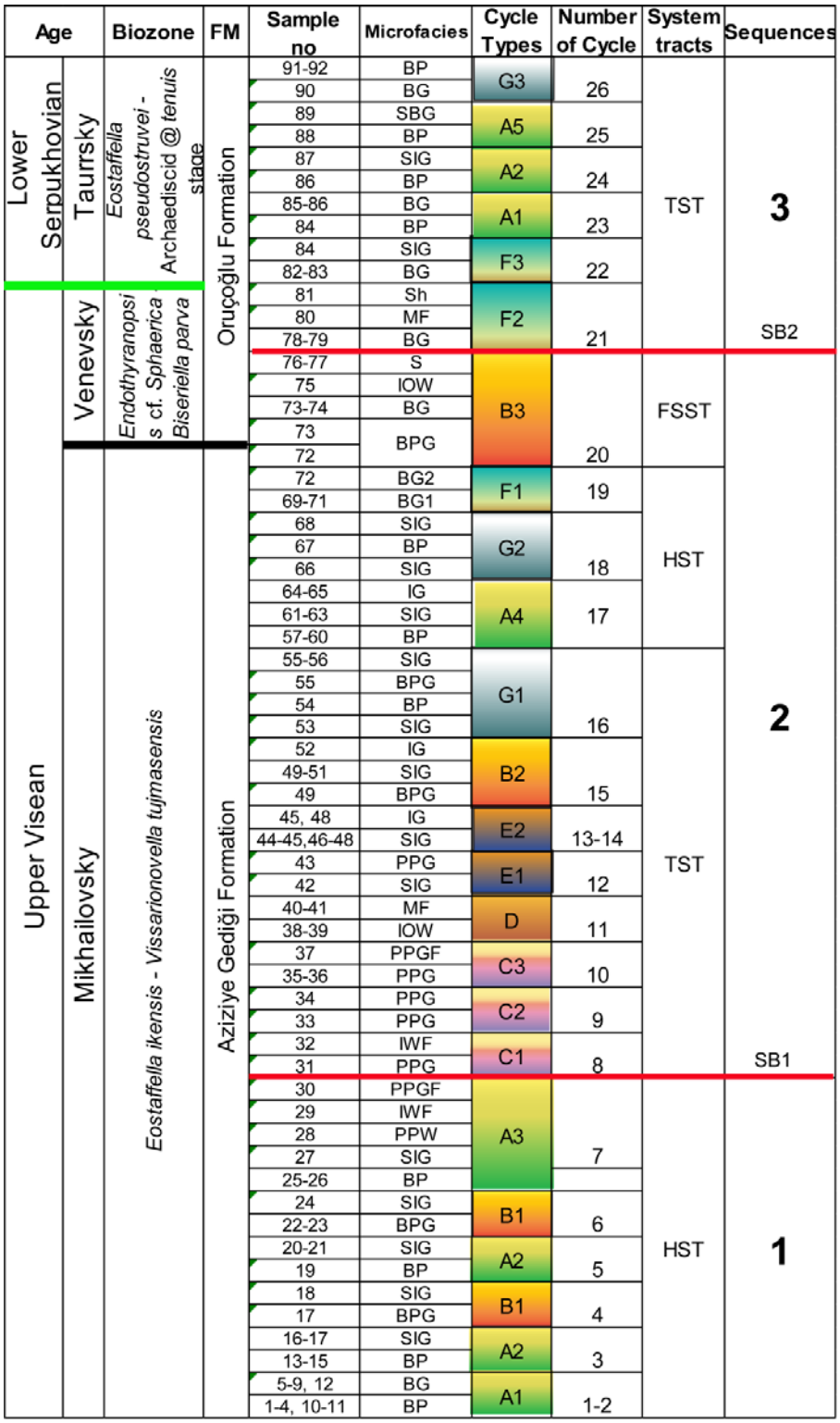

Figure 6.1: Summary table illustrating age, biozones, Formations, microfacies, cycles, system tracts, sequences and sequence boundaries.

To be able to recognize foraminifera a detailed taxonomic work was carried out based on some taxonomical criteria namely, wall structure, diameter, width and form ratio (width/diameter) of test, shape of the umbilical region and periphery, type of coiling, number of volutions and chambers, presence of secondary deposits, shape of chambers, septa and secondary deposits. 145 species belonging to 52 genera and 7 undetermined genera were described in this study. These species were assigned to 8 superfamilies namely; Parathuramminacea, Earlandiacea, Archaediscacea, Biseriamminacea, Endothyracea, Fusulinacea, Paleotextulariacea and Tetrataxacea. Based on the distribution, the first appearance and the last appearance of these taxa three biozones were determined along the studied section. These biozones are *Eostaffella ikensis – Vissarionovella tujmasensis* Zone, *Endothyranopsis* cf. *sphaerica – Biseriella parva* Zone and *Eostaffella pseudostruvei* – Archaediscid @ *tenuis* stage Zone and they correspond to the Russian Mikhailovsky, Venevsky and Taurssky Horizons respectively (Figure 6.1).

In order to understand the depositional history and sedimentary cyclicity of the studied area a detailed microfacies analysis was carried out. Vertical evolution of the microfacies within the studied section reveals the depositional history of the area and a conceptual depositional model was proposed. 3 main depositional environments were determined namely open marine, bioclastic shoal or bank, and tidal flat environments and 3 facies associations were proposed such as open marine facies, bioclastic shoal facies and tidal flat and associated facies. 12 major microfacies and 11 sub-microfacies types were interpreted. Open marine facies are represented by bioclastic packstones. Three sub-microfacies are able to deposit in the open marine environment namely, bioclastic packstone with equally distributed skeletal grains, crinoidal-foraminiferal-pelloidal packstone and crinoidal-foraminiferal packstone with current oriented grains. Shoal facies are composed of the bioclastic packstone to grainstone, bioclastic grainstone, skeletal-intraclast grainstone, intraclastic grainstone and sandy bioclastic grainstone. The bioclastic grainstone has two sub-microfacies which are crinoidal-pelloidal-foraminiferal grainstone and bioclastic grainstone with equally distributed

skeletal grains. The skeletal-intraclast grainstone has three submicrofacies namely; skeletal-intraclast grainstone with some micritized skeletal grains, skeletal-intraclast grainstone with abundant skeletal grains and dark clasts and intraclast – crinoidal foraminiferal grainstone. Tidal flat and associated facies is represented in lagoons and ponds by pelloidal packstone to wackestone; wackestone-mudstone and shale. Wackestone-mudstone is made up of three submicrofacies namely; intraclastic wackestone with ostracods, mudstone with fenestral fabric and intraclastic (dark clast) wackestone with fenestral fabric. In channels pelloidal grainstone or packstone to grainstone including dark clast was deposited. Other facies types of the tidal flat environment are pelloidal packstone to grainstone with fenestral fabric and sandstone.

Since depositional environments are affected in sea level fluctuations, repetitive rises and falls of sea level cause cyclic sedimentation. Based on the vertical association of microfacies, 26 cycles were interpreted in the studied section. Based on the stacking patterns eleven type (A-G) and nineteen sub-types of cycles were identified in the measured section (Figure 6.1). A type cycles are mainly characterized by open marine and shoal facies. This cycle types starts with bioclastic packstone of open marine environment and capped by grainstones of shoal environment. Only, A3 type cycle is capped by the wackestones and grainstone of tidal flat environment. B type cycles are characterized by bioclastic packstone to grainstone at lower, skeletal-intraclast grainstone or intraclastic grainstone at the upper part. B3 type cycle is capped by sandstone as distinct from the other B type cycles. C type cycles are characterized by pelloidal grainstone or pelloidal packstone to grainstone including dark clasts at the bottom. The shallowing trend is indicated by either the abundance of dark clasts or the fenestral fabrics. D types of cycle is mainly represented by wackestone and mudstone microfacies. It starts with mudstone with fenestral fabric and capped by the intraclastic wackestone with ostracods. E type cycles start with skeletal intraclast grainstone capped by either pelloidal grainstone or intraclastic grainstone. F types cycles are mainly characterized by the alternation of bioclastic grainstone of the shoal environment or evolve vertically into mudstone with fenestral fabric and shale. G type

cycles show a deepening trend first then they shallow upwards. The characterizing feature of G type cycles is that they starts with bioclastic grainstones, they deepen with bioclastic packstone or packstone to grainstone and they shallow with skeletal intraclast grainstone.

These high frequency sedimentary cycles are the result of glacioestasy driven by Late Paleozoic Gondwanan glaciation. In addition, Carboniferous is well known with cyclic sedimentation and high frequency cycles are the result of both glacioeustasy and changes of the Earth's orbital parameters. Duration of cycles in this study is approximately 117 ky which can be the result of Milankowitch eccentricity. The reason why duration of cycles in our study is not exactly 100 ky can be related with the nature of cycles described in the present study. There may be hidden cycles beyond our resolution and they may not mistakenly be noticed.

Stacking patterns of cycles are used to determine the sequence stratigraphic framework. Three sequences and two sequence boundaries were detected in the measured section. The first sequence was in the Mikhailovsky horizon and it only consists of the highstand system tracts. Second sequence which was interpreted in the Upper Mikhailovsky an Lower Venevsky horizons and is formed by the transgressive system tracts, highstand system tracts and falling stage system tract. Third sequence that was interpreted in the Upper Venevsky and Lower Serpukhovian and is characterized by only transgressive system tract deposits since the upper limit of the stratigraphic section is within the third system tract (Figure 6.1).

The genetic units and chronostratigraphic units, which are sequence boundaries and biozones respectively, were not coincident but, lithostratigraphic units and some of the chronostratigraphic units were coincident such that Aziziye Gediği Formation ends at the upper limit of the Mikhailovsky horizon represented by *Eostaffella ikensis-Vissarionovella tujmasensis* zone and Oruçoğlu Formation starts at the lower limit of the Venevsky horizon represented by the *Endothyranopsis* cf. *sphaerica-Biseriella parva* zone (Figure 6.1).

Global sea level chart of Haq and Schutter (2008) indicates a sea level fall in the latest Visean and a relative rise between latest Visean and earliest Serpukhovian. This trend is also observed in the studied section such that the sequence boundary corresponds to the uppermost part of the Venevsky Horizon. Deposits of the rest of the Venevsky Horizon and Serpukhovian stage in the measured section belong to the transgressive stand system tract corresponding to the rise of relative sea level (Figure 6.1).

This thesis delineates the Visean-Serpukhovian boundary by calcareous foraminifera and comprises a very detailed taxonomic work on late Visean to Early Serpukhovian foraminifers. For the first time a meter scale cyclicity study on the Lower Carboniferous of the Aladağ Unit in Eastern Taurides was interpreted with this thesis.

REFERENCES

Adams, A.E., Horbury, A.D., Ramsay, A.T.S., 1992. Significance of palaeoberesellids (Chlorophyta) in Dinantian sedimentation, UK. Lethaia, 25,375-382. *In*: Rodríguez-Martínez, M., Reitner, J., 2010. Micro-framework reconstruction from peloidal-dominated mud mounds (Viséan, SW Spain). Facies, 56, 139-156.

Ahmad, A.H.M., Bhat, G.M., Khan, M.H.A., 2006. Depositional environments and diagenesis of the Kuldhar and Keera Dome carbonates (Lat Bathonian-Early Callovian) of western India. Jurnal of Asian Earth Sciences, 27, 765-778.

Aisenverg, D.E., Brazhnikova, N.E., Vassilyuk, N.P., Reitlinger, E.A., Fomina, E.V., Einor, O.L., 1979. The Serpukhovian stage of the Lower Carboniferous of the USSR. *In:* Wagner, R.H., Higgins, A.C., Meyen, S.V. (eds.): The Carboniferous of the USSR, Yorkshire Geological Societey, Occasional Publication no: 4, 49-59.

Aksay, A., 1980. Toroslarda fasiyes yönünden farklı bir Alt Kabonifer istifi (Aladağ Bölgesi). Türkiye Jeoloji Kurumu Bülteni, c. 23, 193-199.

Al-Tawil, A., Read, J.F., 2003. Late Mississippian (Late Meramecian-Chesterian) glacio-eustatic sequence development on an active distal foreland ramp, Kentucky, U.S.A. *SEPM Special Publication* 78, AAPG Memoir 83, 35-55.

Altıner, D., 1981. Recherces stratigraphique et micropaléontologique dans le Taurus Oriental au NW de Pınarbaşı (Turquie). Theses Universite de Geneve, No 2005, Geneve, 450 pp.

Altıner, D., Savini, R, 1995. Pennsylvanian foraminifera and biostratigraphy of the Amazonas and Solimoes basins (North Brazil). Revue de Paleobiologie, 14 (2), 417-453.

Altıner, D., Özgül, N., 2001. Paleoforams 2001; International Conference on Paleozoic Benthic Foraminifera; Carboniferous and Permian of the allochthonous terranes of the Central Tauride Belt, Southern Turkey. *Guide Book*. 35 p.

Altıner, D., Yılmaz, İ. Ö., Özgül, N., Akçar, N., Bayazıtoğlu, M., Gaziulusoy, Z E., 1999. High-resolution sequence stratigraphic correlation in the Upper Jurassic (Kimmeridgian) - Upper Cretaceous (Cenomanian) peritidal carbonate deposits (Western Taurides, Turkey). Geological Journal, 34/1-2, 139-158.

Amirshahkarami, M., Moghaddam, H.V., Taheri, A., 2007. Sedimentary facies and sequence stratigraphy of the Asmari Formation at Chaman-Bolbol, Zagros Basin, Iran. Jurnal of Asian Earth Sicences, 29, 947-959.

Armella C., Cabaleri, N., Leanza, H.A., 2007. Tidally dominated, rimmed-shelf facies of the Picún Leufú Formation (Jurassic/Cretaceous boundary) in southwest Gondwana, Neuquén Basin, Argentina. Cretaceous Research, 28, 961-979.

Atakul, A., 2006. Lower-middle Carboniferous boundary in central Taurides, Turkey (Hadim area): paleontologıcal and sequence straıgraphıcal approach. M. S. Thesis, Middle East Technical University, Ankara, Turkey, 202 pp.

Atakul-Özdemir, A., Altıner, D., Özkan-Altıner, S., Yılmaz İ.Ö., 2011. Foraminiferal biostratigraphy and sequence stratigraphy of across the mid- Carboniferous boundary in the Central Taurides, Turkey. Facies, 57, 705-730.

Athersuch, J., Strank, A.R.E., 1989. Foraminifera and Ostracods from the Dinantian Woodbine Shale and Urswick Limestone, South Cumbria, U.K. Journal of Micropalaeontology, 8, 9-21.

Austin, R.L., Conil, R., Rhodes, F.H.T., 1973. Recognition of the Tournaisian-Visean boundary in the north America and Britain. Annales de la Société Géologique de Belgique, 96, 165-188.

Basan, P.B., 1973. Aspects of sedimentation and developement of a carbonate bank in the BarracudaKeys, south Florida. Jurnal of Sedimentary Research, 43, 42-53. In Pratt, B.R., James, N.P., 1986. The St. George Group (Lower Ordovician) of western Newfoundland: tidal flat island model for carbonate sedimentation in shallow epeiric seas. Sedimentology, 33, 313-343.

Bauer, J., Kuss, J.B., Steuber, T.B., 2002. Platform Environments, Microfacies and Systems Tracts of the Upper Cenomanian - Lower Santonian of Sinai, Egypt. Facies, 47, 1-26.

Blumenthal, M. M. 1944. Bozkır güneyinde Toros sıradağlarının serisi ve yapısı. İstanbul Üniversitesi Fen Fakültesi Mec., V. B. 9, 95-125.

Blumenthal, M. M. 1947. Beyşehir-Seydişehir hinterlandındaki Toros dağlarının jeolojisi. Maden Tetkik Arama Enst. Ankara, seri D, 2, 242 p.

Blumenthal, M. M. 1951. Batı Toroslarda Antalya ardı ülkesinde jeolojik araştırmalar. Maden Tetkik Arama Enst. Ankara, seri D, 5, 194 p.

Blumenthal, M.M. 1956. Karaman Konya Havzası Güney batısında Toros Kenar Silsileleri ve Şist Radyolarit Formasyonu Stratigrafi Meselesi. Maden Tetkik Arama Enst. Derg., 48, 1-36.

Brady, H.B., 1873. On *Archaediscus karreri*, a new type of Carboniferous foraminifera. *Annals and Magazine of Natural History*, series 4, 12, 286-290.

Brazhnikova, N.E., 1962. Quasiendothyra and close forms from the Lower Carboniferous of the Donetsk Basin and other regions of the Ukraine. Akad. Nauk Ukrainsk. SSR, Inst. Geol. Nauk,ser. Strat. Pal., 44, 36-37 (in Russian).

Brazhnikova, N.E., Vakarchuk, G.l., Vdovenko, M.V., Vinnichenko, L.V., Karpova, M.A., Kolomiets, Ya. I., Potievskaya, P.D., Rostovtseva, L.F., and Shevchenko, G.D. 1967. Microfaunal reference horizons of the Carboniferous and Permian deposits of the Dniepr Donets Depression. Akademia Nauk Ukrainskoi SSR, Institut GeoloQicheskii Nauk "Dumka" Kiev, 224 pp. (In Russian with English, French and Germany summaries).

Brazhnikova, N.E., Vassilyuk, N.P., Gorak, S.V., Dunaeva, N.N., Kireeva, G.D., Kotchetkova, N.M., Popov, A.B., Potievskaya, P.D., Reitlinger, E.A., Rotai, A.P., Sergeeva, M.T., Teteryuk, V.K., Fissunenko, O.P., Furduy, R.S., 1979. The Lower Carboniferous-Middle Carboniferous boundary. *In:* Wagner, R.H., Higgins, A.C., Meyen, S.V., Einor, O.L. (eds.): The Carboniferous of the USSR, Yorkshire Geological Societey, Occasional Publication no: 4, 61-81.

Brenckle, P.L., 1990. Foraminiferal division of the Lower Carboniferous / Mississippian in North America. Courier Forsch.-Inst. Senckenberg, 130, 65-78.

Brenckle, P.L., 2004. Late Visean (Mississippian) Calcareous microfossils from the Tarim Basin of Western China. Journal of Foraminiferal Research, 34 (2), 144-164.

Brenckle, P.L. and Grelecki, C.J., 1993. Type Archaediscacean Foraminifers (Carboniferous) from the former Soviet Union and Great Britain, with a description of computer modeling of Archaediscacean coiling, *Cushman Foundation for Foramineral Research,* Special Publication. no.30, 1-59.

Brenckle, P., Lane, H.R., Collinson, C., 1974. Progress toward reconciliation of Lower Mississippian conodont and foraminiferal zonations. Geology, 2 (9), 433-436.

Brenckle, P.L., Marchant, T.R., 1987. Calcareous microfossils, depositional environments and correlation of the Lower Carboniferous UM Bogma Formation at Gebel Nukhul, Snai,Egypt. Jurnal of Foraminiferal Research, 17 (1), 74-91.

Brunn, J.H., Dumont, J.H., Graciansky, P. Ch de,Gutnic, M., Juteau, Th., Marcoux, J., Monod, O., Posson, A., 1971. Outline of the Geology of Western Taurids geology and history of Turkey. Petroleum Exploration Society of Libya, Tripoli, 25-255.

Brunn, J.H., Argyriadis, L., Marcoux, J., Poisson, A., Ricou, L.E., 1973. Antalya Ofiyolit naplarının orijini lehine ve aleyhine kanıtlar. Cumhuriyetin 50. Yılı Yerbilimleri Kong. Tebliğleri, 58-69, Ankara.

Bykova, E.V., 1955. Devonian foraminifera and radiolaria of the Volga-Ural district and central Devonian field, and their significance for stratigraphy. Trudy Vsesoyuznogo Neftyanogo Nauchno-issledovatel'skogo Geologorazvedochnogo instituta, 87, 5-190.

Chamley, H., Proust, J.N., Mansy, J.L., Boulvain, F., 1997. Diagenetic and palaeogeographic significance of clay, carbonate and other sedimentary components in the middle Devonian limestones of western Ardenne, France. Palaeogeography, Palaeoclimatology, Palaeoecology, 129, 369-385.

Chernysheva, N.E., 1941. A new genus of foraminifers from the tournaisan deposits of the Urals. Dokl. Akad. Nauk. SSSR 32 (1), 69-70.

Chernysheva, N.E., 1948. Some new species of foraminifera from the Visean of the Makarov District. Academia Nauk SSSR, Trudy Geologicheskii Institute 62. 246-250 (in Russian).

Colombié, C., Strasser A., 2005. Facies, cycles, and controls on the evolution of a keep-up carbonate platform (Kimmeridgian, Swiss Jura). Sedimentology, 52, 1207-1227.

Conil, R., 1963. Interprétation micropaléontologique de quelques sondages de Campine. Bulletin Société belge Géologie, Paléontologie et Hydrogeologie, 72, 123–135.

Conil, R., 1980. Note sur quelques foraminifères du Struntien et du Dinantien d' Europe Occidentale. Annales de la Société Géologique de Belgique, 103, 43-53.

Conil, R., Longerstaey, P.J., Ramsbottom, W.H.C., 1979. Matériaux pour l' étude micropaléontologique du Dinantian de Grand e-Bretagne. Mém. Inst. Géol. Univ. Louvin, 30, 187 pp.

Conil, R., Lys, M., 1964. Matériaux pour l' étude micropaléontologique du Dinantien de la Belgique et de la France (Avesnois). Mém. Inst. Géol. Univ. Louvin, 22, 1-335.

Conil, R., Lys, M., 1977. Les transgressions Dinantiennes et leur influence sur la dispersion et l' évolution des Foraminifèrs. Mém. Inst. Géol. Univ. Louvin, 29, 9-55.

Conil, R., Pirlet, H., 1963. Sur quelques foraminifères charactéristiques du Viséen supèrieur de la Belgique (Bassin de Namur et de Dinant). Bulletin Societé belge Géologie, Paléontologie et Hydrogeologie, 72, 183-197.

Conil, R., Pirlet, H., 1970. Le calcaire Carbonifère du Synclinorium de Dinant et le sommet du Fammennien, *Colloque sur la stratigraphie du Carbonifère*. Congrès et Colloques de l'Université de Liège, 55, 47-63.

Cózar, P., 2002. Taxonomic value of the diaphanotheca/luminotheca in the classification of Lower Carboniferous endothyroid Foraminiferida; creation of two new species of *Pojarkovella*. Geobios, 34, 283-291.

Cózar, P., 2003. Foraminiferal fauna and zonation from the Lower Carboniferous of the Guadiato area (sw Spain): comparison with European and north African zonal schemes and their paleobiogeographical implications. *SEPM Special Publication* 78, AAPG Memoir 83, 155-169.

Cózar, P., 2004. Foraminiferal and algal evidence for the recognition of the Asbian/Brigantian Boundary in the Guadiato Area (Mississippian, southwestern Spain). Revista Espanola de Micropaleontologia, 36 (3), 367-388.

Cózar, P., Rodriguez, S., 2004. Pendleian (early Serpukhovian) marine carbonates from SW Spain: sedimentology, biostratigraphy and depositional model. Geological Journal, 39, 25–47.

Cózar, P., Somerville, H.E.A., Somerville, I.D., 2005. Foraminifera, calcareous algae and rugose corals in Brigantian (Late Visean) limestones in Ireland. Proceedings of the Yorkshire Geological Society, 55, 287-300.

Cózar, P., Somerville, I.D., Burges, I., 2008. New foraminifers in the Visean/Serpukhovianboundary interval of the Lower Limestone Formation, Midland Valley, Scotland. Jurnal of Paleontology, 82 (5), 906-923.

Cózar, P., Somerville, I.D., 2004. New algal and foraminiferal assemblages and evidence for recognition of the Asbian-Brigantian boundary in northern England. Proceedings of the Yorkshire Geological Society, 55, 43-65.

Cózar, P., Somerville, I.D., Mitchell, W.I., Medina – Varea, P., 2006. Correlation of Mississippian (Upper Visean) foraminiferan, conodont, miospore and ammonoid zonal schemes, and correlation with the Asbian – Brigantian boundary in northwest Ireland. Geological Journal, 41, 221-241.

Cózar, P., Vachard, D., 2001. Dainellinae subfam. nov. (Foraminiferida du Carbonifère inférieur), révision et nouveaux taxons. Geobios, 34(5), 505-526.

Cózar, P., Vachar, D., Somerville, I.D., Berkhli, M., Mediana-Varea, P., Rodriguez, S., Daid, I., 2008. Late Viséan-Serpukhovian foraminiferans and calcareous algea from the Adarouch region (central Morocco), North Africa. Geological Journal, 43, 463-485.

Cummings, R.H., 1955. New genera of foraminifera from the British Lower Carboniferous. Washington Acad. Sci. Journ., 45(1), 1-8.

Cushman, J., 1927. An outline of a reclassification of the foraminifera. Contrib. Cushman Lab. Foram. Research, vol. 3, no. 1, 105 p.

Çelik, Ö.F., Demir, N., Gürbüz, A., Bingöl, E., 2007. Siyah Aladağ Napı'nın stratigrafik ve tektonik özellikleri (Aladağlar, Doğu Toroslar). Hacettepe Üniversitesi Yerbilimleri Uygulama ve Araştırma Merkezi Dergisi, c. 18(2), 113-126.

Davydov, V., Wardlaw, B.R., Gradstein, F.M., 2004. The Carboniferous Period. *In*: Gradstein, F.M., Ogg, J.G., Smith, A.G. (eds.): A Geologic Time Scale 2004. Cambridge University Press, pp. 610.

Dain, L.G. and Grozdilova, L. 1953. Iskopaemye Foraminifery S.S.S.R.:Turneyellidy: Archedistsidy (Fossil foraminifera of the U.S.S.R.: Tournayellidae and Archaediscidae, Trudy Vsesesoyuznogo Neftyanogo Nauchnoissledovatel' skogo Geologorazvedochnogo Instituta (VNIGRI), ser. 74, 1-115.

Dean, W.T., Özgül, N., 1980. Orta Toroslarda Çaltepe Formasyonunun Bağdaşı (Hadim-Konya) yöresindeki yüzeylenmesinde bulunan Kambriyen trilobitleri. MTA Enstitüsü Dergisi, 92, 1-6.

Dean, W.T., Özgül, N., 1994. Cambrian rocks and faunas, Hüdai area, Taurus Mountains, southwestern Turkey. Bull. Ins. Roy. Sc. Nat. Belg., 64, 5-20.

Della Porta, G., Villa, E., Kenter, J.A.M., 2005. Foraminiferal distribution of fusulinida in a Bashkirian-Moscovian (Pennsylvanian)carbonate platform top (Cantabrian Mountins, NW Spain). Jurnal of Foraminiferal Research, 35, 344-367.

Demirkol, C., 1989. Pozantı-Karsantı-Karaisalı (Doğu Toroslar) arasında yer alan karbonat platformunun stratigrafisi ve jeolojik gelişimi. MTA Dergisi, 109, 33 – 44.

Demirtaşlı, E., 1967. Pınarbaşı – Sarız – Mağara civarının jeoloji raporu. Maden Tetkik ve Arama Enstitüsü, Derleme no: 1957, (yayınlanmamış).

Demirtaşlı, E., 1984. Stratigraphy and tectonic of the area between Silifke and Anamur, Central Taurus Mountains. *In:* Tekeli O. and Göncüoğlu M. C. (eds): Geology of the Taurus Belt. Mineral Research and Exploration Institute of Tukey Publication, 101-123.

Demirtaşlı, E., Çatal, E., Dil, N., Kırağlı, C., Salancı, A., 1978. Carboniferous of the Area Between Pınarbaşı and Sarız. Guide Book of Field Excursions of the Carboniferous Stratigraphy of Turkey. IUGS Subcom. Carboniferous Stratigraphy. Guidebook Field Excursion Carboniferous Stratigraphy, Ankara.

Demirtaşlı, E., 1979. Pınarbaşı, Sarız ve Tufanbeyli İlçeleri Arasında kalan Yörenin Jeolojisi: I:Ü.F.F.Min. ve Petr. Kürs., 30 sayfa. Yayınlanmamış, İstanbul.

Derville, P.H., 1931. Les Marbres du Calcaire carbonifere en Bas-Boulonnais. Imprimerie O. Boehm., Strasbourg, 322 pp.

Derville, P.H. 1952. A propos de Calcispheres (rectification). *Soc. Geol. France Compte Rendue Sommaire*, 236-237.

Dumont, J.F., Monod, O., 1976. Dipoyraz Dağ Masifinin Triyasik karbonatlı serisi) Batı Toroslar, Türkiye). MTA Dergisi, 87, 26-38.

Durkina, A.V., 1959. Foraminifera of the Lower Carboniferous deposits of the Timan-Pechora Province. Vsesoyuznogo Neftianogo Nauchno-Issledovatel'skogo Geologorazvedochnogo Instituta (VNIGRI). Mikrofauna SSSR 10, Trudy 136, 132-389 (in Russian).

Eichwald, E., 1860. Lethaea rossica on paleontologie de la Russie, 1, 1657 pp.

Einsele, G., Ricken, W., Seilacher, A., 1991. Cycles and events in stratigraphy. Springer-Verlag, 955 pp.

Emery, D., 1996. Historical perspective. *In*: Emery, D., Myers, K. (eds.): Sequence stratigrahy. Blackwell Science, 297 pp.

Esatoğlu, H., 2011. Foraminiferal paleontology, biostratigraphy and sequence stratigraphy of the Permian – Triassic boundary beds of the Bolkar Dağı (Central

Taurıdes, Turkey). M. S. Thesis, Middle East Technical University, Ankara, Turkey, 184 pp.

Etheridge, R., Jr. 1873. Notes on certain genera and species mentioned in the foregoing lists. *Scotland Geological Survey Memoir*, Explanation of Sheet 23, 93-107.

Ettenshon, F.R., Rice, C.L., Dever, G.R., Chesnut, D.R., 1984. Slade and Paragon Formations –New stratigraphic nomenclature for Mississippian Rocks along the Cumberland Escarpement in Kentucky. US. Geological Survey of America Bulletin, 1605B, 37 pp.

Fielding, C.R., Frank, T.D., Birgenheier, L.P., Michael, C.R., Jones, A.T., Roberts, J., 2008. Stratigraphic imprint of the Late Paleozoic ice age in eastern Australia: a record of alternating glacial and non glacial climate regime. Journal of the Geological Society, 165, 129-140.

Flügel, E., 2004. Microfacies of carbonate rocks: analysis, interpretation and application. Springer, 976 pp.

Fürsich. F.T., Wilmsen. M., Seyed-Emami. K., Schairer. G., Majidifard. M., 2003. Platform-basin transect of a Middle to Late Jurassic large scale carbonate platform system (Shotori Mountains, Tabas area, east-central Iran). Facies, 48, 171-198.

Gallagher, S.J., 1998. Controls on the distribution of calcareous foraminifera in the Lower Carboniferous of Ireland. Marine Micropaleontology, 34, 187-211.

Gallagher, S.J., Somerville, I.D., 2003. Lower Carboniferous (Late Viséan) Platform development and cyclicity in southern Ireland: foraminiferal biofacies and lithofacies evidence. Rivista Italiana di Paleontologia e Stratigrafia, 109, 159-171.

Gallagher, S.J., Macdermot, C.V., Somerville, I.D., Pracht, M., 2006. Biostratigraphy, microfacies and depositional environments of Upper Vise´an limestones from the Burren region, County Clare, Ireland. Geological Journal, 41, 61-91.

Galloway, J.J. and Harlton, B.H. 1928. Some Pennsylvanian foraminifera of Oklahoma with special reference to the genus *Orobias*. Journal of Paleontology, 2, 338-357.

Galloway, J.J. and Ryniker, C. 1930. Foraminifera from the Atoka formation of Oklahoma. *Oklahoma Geological Survey Circular*, 21, 1-36.

Ganelina, R.A., 1951. Eostaffellidae and Millerellidae of Visean and Namurian (stages of Lower Carboniferous) of western part of the Moscow basin. Trudy Vsesesoyuznogo Neftyanogo Nauchno-issledovatel'skogo. 154 *Geologorazvedochnogo Instituta (VNIGRI). Microfauna SSSR*, 56, 179-210 (in Russian).

Ganelina, R.A., 1956. Foraminifera of the Visean of the northwestern regions of the sub-Moscow Basin. Trudy VNIGRI (Microfauna of the U.S.S.R.), 8, 61-159. (in Russian).

Gibshman, N.B., Baranova, D.V., 2003. The foraminiferes *Janischewkina* and '*Millerella*', their evolutionary patterns and biostratigraphyc potential for the Visean-Serpukhovian boundary. *In*: Wrong, Th.E. (Ed.): Proceedings of the XVth International Congress on Carboniferous and Permian Stratigraphy (Utrecht): pp. 269-281.

Göncüoğlu, M.C., 1997. Distribution of Lower Paleozoic units in the Alpine Terranes of Turkey: paleogeographic constraints. *In*: Göncüoğlu, M.C., Derman, A.S. (eds.): Lower Paleozoic Evolution in northwest Gondwana, Turkish Assoc. Petrol. Geol., Spec. Publ., 3, 13-24.

Göncüoğlu, M.C., Çapkınoğlu, Ş., Gürsel, S., Noble, P., Tuhan, N., Tekin, U.K., Okuyucu, C., Göncüoğlu, Y., 2007. The Mississippian in the central and eatern Taurides (Turkey): constrains on the tectonic setting of the Tauride-Anatolide platform. Geologica Carpathica, 58 (5), 427-442.

Göncüoğlu, M.C., Göncüoğlu, Y., Kozur, H.W., Kozlu, H., 2004. Paleozoic stratigraphy of the Geyik Dağı Unit in the Eastern Taurides (Turkey): New age data and implications for Gondwanan evolution. Geologica Carpathica, 55 (6), 433-447.

Gradstein, F., Ogg, J., Smith, A., 2004. A Geologic Time Scale. Cambridge University Press, 589 pp.

Groves, J.R., 1988. Calcerous foraminifers from the Bashkirian stratotype (Midle Carboniferous, South Urals) and their significance for intercontinental correlations and the evolution of the Fusulinidae. Jurnal of Paleontology, 62, 368-399.

Groves, J.R.,Beason, S.R., 2006. Foraminiferal evidence for the age of the Mississippian Pella Formation (southwestern Iowa, USA). Journal of Foraminiferal Research, 36 (4), 379-388.

Groves, J.R., Larghi, C., Nicora, A., Rettori, R., 2003. Mississippian (Lower Carboniferous) microfossils from the Chios Mélange (Chios Island, Greece). Geobios, 36, 379-389.

Grozdilova, L.P., 1953. Arkhedistsidy (Archaediscidae). In: L.G., Dain and L.P., Grozdilova, Iskopaemye foraminifery S.S.S.R., turneiellidy i arkhedistsidy (Fossil foraminifers of the U.S.S.R., Tournayellidae and Archaediscidae). Trudy Vsesoyuznogo Neftyanogo Nauchno-Issle-dovatel'skogo Geologorazvedochnogo Instituta (VNIGRI), Novaya Seriya, publication 74, 65- 123.

Grozdilova, L.P. and Glebovskaia, E.M., 1948. Materials pertinent to the studies of the genus Glomospira and other representatives of the family Ammodiscidae in Viséan sediments of Makarov, Krasnokamsk, Kizel and Moskow districts. Akad. Nauk. SSSR, Trudy Inst. Geol. Nauk, 62, 145-149.

Grozdilova, L.P. and Lebedeva, N.S., 1954. Foraminifers from the Lower Carboniferous and Bashkirian stage of the Middle Carboniferous of the Kolvo-Vishera area. Trudy Vsesesoyuznogo Neftyanogo Nauchno-issledovatel'skogo 156 Geologorazvedochnogo Instituta (VNIGRI), *Microfauna S.S.S.R.*, sbornik 7, 81, 4-236 (in Russian).

Grozdilova, L.P. and Lebedeva, N.S., 1960. Foraminifera from the Carboniferous deposits of the western slope of the Urals and Timan, Trudy Vsesesoyuznogo Neftyanogo Nauchno-issledovatel'skogo Geologorazvedochnogo Istituta (VNIGRI). *Microfauna S.S.S.R.*, 150, 1-264 (in Russian).

Gutnic, M., Monod, O., Poisson, A., Dumont, J. F., 1979. Géologie des Taurides Occidentales (Turquie). Mémoires dela Sociéte geologique de France, 137, 1-112.

Haq, B., U., Hardenbol, J., Vail, P.R., 1987. Chronology of fluctuating sea levels since the Triassic. Science, 235, 1156-1167.

Haq, B., U., Schutter, S.R., 2008. A Chronology of Paleozoic Sea-Level Changes. Science, 322, 64-68.

Hecker, M.R., 2009. Major guide taxa for correlation of the Moscow and Donets Basins Dinantian successions with the type are (Belgium). In: PUCHKOV, V.N., (ed.), Carboniferous Type sections in Russia and Potential Global Stratotypes. Proceedings of the International Field Meeting "The historical type sections, proposed and potential GSSP of the Carboniferous in Russia". Southern Urals Session, Ufa-Sibai, 13-18 August 2009, Ufa Research Center: 198-201.

Hoare, R.D., Skipp, B., 1995. Calcareous microfossils from the Upper Mississippian (Chesterian) Maxville Limestone, southeastern Ohio. Journal of Paleontology, 69 (4), 617-624.

Horbury, A.D., Adams, A.E., 1996. Microfacies associations in Asbian carbonates: an example from the Urswick Limstone Formation of the southern Lake District, northern England. Geological Society of London, Special Publication, 107, 221-237.

Howchin, W., 1888. Additions to the knowledge of the Carboniferous Foraminifera. Royal Microsc. Soc. Jour., part 2, 533-545.

Hunt, D., Tucker, M.E., 1993. Sequence stratigraphy of carbonate shelves with an example from the mid-Cretaceous (Urgonian) of southeast France. *In*: Posamentier, H.W., Summerhayes, C.P., Haq, B.U., Allen, G.P. (eds.): Sequence Stratigraphy and Facies Associations. International Association of Sedimentologists, Special Publication 18, 307–341.

Hüneke, H.G., Joachimski, M., Buggisch, W.E., Lützner, H.J., 1991. Marine carbonate facies in response to climate and nutrient level: The Upper Carboniferous and Permian of central Spitsbergen (Svalbard). Facies, 45, 93-136.

Isbell, J.L., Miller, M.F., Wolfe, K.L., Lenaker, P.A., 2003. Timing of Late Paleozoic glaciation in Gonwana: was glaciation is responsible for the development of northern hemisphere cyclothems?. Geological Society of America Special Paper, 370, 5-24.

Işık, A., 1981. Nohutluk Tepe Alt Karbonifer istifinin foraminifer biyostratigrafisi (Aladağ Bölgesi, Doğu Toroslar). Türkiye Jeoloji Kurumu Bülteni c. 24, 79 – 84.

Joachimski, M.M., 1994. Subaerial exposure and deposition of shallowing upward sequences: evidence from stable isotopes of Purbeckian peritidal carbonates (basal Cretaceous), Swiss and French Jura Mountains. Sedimentology, 41, 805-824.

Kakizaki, Y., Kano, A., 2009. Architecture and chemostratigraphy of Late Jurassic shallow marine carbonates in NE Japan, western Paleo-Pacific. Sedimentary Geology, 214, 49-61.

Kobayashi, F., Altıner D., 2008. Carboniferous and Early Permian fusulinoideans in the Central Taurides, Turkey: biostratigraphy, faunal composition and comparison. Journal of Foraminiferal Research, 38, 59-73.

Krestovnikov, V.N. and Teodorovich, G.I., 1936. A new species of foraminifera of the genus *Archaediscus* from the middle Urals. Moskovskoye Obshchestva Ispytatelei

Prirody Bulletin, Otdelenie Geologii, 44, Geologicheskaya Seria No. 14 (1), 86-90 (in Russian).

Kulagina, E.I., Pazukhin, V.N., Nikolaeva, S.V., Kochetova, N.N., Zainakaeva, G.F., Gibshman, N.B., and Konovalova, V.A., 2009. Serpukhovian and Bashkirian Bioherm Facies of the Kizil Formation in the Southern Urals, in *Tipovye razrezy karbona Rossii i potentsial'nye global'nye stratotipy. Yuzhnoural'skaya sessiya. Materialy Mezhdunarodnogo polevogo soveshchaniya "Stratotipicheskie razrezy, predlagaemye i potentsial'nye TGSG karbona v Rossii. Ufa-Sibai, 13–18 August, 2009"* (Carboniferous Type Sections in Russia, Potential and Global Stratotypes. Southern Urals Session, Proc. Int. Field Meeting of the Int. Subcommission on Carboniferous Stratigraphy "The Historical Type Sections, Proposed and Potential GSSP of the Carboniferous in Russia," Ufa-Sibai, 13–18 avgusta, 2009 g.), Ufa: OOO Dizain Poligraf Servis, pp. 78–96.

Loucks, R.G., Sarg, J. F. (eds.) Carbonate Sequence Stratigraphy – Recent Developments and Applications. American Association of Petroleum Geologists Memoir, 57, p.545.

Lipina, O.A., Reitlinger, E.A., 1970. Stratigraphie zonale et Paléozoo-géographie du Carbonifère Inférieur d'après les Foraminiféres: Compte Rendu, v. 3, Sixth InternationalCongress of Carboniferous Stratigraphy and Geology, Sheffield, 1967, p. 1101-1111.

Lys, M., 1988. Biostratigraphie des dépots marine du Carbonifère et du Permien du sud-Tunisien, Micropaléontologie (foraminiféres) et paléobiogéographie. Bull. Centres Rech. Explr. – Prod. Elf- Aquitaine, Pau, 12 (2), 601-659.

Mackintosh, P.W., Robertson, A.H.F., 2012. Late Devonian–Late Triassic sedimentary development of the central Taurides, S Turkey: Implications for the northern margin of Gondwana. Gondwana Re

Makhlina, M.KH., 1996. Cyclic stratigraphy, facies and fauna of the Lower Carboniferous (Dinantian) of the Moscow Syneclise and Varonezh Anteclise. *In*:

Strogen, P., Somerville, I.D., Jones, G.LI. (eds.): Recent Advances in Lower Carboniferous Geology. The Geological Society, Special Publication, 107, 359-369.

Mamet, B., 1973. Microfacies du Viséen du Boulonnais (Nord, France). Revue de Micropaléontologie, 16 (2), 101-124.

Mamet, B., 1975. Viseidicus, un nouveau genre de Planoarchaediscinae (Archaediscinae [sic.] foraminiféres), Compte Rendu Sommaire des Séances de la Société Géologique de France, 1975, 48-49.

Mamet, B., Mikhailoff, N. and Mortelmans, G., 1970. La stratigraphie du Tournaisien et du Viséen inférieur de Landelies. Comparaison avec les coupes du Tournaisis et du baord nord du synclinal de Namur. Mémoir Societé belge Géologie, Paléontologie, Hydrogéologie, ser. in 8, 9, 81 pp.

Mamet, B., Pinard S., 1990. Note sur la taxonomie de petites foraminiféres du Paleozoique Superieur. Bulletin de la Société belge de Geologie , 99, 373-398.

Mamet, B., Pinard S., Armstrong, A.K., 1993. Micropaleontological Zonation (Foraminifers, Algae) and Stratigraphy, Carboniferous Peratrovich Formation, Southeastern Alaska. U.S. Geological Survey Bulletin 2031, 32 pp., 16 pl.

Manukalova-Grebeniuk, M.F., Ilina, M.T., and Serezhnikova, T.D., 1969. An Atlas of foraminifers from the Middle Carboniferous of the Dneiper-Donetz basin. Ministerstvo Geologii SSSR, Trudy Ukrainskii nauchro Issledovatel'skii Geologo-Razvedochii Institut Ukranigril, 20, 287 pp (inRussian).

Marfenkova, M.M., 1978. Foraminifera and stratigraphy of the Lower and Middle Visean of southern Kazakhstan. Trudy Instituta Gelologii i Geofiziki, Akademiya Nauk SSSR. Sibirskoe otdelenie, 386, 78-99.

Marfenkova, M.M., 1983. Archaediscids from the Visean and Serpukhovian beds of Kazakhstan. Izvestiya Akademiya Nauk KazSSR, Seriya Geologicheskaya 1983(3), 42-53 (in Russian).

Marfenkova, M.M., 1991. Marine Carboniferous of Kazakhstan. Alma-Ata, 1 and 2, 1-98 and 1-19.

Marfenkova, M.M., 2009. Visean and Serpukhovian Koktjubinids (Biseriamminacea, Foraminifera) from Kazakhstan. Paleontological Journal, 43 (3), 251-257.

Maslo, A., Vachard, D., 1997. Inventaire critique des Eostaffellinae (foraminiféres du Carbonifére). Revue de Micropaléontologie, 40 (1), 39-69.

Metin, S., Ayhan, A., Papak, İ., 1986. Doğu Toroslar' ın batı kesiminin jeolojisi (GGD Türkiye). MTA Dergisi, 107, 1-13.

Miklaylov, A.V., 1935. On the question of the phylogeny of Carboniferous foraminifera. Izvestiya Leningradskogo Geologo-Gidro-Geodezicheskogo-Tresta, 2-3 (7-8), 38-42.

Miklaylov, A.V., 1939. Of the Paleozoic Ammodiscidae. Sbornik Leningradskogo Geologicheskogo Upravleniya, Glavnoe Geologicheskoe Upravlenie, 3, 63-69.

Miklukho-Maklay, A.D., 1957. Biostratigraficheskoe razdelenie verkhnego Paleozoya Khr. Kara-Chartyr (Yuzhnaya Fergana), (Biostratigraphic subdivision of the Upper Paleozoic in the Kara-Chartyr Mountain range (southern Fergana)). *Doklady AkademiiNauk S.S.S.R.,* 108, 1152-1155.

Mitchum, R., M., Vail, P., R., Thomson, S. 1977. Seismic stratigraphy and global changes of sea-level, Part 2: The depositional sequences as a basic unit of for stratigraphic analysis. Applications to Hydrocarbon Exploration. AAPG Memoir, 26, 53-62.

Moeller, V.V., 1878. Die Spiral-gewundenen Foraminiferen des rüssichen Kohlenkalks. Mater. Geol. Rossii, 8,1-219.

Moeller, V.V., 1879. Die Foraminiferen des Russischen Kohlenlaks. *Memories de I'Akademie Imperiale des Sciences de St. Petersbourg*, 7 (27), 1- 131.

Monod, O., 1967. Presence d'une faune Ordovicienne dans les schistes de Seydişehir a la base des calcaries du Taurus occidental. MTA Bul., 69, 79-89.

Monod O., 1977. Recherches géologiques dans le Taurus occidental au Sud de Beysehir (Turquie). Université de Paris-Sud, Centre d'Orsay, 442 p.

Monod, O. 1978. Güzelsu Akseki Bölgesindeki Antalya Napları üzerine Açıklama)Orta Batı Toroslar, Türkiye). Türkiye Jeoloji Kurumu Bülteni, c.21, 27-29.

Monod, O. and Akay, E., 1984. Evidence for a late Triassic-Early Jurassic orogenic event in the Taurides. In the Geological evolution of the Eastern Mediterranean, Dixon, J.E. and Robertson, A. H.F. (eds.), Geological Society Special Publication, 824 pp.

Nigmadhaznov, I.M., Nikolaeva, S.V., Konovalova, V.A., Orlov-Labkovsky, O., 2010. Integrated ammonoid, conodont and foraminiferal stratigraphy in the Paltau section, Middle Tienshan, Uzbekhistan. *In*: Newsletters on Carboniferous Stratigraphy, 28, 50-60.

Noe, S.U., 1987., Facies and paleogeography of the marine Upper Permiaan and of the Permian- Triassic boundary in the southern Alps (Bellaraphon Formation, Tesero Horizon). Facies, 16, 89-142. In Ünal, E., Altıner, D., Yılmaz, İ.Ö., Özkan Altıner, S., 2003. Cyclic sedimentation across the Permian – Triassic boundary (central Taurides, Turkey). Rivista Italiana di Paleontologia a Stratigrafia, 109/2, 359-376.

Ogg, J.G., Ogg, Gabi, Gradstein, F.M., 2008. The Concise Geologic Time Scale. Cambridge University Press, 177 pp.

Okuyucu, C., 1999. A new *Multidiscus* ? species (Foraminifera) from a Fusulinacean-rich succession encompassing the Carboniferous – Permian boundary in the Hadim Nappe

(Central Taurus, Turkey) . Rivista Italiana di Paleontologia e Stratigrafia, 105(3), 439 - 444.

Okuyucu, C., Vachard, D., 2006. Late Viséan foraminifers and algea from the Cataloturan Nappe, Aladağ Mountains, Eastern Taurides, southern Turkey. Geobios, 39, 535-554.

Omara, S., Conil, R., 1965. Lower Carboniferous from southwestern Sinai, Egypt, Annales de la Société Géologique de Belgique, 88, B221-B242.

Orlova, I.N. 1955. Novyi rod semeistva Archaediscidae E. Tchern. Akademia Nauk S.S.S.R. Doklady, 102, 621-622.

Özgül, N., 1971. Orta Torosların kuzey kesiminin yapısal gelişiminde blok hareketlerin önemi. TJK Bülteni, 14, 85-101.

Özgül, N., 1976. Toroslar' ın bazı temel jeolojik özellikleri. Türkiye Jeoloji Kurumu Bülteni, c.19, 65-78.

Özgül, N., 1983. Geology of the Central Taurides. Field Guide Book for the Int. Symp. Geol. Taurus Belt, 16 pp.

Özgül, N., 1984. Stratigraphy and tectonic evolution of the Central Taurides. In: O. Tekeli and M.C. Göncüoğlu (Editors), Geology of the Taurus Belt, Mineral research and Exploration Ins. Turkey, Ankara, 77-90.

Özgül, N., 1985. Alanya tektonik penceresi ve batı kesiminin jeolojisi. Ketin Sempozyumu Kitabı, 97-120.

Özgül, N., 1997. Bozkır-Hadim-Taşkent (Orta Toroslar' ın kuzey kesimi) dolaylarında yer alan tektono-stratıgrafik birliklerin stratigrafisi. MTA Dergisi, 119, 113-174.

Özgül, N., Gedik, İ., 1973. Orta Toroslar'da Alt Paleozoyik yaşta Çaltepe Kireçtaşı ve Seydişehir Formasyonu'nun stratigrafisi ve konodont faunası hakkında yeni bilgiler. Türkiye Jeoloji Kurumu Bülteni, 16 (2), 39-52.

Özgül, N., Metin, S., Dean, W., 1972. Doğu Toroslarda Tufanbeyli ilçesi (Adana) dolayının Alt Paleozoik stratigrafisi ve faunası. MTA Dergisi, 79, 9-16.

Özkan, R. 1999. Lower and middle Carboniferous micropaleontology and biostratigraphy of eastern part of pre-Caspian depression, western Kazakhstan. M. S. Thesis, Middle East Technical University, Ankara, Turkey, 246 pp.

Özkan-Altıner, S., Altıner, D., Yılmaz, İ.Ö., Peynircioğlu, A., 2007. Türkiye' nin denizel Karboniferde kat sınır stratotip tanımlamasına yönelik araştırma. TUBİTAK Proje no: 103Y190, 165 pp.

Pazukhin, V. N., Kulagina, E.I., Nikolaeva, S.V., Kochetova, N.N., Konovalova, V.A., 2010. The Serpukhovian Stage in the Verkhnyaya Kardailovka Section, South Urals. Stratigraphy and Geological Correlation, 18 (3), 269-289.

Perret, M.F., 1993. Recherches micropaléontologique et biostratigraphique (Conodontes-Foraminifères) dans le Carbonifère Pyrenéen. Actes Lab. Géol. Sediment. Paléontol. Univ. Paul-Sabatier Toulouse, 21 (2), 1-597. *In*: Cózar, P., 2002. Taxonomic value of the diaphanotheca/luminotheca in the classification of Lower Carboniferous endothyroid Foraminiferida; creation of two new species of *Pojarkovella*. Geobios, 34, 283-291.

Phillips, J., 1846. On the remains of microscopic animals in the rocks of Yorkshire. *Geol. Polytech. Soc.*, West Riding, Yorkshire, 2, 274-285.

Pillet, L., Vachard, D., Argyriadis, I., Aretz, M., 2010. Revision of the late Visean-Serpukhovian (Mississippian) calcareous algae, foraminifers and microproblematica from Balia-Maden (NW Turkey). Geobios, 43 (5), 531-546.

Plint, A.G.,Nummedal, D., 2000. The falling stage systems tract: recognition and importance in sequence stratigraphic analysis. *In*: Hunt, D., Gawthorpe, R.L., (Eds.): Sedimentary Response to Forced Regression. Geological Society of London Special Publication 172, pp. 1–17.

Plummer, H.J., 1930. Calcareous foraminifera in the Brownwood Shale near Bridgeport, Texas. Bulletin University of Texas Bureau o Economic Geology and Technology, 3101, 5-21.

Posamentier, H.W., James, D.P., 1993. An Overview of sequence – stratigraphic concepts: uses and abuses. *In*: Posamentier, H.W., Summerhayes, C.P., Haq B.U., Allen, G.P. (eds.): Sequence Stratigraphy and Facies Associations. International Association of Sedimentologists, Special Publication **18**, 3-18.

Posamentier, H.W., Jervey, M.T., Vail, P.R., 1988. Eustatic controls on clastic Deposition I - Conceptual framework. Sea-Level Changes – An Integrated Approach. The Society of Economic Paleontologist and Mineralogists, Special Publication, 42, 109-124.

Pratt, B.R., James, N.P., 1986. The St. George Group (Lower Ordovician) of Western Newfoundland: tidal flat island model for carbonate sedimentation in shallow epeiric seas. Sedimentology, 33, 313-343.

Pronina, T.V., 1963. Foraminifera of the Carboniferous Berezov beds of the eastern slope of the southern Urals. Trudy Instituta Geologicheskikh Nauk, Akademiya Nauk SSSR, Ural'skiy Filial, 65, 119-176 (in Russian).

Raspini, A., 2001. Stacking pattern of cyclic carbonate platform strata: Lower Cretaceous of Southern Apennines, Italy. Jurnal of the Geological Society, London, 158, 353-366.

Rauser-Chernousova, D.M., 1948. Materials and foraminiferal fauna from the Carboniferous deposits of central Kazakhstan, Akademiva Nauk SSSR, Trudy Institut Geologicheskii Nauk, 66. *Geologicheskaya Seriva*, **21**, 1-243 (in Russian).

Rauser-Chernousova, D.M., Beliaev, G.M. and Reitlinger, E.A., 1936. Verkhnepaleozoyskie foraminifery Pechorskogo kraya, (Upper Paleozoic foraminifera from the Pechora territory). *Trudy Polyarnoy Komissii, Akademia Nauk,* S.S.S.R., 28, 159-232.

Rauser-Chernousova, D.M., Bensh, F.R., Vdovenko, M.V., Gibshman, N.B., Leven, E. Ya., Lipina, O.A., Reitlinger, E.A., Solovieva, M.N., Chedija, I.O., 1996. On the systematics of Paleozoic foraminifera (Endothyroida, Fusulinoida). Akademiya Nauk SSSR, "Nauka", Moscow (in Russian).

Rauser-Chernousova, D.M. and Fursenko, A.V., 1937. Determination of foraminifera from the oil-producing regions of the USSR. Glavnova Redaktsya Gorno-Toplivnoi Literatury Leningrad, Moskova, 315 p. (in Russian).

Reitlinger, E.A., 1949. An account of the smaller foraminifera in the lower part of Middle Carboniferous in the central Ural and Kama regions, Akademia Nauk SSSR. Isvestia Seria Geologii, 6, 149-164, (in Russian).

Reitlinger, E.A., 1950. Foraminifera from the Middle Carboniferous deposits of the central part of the Russian Platform (excluding family Fusulinidae). Akademia Nauk SSSR. Trudy Institut Geologicheskii Nauk, 126 (47), 1 - 127 (in Russian).

Reitlinger, E.A., 1959. Atlas of microscopical organic remains and problematica of ancient strata of Siberia. Akad. Nauk SSSR, Trudy Geol. Inst., 25, 1-59.

Rich, M., 1982. Foraminiferal zonation of the Floyd Formation (Mississippian) in the type area near Rome, Floyd County, Georgia. Jour nal of Foraminiferal Research, 12 (3), 242-260.

Richards, B. Aretz, M., Barnette, A., Barskow, I., Blanco-Ferrara, S., Brenckle P., Clayton, G., Dean, M., Brooks, E., Gibsman, N., Hecker, M., Konovola, V., Corn, D., Kulagina, E., Lane, R., Mamet, B., Nemyrovska, T., Nikoloeva, S., Pazukhin, V., Qui, Yu-ping, Sanz-Lopez, J., Saltzman, M., Titus, A., Utting, J., Wang, X., 2010. Report of the task group to establish a GSSP close to the existing Visean – Serpukhovian boundary. *In*: Newsletters on Carboniferous Stratigraphy, 28, 30-34.

Rodríguez-Martínez, M., Reitner, J., 2010. Micro-framework reconstruction from peloidal-dominated mud mounds (Viséan, SW Spain). Facies, 56, 139-156.

Ross, C.A., Ross, J.R.P., 1985. Late Paleozoic depositional sequences are synchrounus and worldwide. Geology, 13, 194-197.

Rozovskaya, S.E., 1961. On the systematics of the families Endothyridae and Ozawainellidae. *Paleontologicheskii Zhurnal,* No. 3, 19-21 (in Russian).

Rozvskaya, S.E., 1963. The earliest fusulinids and their ancestors. Trudy Paleontologicheskogo Instituta, Akademiya Nauk SSSR, 97, 1-127. (in Russian).

Rygel, M.C., Fielding, C.R., Frank, T.D., Birgenheier, L.P., 2008. The magnitude of Late Paleozoic glacioeustatic fluctuations: a synthesis. Journal of Sedimentary Research, 78, 500-511.

Sarg, J.F., 1988. Carbonate sequence stratigraphy. *In*: Wilgus, C.K., Hastings, B.S. et al. (Eds.): Sea level changes: An integrated approach. Society of Economic Paleontologist and Mineralogist, Special Publication 42, 155-181.

Schlager, W., 2005. Carbonate sedimentology and sequence stratigraphy. SEPM (Society of Sedimentary Geology) Concepts in Sedimentology and Paleontology, n. 8, Tulsa, Oklahoma, 200 p.

Schlykova, T.I., 1951. Foraminifères du Viséen et du Namurien du bord occidental du basin de Moscou in Stratigraphie et microfaunes du Carbonifère inférieur de la partie occidentale du Bassin de Moscou. Trav. VNIGRI, n.s., 56, 109-178.

Schubert, R.J., 1921. Paleontologische daten zur Stammesgeschichte der Protozoen. *Palaontogische Zeitschrift* (1920), **3**, 129-188.

Schulze, F., Kuss, J., Marzouk, A., 2005. Platform configuration, microfacies and cyclicities of the upper Albian to Turonian of west-central Jordan. Facies, 50, 505-527.

Schwarzacher, W., 1991. Milankovitch cycles and the measurement of time. *In*: Einsele, G., Ricken, W., Seilacher, A. (eds.): Cycles and events in stratigraphy. Springer-Verlag, 955 pp.

Schwarzacher, W., 1993. Cyclostratigraphy and the Milankovitch Theory. Elsevier, 225 pp.

Sebbar, A., Lys, M., 1989. Biostratigraphy de Carbonifère Inférieur: Serpukhovian du Djebel Arlal, Bassin de Béchar, Algérie. Revue de Micropaléontologie, 32 (1), 53-62.

Shinn, E., 1983. Tidal Flats. *In*: Scholle. P.A., et al. (Eds.): Carbonate Depositional Environments. American Association of Petroleum Geologist Memoir, 33, 171-210. In Amirshahkarami, M., Moghaddam, H.V., Taheri, A., 2007. Sedimentary facies and sequence stratigraphy of the Asmari Formation at Chaman-Bolbol, Zagros Basin, Iran. Jurnal of Asian Earth Sicences, 29, 947-959.

Simonova, Z.G., Zub, V.V., 1975. New representatives of the family quasiendothyridae from Middle and Upper Viséan strata of northen Tian-Shan and Lesser Karatau. Geologiya, Kazakhskiy Politeckhnicheskikh Institut 9, Alma –Ata, 19-35 (in Russian).

Skompski, S., Conil, R., Laloux, M., Lys, M., 1989. Etude micropaléontologique de calcaires du Viséen Terminal et du Namurien dans le bassin Carbonifère de Lublin a l'est de la Pologne. Bulletin de la Société belge de Géologie, 98, 353-369.

Sloss, L.L., 1963. Sequences in the cratonic interior of North America. Geological Society of America Bull., 74, 93-114.

Someville, I.D., 2008. Biostratigraphic zonation and correlation of Mississippian rocks in Western Europe: some case studies in the late Visean/Serpukhovian. Geological Journal, 43, 209-240.

Someville, I.D., Cózar, P., 2005. Late Asbian to Brigantian (Mississippian) foraminifera from southeast Ireland: comparison with northern England assemblages. Journal of Micropaleontology, 24, 131-141.

Strank, A.R.E., 1982. Asbian and Holkerian foraminifera from the Beckermonds Scar Borehole. Proceedings of the Yorkshire Geological Society, 44,103-108.

Strank, A.R.E., 1983. New stratigraphically significant foraminifera from the Dinantian of Great Britain. Paleontology, 26 (2), 435-442.

Strasser, A., 1983. Black-pebble occurrence and genesis in Holocene carbonate sediments (Florida Keys, Bahamas, and Tunisia). Jurnal of Sedimentary Petrology, 54, 1097-1109.

Strasser, A., Samankasou, E., 2003. Carbonate sedimentation rates today and in the past: Holocene of Florida Bay, Bahamas and Bermuda vs. Upper Jurassic and Lower Cretaceous of the Jura Mountins (Switzerland and France). Geologia Croatica, 56(1), 1-18.

Suleymanov, I.S., 1945. Some new species of small foraminifers from the Tournaisian of the Ishimbayevo oil-bearing region. Compte Rendus (Doklady) de l' Académie des Sciences de l' URSS, 48, 124-127.

Şenel, M. 1999. Stratigraphic and tectonic features of the tecnostratigraphic units in the Taurus Belt, and the redefinition of these units. Proceeding of the 52nd Geological Congress of Turkey, 376-378.

Şenel, M., Gedik, İ., Dalkılıç, H., Serdaroğlu, M., Bilgin, A.Z., Uğuz, M.F., Bölükbaşı, A.S., Korucu, M., Özgül, N., 1996. Isparta Büklümü Doğusunda, Otokton ve Allokton Birimlerin Stratigrafisi (Batı Toroslar). MTA Dergisi, 118, 111-160.

Şenel, M., Dalkılıç, H., Gedik, İ., Serdaroğlu, M., Metin, S., Esentürk, K., Bölükbaşı, A.S., Özgül, N., 1998. Orta Toroslar'da Güzelsu Koridoru ve kuzeyinin jeolojisi. MTA Dergisi, 120, 171-197.

Şengör, A. M. C., Yılmaz, Y., 1981. Tethyan evolution of Turkey: a plate tectonic approach. Tectonophysics, 75, 181-241.

Tekeli, O., 1980. Toroslar' da Aladağlarin yapısal evrimi. Türkiye Jeoloji Kurumu Bülteni, 23. 11-14.

Tekeli, O., Aksoy, A., Ürgün, B.M., and Işık, A., 1984. Geology of the Aladağ Mountains. *In*: Tekeli, O., Göncüoğlu, M.C. (eds.): Geology of the Taurus Belt, Mineral Research and Exploration Institute of Tukey Publication, 143-158.

Tresch, J., Strasser, A., 2010. History of the Middle Berriasian transgression on the Jura carbonate platform: revealed by high-resolution sequence- and cyclostratigraphy (Switzerland and France). International Jurnal of Earth Sciences, 99, 139-163.

Thompson, M.L., 1942. New genera of Pennsylvanian fusulinids. American Journal of Science, 240, 403-420.

Tucker, M.E., Calvet, F., Hunt, D., 1993. Sequence stratigraphy of carbonate ramps: systems tracts, models and application to the Muschelkalk carbonate platforms of eastern Spain. *In*: Posamentier, H.W., Summerhayes, C.P., Haq B.U., Allen, G.P. (eds.): Sequence Stratigraphy and Facies Associations. International Association of Sedimentologists, Special Publication **18**, 397–415.

Tucker M., Wright V.P., 1990. Carbonate Sedimentology. Blackwell Scientific Press, 482 pp.

Ueno, K., Miyazaki, T., 2009. Mississippian foraminifers from the Onimaru Formation in the Hikoroichi area, South Kitakami Belt, Northeast Japan. Acta Geoscientica Sinica, 30 (1), 82-86.

Ueno, K. and Nakazawa, T., 1993. Carboniferous foraminifers from the lowermost part of the Omi Limestone Group, Niigata Prefecture, central Japan. Science Reports of the Institute of Geoscience, University of Tsukuba, section B, Geological Sciences, 14, 1-51.

Ünal, E., Altıner, D., Yılmaz, İ. Ö., Özkan-Altiner, S., 2003. Cyclic sedimentation across the Permian-Triassic boundary (central Taurides, Turkey). Rivista Italiana di Paleontologia e Stratigrafia, 109 (2), 359-376.

Vachard, D., 1977. Etude stratigraphique et micropaléontologique (algues et foraminifères du Viséen de la Montagne Noir (Hérault, France). Mém. Inst, Géol. Univ. Louvain, t. 29, 11-195.

Vachard D., 1988. Towards a rasonable classification of the archaediscidae (Foraminifera, Lower-Middel Carboniferous). Revue de Paléobiologie, 2, 103-123.

Vachard, D.,Aretz, M., 2004. Biostratigraphival precisions on Early Serpukhovian (Late Mississippian), by means of a carbonate algal microflora (cyanobacteria, algea and pseudoalgea) from la Serre (Montaigne Noir, France). Geobios, 37, 643-666.

Vachard, D., Beckary, S., 1991. Algues et foraminifères bachkiriens des Coal Balls de la Mine Rosario (Truebano, Leon, Espagne). Rev. Paléobiol, 10, 315-357. *In:* Cózar, P., 2002. Taxonomic value of the diaphanotheca/luminotheca in the classification of Lower Carboniferous endothyroid Foraminiferida; creation of two new species of *Pojarkovella*. Geobios, 34, 283-291.

Vachard, D., Laveine, J.P., Zhang, S., Deng, G., Lemoigne, Y., 1991. Calcareous microfossils (foraminiferes, algae, pseudo-algea) from the Uppermost Visean of Jiu Hu near Guangzhou (Canton), People's Republic of China. Geobios, 24 (4), 675-681.

Vachard, D., Gaillot, J., Pille, L., Blazejowski, B., 2006. Problems on Biseriamminoidea, Mississippian-Permian biserially coiled foraminifera. A Reappraisal with proposals. Revista Espanola de Micropaleontologia, 38 (2-3), 453-492.

Vachard, D., Orberger, B., Rividi N., Pille, L., Berkhli, M., 2006. New Late Asbian/Early Brigantian (Late Visean, Mississippian) dates in the Mouchenkour Formation (central Morocco): palaeogeographical consequences. General Paleontology, 5, 769-777.

Vail, P., R., Audemard, F., Bowman, S.A., Eisner, P.N., Perez-Cruz, C., 1991. *In:* Einsele, G., Ricken, W., Seilacher, A. (eds.): Cycles and events in stratigraphy. Springer-Verlag, 955 pp.

Vail, P., R., Hardenbol, J., Todd, R., G., 1984. Jurassic unconformities, chronostratigraphy and sea level changes from seismic stratigraphy. *In:* Schlee J.S. (ed.): Interregional Unconformities and Hydrocarbon Exploration. Memoir of the AAPG, Tulsa, 33, 129-144.

Vail, P.R., Mitchum, J.R, 1977. Seismic stratigraphy and global changes of sea level, Part 1: Overview-Applications to Hydrocarbon Exploration. AAPG Memoir, 26, 63-81.

Vail, P. R., Mitchum, R. M. and Thompson, S. 1977. Seismic stratigraphy and global changes of sea level, Part 4: Global cycles of relative changes of the sea level, in payton, C. E., eds., seismic stratigraphy. Application to Hydrocarbon Exploration. AAPG Memoir, 26, 83-97.

Van Wagoner, J.C., Mithchum, R.M.,, Campion, K.M., Rahmaian, V.D., 1990. Siliciclastic sequence stratigraphy in well logs, core and outcrop: concepts for high-resolution correlation of time and facies. American Association of Petroleum Geologist, Methods Exploration, 7, 55 pp.

Van Wagoner, J.C., Posamentier, H.W., Mithchum, R.M., Vail, P.R., Sarg, J.F., Loutit, T.S., Hardenbol, J., 1988. An overview of the fundamentals of sequence stratigraphy

and key definitions. Sea-Level Changes-An Integrated Approach. The Society of Economic Paleontologist and Mineralogist, Special Publication, 42, 40-44.

Vdovenko, M.V., Aisenverg, D.Ye., Nemirovskaya, T.I., Poletaev, V.I., 1990. An overview of Lower Carboniferous biozones of the Russioan Platform. Journal of Foraminiferal Research, 20 (3), 184-194.

Vdovenko, M.V., Aisenverg, D. YE., Nemirovskaya, T.I., Poletaev, V.I., 1990. An overview of Lower Carboniferous biozones of the Russian Platform. Journal of Foraminiferal research,20 (3), 184-194.

Védrine , S., Strasser, A., 2009. High-frequency palaeoenvironmental changes on a shallow carbonate platform during a marine transgression (Late Oxfordian, Swiss Jura Mountains). Swiss Jurnal of Geosciences, 102, 247-270.

Vissarionova, A.Ya., 1948. Primitive Fusulinidae from the Lower Carboniferous of the Eauropean part of the USSR. Trudy Geologicheskogo Instituta, Akademiya Nauk SSSR, 62, 216-226 (in Russian).

Vladimir, I.D., Crowley J.L., Schmitz, M.D., Poletaev, V.I., 2010. New high – precision calibration of the Global Carboniferous Time Scale: The records from Donets Basin, Ukraine. *In:* Aretz, M., Richards, B. (eds.): Newsletter on Carboniferous Stratigraphy. International Union of Geological Sciences. Subcommission on Carboniferous Stratigraphy. 28, pp: 1-86.

Wilson , J.L., 1975. Carbonate facies in geologic history. Springer-Verlag, New York, 471 pp.

Wright, V.P., Vanstone, S.D., 2001. Onset of Late Paleozoic glacioeustasy and the evolving climates of low latitude areas: a synthesis of current understanding. Journal of the Geological Society, London, 158, 579-582.

Yılmaz, İ. Ö., Altıner, D., 2001. Use of sedimentary structures in the recognition of sequence boundaries in the Upper Jurassic (Kimmeridgian) – Upper Cretaceous (Cenomanian) peritidal carbonates of the Fele (Yassıbel) area (Western Taurides, Turkey). International Geological Review, 43 (8), 736-753.

Yılmaz, İ. Ö., Altıner, D., 2006. Cyclic paleokarst surfaces in Aptian peritidal carbonate successions (Taurides, SW Turkey): internal structure and response to mid-Aptian sea-level fall. Cretaceous Research, 27, 814-827.

Yılmaz, İ. Ö., Altıner, D., 2007. Cyclostratigraphy and sequence boundaries of inner platform mixed carbonate-siliciclastic successions (Barremian-Aptian) (Zonguldak, NW Turkey). International Journal of Asian Sciences, 30 (2), 253-270.

Young, J., Armstrong, J., On the Carboniferous fossils of the west of Scotland. Transaction of the Geological Society of Glasgow, 3, 1-103.

Zeller, D.E.N., Endothyroid foraminifera and ancestral fusulinids from the type Chesteran (Upper Mississippian). Jour. Pal., 27, 183-199.

Zhijun, N., Qifa, D., Jianxiong, W., Yunshan, B., Bing, T., Jianjun, B., 2005. Early Carboniferous foraminiferal faunas in the Zhidoi and Zadoi area, southern Qinghai. Acta Micropalaeontologica Sinica, 22(4), 329-345.

APPENDIX A

EXPLANATION OF PLATES

PLATE I

Figure 1: *Diplosphearina inequalis*, sample no: SC-74 (Scale bar: 0.1 mm)

Figure 2: *Diplosphearina inequalis*, sample no: SC-90 (Scale bar: 0.1 mm)

Figure 3: *Diplosphearina inequalis*, sample no: SC-74 (Scale bar: 0.1 mm)

Figure 4: *Diplosphearina inequalis*, sample no: SC-90 (Scale bar: 0.1 mm)

Figure 5: *Diplosphearina inequalis*, sample no: SC-86 (Scale bar: 0.1 mm)

Figure 6: *Calcisphaera* sp., sample no: SC-35 (Scale bar: 0.1 mm)

Figure 7: *Calcisphaera* sp., sample no: SC-30 (Scale bar: 0.1 mm)

Figure 8: *Parathurammina* sp., sample no: SC-30 (Scale bar: 0.1 mm)

Figure 9: *Parathurammina* sp., sample no: SC-30 (Scale bar: 0.1 mm)

Figure 10: *Eotuberitina* sp., sample no: SC-82 (Scale bar: 0.1 mm)

Figure 11: *Eotuberitina* sp., sample no: SC-87 (Scale bar: 0.1 mm)

Figure 12: *Earlandia elegans*, sample no: SC-20 (Scale bar: 0.1 mm)

Figure 13: *Earlandia elegans*, sample no: SC-9 (Scale bar: 0.1 mm)

Figure 14: *Hemithurammina fimbriata*?, sample no: SC-86a (Scale bar: 0.1 mm)

Figure 15: *Hemithurammina fimbriata*, sample no: SC-86 (Scale bar: 0.1 mm)

Figure 16: *Hemithurammina fimbriata*, sample no: SC-46 (Scale bar: 0.1 mm)

PLATE I

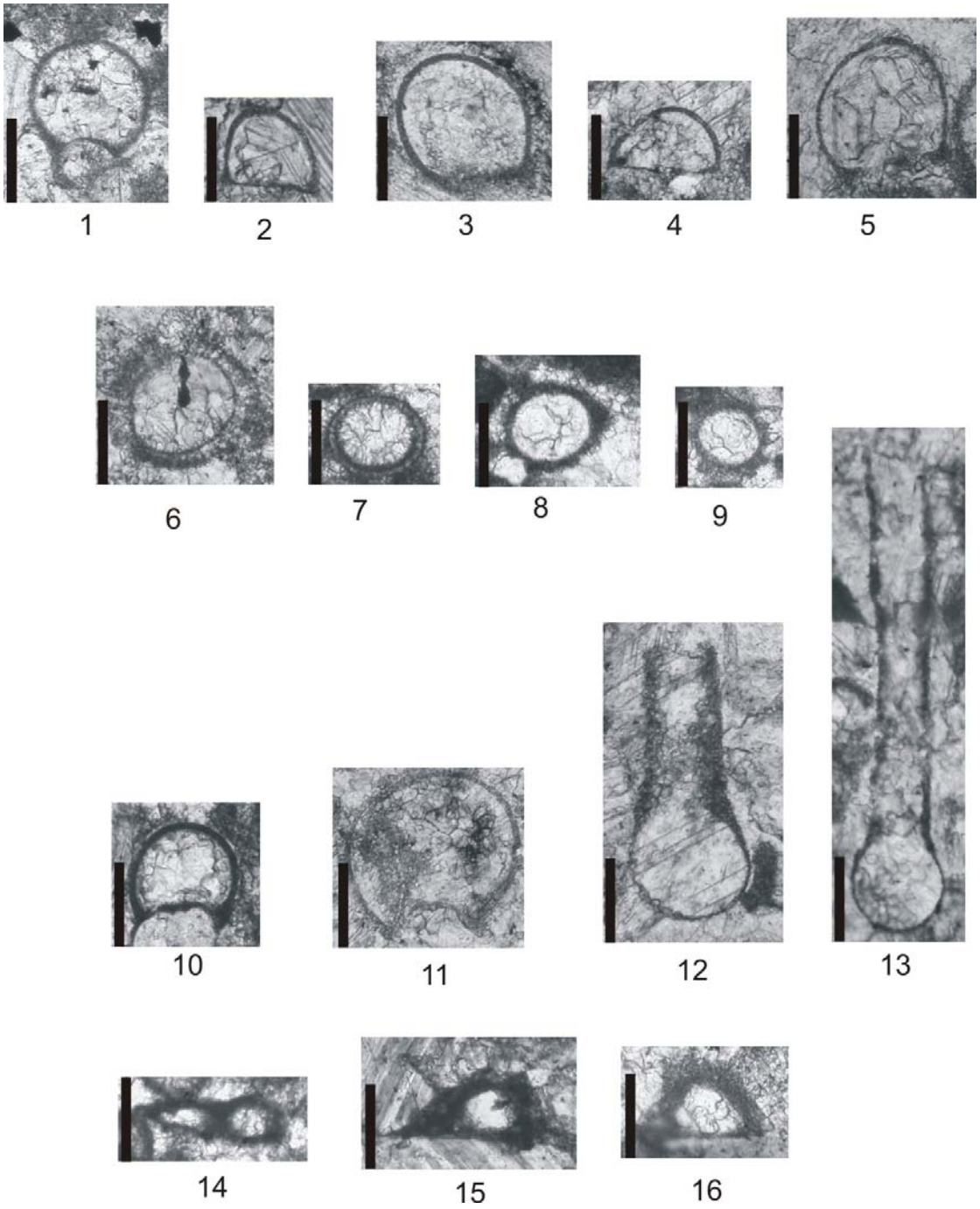

PLATE II

Figure 1: *Brunsia spirillinoides*, sample no: SC-18 (Scale bar: 0.1 mm)

Figure 2: *Brunsia spirillinoides*, sample no: SC-24 (Scale bar: 0.1 mm)

Figure 3: *Brunsia pulchra*, sample no: SC-23 (Scale bar: 0.1 mm)

Figure 4: *Brunsia pulchra*, sample no: SC-23 (Scale bar: 0.1 mm)

Figure 5: *Brunsia pulchra*, sample no: SC-23 (Scale bar: 0.1 mm)

Figure 6: *Brunsia* sp. , sample no: SC-44 (Scale bar: 0.1 mm)

Figure 7: *Brunsia* sp. , sample no: SC-33 (Scale bar: 0.1 mm)

Figure 8: *Brunsia* sp. , sample no: SC-7 (Scale bar: 0.1 mm)

Figure 9: *Brunsia* sp. , sample no: SC-7 (Scale bar: 0.1 mm)

Figure 10: *Brunsia sygmoidalis,* sample no: SC-22 (Scale bar: 0.1 mm)

Figure 11: *Pseudoammodiscus* sp., sample no: SC-4 (Scale bar: 0.1 mm)

Figure 12: *Pseudoammodiscus* sp., sample no: SC-22 (Scale bar: 0.1 mm)

Figure 13: *Pseudoammodiscus* sp., sample no: SC-27 (Scale bar: 0.1 mm)

Figure 14: *Pseudoammodiscus* sp., sample no: SC-16 (Scale bar: 0.1 mm)

PLATE II

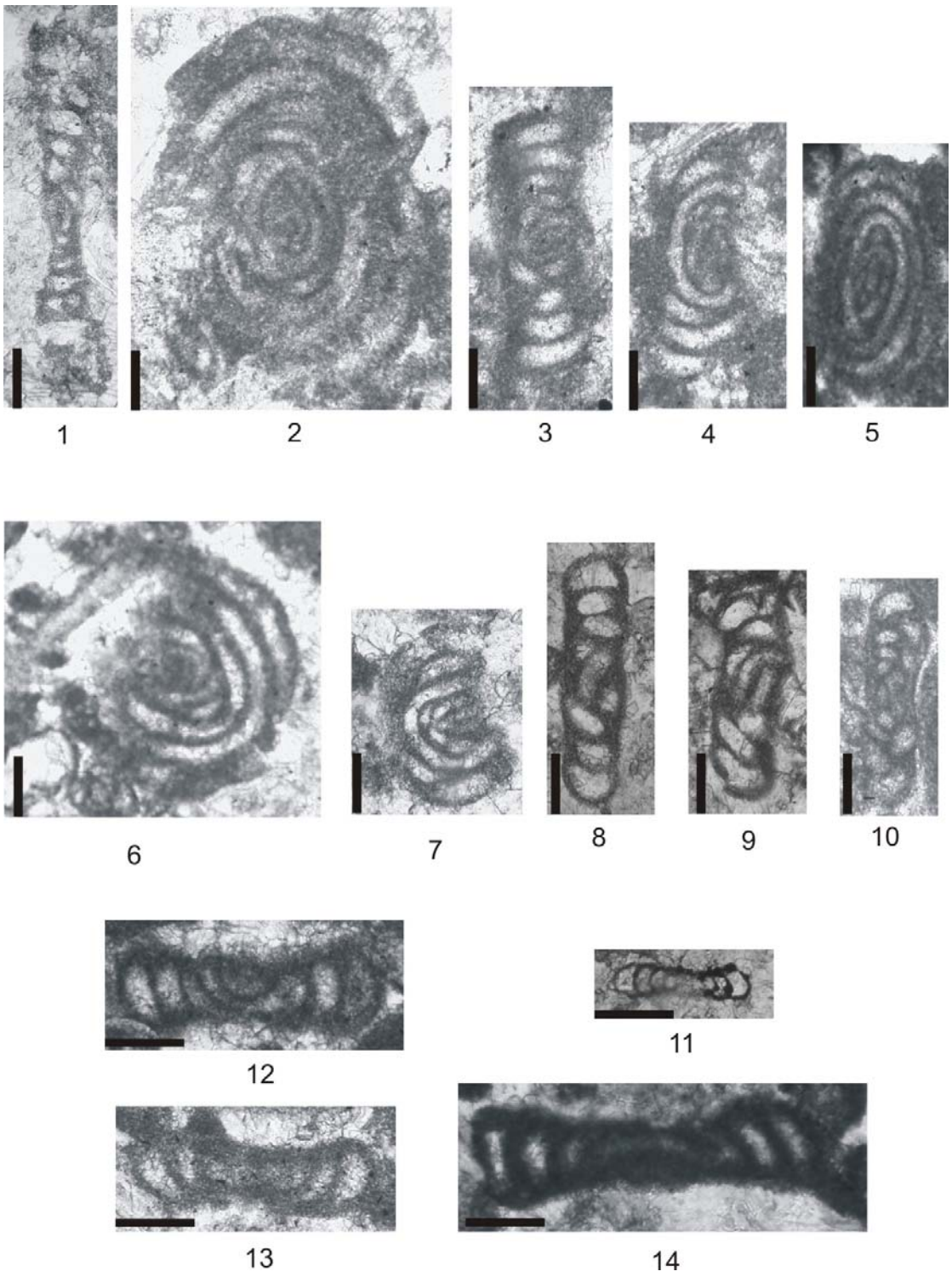

PLATE III

Figure 1: *Pseudoglomospira* sp.1, sample no: SC- 90 (Scale bar: 0.1 mm)

Figure 2: *Pseudoglomospira* sp.1, sample no: SC-86a (Scale bar: 0.1 mm)

Figure 3: *Pseudoglomospira* sp.1, sample no: SC-86a (Scale bar: 0.1 mm)

Figure 4: *Pseudoglomospira* sp.1, sample no: SC-86a (Scale bar: 0.1 mm)

Figure 5: *Pseudoglomospira* sp.1, sample no: SC-89 (Scale bar: 0.1 mm)

Figure 6: *Pseudoglomospira* sp.1, sample no: SC-87 (Scale bar: 0.1 mm)

Figure 7: *Pseudoglomospira* sp.1, sample no: SC-86a (Scale bar: 0.1 mm)

Figure 8: *Pseudoglomospira* sp.1, sample no: SC-91 (Scale bar: 0.1 mm)

Figure 9: *Pseudoglomospira* sp.2, sample no: SC-83 (Scale bar: 0.1 mm)

Figure 10: *Pseudoglomospira* sp.2, sample no: SC-92 (Scale bar: 0.1 mm)

Figure 11: *Pseudoglomospira* sp.3, sample no: SC-86a (Scale bar: 0.1 mm)

Figure 12: : *Pseudoglomospira* sp.3, sample no: SC-86a (Scale bar: 0.1 mm)

Figure 13: *Pseudoglomospira* sp.3, sample no: SC-84 (Scale bar: 0.1 mm)

Figure 14: *Pseudoglomospira* sp.3, sample no: SC-84 (Scale bar: 0.1 mm)

Figure 15: *Pseudoglomospira* sp.3, sample no: SC-91 (Scale bar: 0.1 mm)

Figure 16: *Pseudoglomospira* sp. , sample no: SC-91 (Scale bar: 0.1 mm)

Figure 17: *Pseudoglomospira* sp. , sample no: SC-86a (Scale bar: 0.1 mm)

Figure 18: *Pseudoglomospira* sp. , sample no: SC-91 (Scale bar: 0.1 mm)

Figure 19: *Pseudoglomospira*? sp. , sample no: SC-39 (Scale bar: 0.1 mm)

Figure 20: *Pseudoglomospira*? sp. , sample no: SC-50 (Scale bar: 0.1 mm)

Figure 21: *Pseudoglomospira*? sp. , sample no: SC-86a (Scale bar: 0.1 mm)

Figure 22: *Scalebrina sp.*, sample no: SC-89 (Scale bar: 0.1 mm)

PLATE III

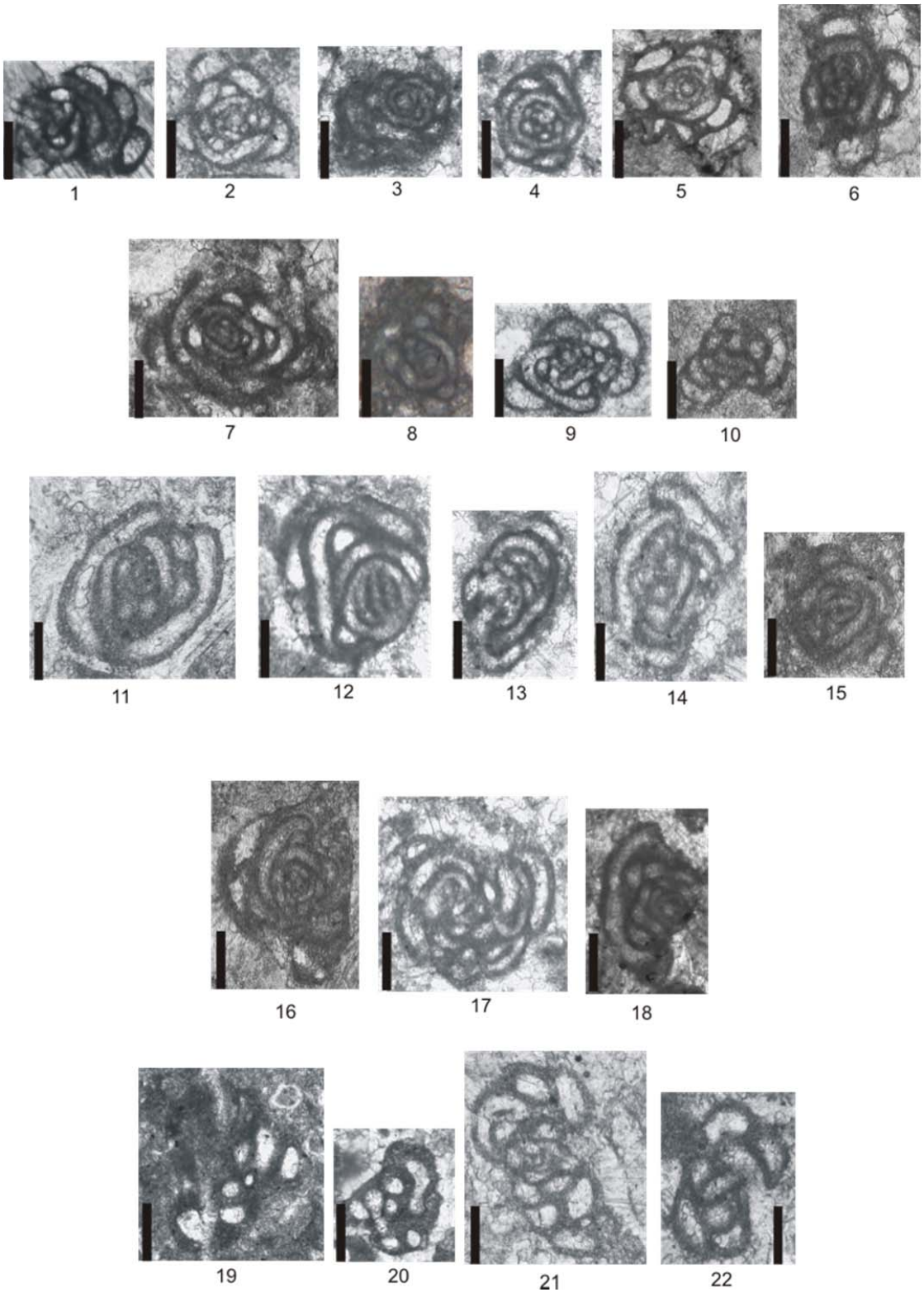

PLATE IV

Figure 1: *Viseidiscus monstratus*, sample no: Sc-21(Scale bar: 50 μm)

Figure 2: *Viseidiscus umbogmaensis*, sample no: SC-4 (Scale bar: 50 μm)

Figure 3: *Viseidiscus umbogmaensis*, sample no: SC5 (Scale bar: 50 μm)

Figure 4: *Viseidiscus umbogmaensis*?, sample no: SC21 (Scale bar: 50 μm)

Figure 5: *Viseidiscus umbogmaensis*, sample no: SC-2 (Scale bar: 50 μm)

Figure 6: *Viseidiscus* sp., sample no: SC-17 (Scale bar:50 μm)

Figure 7: *Viseidiscus* sp., sample no: SC-7 (Scale bar: 50 μm)

Figure 8: *Paraarchaediscus koktjubensis*, sample no: SC-87(Scale bar: 0.1 mm)

Figure 9: *Paraarchaediscus koktjubensis*, sample no: SC-82 (Scale bar: 0.1 mm)

Figure 10: *Paraarchaediscus koktjubensis*, sample no: SC79 (Scale bar: 0.1 mm)

Figure 11: *Paraarchaediscus koktjubensis*, sample no: SC-70 (Scale bar: 0.1 mm)

Figure 12: *Paraarchaediscus koktjubensis* sample no: SC-90 (Scale bar: 0.1 mm)

Figure 13: *Paraarchaediscus koktjubensis* sample no: SC-82 (Scale bar: 0.1 mm)

Figure 14: *Paraarchaediscus koktjubensis* sample no: SC-82 (Scale bar: 0.1 mm)

Figure 15: *Paraarchaediscus koktjubensis*, sample no: SC-27 (Scale bar: 0.1 mm)

Figure 16: *Paraarchaediscus koktjubensis* sample no: SC-79 (Scale bar: 0.1 mm)

Figure 17: *Paraarchaediscus koktjubensis*, sample no: SC67 (Scale bar: 0.1 mm)

Figure 18: *Paraarchaediscus koktjubensis* sample no: SC-79 (Scale bar: 0.1 mm)

Figure 19: *Paraarchaediscus koktjubensis* sample no: SC-79 (Scale bar: 0.1 mm)

Figure 20: *Paraarchaediscus koktjubensis* sample no: SC-3 (Scale bar: 0.1 mm)

Figure 21: *Paraarchaediscus koktjubensis* sample no: SC-86 (Scale bar: 0.1 mm)

Figure 22: *Paraarchaediscus koktjubensis*, sample no: SC-79 (Scale bar: 0.1 mm)

Figure 23: *Paraarchaediscus koktjubensis*, sample no: SC-85 (Scale bar: 0.1 mm)

Figure 24: *Paraarchaediscus koktjubensis*, sample no: SC-82 (Scale bar: 0.1 mm)

PLATE IV

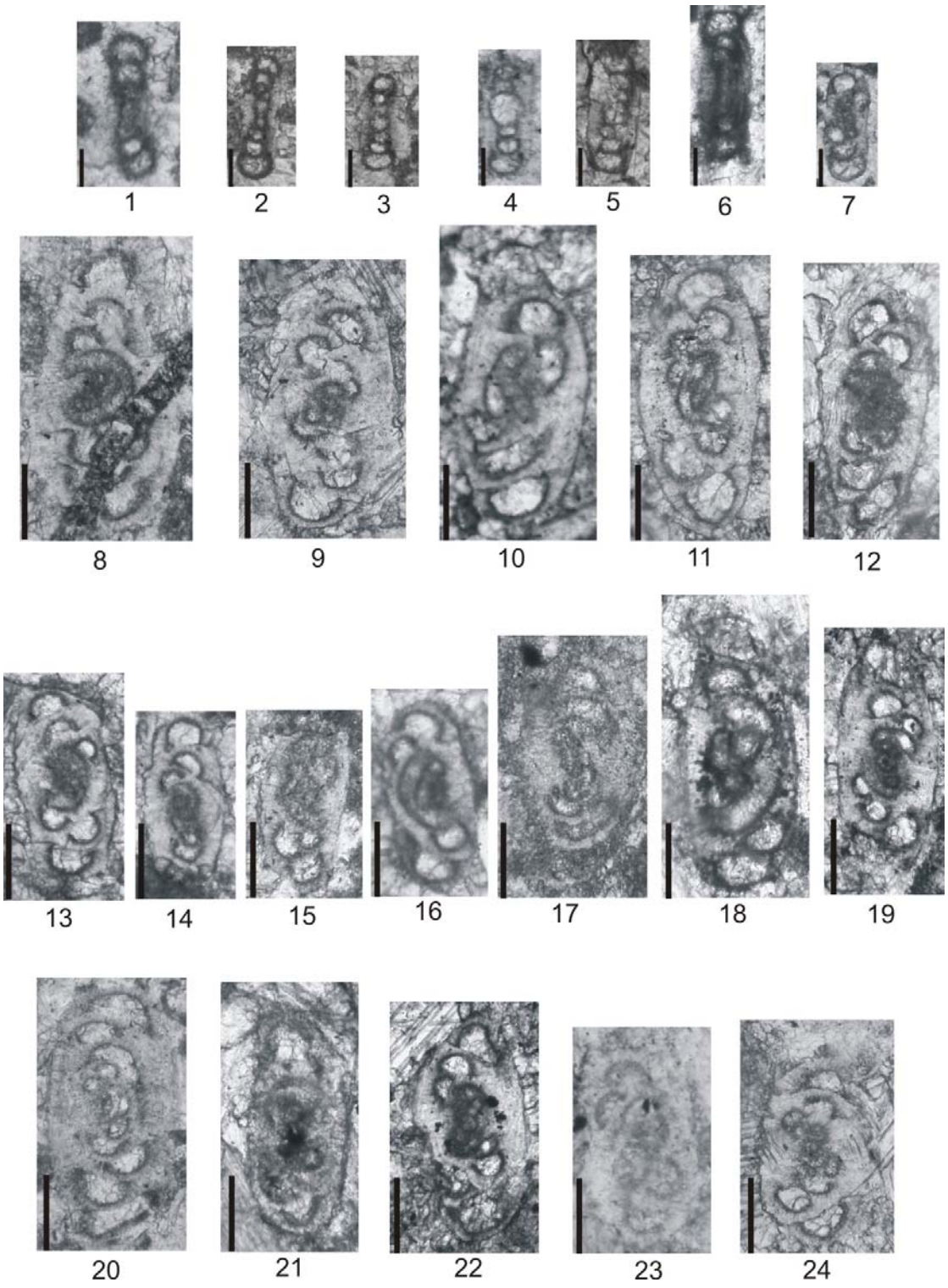

PLATE V

Figure 1: *Paraarchaediscus koktjubensis*?, sample no: SC-82 (Scale bar: 0.1 mm)

Figure 2: *Paraarchaediscus* sp., sample no: SC-11 (Scale bar: 0.1 mm)

Figure 3: *Paraarchaediscus* sp., sample no: SC-86 (Scale bar: 0.1 mm)

Figure 4: *Paraarchaediscus* sp., sample no: SC-82 (Scale bar: 0.1 mm)

Figure 5: *Paraarchaediscus* sp., sample no: SC-83 (Scale bar: 0.1 mm)

Figure 6: *Paraarchaediscus* sp., sample no: SC-85 (Scale bar: 0.1 mm)

Figure 7: *Paraarchaediscus* sp., sample no: SC-82 (Scale bar: 0.1 mm)

Figure 8: *Paraarchaediscus* sp., sample no: SC-82 (Scale bar: 0.1 mm)

Figure 9: *Paraarchaediscus* sp., sample no: SC-66 (Scale bar: 0.1 mm)

Figure 10: *Paraarchaediscus* sp., sample no: SC-79 (Scale bar: 0.1 mm)

Figure 11: *Paraarchaediscus* sp., sample no: SC-58 (Scale bar: 0.1 mm)

Figure 12: *Paraarchaediscus* sp., sample no: SC-86 (Scale bar: 0.1 mm)

Figure 13: *Paraarchaediscus* sp., sample no: SC-86 (Scale bar: 0.1 mm)

Figure 14: *Paraarchaediscus* sp., sample no: SC-90 (Scale bar: 0.1 mm)

Figure 15: *Archaediscus karreri*, sample no: SC-90 (Scale bar: 0.1 mm)

PLATE V

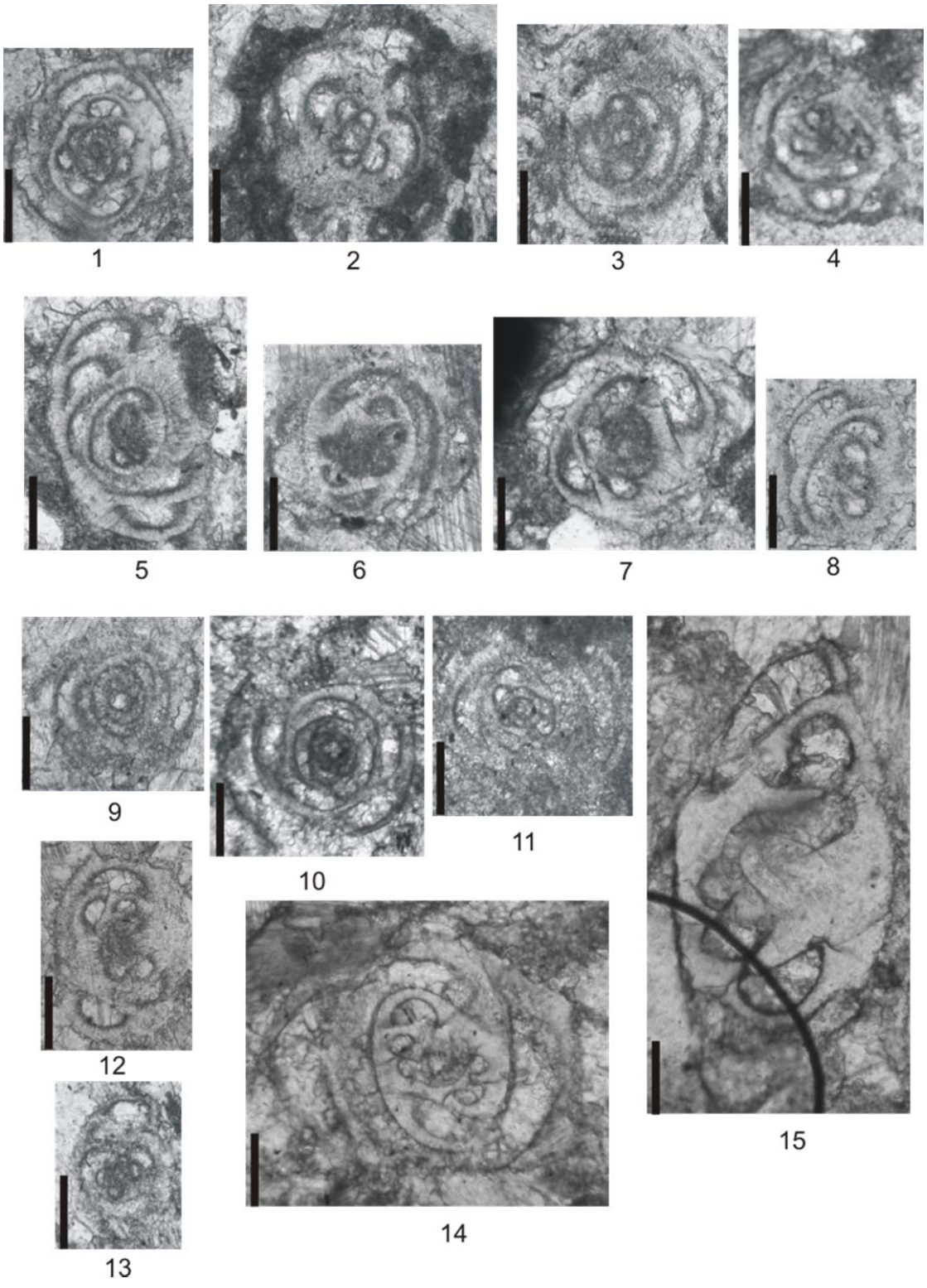

PLATE VI

Figure 1: *Paraarchaediscus convexus*, sample no: SC-85 (Scale bar: 0.1 mm)

Figure 2: *Paraarchaediscus convexus*, sample no: SC-82 (Scale bar: 0.1 mm)

Figure 3: *Paraarchaediscus convexus*, sample no: SC-85 (Scale bar: 0.1 mm)

Figure 4: *Paraarchaediscus convexus*, sample no: SC-79 (Scale bar: 0.1 mm)

Figure 5: *Paraarchaediscus convexus*, sample no: SC-82 (Scale bar: 0.1 mm)

Figure 6: *Betpakodiscus attenuatus*, sample no: SC-57 (Scale bar: 0.1 mm)

Figure 7: *Paraarchaediscus stilus*, sample no: SC-86 (Scale bar: 0.1 mm)

Figure 8: *Paraarchaediscus stilus*, sample no: SC82 (Scale bar: 0.1 mm)

Figure 9: *Paraarchaediscus stilus*, sample no: SC-60 (Scale bar: 0.1 mm)

Figure 10: *Paraarchaediscus* ex gr. *stilus*, sample no: SC-69 (Scale bar: 0.1 mm)

Figure 11: *Paraarchaediscus* ex gr. *stilus*, sample no: SC-58 (Scale bar: 0.1 mm)

Figure 12: *Paraarchaediscus* ex gr. *stilus*, sample no: SC-57 (Scale bar: 0.1 mm)

Figure 13: *Paraarchaediscus* ex gr. *stilus*, sample no: SC-82 (Scale bar: 0.1 mm)

Figure 14: *Paraarchaediscus* ex gr. *stilus*, sample no: SC-88 (Scale bar: 0.1 mm)

Figure 15: *Paraarchaediscus* ex gr. *stilus*, sample no: SC-5 (Scale bar: 0.1 mm)

Figure 16: A*rchaediscus moelleri*, sample no: SC-90 (Scale bar: 0.1 mm)

Figure 17: *Paraarchaediscus* sp. 1, sample no: SC-55 (Scale bar: 50 μm)

Figure 18: *Paraarchaediscus* sp. 1, sample no: SC-21 (Scale bar: 50 μm)

Figure 19: *Paraarchaediscus* sp. 1, sample no: SC-85 (Scale bar: 50 μm)

Figure 20: *Paraarchaediscus* sp. 1, sample no: SC-87 (Scale bar: 50 μm)

Figure 21: *Paraarchaediscus* sp., sample no: SC-86 (Scale bar: 0.1 mm)

Figure 22: *Paraarchaediscus* sp., sample no: SC-21 (Scale bar: 0.1 mm)

PLATE VI

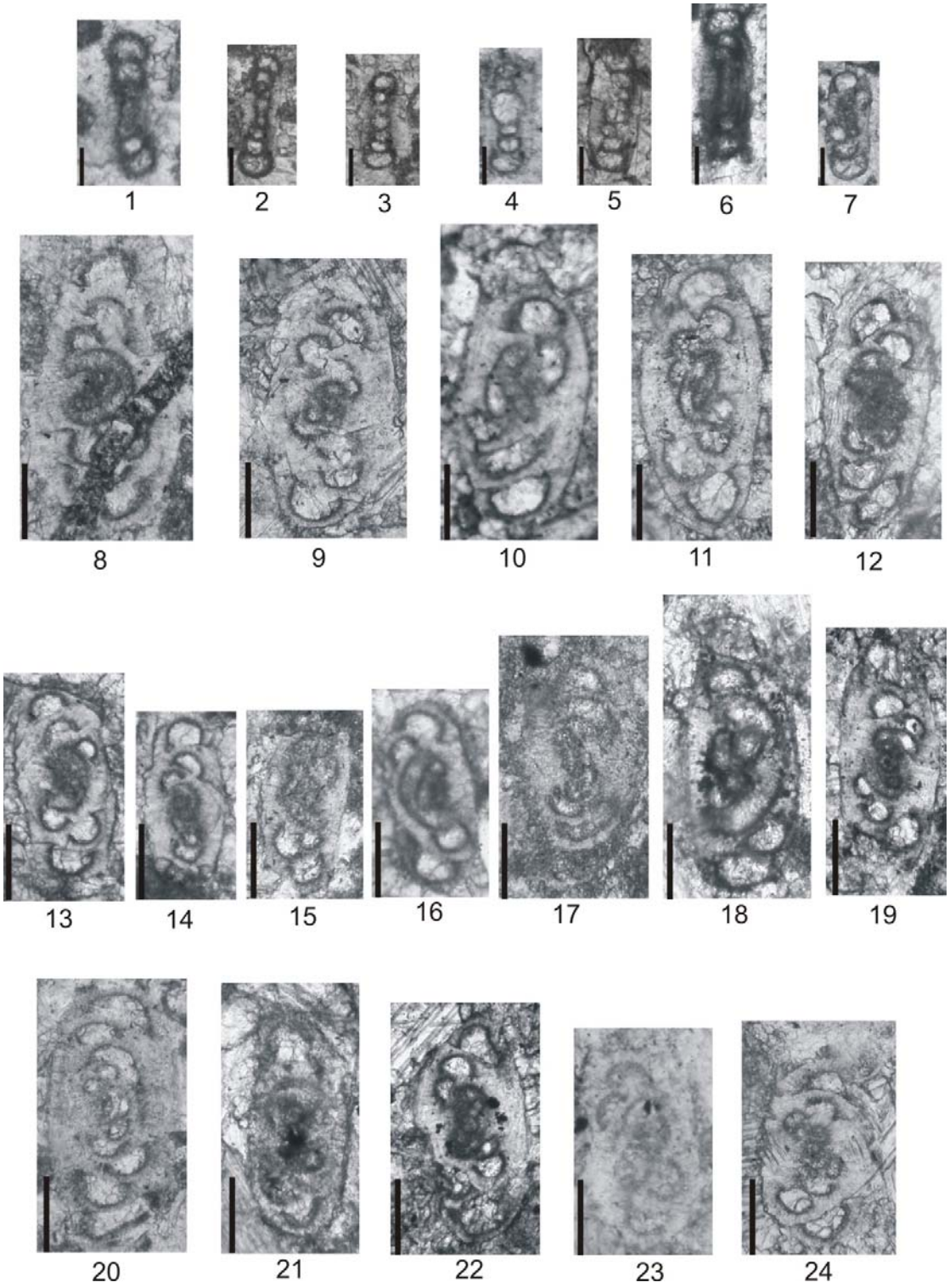

PLATE VII

Figure 1: *Asteroarchaediscus rugosus*, sample no: 83 (Scale bar: 0.1 mm)

Figure 2: *Asteroarchaediscus rugosus*, sample no: 85 (Scale bar: 0.1 mm)

Figure 3: *Asteroarchaediscus rugosus*, sample no: 85 (Scale bar: 0.1 mm)

Figure 4: *Asteroarchaediscus rugosus*, sample no: 85 (Scale bar: 0.1 mm)

Figure 5: *Asteroarchaediscus* sp., sample no: 85 (Scale bar: 0.1 mm)

Figure 6: *Asteroarchaediscus* sp., sample no: 84 (Scale bar: 0.1 mm)

Figure 7: *Neoarchaediscus incertus*, sample no: SC-82 (Scale bar: 0.1 mm)

Figure 8: *Neoarchaediscus incertus*, sample no: SC-85 (Scale bar: 0.1 mm)

Figure 9: *Neoarchaediscus parvus*, sample no: SC-82 (Scale bar: 0.1 mm)

Figure 10: *Neoarchaediscus parvus*, sample no: SC-82 (Scale bar: 0.1 mm)

Figure 11: *Neoarchaediscus parvus*, sample no: SC-82 (Scale bar: 0.1 mm)

Figure 12: *Neoarchaediscus probatus*, sample no: SC-85 (Scale bar: 0.1 mm)

Figure 13: *Neoarchaediscus probatus*, sample no: SC-88 (Scale bar: 0.1 mm)

Figure 14: *Neoarchaediscus* ex. gr. *subbaschkiricus*, sample no: SC-92 (Scale bar: 0.1 mm)

Figure 15: *Neoarchaediscus* ex. gr. *subbaschkiricus*, sample no: SC-84 (Scale bar: 0.1 mm)

Figure 16: *Neoarchaediscus* sp., sample no: SC-82 (Scale bar: 0.1 mm)

Figure 17: *Neoarchaediscus* sp., sample no SC-82 (Scale bar: 0.1 mm)

Figure 18: *Neoarchaediscus* sp., sample no: SC82 (Scale bar: 0.1 mm)

Figure 19: *Neoarchaediscus* sp. (@tenuis stage) , sample no: SC-82 (Scale bar: 0.1 mm)

Figure 20: Neoarchaediscus? sp., sample no: SC-72 (Scale bar: 0.1 mm)

Figure 21: *Neoarchaediscus* sp. , sample no: SC-78 (Scale bar: 0.1 mm)

Figure 22: *Neoarchaediscus* sp., sample no: SC-85 (Scale bar: 0.1 mm)

Figure 23: *Neoarchaediscus* sp., sample no: SC-91 (Scale bar: 0.1 mm)

PLATE VII

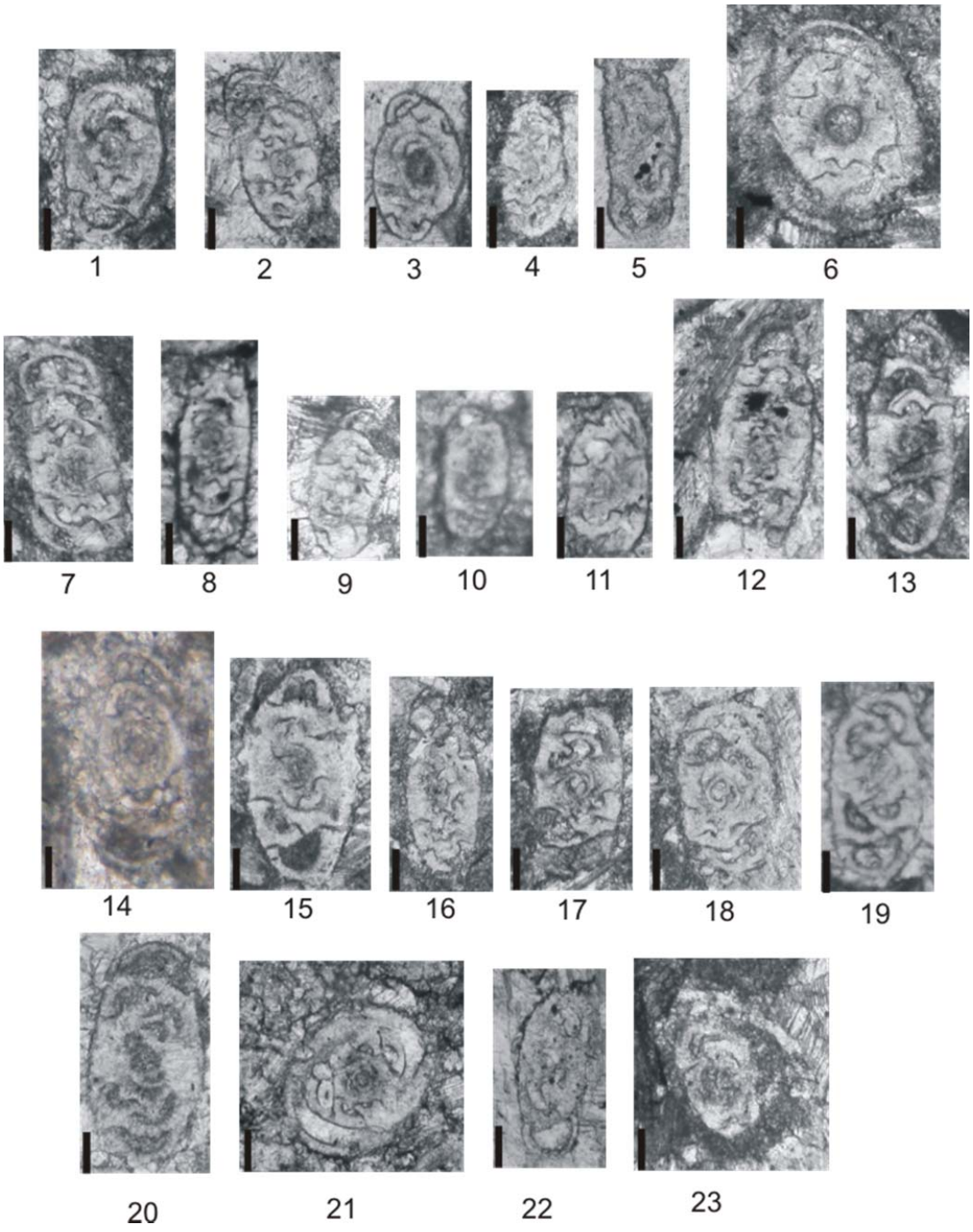

PLATE VIII

Figure 1: *Biseriella parva*, sample no: SC-86 (Scale bar: 0.1 mm)

Figure 2: *Biseriella parva*, sample no: SC-78 (Scale bar: 0.1 mm)

Figure 3: *Biseriella parva*, sample no: SC-83 (Scale bar: 0.1 mm)

Figure 4: *Biseriella parva*, sample no: SC-83 (Scale bar: 0.1 mm)

Figure 5: *Biseriella parva*, sample no: SC-82 (Scale bar: 0.1 mm)

Figure 6: *Biseriella parva*, sample no: SC-90 (Scale bar: 0.1 mm)

Figure 7: *Biseriella parva*, sample no: SC-88 (Scale bar: 0.1 mm)

Figure 8: *Biseriella parva*, sample no: SC-82(Scale bar: 0.1 mm)

Figure 9: *Biseriella parva*, sample no: SC-86 (Scale bar: 0.1 mm)

Figure 10: *Biseriella parva*, sample no: SC-83 (Scale bar: 0.1 mm)

Figure 11: *Biseriella parva*, sample no: SC-79 (Scale bar: 0.1 mm)

Figure 12: *Biseriella parva*?, sample no: SC-86a (Scale bar: 0.1 mm)

Figure 13: *Globivalvulina bulloides*, sample no: SC-86a (Scale bar: 0.1 mm)

Figure 14: *Globivalvulina bulloides*, sample no: SC-79 (Scale bar: 0.1 mm)

Figure 15: *Globivalvulina bulloides*?, sample no: SC-86a (Scale bar: 0.1 mm)

Figure 16: *Globivalvulina* sp. 1, sample no: SC-88 (Scale bar: 0.1 mm)

Figure 17: *Globivalvulina* sp. 1, sample no: SC-87 (Scale bar: 0.1 mm)

Figure 18: *Globivalvulina* sp. 1, sample no: SC-85 (Scale bar: 0.1 mm)

Figure 19: *Globivalvulina* sp.1, sample no: SC-86a (Scale bar: 0.1 mm)

Figure 20: *Globivalvulina* sp. 1, sample no: SC-86 (Scale bar: 0.1 mm)

PLATE VIII

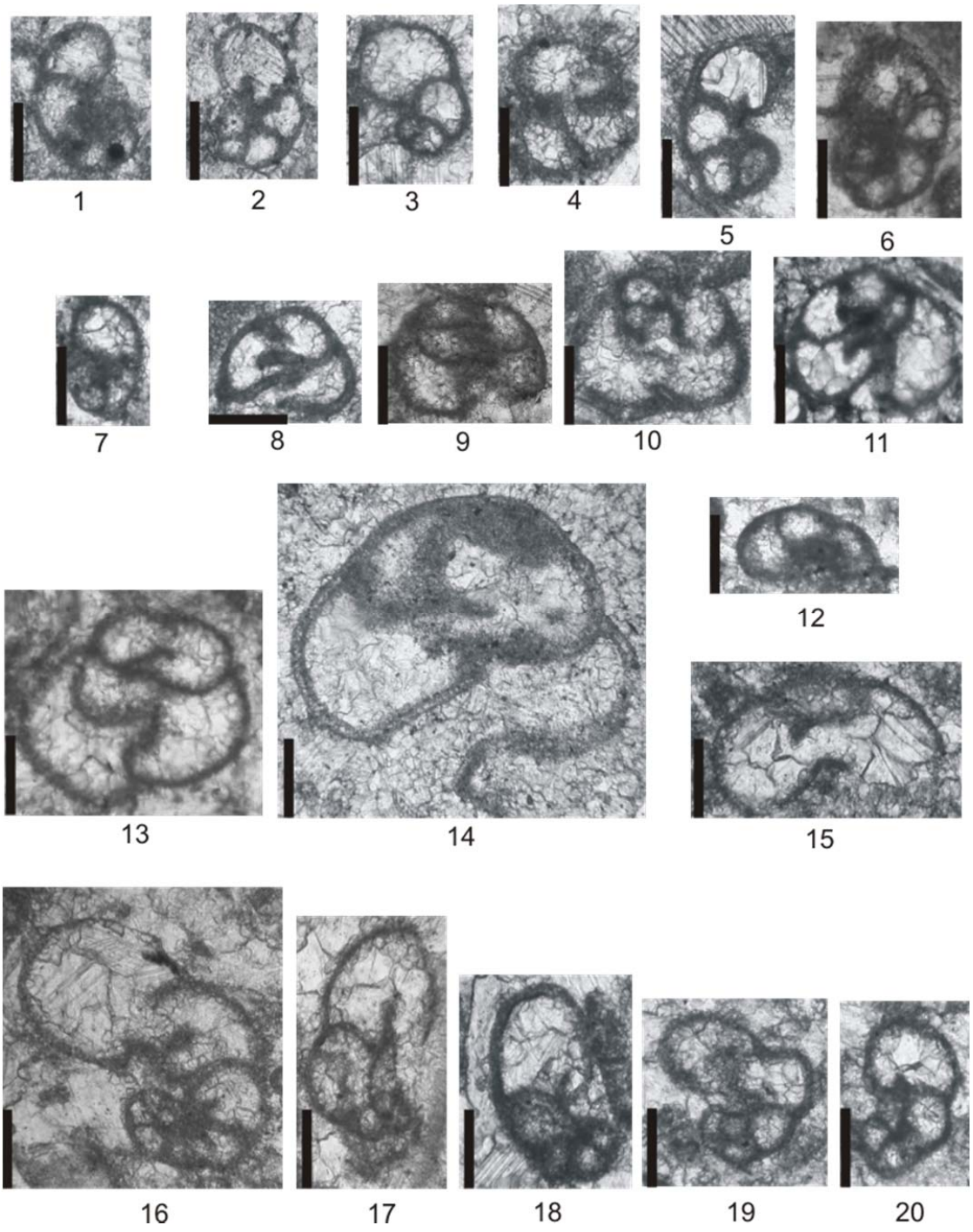

PLATE IX

Figure 1: *Globivalvulina* sp., sample no: SC-89 (Scale bar: 0.1 mm)

Figure 2: *Globivalvulina* sp., sample no: SC-90 (Scale bar: 0.1 mm)

Figure 3: *Globivalvulina* sp., sample no: SC-92 (Scale bar: 0.1 mm)

Figure 4: *Globivalvulina* sp., sample no: SC-86 (Scale bar: 0.1 mm)

Figure 5: *Globivalvulina* sp., sample no: SC-45 (Scale bar: 0.1 mm)

Figure 6: *Globivalvulina* sp., sample no: SC-90 (Scale bar: 0.1 mm)

Figure 7: *Globivalvulina*? sp., sample no: SC-92 (Scale bar: 0.1 mm)

Figure 8: *Globivalvulina* sp., sample no: SC-86 (Scale bar: 0.1 mm)

Figure 9: Koktjubinidae, sample no: SC-90 (Scale bar: 0.1 mm)

Figure 10: Koktjubinidae, sample no: SC-89 (Scale bar: 0.1 mm)

Figure 11: Koktjubinidae, sample no: SC-86 (Scale bar: 0.1 mm)

Figure 12: Koktjubinidae, sample no: SC-92 (Scale bar: 0.1 mm)

Figure 13: Koktjubinidae, sample no: SC-90 (Scale bar: 0.1 mm)

PLATE IX

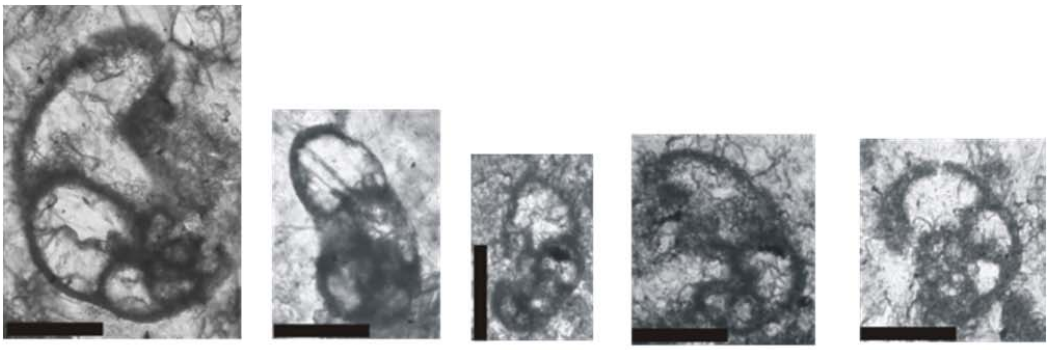

1 2 3 4 5

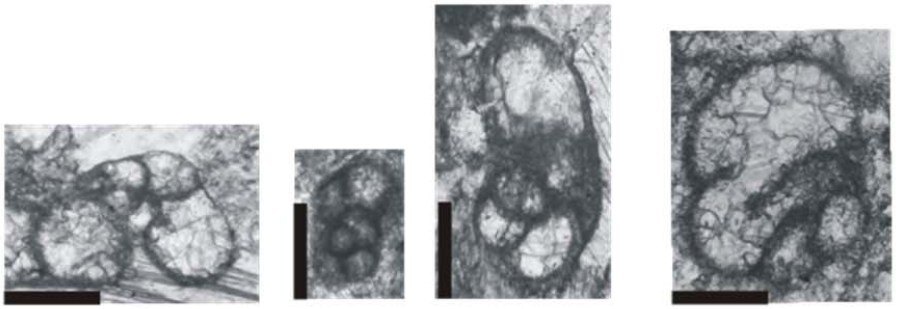

6 7 8 9

10

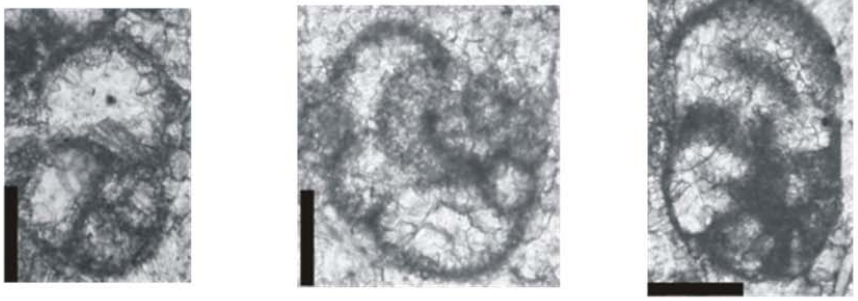

11 12 13

PLATE X

Figure 1: *Bradyina* sp., sample no: SC-90 (Scale bar: 0.2 mm)

Figure 2: *Bradyina* sp., sample no: SC-90 (Scale bar: 0.2 mm)

Figure 3 *Bradyina* sp., sample no: SC-90 (Scale bar: 0.2 mm)

Figure 4: *Bradyina* sp., sample no: SC-79 (Scale bar: 0.2 mm)

Figure 5: *Bradyina* sp., sample no: SC-86 (Scale bar: 0.2 mm)

Figure 6: *Bradyina* sp., sample no: SC-90 (Scale bar: 0.2 mm)

Figure 7: *Bradyina* sp., sample no: SC-86 (Scale bar: 0.2 mm)

Figure 8: *Bradyina* sp., sample no: SC-85 (Scale bar: 0.2 mm)

Figure 9: *Bradyina* sp., sample no: SC-83 (Scale bar: 0.2 mm)

Figure 10: *Bradyina* sp., sample no: SC-85 (Scale bar: 0.2 mm)

Figure 11: *Bibradya*? sp., sample no: SC-18 (Scale bar: 0.2 mm)

Figure 12: *Bibradya*? sp., sample no: SC-66 (Scale bar: 0.2 mm)

PLATE X

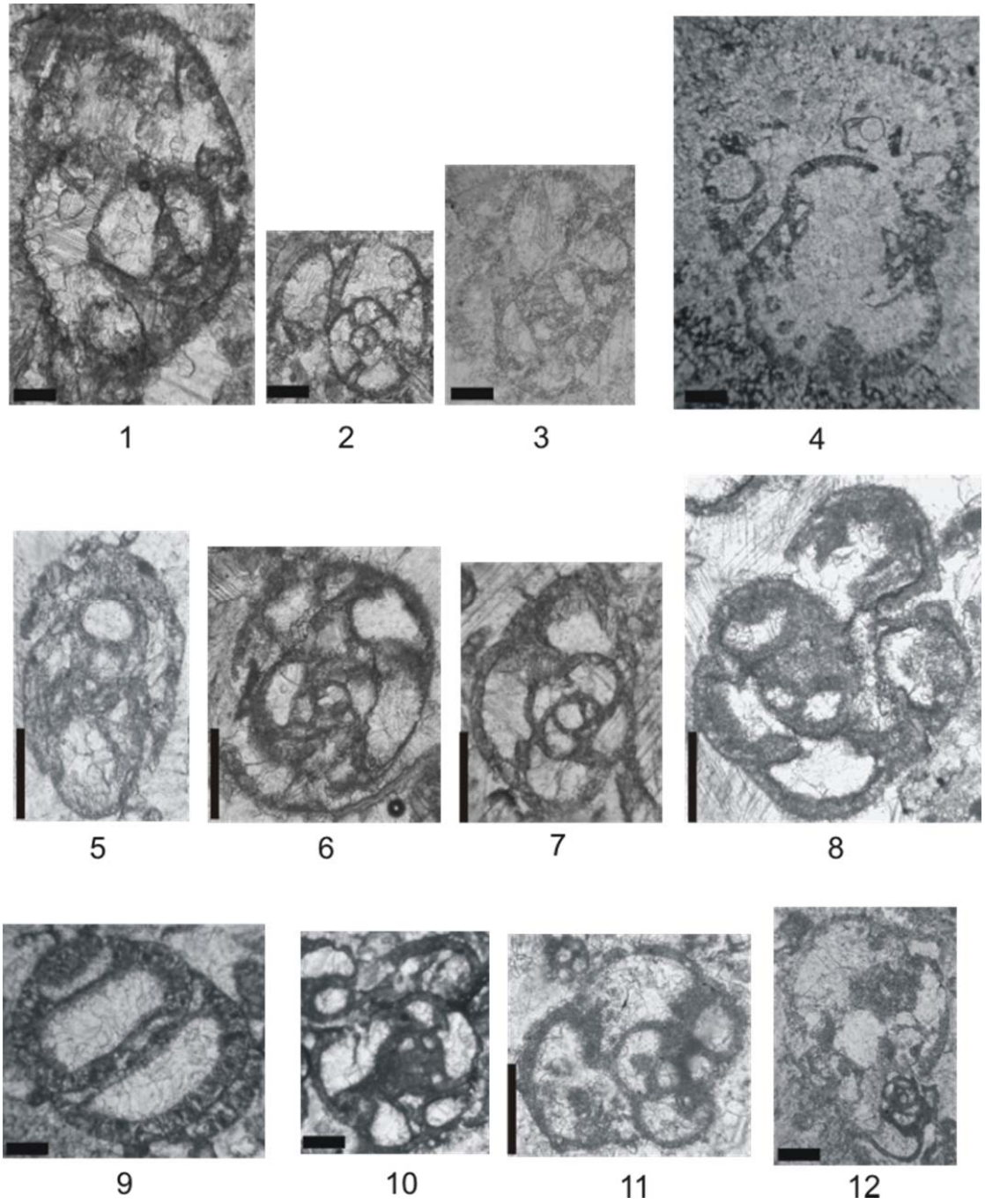

PLATE XI

Figure 1: *Globoendothyra* sp., sample no: SC-66 (Scale bar: 0.2 mm)

Figure 2: *Globoendothyra* sp., sample no: SC-57 (Scale bar: 0.2 mm)

Figure 3: *Globoendothyra* sp., sample no: SC-53 (Scale bar: 0.2 mm)

Figure 4: *Globoendothyra* sp., sample no: SC-82 (Scale bar: 0.2 mm)

Figure 5: *Globoendothyra* sp., sample no: SC-5 (Scale bar: 0.2 mm)

Figure 6: *Globoendothyra* sp., sample no: SC-6 (Scale bar: 0.2 mm)

Figure 7: *Globoendothyra* sp., sample no: SC-5 (Scale bar: 0.2 mm)

Figure 8: *Globoendothyra* sp., sample no: SC-20 (Scale bar: 0.2 mm)

Figure 9: *Globoendothyra* sp., sample no: SC-55 (Scale bar: 0.2 mm)

Figure 10: *Globoendothyra* sp., sample no: SC-75 (Scale bar: 0.2 mm)

Figure 11: *Banffella* sp. 1, sample no: SC-48 (Scale bar: 0.2 mm)

Figure 12: *Banffella* sp. 1, sample no: SC-46 (Scale bar: 0.2 mm)

Figure 13: *Banffella*? sp. 2, sample no: SC-47 (Scale bar: 0.2 mm)

Figure 14: *Banffella*? sp. 2, sample no: SC-48 (Scale bar: 0.2 mm)

Figure 15: *Banffella*? sp. 2, sample no: SC-55 (Scale bar: 0.2 mm)

PLATE XI

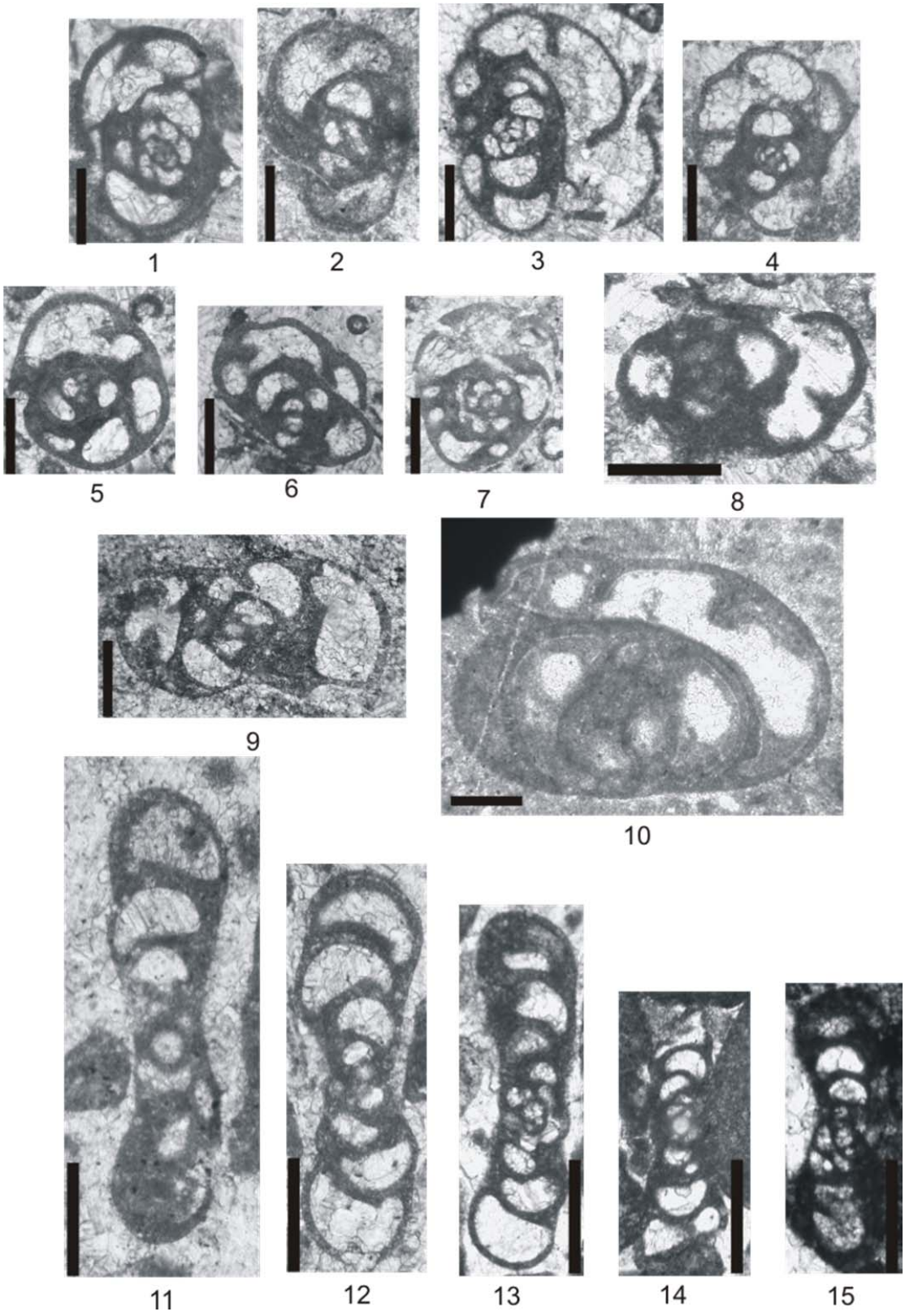

PLATE XII

Figure 1: *Omphalotis minima*, sample no: SC-3 (Scale bar: 0.2 mm)

Figure 2: *Omphalotis minima*, sample no: SC-5 (Scale bar: 0.2 mm)

Figure 3: *Omphalotis minima*, sample no: SC-5 (Scale bar: 0.2 mm)

Figure 4: *Omphalotis minima*, sample no: SC-3 (Scale bar: 0.2 mm)

Figure 5: *Omphalotis minima*, sample no: SC-1 (Scale bar: 0.2 mm)

Figure 6: *Omphalotis minima*, sample no: SC-3 (Scale bar: 0.2 mm)

Figure 7: *Omphalotis minima*, sample no: SC-3 (Scale bar: 0.2 mm)

Figure 8: *Omphalotis* sp., sample no: SC-4 (Scale bar: 0.2 mm)

Figure 9: *Omphalotis* sp., sample no: SC-6 (Scale bar: 0.2 mm)

Figure 10: *Omphalotis*? sp., sample no: SC-20 (Scale bar: 0.2 mm)

Figure 11: *Omphalotis*? sp., sample no: SC-20 (Scale bar: 0.2 mm)

Figure 12: *Omphalotis* sp., sample no: SC-74 (Scale bar: 0.2 mm)

Figure 13: *Endospiroplectammina* sp. 1, sample no: SC-4 (Scale bar: 0.2 mm)

Figure 14: *Endospiroplectammina* sp. 1, sample no: SC-5 (Scale bar: 0.2 mm)

Figure 15: *Endospiroplectammina* sp. 1, sample no: SC-25 (Scale bar: 0.2 mm)

Figure 16: *Endospiroplectammina* sp. 2, sample no: SC-28 (Scale bar: 0.2 mm)

PLATE XII

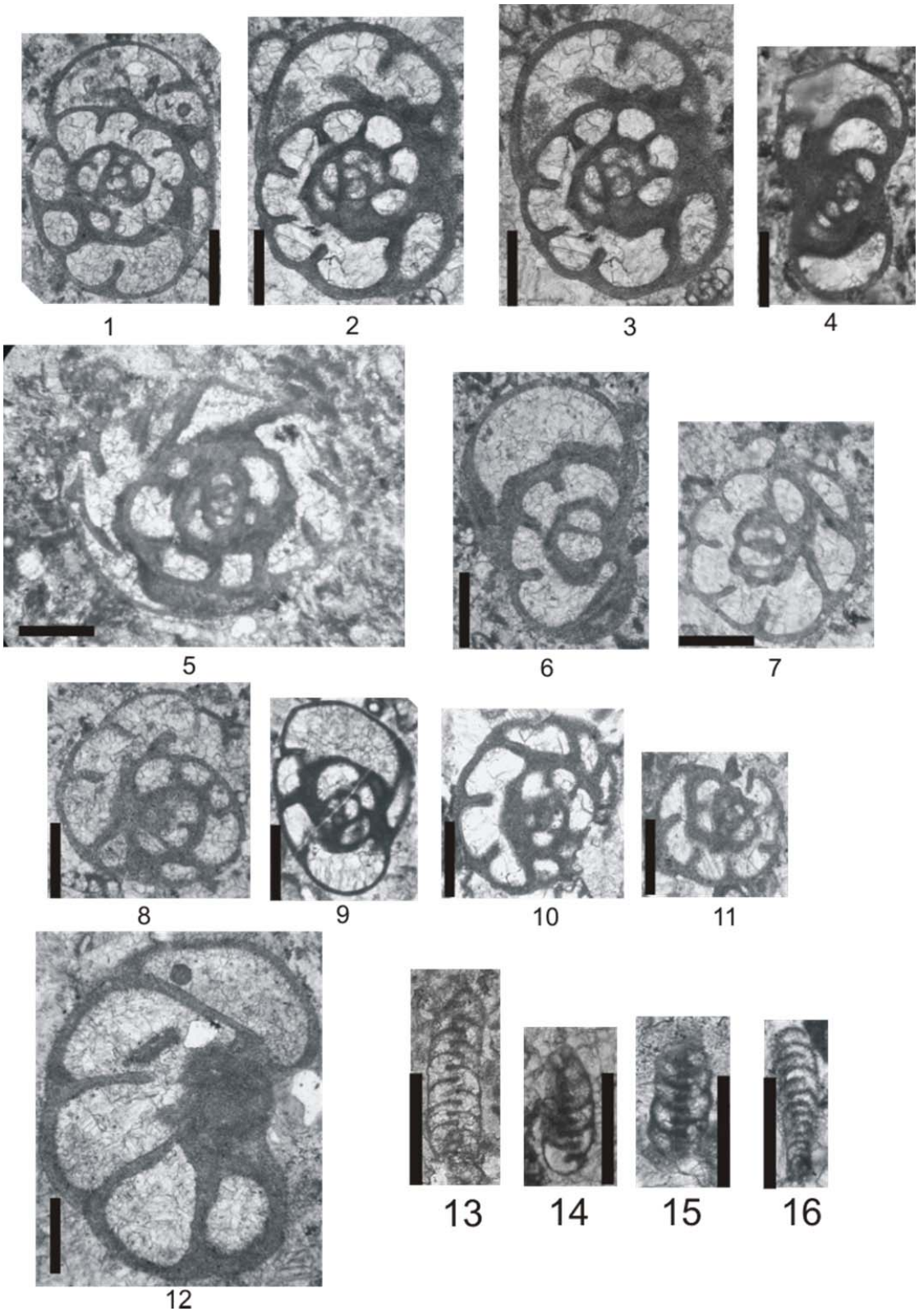

PLATE XIII

Figure 1: *Endothyra similis*, sample no: SC-78 (Scale bar: 0.1 mm)

Figure 2: *Endothyra similis*, sample no: SC-79 (Scale bar: 0.1 mm)

Figure 3: *Endothyra similis*, sample no: SC-67 (Scale bar: 0.1 mm)

Figure 4: *Priscella prisca*, sample no: 26 (Scale bar: 0.1 mm)

Figure 5: *Priscella prisca*, sample no: 50 (Scale bar: 0.1 mm)

Figure 6: *Priscella prisca*, sample no: 20 (Scale bar: 0.1 mm)

Figure 7: *Priscella prisca*, sample no: SC-60 (Scale bar: 0.1 mm)

Figure 8: *Priscella prisca*, sample no: SC-4 (Scale bar: 0.1 mm)

Figure 9: *Endothyra phrissa*, sample no: SC-79 (Scale bar: 0.1 mm)

Figure 10: *Endothyra archerbecki*, sample no: SC-79 (Scale bar: 0.1 mm)

Figure 11: *Endothyra archerbecki*, sample no: SC-82 (Scale bar: 0.1 mm)

Figure 12: *Endothyra* sp. 1, sample no: SC-83 (Scale bar: 0.1 mm)

Figure 13: *Endothyra* sp. 1, sample no: SC-86 (Scale bar: 0.1 mm)

Figure 14: *Endothyra excellens*, sample no: SC-87 (Scale bar: 0.2 mm)

Figure 15: *Endothyra cuneisepta*, sample no: SC-21 (Scale bar: 0.1 mm)

Figure 16: *Endothyra obselata*, sample no: SC-22 (Scale bar: 0.2 mm)

Figure 17: *Endothyra bowmani*, sample no: SC-2 (Scale bar: 0.1 mm)

Figure 18: *Endothyra bowmani*, sample no: SC-1 (Scale bar: 0.1 mm)

Figure 19: *Endothyra bowmani*, sample no: SC-24 (Scale bar: 0.1 mm)

Figure 20: *Endothyra* sp. , sample no: SC-74 (Scale bar: 0.1 mm)

Figure 21: *Endothyra* sp. , sample no: SC-78 (Scale bar: 0.1 mm)

Figure 22: *Endothyra* sp. , sample no: SC-66 (Scale bar: 0.1 mm)

Figure 23: *Endothyra* sp. 2, sample no: SC-80 (Scale bar: 0.1 mm)

Figure 24: *Endothyra* sp. 2, sample no: SC-84 (Scale bar: 0.1 mm)

Figure 25: *Endothyra* sp. , sample no: SC-1 (Scale bar: 0.1 mm)

Figure 26: *Endothyra* sp. , sample no: SC-21 (Scale bar: 0.1 mm)

PLATE XIII

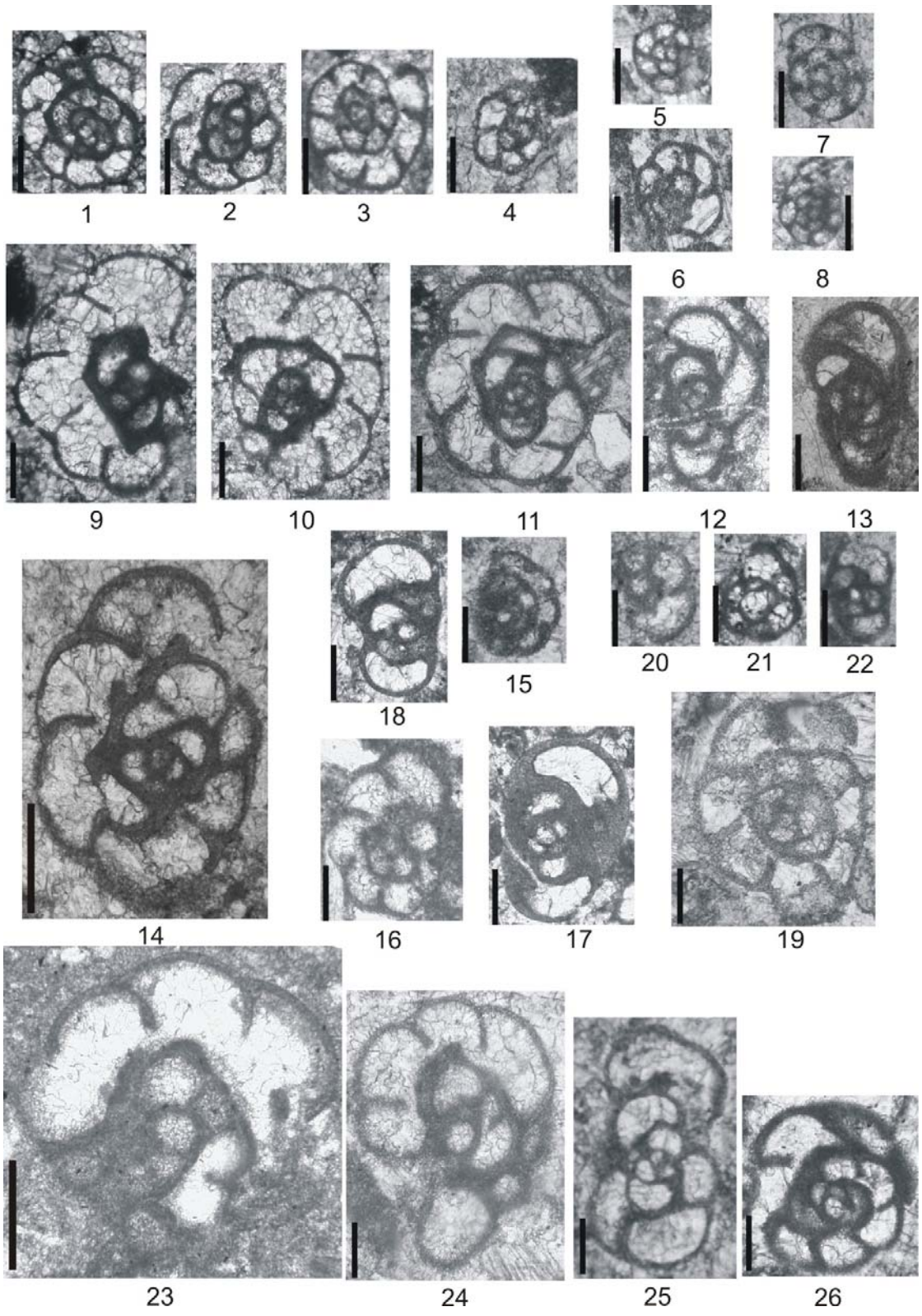

PLATE XIV

Figure 1: *Haplophragmella fallax*, sample no: SC-2 (Scale bar: 0.2 mm)

Figure 2: *Mikhaiolovella gracilis*, sample no: SC-34 (Scale bar: 0.2 mm)

Figure 3: *Mikhaiolovella* sp., sample no: SC-6 (Scale bar: 0.2 mm)

Figure 4: "*Endothyranopsis"* sp., sample no: SC-60 (Scale bar: 0.2 mm)

Figure 5: "*Endothyranopsis"* sp., sample no: SC-5 (Scale bar: 0.2 mm)

Figure 6: "*Endothyranopsis"* sp., sample no: SC-85 (Scale bar: 0.2 mm)

Figure 7: "*Endothyranopsis"* sp., sample no: SC-58 (Scale bar: 0.2 mm)

Figure 8: "*Endothyranopsis"* sp., sample no: SC-27 (Scale bar: 0.2 mm)

Figure 9: *Endothyranopsis* cf. *sphaerica*, sample no: SC-72 (Scale bar: 0.2 mm)

Figure 10: *Endothyranopsis* sp., sample no: SC-47 (Scale bar: 0.2 mm)

Figure 11: *Endothyranopsis* sp., sample no: SC-55 (Scale bar: 0.2 mm)

Figure 12: *Endothyranopsis* sp., sample no: SC-50 (Scale bar: 0.2 mm)

Figure 13: *Endothyranopsis hirosei*?, sample no: SC-5 (Scale bar: 0.2 mm)

Figure 14: *Endothyranopsis*? sp., sample no: SC-69 (Scale bar: 0.2 mm)

Figure 15: *Plectogyrnopsis convexa*, sample no: SC-2 (Scale bar: 0.2 mm)

Figure 16: *Plectogyrnopsis convexa*, sample no: SC-1 (Scale bar: 0.2 mm)

Figure 17: *Plectogyrnopsis convexa*, sample no: SC-6 (Scale bar: 0.2 mm)

Figure 18: *Plectogyrnopsis ampla*, sample no: SC-6 (Scale bar: 0.2 mm)

Figure 19: *Plectogyrnopsis ampla*, sample no: SC-3 (Scale bar: 0.2 mm)

Figure 20: *Plectogyrnopsis*? sp.1, sample no: SC-53 (Scale bar: 0.2 mm)

Figure 21: *Plectogyrnopsis* sp., sample no: SC-12 (Scale bar: 0.2 mm)

Figure 22: *Plectogyrnopsis* sp., sample no: SC-8 (Scale bar: 0.2 mm)

PLATE XIV

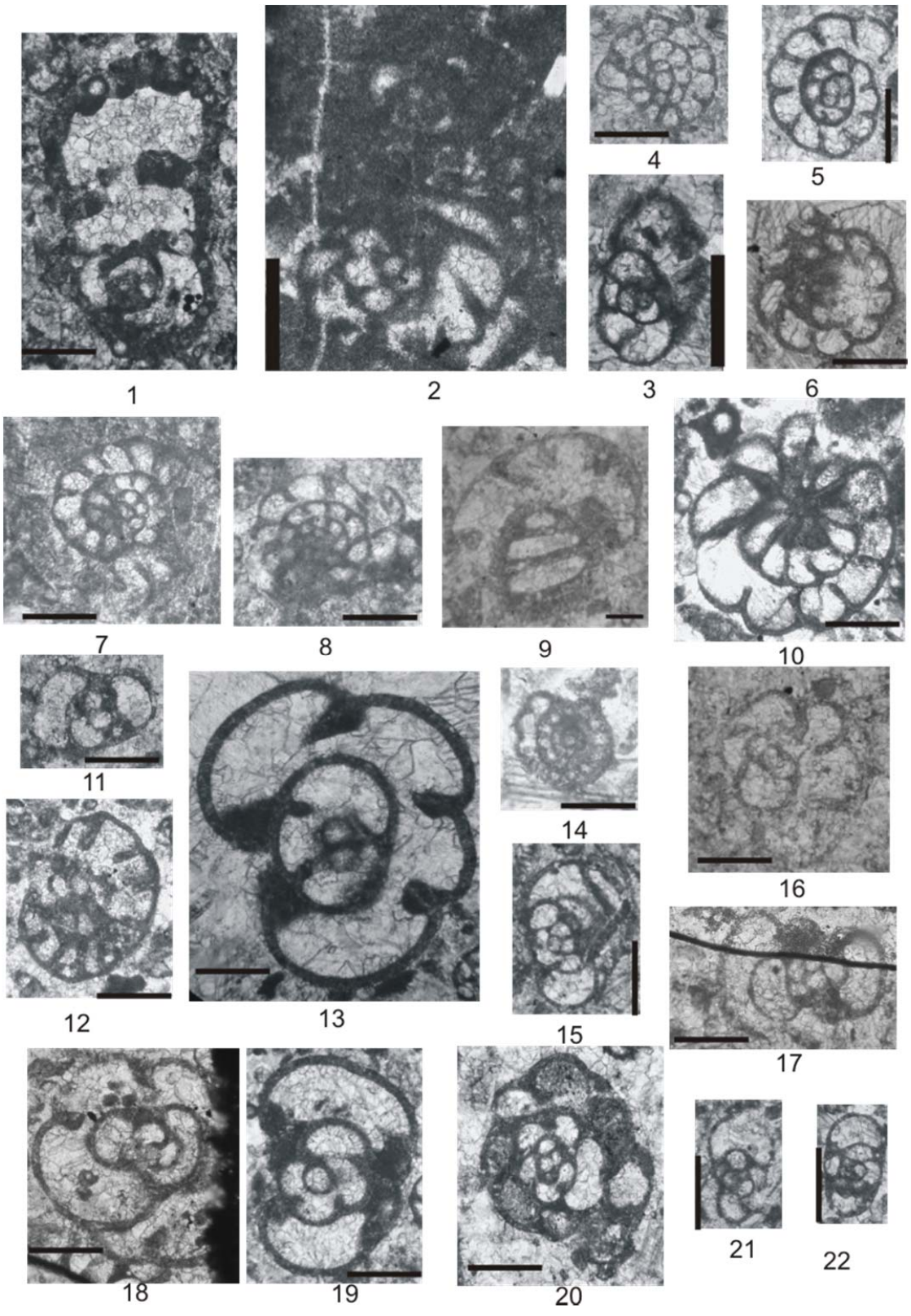

PLATE XV

Figure 1: *Endostaffella delicata*?, sample no: SC-5 (Scale bar: 0.1 mm)

Figure 2: *Endostaffella delicata*?, sample no: SC-2 (Scale bar: 0.1 mm)

Figure 3: *Endostaffella fucoides*, sample no: SC-21 (Scale bar: 0.1 mm)

Figure 4: *Endostaffella fucoides*?, sample no: SC-3 (Scale bar: 0.1 mm)

Figure 5: *Endostaffella fucoides*, sample no: SC- 17 (Scale bar: 0.1 mm)

Figure 6: *Endostaffella rozovskayae*, sample no: SC-69 (Scale bar: 0.1 mm)

Figure 7: *Endostaffella rozovskayae*, sample no: SC-8 (Scale bar: 0.1 mm)

Figure 8: *Endostaffella* sp. 1, sample no: SC-74 (Scale bar: 0.2 mm)

Figure 9: *Endostaffella* sp. 1, sample no: SC-4 (Scale bar: 0.2 mm)

Figure 10: *Endostaffella* sp. , sample no: SC-1 (Scale bar: 0.1 mm)

Figure 11: *Endostaffella* sp. , sample no: SC- 60 (Scale bar: 0.1 mm)

Figure 12: *Endostaffella* sp. , sample no: SC- 4 (Scale bar: 0.1 mm)

Figure 13: *Endostaffella* sp. , sample no: SC- 34 (Scale bar: 0.1 mm)

Figure 14: *Endostaffella* sp., sample no: SC-34 (Scale bar: 0.1 mm)

Figure 15: *Endostaffella* sp., sample no: SC- 62 (Scale bar: 0.1 mm)

Figure 16: *Endostaffella* sp. , sample no: SC-4 (Scale bar: 0.1 mm)

Figure 17: *Endostaffella* sp., sample no: SC-6 (Scale bar: 0.1 mm)

Figure 18: *Endostaffella* sp. , sample no: SC- 60 (Scale bar: 0.1 mm)

Figure 19: *Endostaffella* sp., sample no: SC- 13 (Scale bar: 0.1 mm)

Figure 20: *Endostaffella* sp., sample no: SC- 82 (Scale bar: 0.1 mm)

Figure 21: *Endostaffella* sp. , sample no: SC-11 (Scale bar: 0.1 mm)

PLATE XV

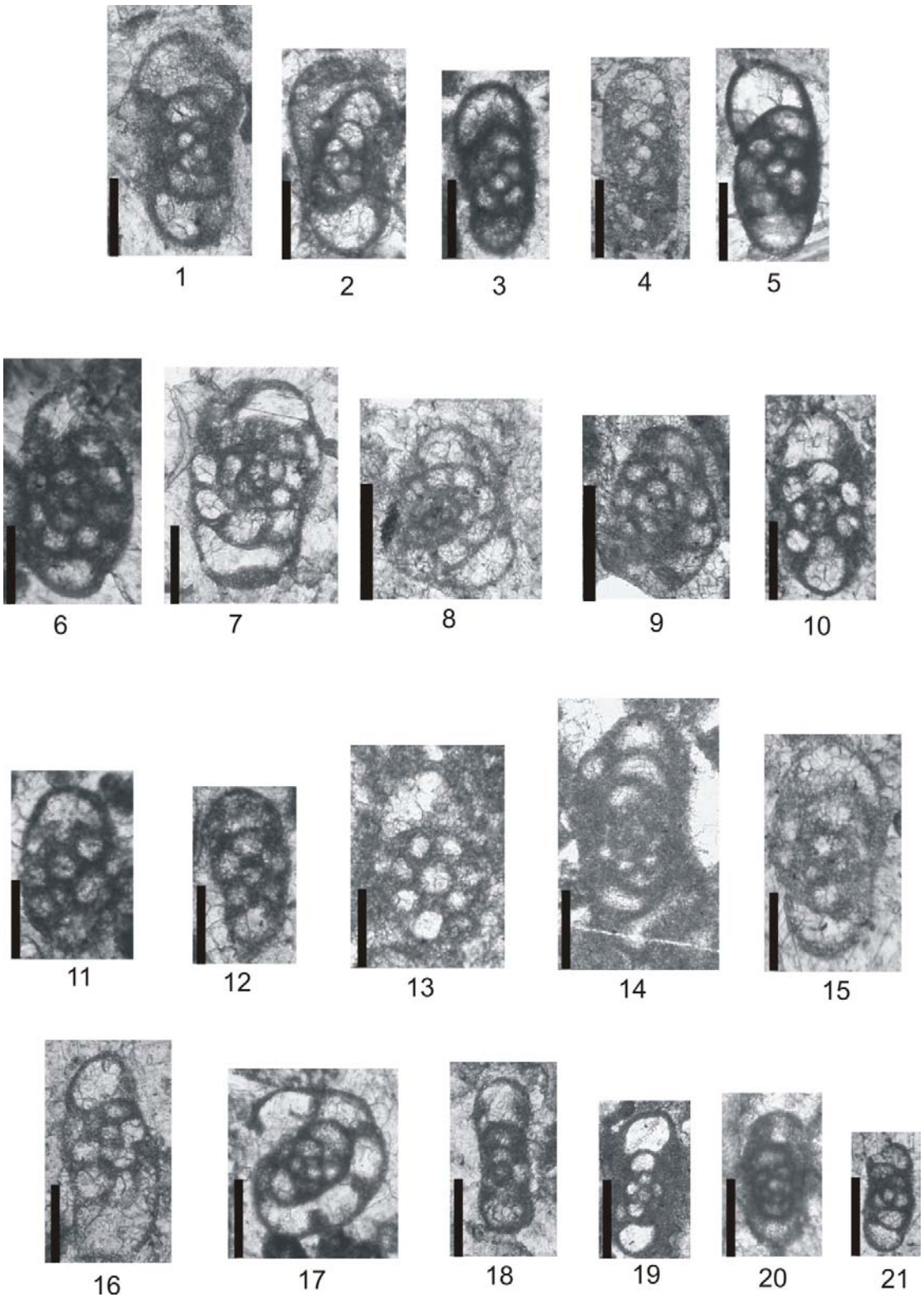

PLATE XVI

Figure 1: *Planoendothyra* sp., sample no: SC-35 (Scale bar: 0.2 mm)

Figure 2: *Planoendothyra* sp., sample no: SC-82 (Scale bar: 0.2 mm)

Figure 3: *Planoendothyra* sp., sample no: SC-7 (Scale bar: 0.2 mm)

Figure 4: *Planoendothyra* sp., sample no: SC-83 (Scale bar: 0.2 mm)

Figure 5: *Planoendothyra* sp., sample no: SC-86 (Scale bar: 0.2 mm)

Figure 6: *Planoendothyra* sp., sample no: SC-27 (Scale bar: 0.2 mm)

Figure 7: *Euxinita efremovi*, sample no: SC-20 (Scale bar: 0.2 mm)

Figure 8*:* *Euxinita efremovi*?, sample no: SC-71 (Scale bar: 0.2 mm)

Figure 9: *Loeblichia minima*, sample no: SC-44 (Scale bar: 0.2 mm)

Figure 10: *Loeblichia* ? sp., sample no: SC-14 (Scale bar: 0.2 mm)

PLATE XVI

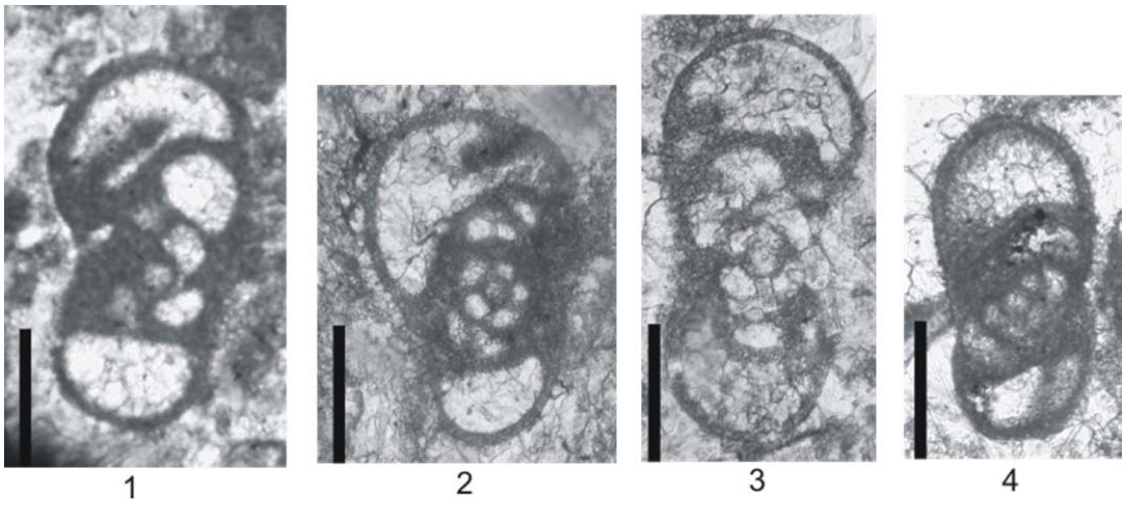

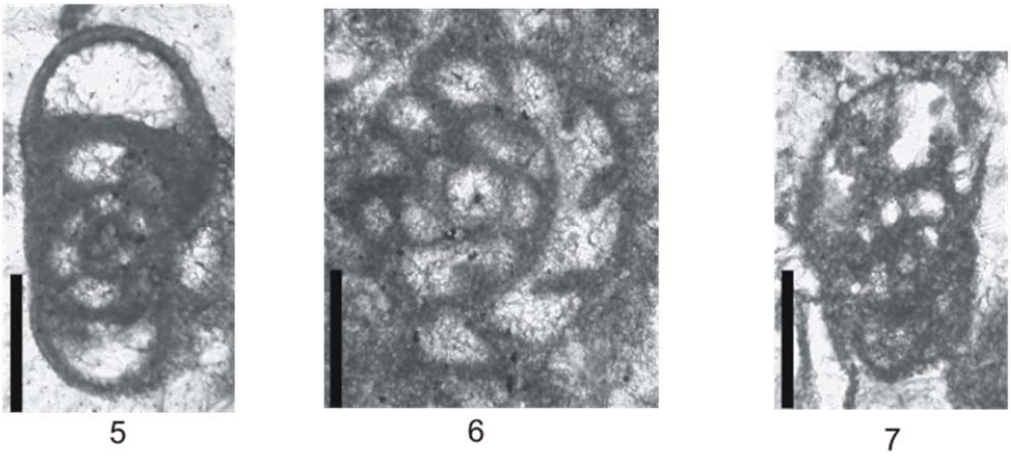

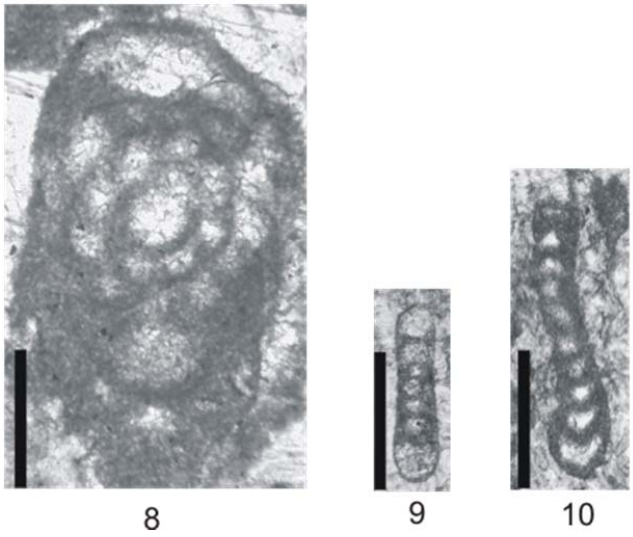

PLATE XVII

Figure 1: *Pojarkovella guadiatensis*, sample no: SC-44 (Scale bar: 0.2 mm)

Figure 2: *Pojarkovella guadiatensis*, sample no: SC-53 (Scale bar: 0.2 mm)

Figure 3: *Pojarkovella guadiatensis*, sample no: SC-68 (Scale bar: 0.2 mm)

Figure 4: *Pojarkovella guadiatensis*, sample no: SC-61 (Scale bar: 0.2 mm)

Figure 5: *Pojarkovella* cf. *guadiatensis*, sample no: SC-54 (Scale bar: 0.2 mm)

Figure 6: *Pojarkovella* ex gr. *guadiatensis*, sample no: SC-20 (Scale bar: 0.2 mm)

Figure 7: *Pojarkovella* ex gr. *guadiatensis*, sample no: SC-21 (Scale bar: 0.2 mm)

Figure 8: *Pojarkovella* sp., sample no: SC-59 (Scale bar: 0.1 mm)

Figure 9: *Pojarkovella* sp., sample no: SC-44 (Scale bar: 0.1 mm)

Figure 10: *Pojarkovella* sp., sample no: SC-47 (Scale bar: 0.1 mm)

Figure 11: *Pojarkovella* sp., sample no: SC-6/116

Figure 12: *Pojarkovella* sp., sample no: SC-22 (Scale bar: 0.2 mm)

Figure 13: *Pojarkovella* sp., sample no: SC-68 (Scale bar: 0.2 mm)

Figure 14: *Pojarkovella* sp., sample no: SC-54 (Scale bar: 0.2 mm)

Figure 15: *Pojarkovella* sp., sample no: SC-21 (Scale bar: 0.2 mm)

Figure 16: *Pojarkovella* sp., sample no: SC-22 (Scale bar: 0.2 mm)

Figure 17: *Pojarkovella* sp., sample no: SC-13 (Scale bar: 0.2 mm)

PLATE XVII

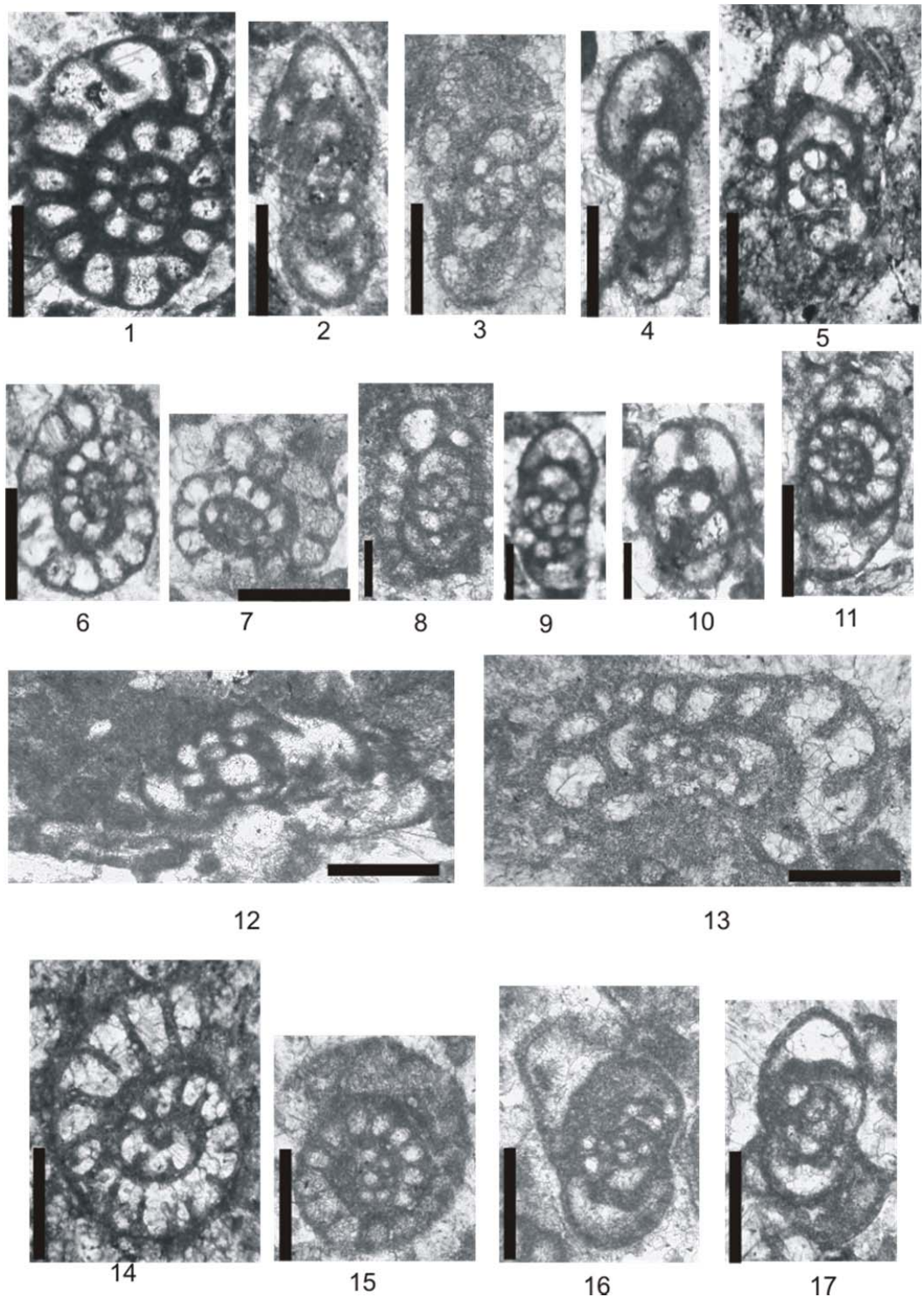

PLATE XVIII

Figure 1: *Pojarkovella nibelis*, sample no: SC-1 (Scale bar: 0.2 mm)

Figure 2: *Pojarkovella nibelis*, sample no: SC-51 (Scale bar: 0.2 mm)

Figure 3: *Pojarkovella nibelis*, sample no: SC-6 (Scale bar: 0.2 mm)

Figure 4: *Pojarkovella nibelis*, sample no: SC-3 (Scale bar: 0.2 mm)

Figure 5: *Pojarkovella nibelis*, sample no: SC-49 (Scale bar: 0.2 mm)

Figure 6: *Pojarkovella nibelis*, sample no: SC-7 (Scale bar: 0.2 mm)

Figure 7: *Pojarkovella nibelis*, sample no: SC-8 (Scale bar: 0.2 mm)

Figure 8: *Pojarkovella nibelis*, sample no: SC-53 (Scale bar: 0.2 mm)

Figure 9: *Pojarkovella nibelis*, sample no: SC-1 (Scale bar: 0.2 mm)

Figure 10: *Pojarkovella* sp. 1, sample no: SC-8 (Scale bar: 0.2 mm)

Figure 11: *Pojarkovella* sp. 1, sample no: SC-6 (Scale bar: 0.2 mm)

Figure 12: *Pojarkovella* sp. 2, sample no: SC-51 (Scale bar: 0.2 mm)

Figure 13: *Pojarkovella* sp. 2, sample no: SC-51 (Scale bar: 0.2 mm)

PLATE XVIII

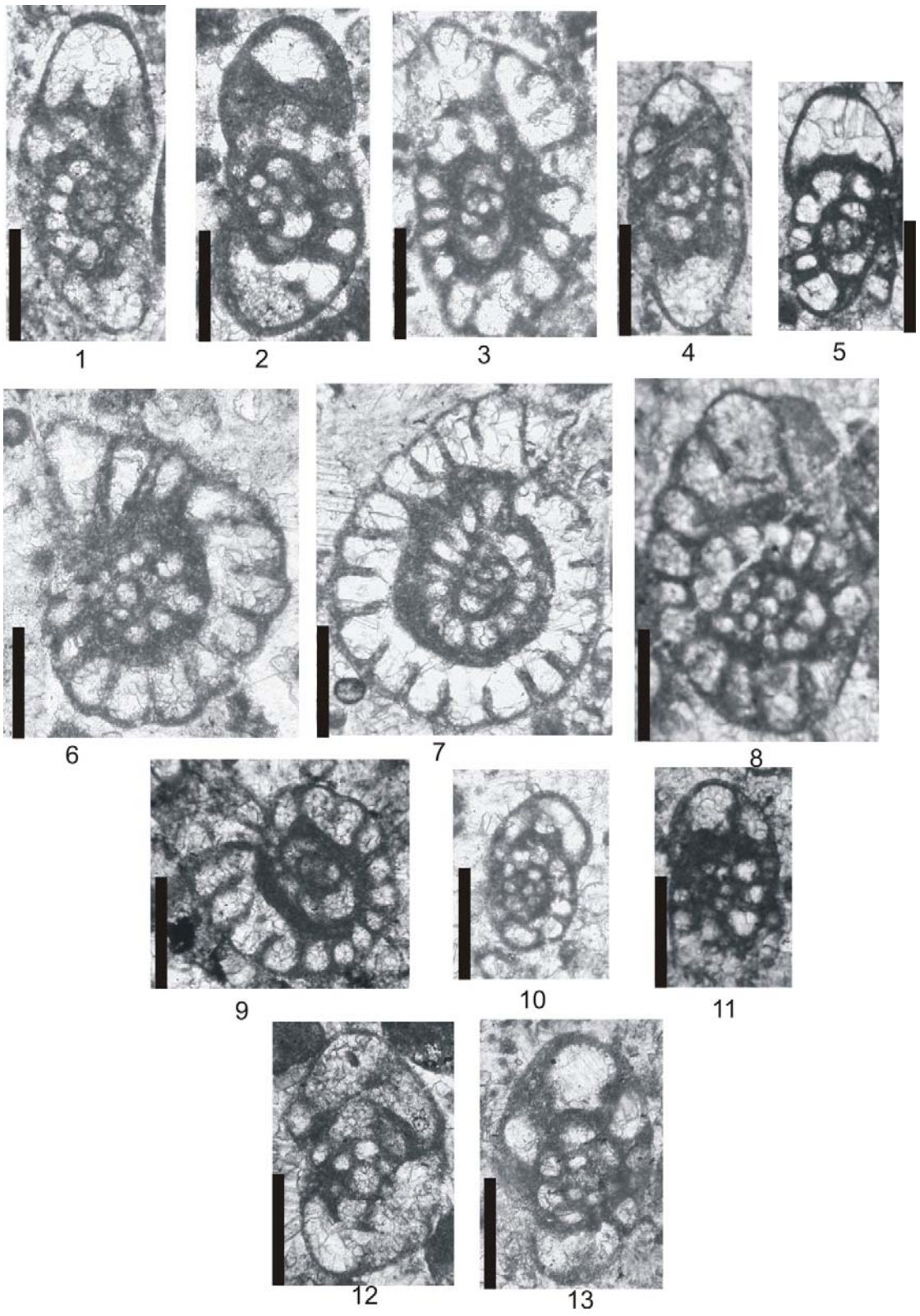

PLATE XIX

Figure 1: *Vissarionovella tujmasensis*, sample no: SC-5 (Scale bar: 0.2 mm)

Figure 2: *Vissarionovella tujmasensis*, sample no: SC-4 (Scale bar: 0.2 mm)

Figure 3: *Vissarionovella tujmasensis*, sample no: SC-5 (Scale bar: 0.2 mm)

Figure 4: *Vissarionovella tujmasensis*, sample no: SC-21 (Scale bar: 0.2 mm)

Figure 5: *Vissarionovella tujmasensis*, sample no: SC-4 (Scale bar: 0.2 mm)

Figure 6: *Vissarionovella tujmasensis*, sample no: SC-33 (Scale bar: 0.2 mm)

Figure 7: *Vissarionovella tujmasensis*, sample no: SC-24 (Scale bar: 0.2 mm)

Figure 8: *Vissarionovella* sp., sample no: SC-33 (Scale bar: 0.2 mm)

Figure 9: *Vissarionovella* sp. 1, sample no: SC-71 (Scale bar: 0.2 mm)

Figure 10: *Vissarionovella* sp. 1, sample no: SC-21 (Scale bar: 0.2 mm)

Figure 11: *Vissarionovella* sp. 1, sample no: SC-4 (Scale bar: 0.2 mm)

Figure 12: *Vissarionovella* sp 1., sample no: SC-5 (Scale bar: 0.2 mm)

Figure 13: *Vissarionovella* sp., sample no: SC-24 (Scale bar: 0.2 mm)

Figure 14: *Vissarionovella* sp., sample no: SC-20 (Scale bar: 0.2 mm)

Figure 15: *Vissarionovella* sp., sample no: SC-21 (Scale bar: 0.2 mm)

PLATE XIX

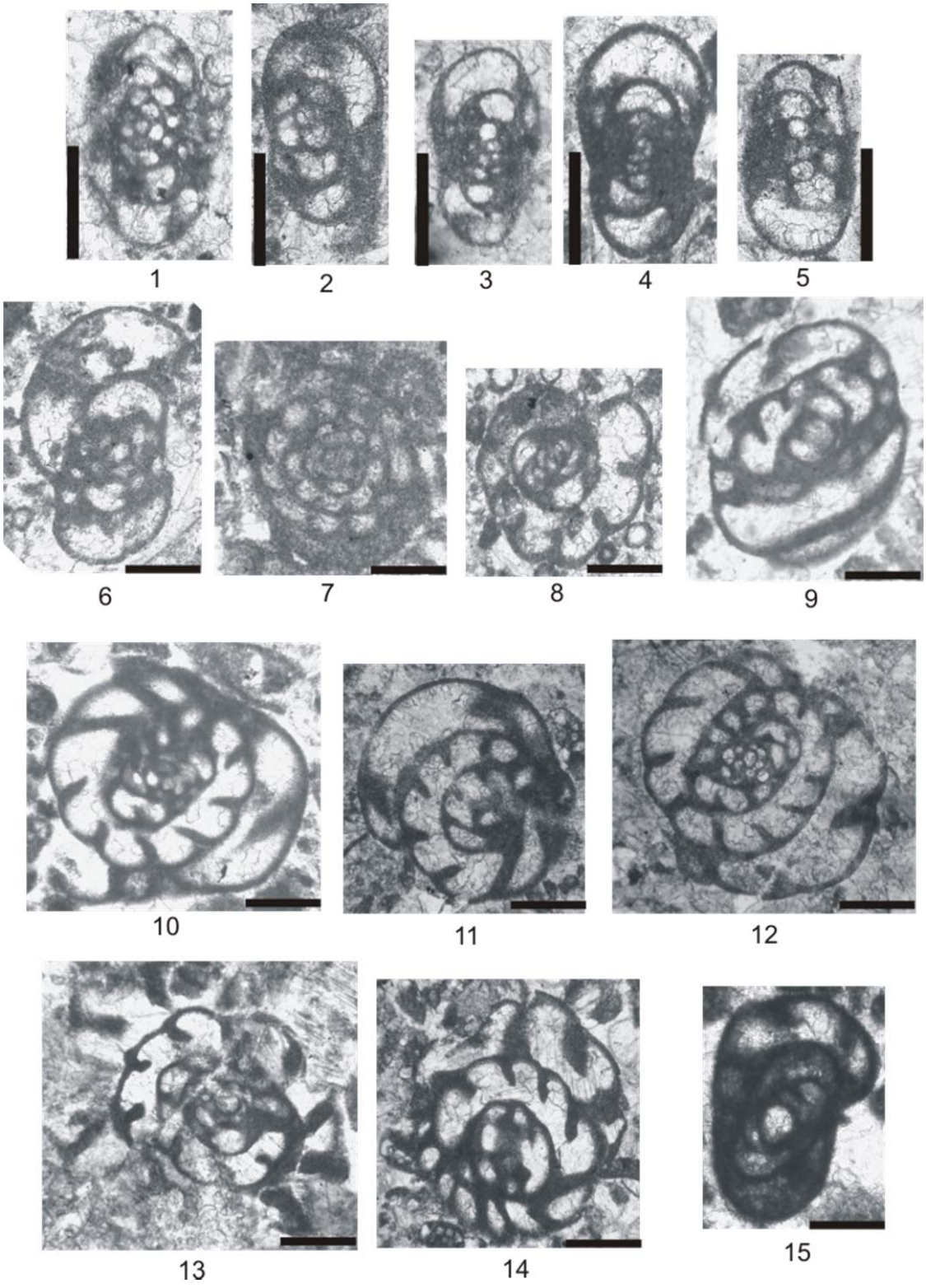

PLATE XX

Figure 1: *Condrustella* sp., sample no: SC-1 (Scale bar: 0.2 mm)

Figure 2: *Condrustella* sp., sample no: SC-3 (Scale bar: 0.2 mm)

Figure 3: *Condrustella* sp., sample no: SC-5 (Scale bar: 0.2 mm)

Figure 4: *Condrustella* sp., sample no: SC-5 (Scale bar: 0.2 mm)

Figure 5: *Mistinia* sp., sample no: SC-28 (Scale bar: 0.2 mm)

Figure 6: *Mistinia* sp., sample no: SC-22 (Scale bar: 0.2 mm)

Figure 7: *Forschia parvula*, sample no: SC-47 (Scale bar: 0.1 mm)

Figure 8: *Forschia subangulata,* sample no: SC-3 (Scale bar: 0.2 mm)

Figure 9: *Forschia subangulata*, sample no: SC-9 (Scale bar: 0.2 mm)

Figure 10: *Forschia subangulata*, sample no: SC-1 (Scale bar: 0.2 mm)

Figure 11: *Forschia* sp., sample no: SC-50 (Scale bar: 0.2 mm)

Figure 12: *Forschia* sp., sample no: SC-46 (Scale bar: 0.2 mm)

Figure 13: *Forschia* sp., sample no: SC-1 (Scale bar: 0.2 mm)

Figure 14: F*orschiella* sp.1, sample no: SC-50 (Scale bar: 0.2 mm)

Figure 15: F*orschiella* sp.1, sample no: SC-48 (Scale bar: 0.2 mm)

Figure 16: F*orschiella* sp.2, sample no: SC-35 (Scale bar: 0.2 mm)

Figure 17: F*orschiella* sp., sample no: SC-2 (Scale bar: 0.2 mm)

PLATE XX

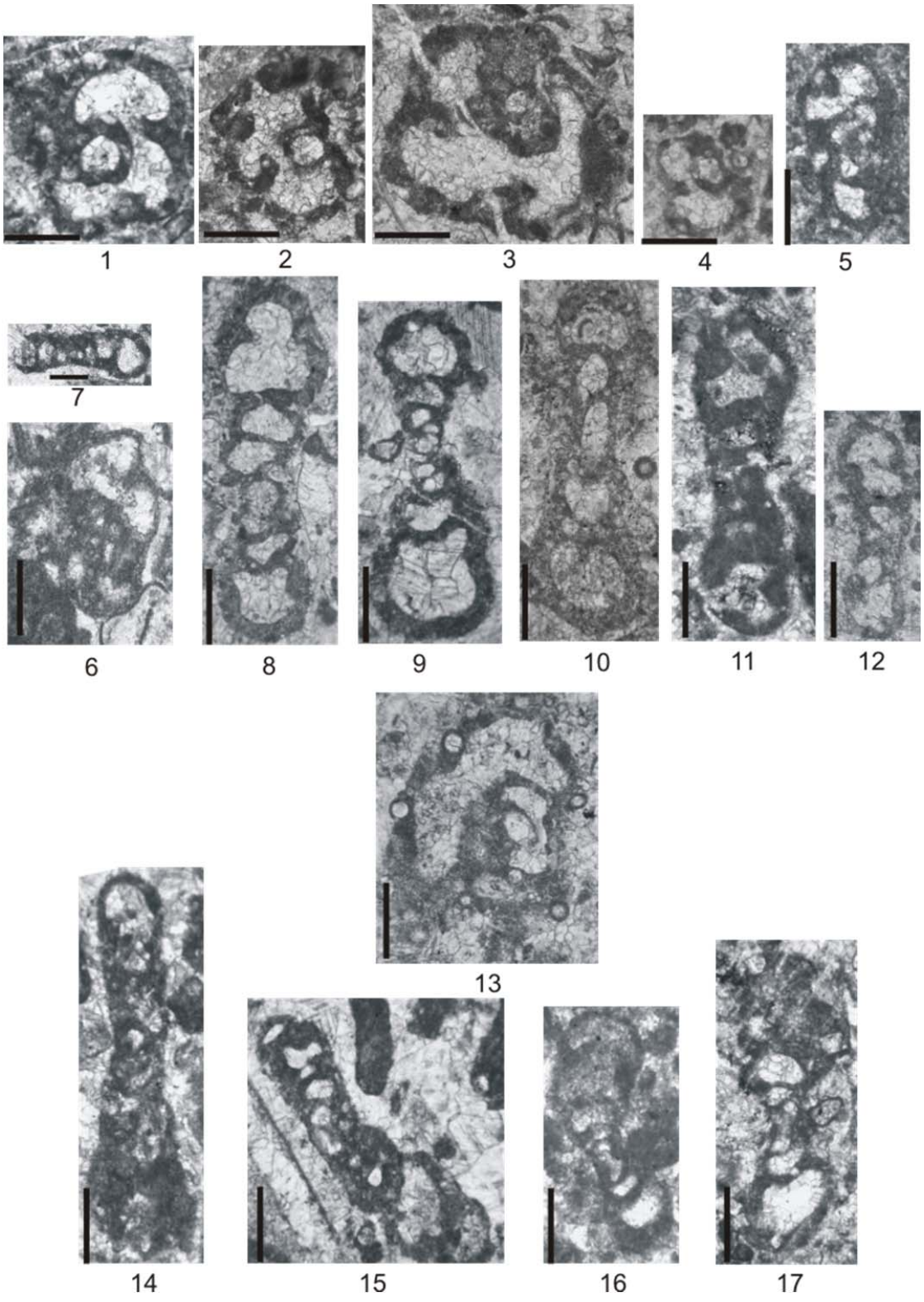

PLATE XXI

Figure 1: *Eostaffella ikensis*, sample no: SC-49 (Scale bar: 0.2 mm)

Figure 2: *Eostaffella ikensis*, sample no: SC-82 (Scale bar: 0.2 mm)

Figure 3: *Eostaffella ikensis*, sample no: SC-3 (Scale bar: 0.2 mm)

Figure 4: *Eostaffella ikensis*, sample no: SC-82 (Scale bar: 0.2 mm)

Figure 5: *Eostaffella ikensis*, sample no: SC-5 (Scale bar: 0.2 mm)

Figure 6: *Eostaffella ikensis*, sample no: SC-82 (Scale bar: 0.2 mm)

Figure 7: *Eostaffella ikensis*, sample no: SC-6 (Scale bar: 0.2 mm)

Figure 8: *Eostaffella tenebrosa*, sample no: SC-85 (Scale bar: 0.2 mm)

PLATE XXI

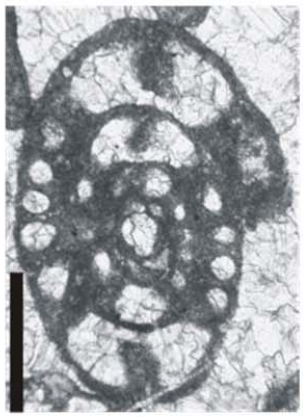

1

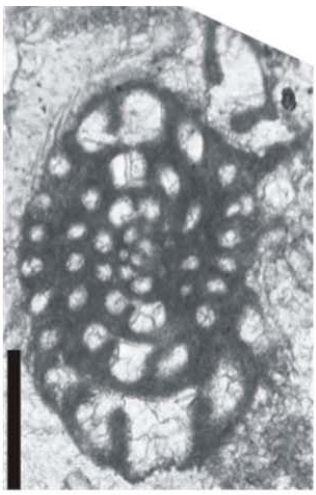

2

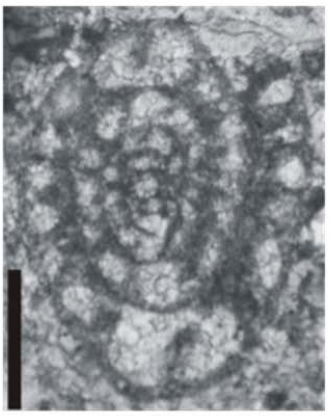

3

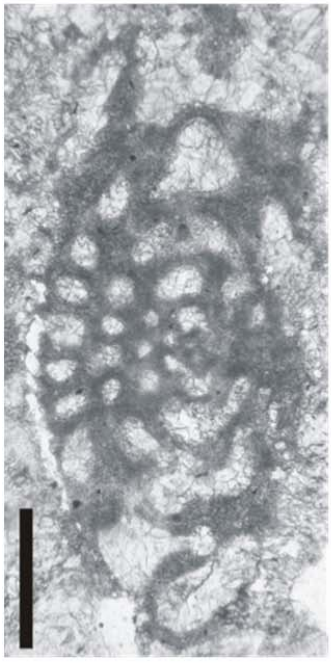

4

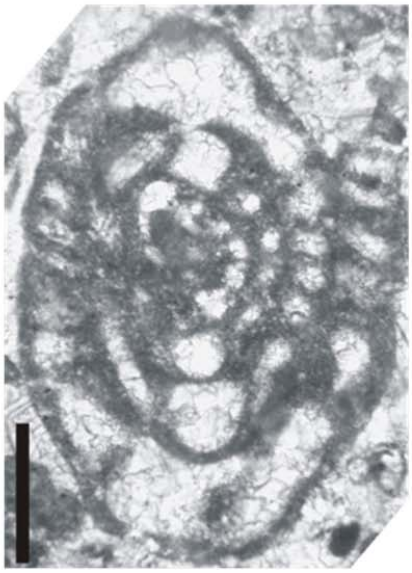

5

6

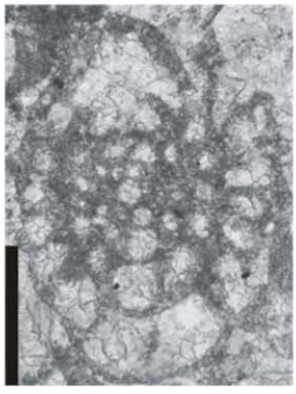

7

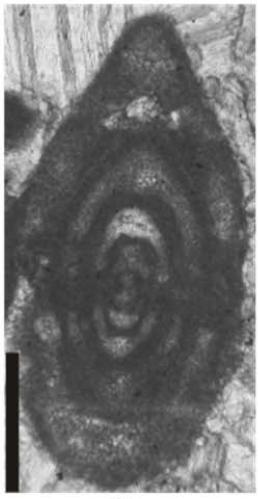

8

PLATE XXII

Figure 1: *Eostaffella parastruvei*, sample no: SC-54 (Scale bar: 0.2 mm)

Figure 2: *Eostaffella parastruvei*, sample no: SC-33 (Scale bar: 0.2 mm)

Figure 3: *Eostaffella parastruvei*, sample no: SC-5 (Scale bar: 0.2 mm)

Figure 4: *Eostaffella parastruvei*, sample no: SC-2 (Scale bar: 0.2 mm)

Figure 5: *Eostaffella parastruvei*, sample no: SC-47 (Scale bar: 0.2 mm)

Figure 6: *Eostaffella parastruvei*, sample no: SC-12 (Scale bar: 0.2 mm)

Figure 7: *Eostaffella parastruvei*, sample no: SC-50 (Scale bar: 0.2 mm)

Figure 8: *Eostaffella parastruvei*, sample no: SC- 47 (Scale bar: 0.2 mm)

Figure 9: *Eostaffella parastruvei*, sample no: SC-57 (Scale bar: 0.2 mm)

Figure10: *Eostaffella parastruvei*, sample no: SC-47 (Scale bar: 0.2 mm)

Figure 11: *Eostaffella parastruvei*, sample no: SC-2 (Scale bar: 0.2 mm)

Figure 12: *Eostaffella mosquensis*, sample no: SC-46 (Scale bar: 0.2 mm)

Figure 13: *Eostaffella compacta*, sample no: SC-59 (Scale bar: 0.2 mm)

Figure 14: *Eostaffella compacta*, sample no: SC-47 (Scale bar: 0.2 mm)

PLATE XXII

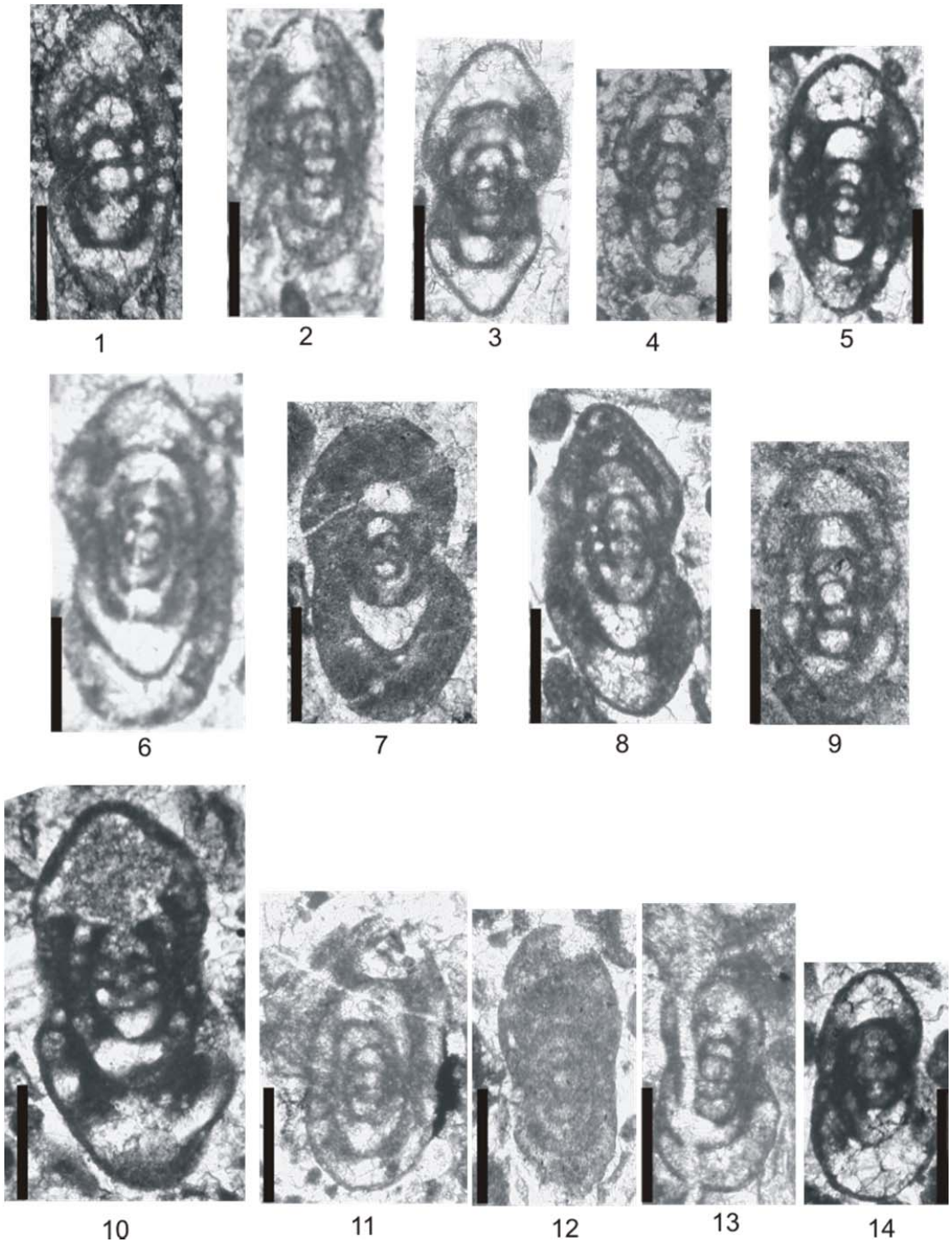

PLATE XXIII

Figure 1: *Eostaffella ovoidea*, sample no: SC-79 (Scale bar: 0.1 mm)

Figure 2: *Eostaffella ovoidea*, sample no: SC-85 (Scale bar: 0.1 mm)

Figure 3: *Eostaffella ovoidea*, sample no: SC-89 (Scale bar: 0.1 mm)

Figure 4: *Eostaffella* cf. *ovoidea*, sample no: SC-59 (Scale bar: 0.1 mm)

Figure 5: *Eostaffella* cf. *ovoidea*, sample no: SC-79 (Scale bar: 0.1 mm)

Figure 6: *Eostaffella* cf. *ovoidea*, sample no: SC-78 (Scale bar: 0.1 mm)

Figure 7: *Eostaffella ovesa*?, sample no: SC-84 (Scale bar: 0.1 mm)

Figure 8: *Eostaffella pseudostruvei*, sample no: SC-86 (Scale bar: 0.1 mm)

Figure 9: *Eostaffella pseudostruvei*, sample no: SC-91 (Scale bar: 0.1 mm)

Figure 10: *Eostaffella pseudostruvei*, sample no: SC-82 (Scale bar: 0.1 mm)

Figure 11: *Eostaffella* sp. 1, sample no: SC-505 (Scale bar: 0.1 mm)

Figure 12: *Eostaffella* sp. 1, sample no: SC-6 (Scale bar: 0.1 mm)

Figure 13: *Eostaffella* sp. 1, sample no: SC-78 (Scale bar: 0.1 mm)

Figure 14 : *Eostaffella* sp. 1, sample no: SC-20 (Scale bar: 0.1 mm)

Figure 15: *Eostaffella* sp. 2, sample no: SC-51 (Scale bar: 0.1 mm)

Figure 16: *Eostaffella* sp. 2, sample no: SC-50 (Scale bar: 0.1 mm)

Figure 17: *Eostaffella* sp 3, sample no: SC-48 (Scale bar: 0.1 mm)

Figure 18: *Eostaffella*? sp., sample no: SC-1 (Scale bar: 0.1 mm)

Figure 19: *Eostaffella*? sp., sample no: SC-57 (Scale bar: 0.1 mm)

Figure 20: *Eostaffella* sp., sample no: SC-57 (Scale bar: 0.1 mm)

Figure 21: *Eostaffella* sp., sample no: SC-20 (Scale bar: 0.1 mm)

Figure 22: *Eostaffella* sp., sample no: SC-2 (Scale bar: 0.1 mm)

Figure 23: *Eostaffella* sp., sample no: SC-2 (Scale bar: 0.1 mm)

Figure 24: *Eostaffella* sp., sample no: SC-2 (Scale bar: 0.1 mm)

Figure 25: *Eostaffella* sp., sample no: SC-50 (Scale bar: 0.1 mm)

Figure 26: *Eostaffella* sp., sample no: SC-21 (Scale bar: 0.1 mm)

PLATE XXIII

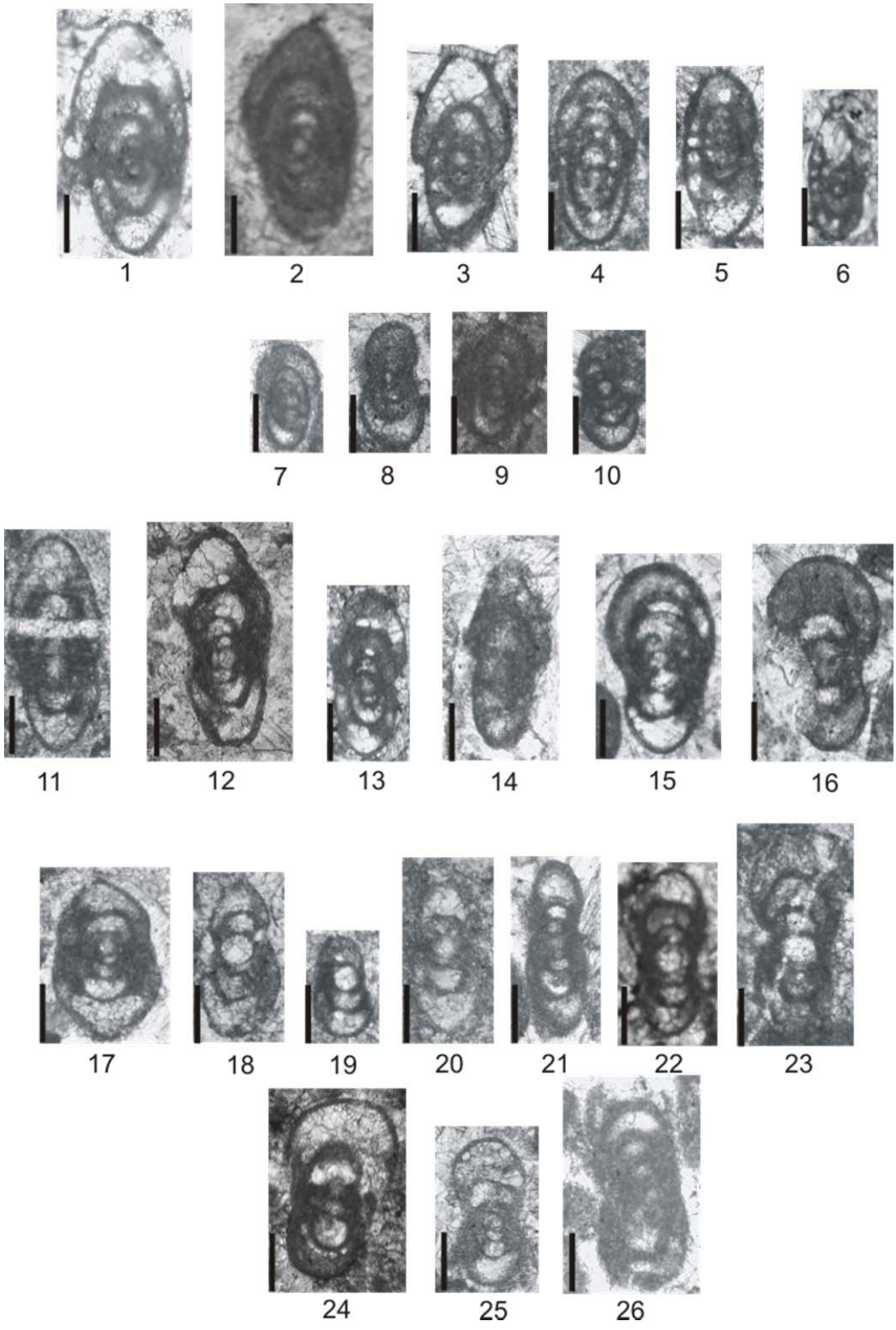

PLATE XXIV

Figure 1: *Eostaffella* sp.4, sample no: SC-35 (Scale bar: 0.1 mm)

Figure 2: *Eostaffella* sp.4, sample no: SC-57 (Scale bar: 0.1 mm)

Figure 3: *Eostaffella* sp.4, sample no: SC-1 (Scale bar: 0.1 mm)

Figure 4: *Eostaffella* sp.4, sample no: SC-2 (Scale bar: 0.1 mm)

Figure 5: *Eostaffella* sp.4, sample no: SC-54 (Scale bar: 0.1 mm)

Figure 6: *Eostaffella* sp.5, sample no: SC-35 (Scale bar: 0.1 mm)

Figure 7: *Eostaffella* sp.5, sample no: SC-49 (Scale bar: 0.1 mm)

Figure 8: *Eostaffella* sp.5, sample no: SC-46 (Scale bar: 0.1 mm)

Figure 9: *Eostaffella* sp.5, sample no: SC-3 (Scale bar: 0.1 mm)

Figure 10: *Eostaffella* sp.5, sample no: SC-56 (Scale bar: 0.1 mm)

Figure 11: *Eostaffella* sp.5, sample no: SC-20 (Scale bar: 0.1 mm)

Figure 12: *Eostaffella* sp.6, sample no: SC-49 (Scale bar: 0.2 mm)

Figure 13: *Eostaffella* sp.6, sample no: SC-45 (Scale bar: 0.2 mm)

Figure 14: *Eostaffella* sp.6, sample no: SC-31 (Scale bar: 0.2 mm)

Figure 15: *Eostaffella* sp.6, sample no: SC-49 (Scale bar: 0.2 mm)

PLATE XXIV

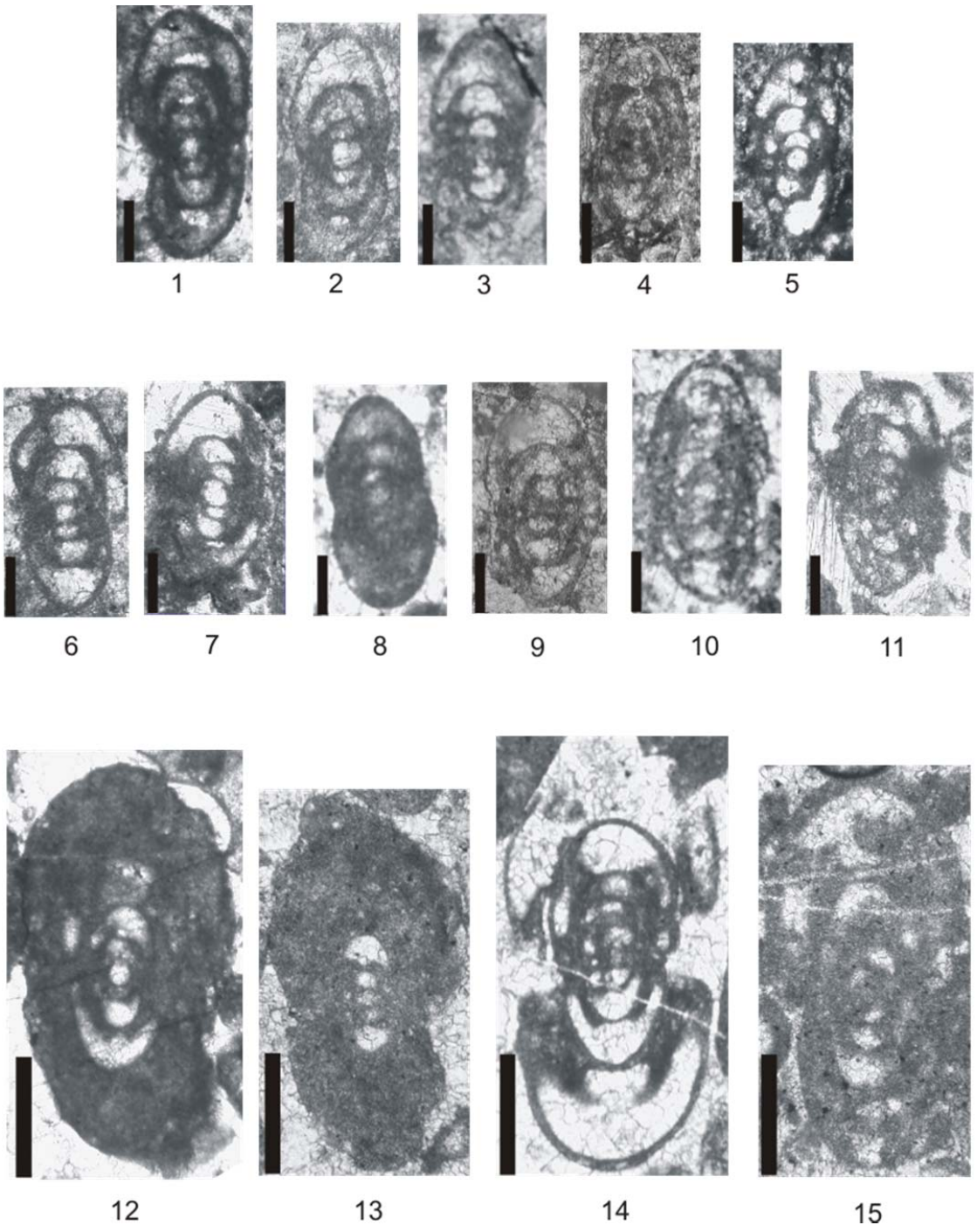

PLATE XXV

Figure 1: *Eostaffella* sp.6., sample no: SC-49 (Scale bar: 0.2 mm)

Figure 2: *Eostaffella* sp.6, sample no: SC-33 (Scale bar: 0.2 mm)

Figure 3: *Eostaffella*? sp7., sample no: SC-4 (Scale bar: 0.1 mm)

Figure 4: *Eostaffella*? sp7., sample no: SC-2 (Scale bar: 0.1 mm)

Figure 5: *Eostaffella*? sp7., sample no: SC-2 (Scale bar: 0.1 mm)

Figure 6: *Eostaffella* sp., sample no: SC-86a (Scale bar: 0.2 mm)

Figure 7: *Eostaffella* sp., sample no: SC-2 (Scale bar: 0.2 mm)

Figure 8: *Eostaffella* sp., sample no: SC-1 (Scale bar: 0.2 mm)

Figure 9: *Eostaffella* sp., sample no: SC-79 (Scale bar: 0.1 mm)

Figure 10: *Eostaffella* sp., sample no: SC-6 (Scale bar: 0.1 mm)

Figure 11: *Eostaffella* sp., sample no: SC-84 (Scale bar: 0.1 mm)

PLATE XXV

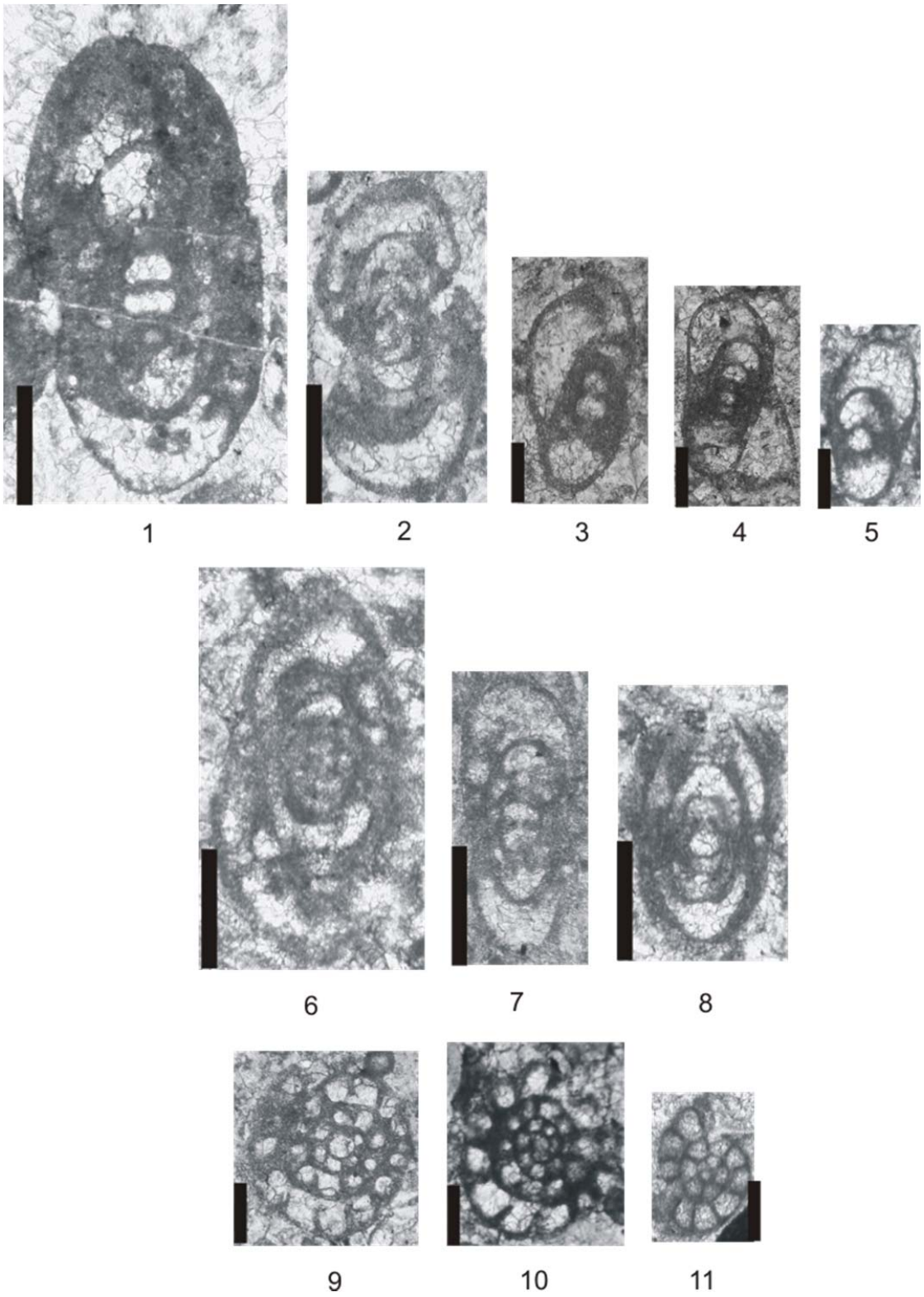

PLATE XXVI

Figure 1: *Mediocris mediocris*, sample no: SC-3 (Scale bar: 0.2 mm)

Figure 2: *Mediocris mediocris*, sample no: SC-1 (Scale bar: 0.2 mm)

Figure 3: *Mediocris mediocris*, sample no: SC-1 (Scale bar: 0.2 mm)

Figure 4: *Mediocris mediocris*, sample no: SC-7 (Scale bar: 0.2 mm)

Figure 5: *Mediocris mediocris*, sample no: SC-21 (Scale bar: 0.2 mm)

Figure 6: *Mediocris mediocris*, sample no: SC-12 (Scale bar: 0.2 mm)

Figure 7: *Mediocris mediocris*, sample no: SC-21 (Scale bar: 0.2 mm)

Figure 8: *Mediocris mediocris*, sample no: SC-23 (Scale bar: 0.2 mm)

Figure 9: *Mediocris mediocris*, sample no: SC-4 (Scale bar: 0.2 mm)

Figure 10: *Mediocris mediocris*, sample no: SC-3 (Scale bar: 0.2 mm)

Figure 11: *Mediocris breviscula*, sample no: SC-5 (Scale bar: 0.1 mm)

Figure 12: *Mediocris breviscula*, sample no: SC-4 (Scale bar: 0.1 mm)

Figure 13: *Mediocris breviscula*, sample no: SC-26 (Scale bar: 0.1 mm)

Figure 14: *Mediocris breviscula*, sample no: SC-44 (Scale bar: 0.1 mm)

Figure 15: *Mediocris breviscula*, sample no: SC-7 (Scale bar: 0.1 mm)

Figure 16: *Chomatomediocris* sp. , sample no: SC-18 (Scale bar: 0.2 mm)

PLATE XXVI

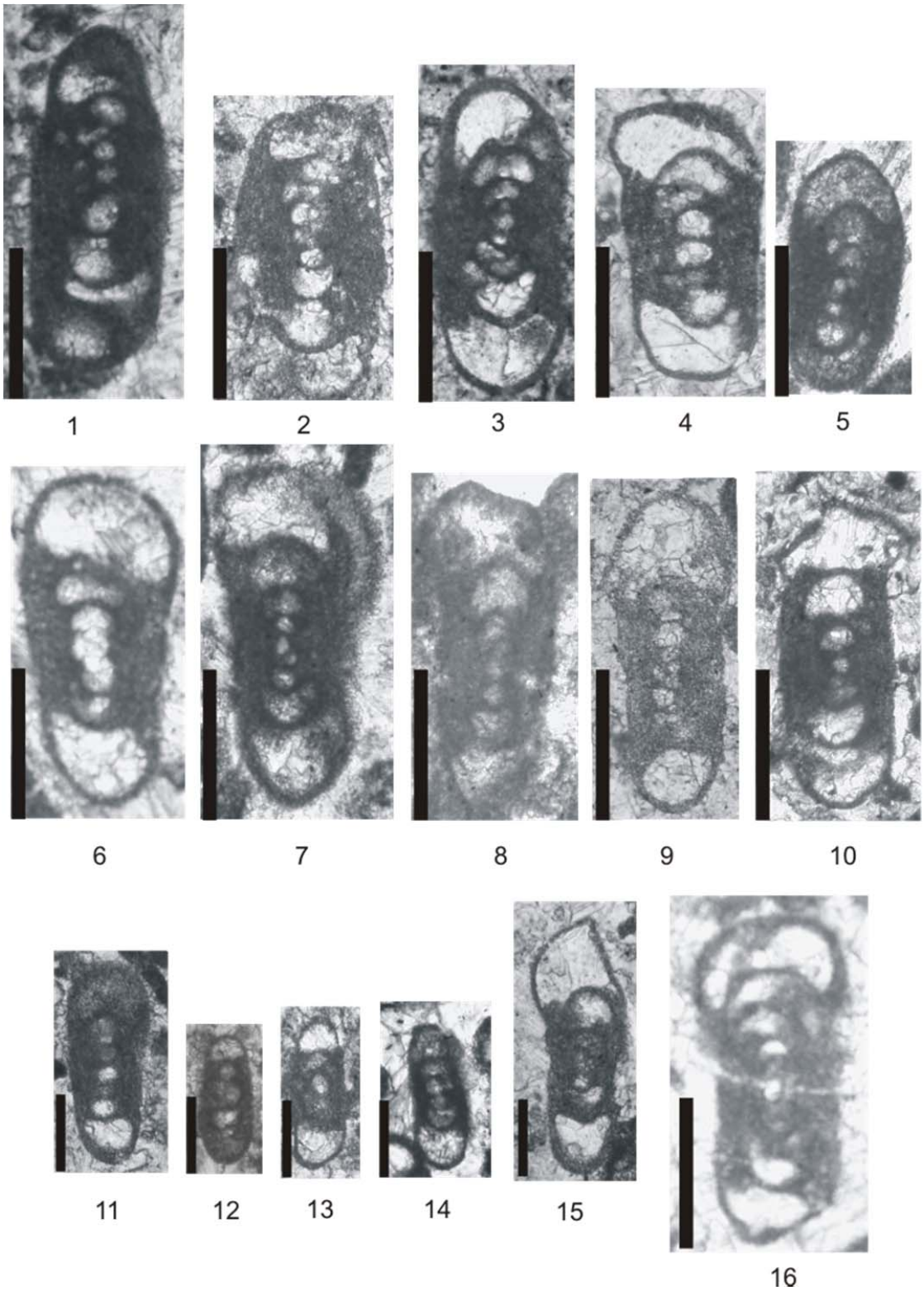

PLATE XXVII

Figure 1: *Mediocris* sp., sample no: SC-7 (Scale bar: 0.1 mm)

Figure 2: *Mediocris* sp., sample no: SC-5 (Scale bar: 0.1 mm)

Figure 3: *Mediocris* sp., sample no: SC-66 (Scale bar: 0.1 mm)

Figure 4: *Mediocris* sp., sample no: SC-74 (Scale bar: 0.1 mm)

Figure 5: *Mediocris* sp., sample no: SC-5 (Scale bar: 0.1 mm)

Figure 6: *Mediocris* sp., sample no: SC-89 (Scale bar: 0.1 mm)

Figure 8: *Mediocris* sp., sample no: SC-21 (Scale bar: 0.1 mm)

Figure 9: *Mediocris* sp., sample no: SC-5 (Scale bar: 0.1 mm)

Figure 10: *Mediocris* sp., sample no: SC-44 (Scale bar: 0.1 mm)

Figure 11: *Mediocris* sp., sample no: SC-2 (Scale bar: 0.1 mm)

Figure 12: *Mediocris* sp., sample no: SC-52 (Scale bar: 0.1 mm)

Figure 13: *Mediocris* sp., sample no: SC-44 (Scale bar: 0.1 mm)

Figure 14: *Eostaffella pseudostruvei*, sample no: SC-87 (Scale bar: 0.1 mm)

Figure15: *Eostaffella pseudostruvei*, sample no: SC-86 (Scale bar: 0.1 mm)

Figure16: *Eostaffella pseudostruvei*, sample no: SC-86 (Scale bar: 0.1 mm)

Figure 17: *Millerella* sp., sample no: SC-63 (Scale bar: 0.2 mm)

Figure 18: *Millerella* sp., sample no: SC-55 (Scale bar: 0.2 mm)

Figure 19: *Millerella* sp., sample no: SC-60 (Scale bar: 0.2 mm)

PLATE XXVII

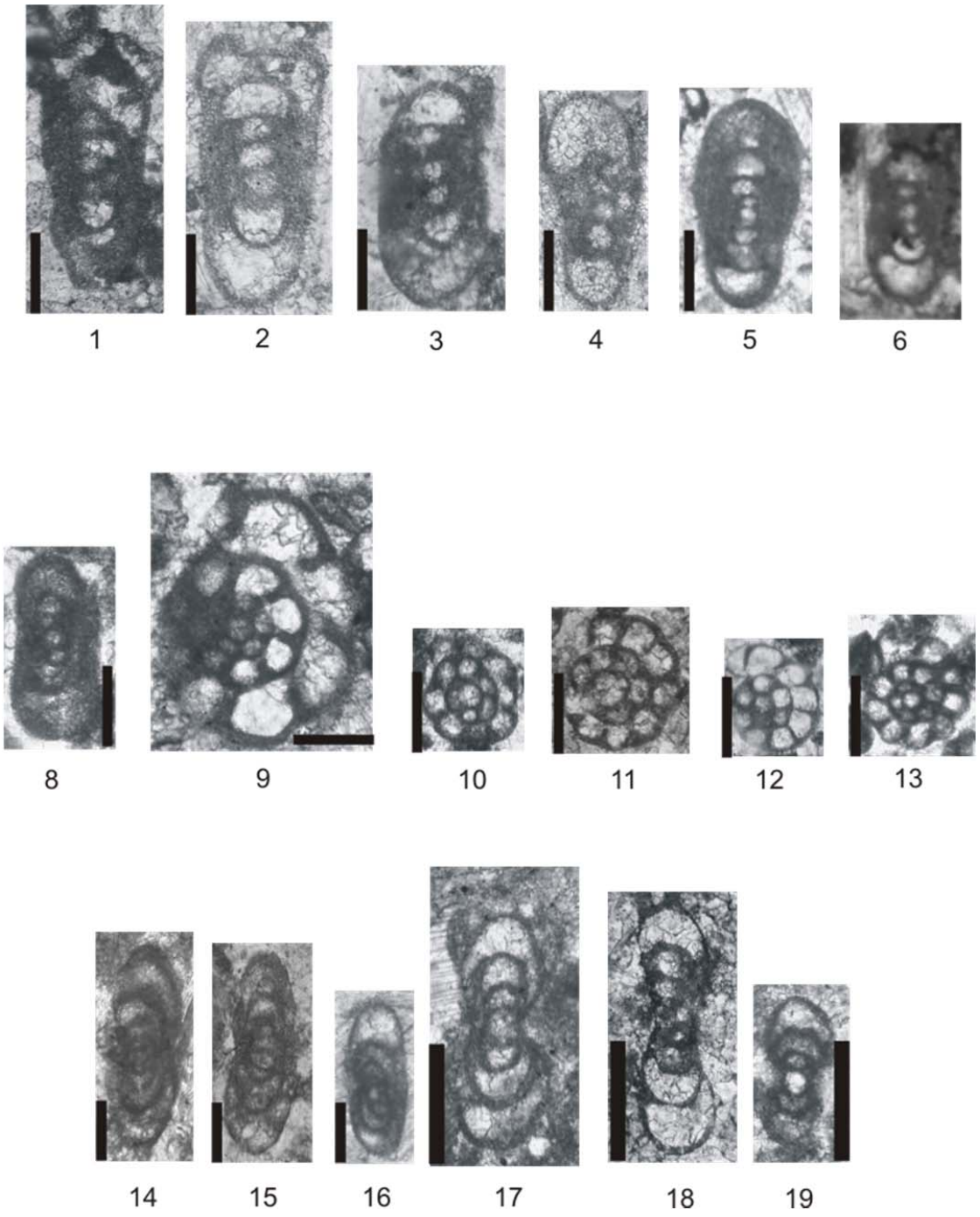

PLATE XXVIII

Figure 1: *Praeostaffellina macdonaldensis*, sample no: SC-53 (Scale bar: 0.1 mm)

Figure 2: *Paraeplectostaffella anvilensis*, sample no: SC-8 (Scale bar: 0.1 mm)

Figure 3: *Paraeplectostaffella anvilensis*, sample no: SC-4 (Scale bar: 0.1 mm)

Figure 4: *Paraeplectostaffella anvilensis*, sample no: SC-55 (Scale bar: 0.1 mm)

Figure 5: *Paraeplectostaffella anvilensis*, sample no: SC-3 (Scale bar: 0.1 mm)

Figure 6: *Paraeplectostaffella anvilensis*, sample no: SC-44 (Scale bar: 0.1 mm)

Figure7: *Paraeplectostaffella anvilensis*, sample no: SC-12 (Scale bar: 0.1 mm)

Figure 8: *Paraeplectostaffella anvilensis*, sample no: SC-2 (Scale bar: 0.1 mm)

Figure 9: *Paraeplectostaffella anvilensis*, sample no: SC-5 (Scale bar: 0.1 mm)

Figure 10: *Paraeplectostaffella anvilensis*?, sample no: SC-53 (Scale bar: 0.1 mm)

Figure 11: *Paraeplectostaffella anvilensis*, sample no: SC-51 (Scale bar: 0.1 mm)

Figure 12: *Paraeplectostaffella anvilensis,* sample no: SC- 82 (Scale bar: 0.1 mm)

Figure 13: *Paraeplectostaffella* sp., sample no: SC-35 (Scale bar: 0.1 mm)

Figure 14: *Paraeplectostaffella* sp., sample no: SC-50 (Scale bar: 0.1 mm)

PLATE XXVIII

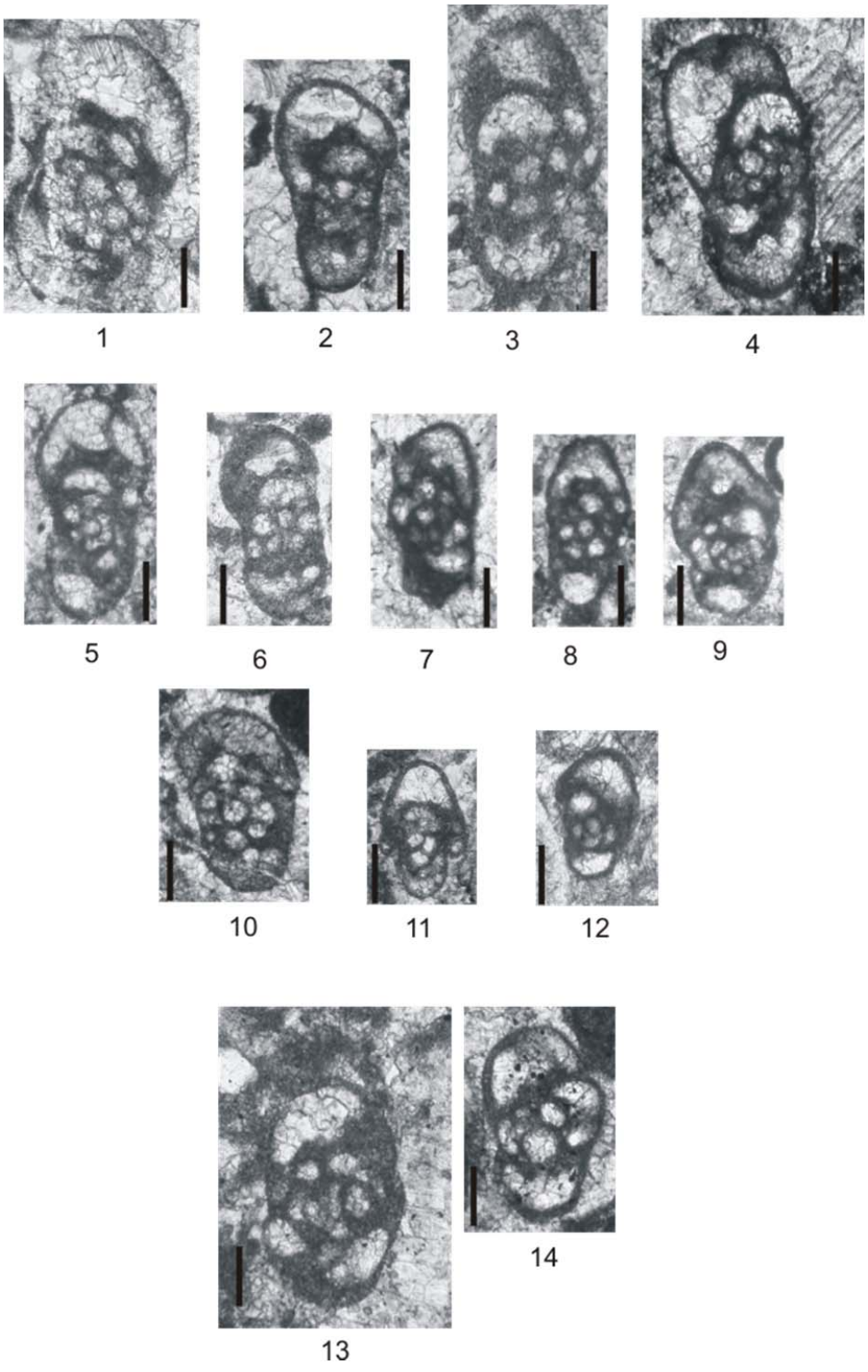

PLATE XXIX

Figure 1: *Pseudoendothyra struvei*, sample no: SC-51 (Scale bar: 0.2 mm)

Figure 2: *Pseudoendothyra struvei*, sample no: SC-4 (Scale bar: 0.2 mm)

Figure 3: *Pseudoendothyra* ex gr. *struvei*, sample no: SC-9 (Scale bar: 0.2 mm)

Figure 4: *Pseudoendothyra* ex gr. *struvei*, sample no: SC-68 (Scale bar: 0.2 mm)

Figure 5: *Pseudoendothyra* ex gr. *struvei*, sample no: SC-8 (Scale bar: 0.2 mm)

Figure 6: *Pseudoendothyra* ex gr. *struvei*, sample no: SC-4 (Scale bar: 0.2 mm)

Figure 7: *Pseudoendothyra* ex gr. *struvei*, sample no: SC-48 (Scale bar: 0.2 mm)

Figure 8: *Pseudoendothyra* ex gr. *struvei*, sample no: SC-65 (Scale bar: 0.2 mm)

Figure 9: *Pseudoendothyra* ex gr. *struvei*, sample no: SC-58 (Scale bar: 0.2 mm)

Figure 10: *Pseudoendothyra* sp., sample no: SC-50 (Scale bar: 0.2 mm)

Figure 11: *Pseudoendothyra* ex gr. *bona*, sample no: SC-5 (Scale bar: 0.2 mm)

Figure 12: *Pseudoendothyra* ex gr. *bona*, sample no: SC-5 (Scale bar: 0.2 mm)

Figure 13: *Pseudoendothyra* ex gr. *bona*, sample no: SC-5 (Scale bar: 0.2 mm)

PLATE XXIX

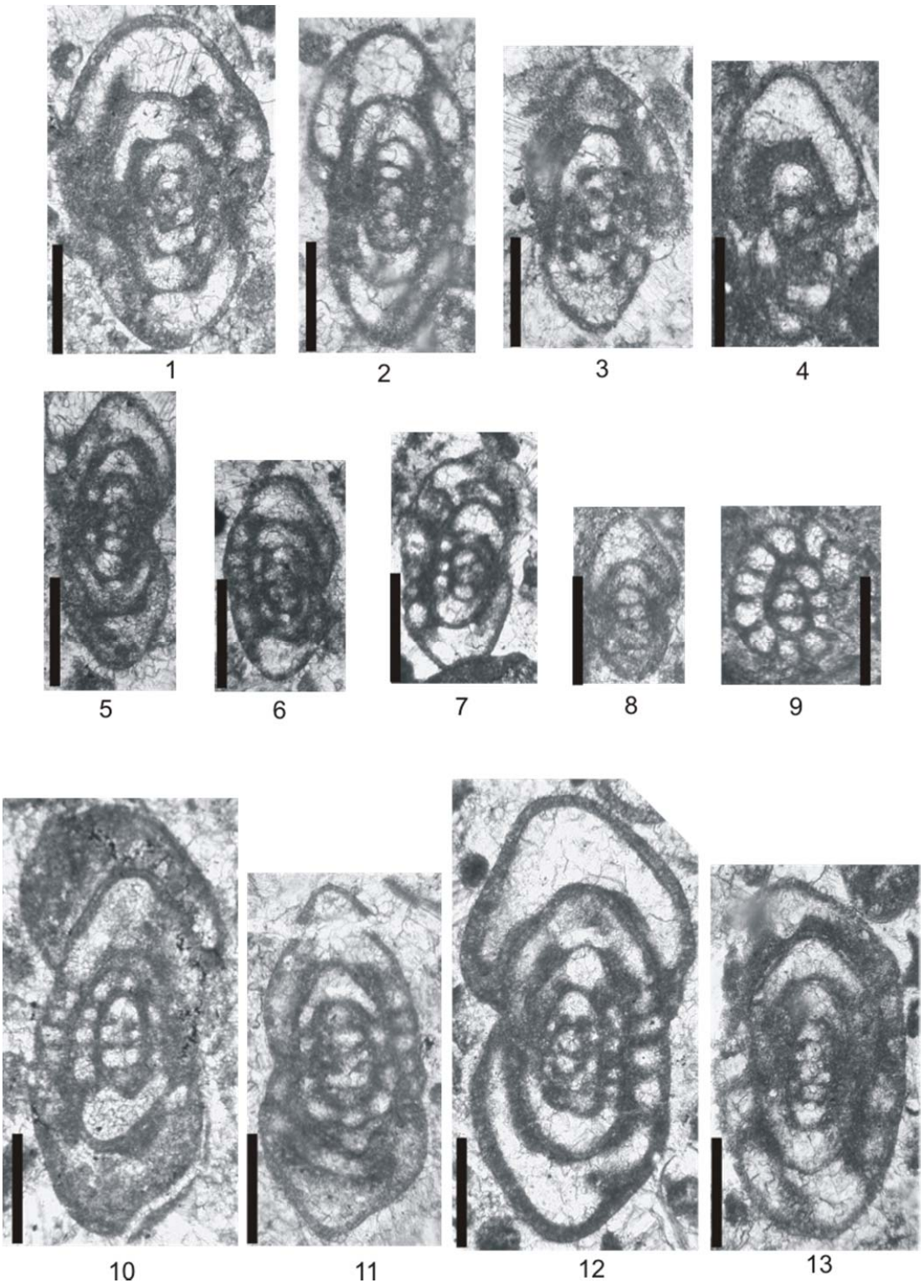

PLATE XXX

Figure 1: *Pseudoendothyra* sp 1 , sample no: SC-89 (Scale bar: 0.2 mm)

Figure 2: *Pseudoendothyra concinna*, sample no: SC- 49 (Scale bar: 0.2 mm)

Figure 3: *Pseudoendothyra* ex gr. *ornata*, sample no: SC-61 (Scale bar: 0.2 mm)

Figure 4: *Pseudoendothyra* ex gr. *ornata*, sample no: SC-72 (Scale bar: 0.2 mm)

Figure 5: *Pseudoendothyra* ex gr. *ornata*, sample no: SC-58 (Scale bar: 0.2 mm)

Figure 6: *Pseudoendothyra sublimis*, sample no: SC-70 (Scale bar: 0.2 mm)

Figure 7: *Pseudoendothyra sublimis*, sample no: SC-75 (Scale bar: 0.2 mm)

Figure 8: *Pseudoendothyra* sp., sample no: SC-2 (Scale bar: 0.2 mm)

Figure 9: *Pseudoendothyra* sp., sample no: SC-22 (Scale bar: 0.2 mm)

Figure 10: *Pseudoendothyra* sp., sample no: SC-5 (Scale bar: 0.2 mm)

Figure 11: *Pseudoendothyra sublimis*, sample no: SC-75 (Scale bar: 0.2 mm)

Figure 12: *Pseudoendothyra* sp 2., sample no: SC-2 (Scale bar: 0.2 mm)

Figure 13: *Pseudoendothyra* sp 3., sample no: SC-60 (Scale bar: 0.2 mm)

Figure 14: *Pseudoendothyra* sp 3., sample no: SC-57 (Scale bar: 0.2 mm)

PLATE XXX

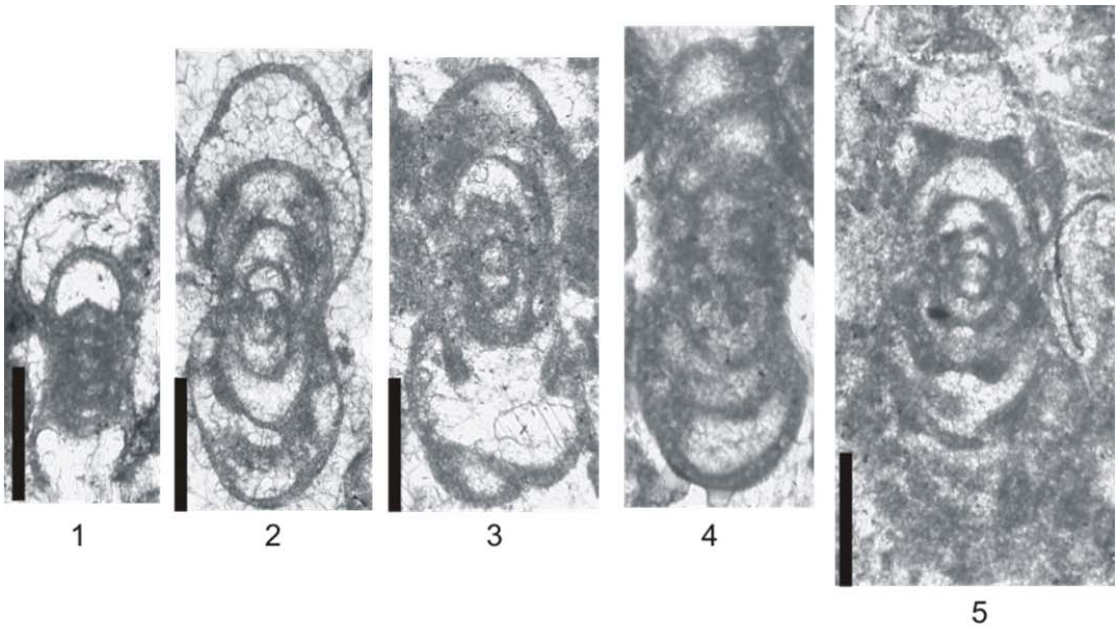

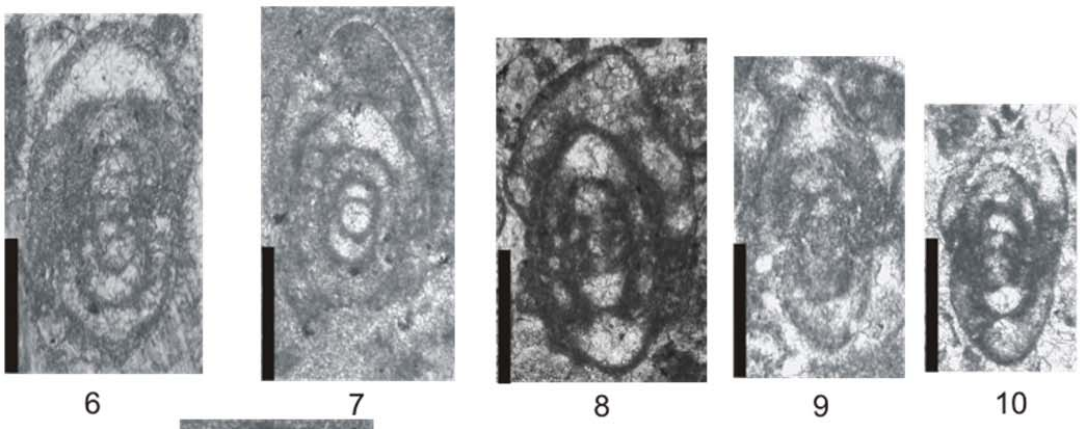

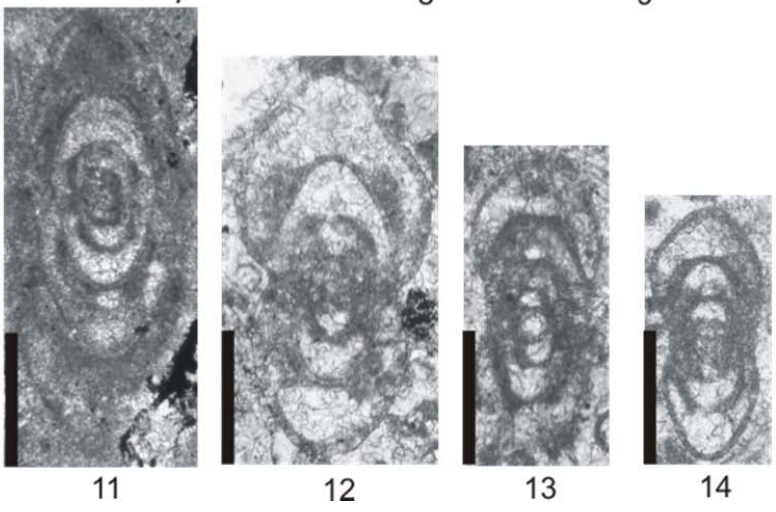

PLATE XXXI

Figure 1: *Paleotextularia* sp. 1, sample no: SC-84 (Scale bar: 0.2 mm)

Figure 2: *Paleotextularia* sp. 1, sample no: SC-85 (Scale bar: 0.2 mm)

Figure 3: *Paleotextularia* sp. 2, sample no: SC-78 (Scale bar: 0.2 mm)

Figure 4: *Paleotextularia* sp. 3, sample no: SC-85 (Scale bar: 0.2 mm)

Figure 5: *Paleotextularia* sp. 4, sample no: SC-79 (Scale bar: 0.2 mm)

Figure 6: *Paleotextularia* sp. 5, sample no: SC-90 (Scale bar: 0.2 mm)

Figure 7: *Paleotextularia* sp. 5, sample no: SC-85 (Scale bar: 0.2 mm)

Figure 8: *Paleotextularia* sp. 5, sample no: SC-84 (Scale bar: 0.2 mm)

Figure 9: *Paleobigenerina* sp., sample no: SC-83 (Scale bar: 0.2 mm)

Figure 10: *Paleobigenerina* sp., sample no: SC-78 (Scale bar: 0.2 mm)

Figure 11: *Climacammina* sp., sample no: SC-83 (Scale bar: 0.2 mm)

Figure 12: *Climacammina* sp., sample no: SC-22 (Scale bar: 0.2 mm)

Figure 13: *Tetrataxis* sp., sample no: SC-75 (Scale bar: 0.2 mm)

PLATE XXXI

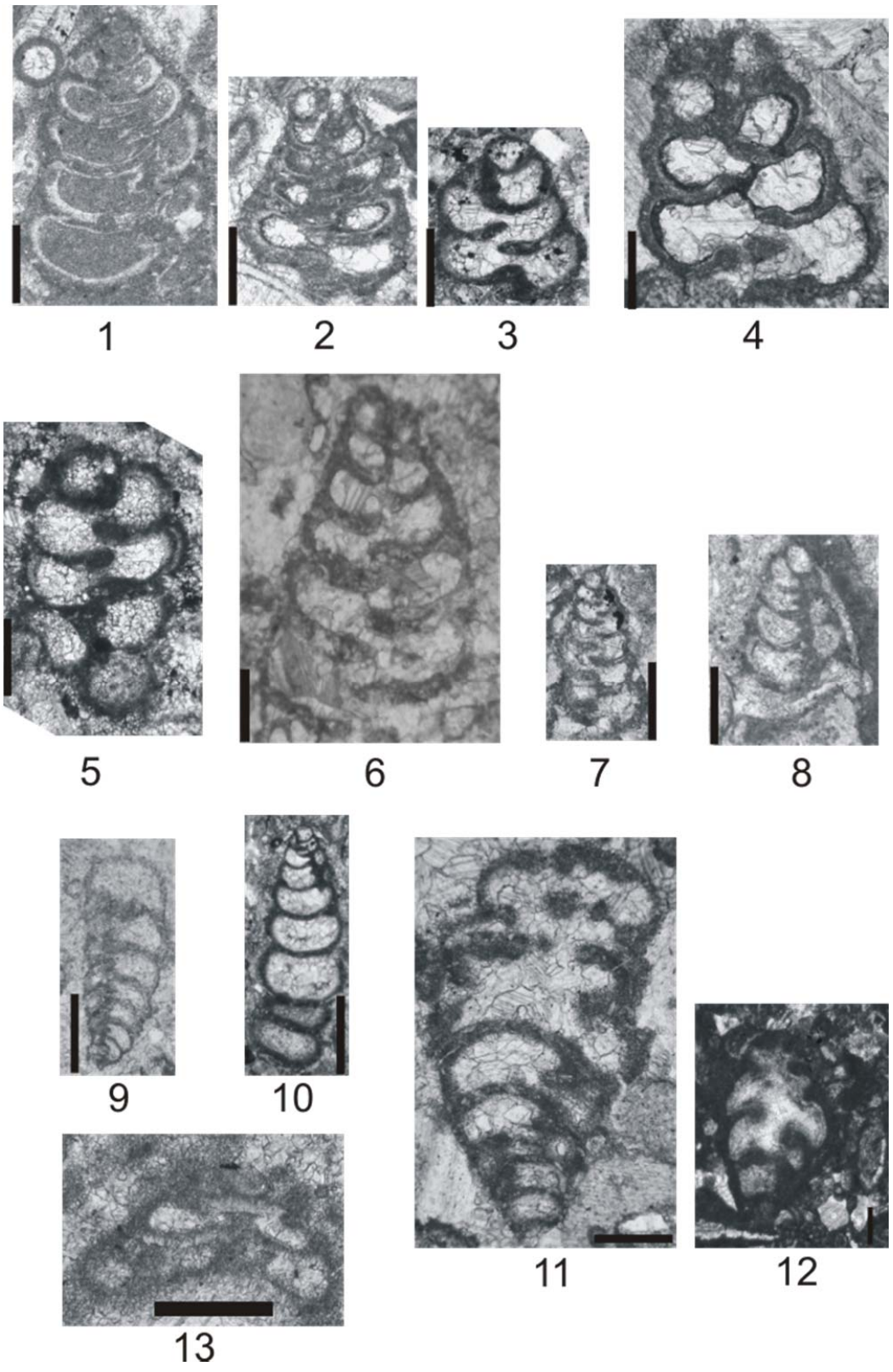

PLATE XXXII

Figure 1: *Consobrinella* sp.1, sample no: SC-85 (Scale bar: 0.1 mm)

Figure 2: *Consobrinella* sp.1, sample no: SC-84 (Scale bar: 0.1 mm)

Figure 3: *Consobrinella* sp.1, sample no: SC-74 (Scale bar: 0.1 mm)

Figure 4: *Consobrinella* sp.1, sample no: SC-83 (Scale bar: 0.1 mm)

Figure 5: *Consobrinella* sp.1, sample no: SC-2 (Scale bar: 0.1 mm)

Figure 6: *Consobrinella* sp.2, sample no: SC-79 (Scale bar: 0.1 mm)

Figure 7: *Consobrinella* sp.3, sample no: SC-9 (Scale bar: 0.1 mm)

Figure 8: *Consobrinella* sp.3, sample no: SC-36 (Scale bar: 0.1 mm)

Figure 9: *Consobrinella* sp. 2?, sample no: SC-2 (Scale bar: 0.1 mm)

Figure 10: *Koskinobigerina* sp. 1, sample no: SC-87 (Scale bar: 0.2 mm)

Figure 11: *Koskinobigerina*? sp., sample no: SC-8 (Scale bar: 0.1 mm)

Figure 12: *Koskinobigerina*? sp., sample no: SC-5 (Scale bar: 0.1 mm)

Figure 13: *Koskinobigerina*? sp., sample no: SC-85 (Scale bar: 0.1 mm)

Figure 14: *Koskinobitextularia* sp., sample no: SC-7 (Scale bar: 0.1 mm)

Figure 15: *Koskinotextulari* sp., sample no: SC-79 (Scale bar: 0.1 mm)

Figure 16: *Koskinobitextulari* sp., sample no: SC-4 (Scale bar: 0.1 mm)

Figure 17: *Koskinobitextulari* sp., sample no: SC-84 (Scale bar: 0.1 mm)

PLATE XXXII

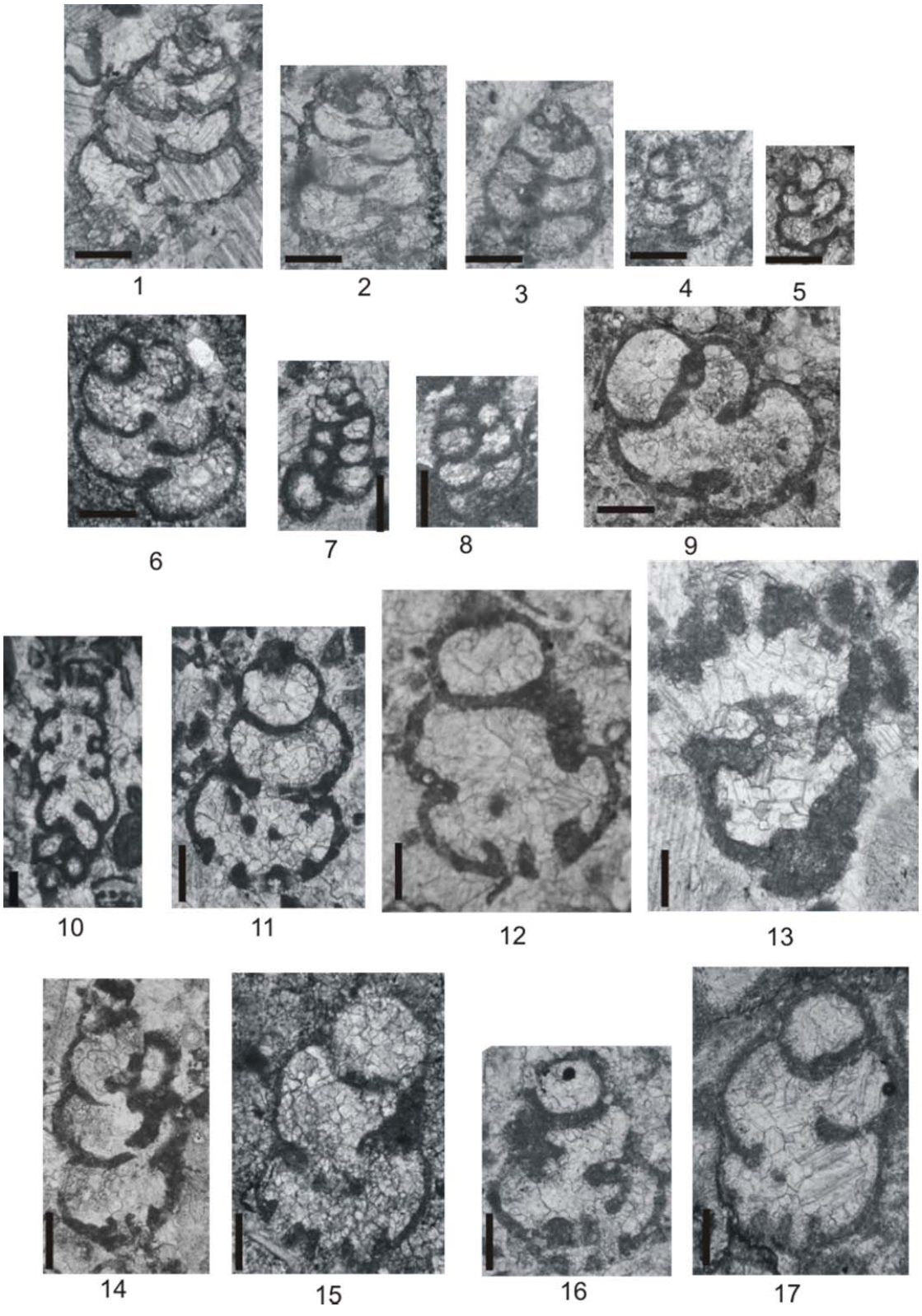

PLATE XXXIII

Figure 1: Unidentified genus 1, sample no: SC-5 (Scale bar: 0.2 mm)

Figure 2: Unidentified genus 1**,** sample no: SC-3 (Scale bar: 0.2 mm)

Figure 3: Unidentified genus 1**,** sample no: SC-4 (Scale bar: 0.2 mm)

Figure 4: Unidentified genus 1**,**sample no: SC-4 (Scale bar: 0.2 mm)

Figure 5: Unidentified genus 1**,**sample no: SC-3 (Scale bar: 0.2 mm)

Figure 6: Unidentified genus 1**,**sample no: SC-1 (Scale bar: 0.2 mm)

Figure 7: Unidentified genus 1**,** sample no: SC-35 (Scale bar: 0.2 mm)

Figure 8: Unidentified genus 1**,** sample no: SC-55 (Scale bar: 0.1 mm)

Figure 9: Unidentified genus 1, sample no: SC-16 (Scale bar: 0.2 mm)

Figure 10: Unidentified genus 2**,** sample no: SC-1 (Scale bar: 0.1 mm)

Figure 11: Unidentified genus 3**,** sample no: SC-1 (Scale bar: 0.1 mm)

Figure 12: Unidentified genus 2**,** sample no: SC-30 (Scale bar: 0.2 mm)

Figure 13: Unidentified genus 5**,** sample no: SC-28 (Scale bar: 0.2 mm)

Figure 14: Unidentified genus 6**,** sample no: SC-16 (Scale bar: 0.2 mm)

Figure 15: Unidentified genus 7, sample no: SC- 35 (Scale bar: 0.1 mm)

Figure 16: Unidentified genus 7, sample no: SC- 31(Scale bar: 0.1 mm)

Figure 17: Unidentified genus 8, sample no: SC-26 (Scale bar: 0.1 mm)

PLATE XXXIII